Bacterial Branching Enzymes as Agents for Modifying Glucan Structure in Industrial Processing

by

Lily Nasanovsky

A Thesis
presented to
The University of Guelph

In partial fulfillment of the requirements
for the degree of
Doctor of Philosophy
in
Molecular and Cellular biology

Guelph, Ontario, Canada

ABSTRACT

Bacterial Branching Enzymes as Agents for Modifying Glucan Structure in Industrial Processing

Lily Nasanovsky
University of Guelph, 2017

Advisor:
Dr. Ian J. Tetlow

Starch is used as a cheap, renewable, chemically-reactive matrix in many industrial processes. During processing, access to chemically-reactive groups on starch is essential and largely depends on their exposure, which is in part, a function of the branching frequency within starch. The amylose component of starch increases retrogradation (gelling property) of the cooked polymer at lower temperatures, forcing industries to use high temperatures throughout processing. The ability to manipulate glucan branching in starch and other polyglucans and remove amylose, offers many industrial end users (*e.g.* paints/inks, coatings, adhesives sectors) with superior performance bio-products. Branching enzymes (BEs) introduce α-1,6 branch points in starch and thus increase the number of reactive non-reducing chemical groups making post-harvest starch more chemically-reactive, facilitating its solubility and reducing retrogradation. Starch-derived polyglucans tend to gel rapidly, particularly in the presence of linear amylose chains, which hinders industrial processing and reduces polyglucan usability. BEs are promising industrial tools for increasing branch frequency and producing starches with improved physicochemical properties, and for reducing glucan chain length (by removing amylose) and alleviating retrogradation, and thus improving the solubility properties of post-

harvest starch. Presented here is a detailed biochemical and functional characterization of recombinant glycogen branching enzymes from *Thermus thermophilus* and *Deinococcus radiodurans* (DrGBE). Additionally, the presented work shows a proof of concept and demonstrates a novel application of DrGBE to modify a commercial starch-based polyglucan to reduce gelling, improve stability and solubility, and produce a visco-stable product.

ACKNOWLEDGEMENTS

I would like to thank my advisor, Dr. Ian Tetlow, for his continuous support and guidance throughout my PhD work. I could not thank you enough for listening to me and guiding me through the hard times. I would also like to express my gratitude to all the past and present members of the Emes/Tetlow lab for their pertinent advice and moral support. A special thank you to Dr. Amina Makhmoudova for the valuable discussions, suggestions and constant help.

I would like to extend a special thank you to all my friends who have been there for me throughout this life-changing journey. Especially, my besties Danve Castroverde and Emily Padhi, who have lent me an ear during difficult times, always offered sincere support and valuable suggestions. I love and appreciate you guys, and I'm looking forward to many more shared adventures.

A very warm and special thank you to my love, Martin, who has always supported me and helped me all throughout. Words cannot express the feeling of my love, devotion, thanks and gratitude to you. You mean the world to me.

Finally, I would like to thank my parents who have been an incredible source of inspiration and a solid support for me throughout my life. Thank you for loving, encouraging, and pushing me to make my dreams come true.

TABLE OF CONTENTS

LIST OF FIGURES

LIST OF TABLES

LIST OF ABBREVIATIONS

AaGBE	*Aquifex aeolicus* glycogen branching enzyme
ADP	adenosine 5’-diphosphate
ae-	*amylose-extender*
AgGBE	*Anaerobranca gottschalkii* glycogen branching enzyme
AGPase	adenosine 5’-diphosphate glucose pyrophosphorylase
Ala	alanine
AMP	adenosine monophosphate
ANN	annealing treatment
Arg	arginine
Asp	aspartic acid
ATP	adenosine triphosphate
BE	branching enzyme
BSA	bovine serum albumin
CBD	chitin-binding domain
CBM48	family 48 carbohydrate-binding-module
CD	circular dichroism spectroscopy
CGTase	cyclodextrin glycosyltransferase
CLD	chain length distribution
C-terminal	carboxy-terminal
Da	dalton
DgGBE	*Deinococcus geothermalis* glycogen branching enzyme
DP	degree of polymerization
DrGBE	*Deinococcus radiodurans* glycogen branching enzyme

DTT	dithiothreitol
E. coli	*Escherichia coli*
EcGBE	*Escherichia coli* glycogen branching enzyme
EDTA	ethylenediaminetetraacetic acid
G1P	glucose-1-phosphate
GBE	glycogen branching enzyme
GH13	hydrolase 13 family
GH57	glycoside hydrolase 57 family
GI	glycemic index
Gln	glutamine
Glu	glutamic acid
GPC	gel permeation chromatography
GS	glycogen synthase
GSD IV	glycogen storage disease IV
His	histidine
HMT	heat-moisture treatment
HPAEC	high-performance anion exchange chromatography
IMPACT	Intein Mediated Purification with an Affinity Chitin-binding Tag
IPTG	isopropyl β-D-1-thiogalactopyranoside
KOD	*Thermococcus kodakaraensis* KOD1
LALS	low-angle light scattering
LB	Luria-Bertani
Leu	leucine
MDs	maltodextrins

MES	2-(N-morpholino)-ethanesulfonic acid
Mn	number average molecular weight
MOPS	3-morpholinopropane-1-sulfonic acid
MOS	maltooligosaccharides
mSBEI	maize starch branching enzyme I
mSBEIIb	maize starch branching enzyme IIb
MtGBE	*Mycobacterium tuberculosis* glycogen branching enzyme
Mw	weight average molecular weight
MWCO	molecular weight cut-off
NH2- (N-)	amino-terminal
NMR	nuclear magnetic resonance
PAD	pulsed amperometric detector
PCR	polymerase chain reaction
PPi	pyrophosphate
RALS	right-angle light scattering
RI	refractive index
SBE	starch branching enzyme
SDS	sodium dodecyl sulphate-polyacrylamide gel electrophoresis
Ser	serine
SOC	Super Optimal broth with Catabolite repression
SS	starch synthase
TkGBE	*Thermococcus kodakaraensis* KOD1 glycogen branching enzyme
TPS1	trehalose-6-phosphate synthase
Trp	tryptophan

TtGBE	*Thermus thermophilus* glycogen branching enzyme
Tyr	tyrosine
UDP	uridine 5’-diphosphate
UGPase	uridine 5’-diphosphate glucose pyrophosphorylase

Chapter 1 - General Introduction

1.1 Introduction

The biosynthesis of starch and glycogen, major carbohydrate reserves in most organisms, is an important process whereby living organisms accrue energy reserves for use when availability of carbon is depleted or reduced in the environment (Iglesias and Preiss, 1992; Preiss, 1984; Seo et al., 2002). Glycogen is one of the most abundant polyglucans and is produced by bacteria, various species of archaea, yeasts and mammals (Bräsen *et al*., 2014; Manners, 1991; Patron and Keeling, 2005). Starch, on the other hand, is an essential short- and long-term reserve carbohydrate synthesized in the cytoplasm of Rhodophyceae (red algae) and Glaucophyta (Dauvillée *et al*., 2009), as well as in plastids of green algae and land plants (Tetlow, 2011).

Starch (comprised of amylose and amylopectin) and glycogen are both composed of glucan chains, which are essentially glucose monomers linked in an α-1,4 fashion with recurring α-1,6 branch points, the latter facilitating packing of more glucan chains into the polymer, exerting minimal effect on the internal osmotic pressure in the cell (Manners, 1991; Iglesias and Preiss, 1992). Branching in glycogen is uniformly distributed throughout the polyglucan and occurs at a higher degree (8 - 10%) compared with branching in the amylopectin component of starch (3 - 5%), in which different size branch points are organized in a periodic manner (Gunja-Smith *et al*., 1970; Hizukuri, 1986; Roach, 2002). Interestingly, some of the differences in the physicochemical properties and function of the two polyglucans are influenced by the positioning and frequency of the α-1,6 branch points.

Glycogen has an open, water-soluble structure, facilitating degradability for rapid release of energy, whereas the water-insoluble, semi-crystalline structure of tightly packed glucan chains forming the starch granule, is ideally suited as a long-term store of carbon (Bell, 1948; Manners, 1989; Myers *et al*., 2000; Tetlow, 2011). The branching patterns of glycogen and starch are established by branching enzymes (BEs) (1,4-α-glucan: 1,4-α-glucan 6-glucosyl-transferase: E.C. 2.4.1.18). BEs catalyze the formation of α-1,6 branch points in glycogen and starch, yielding different branch frequencies and branch chain-length in these polyglucans (Seo *et al*., 2002; Tetlow, 2011). BE catalytic activity was originally detected by Haworth *et al*. (1944) in potato. It was initially thought that polyglucan chain elongation occurred entirely through the action of phosphorylase (E.C. 2.4.1.1), termed P-enzyme (Haworth *et al*., 1944). However, chain elongation was observed to occur in concert with branching, and the enzyme responsible was termed Q-enzyme (Haworth *et al*., 1944; Gilbert and Patrick, 1952).

In plants, there are various isoforms of starch branching enzymes (SBEs) that influence the physical structure and properties of starch, and therefore their relative activities in crop plants dictate various end-uses (Table 1) (Burrell, 2003; Jobling, 2004). In the food industry for example, SBE activities influence digestibility and processing characteristics of starches (Annison and Topping, 1994; Cassidy *et al*., 1994). For instance, 'high-amylose' starches, which compared to wild- type starches possess a lower branch frequency and a higher proportion of relatively long-chain branch points in their modified amylopectin component (which has some amylose-like properties), can be processed into "resistant starches" that are advocated as beneficial for human health, yielding lower glycemic index values upon consumption, as well as promoting colonic

health (Cassidy *et al*., 1994; Annison and Topping, 1994). BEs are also promising tools for industries such as paints and coatings, where highly-branched starches with favourable dispersion properties can facilitate generation of desirable polymers (Kiel *et al*., 1991; Röper, 2002).

Table 1 Examples of Various Starch End-uses.

Food and Drinks	Animal Feed	Agriculture	Plastic	Pharmacy	Building	Paper	Miscelleneous
- Mayonnaise - Baby food - Bread - Soft drinks - Meat products - Confectionery	- Pellets - By products	- Seed coating - Fertilizer	- Biodegradable plastic	- Tablets - Dusting powder	- Mineral fibre - Gypsum board - Concrete	- Corrugated board - Cardboard paper	- Oil drilling - Water treatment - Glue

Starch is a cost-effective, renewable, chemically-reactive matrix used in many industrial processes (Röper, 2002; Smith, 2008; Tetlow, 2011). The ability to manipulate starch glucan branching offers many industrial end-users, in particular the paints/inks, coatings and adhesives sectors a substrate for many types of polymerization and chemical modification reactions. Highly-branched starches with favourable dispersion properties possess an abundance of functional, reactive chemical groups, making these starches ideally suited for the production of bio-based polymers. Post-harvest starches are often chemically modified to improve physicochemical properties, and although chemically modified starches have been developed to maximize the usefulness of starch for industrial applications, there are many disadvantages to this approach (Jobling, 2004; Röper, 2002). These include increased costs of chemical modification to manufacturers, generation of wastes hazardous to the environment, and dependence on petroleum-derived materials.

Currently manufacturers (*e.g*. those in the paints/inks, coatings, and adhesives sectors) rely on importing costly *Waxy* starches (mutant variety), which are essentially free of amylose, as amylose tends to hinder post-harvest starch processing (see details below). Normal crops are naturally higher yielding in starch (than mutant genotypes) and therefore the ability to increase the branching frequency of amylose and amylopectin in normal starches can be beneficial, in particular for improving the functionality of starches for biopolymer applications (Jobling, 2004; Tetlow, 2006). The high degree of branching by BEs has an important impact on the structure and function of the polyglucan as increasing the number of non-reducing ends makes the polymer more reactive to synthesis and degradation, as well as potentially promotes its solubility in water (often a component in industrial processing).

The research described in this thesis aimed to characterize and develop recombinant thermo-tolerant BEs, and chimeric BEs, suited for a variety of industrial processing conditions, providing a new potential industrial tool for bio-product development, while reducing reliance on petroleum-based materials and circumventing production of environmentally-hazardous wastes.

1.2 Starch and Glycogen Structure

Carbohydrate reserves found in the form of starch in tissues of higher plants are normally formed as discrete granules (range in size of ~5 – 50 μm) in various plant plastids (Ahmed *et al*., 2015; Jobling, 2004; Tetlow, 2011). The starch granule is a water-insoluble structure with a hierarchical order composed of two distinct types of glucose polymer (Figure 1.2.1); amylose, an essentially unbranched polyglucan composed of

linear α-1,4-linked glucan chains (Figure 1.2.1 A), and amylopectin, a larger, highly and asymmetrically branched polysaccharide, composed of α-1,4-linked glucan chains that are interlinked by α-1,6-branches (Figure 1.2.1 A) (Ball et al., 1996; Buléon et al., 1998a; Leach and Schoch, 1961; Smith et al., 1997; Tetlow, 2006). Typically, the starch granule is comprised of 20 - 30% amylose, a sparsely branched polyglucan (less than 1%), and 70 - 80% amylopectin, a larger and highly-branched (~5%) glucan polymer (French, 1984; Manners, 1989; Tetlow, 2011). The pattern of distribution of glucan chain lengths and the clustering of branch points within amylopectin facilitate packaging of the short linear chains as parallel left-handed double helices (Figure 1.2.1 B) (French, 1984; Smith et al., 1997). These in turn cluster in ordered arrays, bestowing the semi-crystalline nature upon a majority of the starch granule matrix, and giving starch its water-insoluble characteristic (Figure 1.2.1 B and C) (French, 1984; Liu et al., 2012; Smith et al., 1997). The packed double helices form the crystalline lamellae of amylopectin structure, while the branch points of the polymer assemble into amorphous lamellae that separate the alternating crystalline lamellae (Figure 1.2.1 B and C) (French, 1984; Smith et al., 1997). The alternating amorphous and crystalline lamella form the semi-crystalline growth rings of the starch granule (Figure 1.2.1 C and D; semi-crystalline zone) (Gallant et al., 1997; Pilling and Smith, 2003; Smith et al., 1997). Starch granule formation is established by both the semi-crystalline properties of amylopectin, attributed to the length of its linear chains, and the frequency and clustering of branch points (α-1,6-linkages) within amylopectin (Figure 1.2.1 C and D) (Robin *et al*., 1974; Smith *et al*., 1999; Tetlow, 2011). Amylose is most likely found interspersed within the amorphous lamellae of amylopectin as single-helical or random-coil formations (Jane *et al*., 1992; Jenkins and

Donald, 1995). However, the exact location of amylose within the granule has not yet been determined and is a topic of much debate.

Starch granules are classified into three types of higher-ordered crystalline organization (allomorphs) based on their X-ray diffraction patterns, termed A-, B-, and C-type, which represent differences in helix packing (Katz, 1930). The A-type allomorphs, characteristic of cereal starches, have small intercluster chain lengths, and thus are the most tightly packed starches, while B-type starch allomorphs (tuber starches) have a more open, less packed structure with more water molecules entrapped between helices, and the C-type starch (*e.g.* pea starch) allomorphs are considered to be a combination of A- and B-types (Buléon *et al*., 1998b; Hizukuri *et al*., 1983; Wu and Sarko, 1978).

Glycogen, in contrast to amylopectin, is more highly-branched and has an amorphous open structure that expands in a globular fashion (Figure 1.2.2) (Craig *et al*., 1988; Gunja-Smith *et al*., 1970; Roach, 2002). Although the fine structure of glycogen has not yet been fully elucidated, studies, mainly focused on enzymatic degradation of glycogen, yielded a well accepted model for glycogen structure, which suggests that glycogen is composed of two types of chains; B-chains, classified as glycogen inner chains normally containing two branches, and A-chains, the outer unbranched chains (Goldsmith *et al*., 1982; Gunja-Smith *et al*., 1970). Glycogen structural studies suggest that the average length of A- and B-chains is 13 glucose residues (Meléndez-Hevia *et al*., 1993; Meléndez *et al*., 1997). The model also pinpoints that the glycogen molecule is spherical and is organized into concentric tiers, with B-chains in the inner tiers, and A-chains in the outer tiers (Goldsmith *et al*., 1982; Gunja-Smith *et al*., 1970; Meléndez-

Hevia *et al*., 1993). As the glycogen molecule grows in tiers, new A-chains are added, and chains that were formerly A-type, become B-type. However, such a structure is self-limiting as the packing density increases due to the doubling of the number of chains in each layer, and the resulting steric hindrance at the surface of the molecule prevents further growth (Goldsmith *et al*., 1982; Madsen and Cori, 1958). Interestingly, by contrast to glycogen, the branches in amylopectin are not evenly distributed and the cluster-like organization of glucan chains within amylopectin allow the virtually infinite growth of the macromolecule (Bertoft, 2007; Hizukuri, 1986). The mature glycogen molecule, referred to as a β-particle, has 12 tiers, is ~40 nm in diameter, and has a molecular mass of ~10^7 dalton (Da) (Goldsmith *et al*., 1982; Madsen and Cori, 1958; Meléndez-Hevia *et al*., 1993).

At the core of the glycogen molecule, is glycogenin, a self-glucosylating protein, which forms an oligosaccharide primer chain (Pitcher *et al*., 1987; Smythe and Cohen, 1991). Glycogenin transfers glucose from uridine 5'-diphosphate glucose (UDP-glucose) to a tyrosine residue within itself and then forms α-1,4-glycosidic linkages until the oligosaccharide chain is approximately 10 – 20 glucose residues long (Pitcher *et al*., 1987; Smythe and Cohen, 1991). The commonly accepted theory is that in eukaryotic cells, glycogenin generates the primer for glycogen synthesis by glycogen synthase (GS) (Hurley *et al*., 2006; Roach *et al*., 2012). However, recent studies have shown that glycogen biogenesis can occur in eukaryotic cells in the absence of glycogenin. Typically, *Saccharomyces cerevisiae* cells deficient in glycogenin (deletion of glycogenin *GLG1* and *GLG2* genes) abolish glycogen synthesis; however, in a recent study a small *glg1glg2* mutant population (<3%) of colonies (on agar plate) was found to accumulate

glycogen (Torija *et al*., 2005). The study showed that the capacity of *glg1glg2* mutants to accumulate glycogen was further enhanced by transformation of *glg1glg2* mutants with a high-copy-number plasmid encoding a hyperactive form of glycogen synthase (*GSY*2D643), and upon deletion of the *TPS1* (trehalose-6-phosphate synthase) gene, which caused an increase in accumulation of UDP-glucose and glucose 6-phosphate, the substrate and the positive effector of glycogen synthase, respectively (Torija *et al*., 2005). The authors therefore proposed the existence of an alternative initiator molecule that serves to prime glycogen synthesis in the absence of glycogenin in yeast cells, challenging the dogma of glycogen synthesis in eukaryotic cells (Torija *et al*., 2005). Currently no new research has emerged to confirm or refute an alternative glycogen primer.

Glycogen contains regularly spaced α-1,6 branches, which lead to its spherical structure wherein the glucan chains are hidden away within the sphere while their nonreducing ends are exposed, conferring water solubility to the glycogen molecule (Figure 1.2.2) (Meléndez-Hevia *et al*., 1993). In contrast, in amylopectin the branch chains cluster together forming double helices, and the vicinal double helices subsequently stack causing the water insolubility of the starch molecule (Figure 1.2.1 B and C) (Pérez and Bertoft, 2010; Robin *et al*., 1974). Therefore, the major differences between the water-soluble amorphous glycogen and the insoluble crystalline starch stem from the asymmetric distribution of amylopectin branch points, and the overall decrease of frequency of branching observed in amylopectin, ~5% vs. the ~9% in glycogen (Manners, 1989, 1991; Meléndez *et al*., 1998).

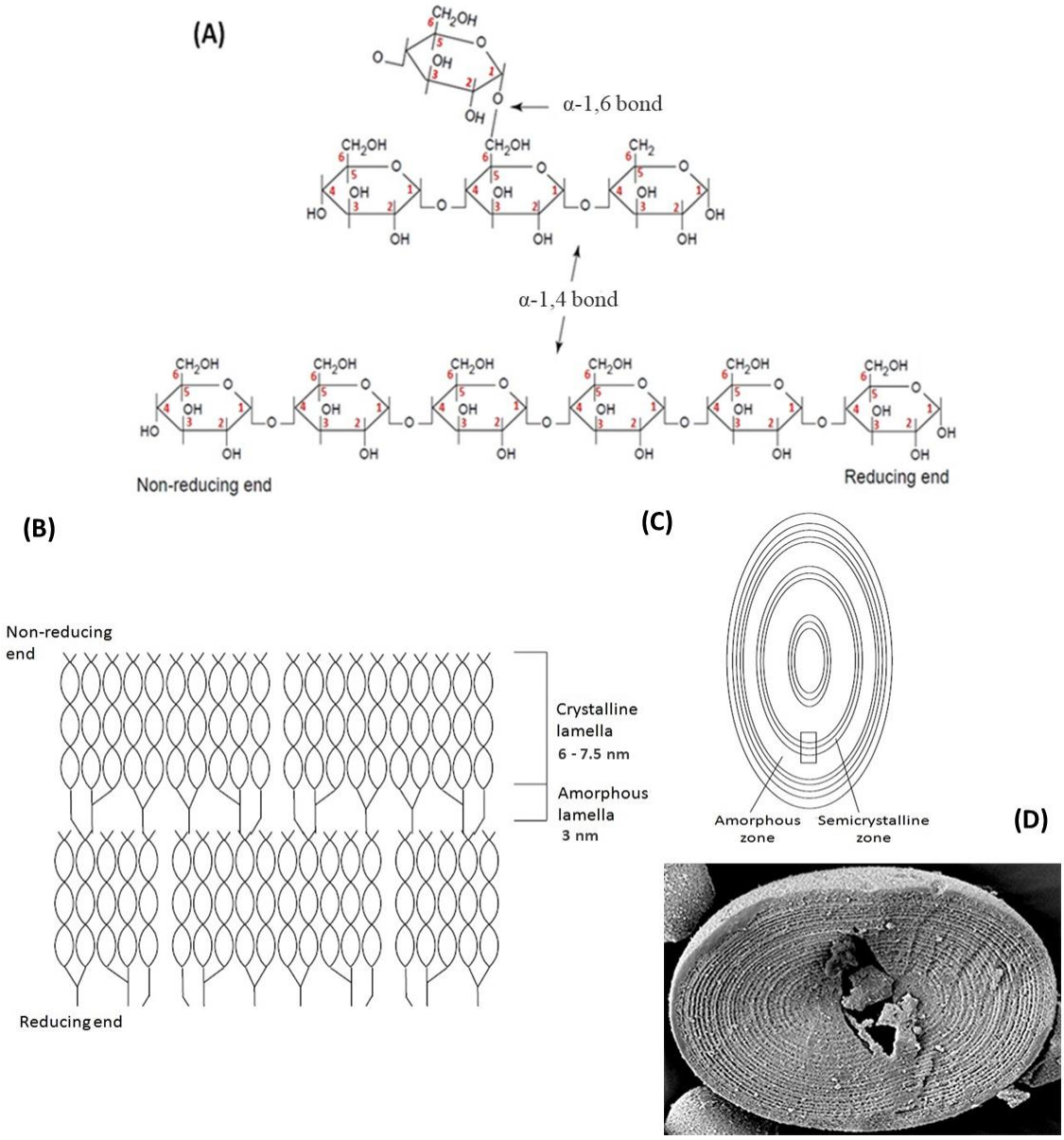

Figure 1.2.1 Schematic representation of the molecular structure of starch, and starch granule organization. (A) Molecular structure of glycogen and starch. Glucose units are linked *via* α-1,4-linkages. BEs cleave α-1,4-bonds, and transfer cleaved chain onto another chain, creating an α-1,6-branch point. (B) Arrangement of the alternating crystalline and amorphous lamellae within growth rings. Each crystalline lamella is composed of clusters of parallel α-1,4-linked glucan chains packed together in a helical configuration. At the bases of the helices, α-1,6-branch points form the amorphous lamella and join the crystalline lamella together. (C) Schematic representation of the starch granule structure showing alternating amorphous and semi-crystalline zones termed growth rings (~100 - 400 nm thick). The amorphous zones are thought to contain amylopectin (in a less-ordered state) along with amylose. (D) Cross-section of a starch granule, following treatment with α-amylase, showing growth rings (reproduced from Pilling and Smith, 2003).

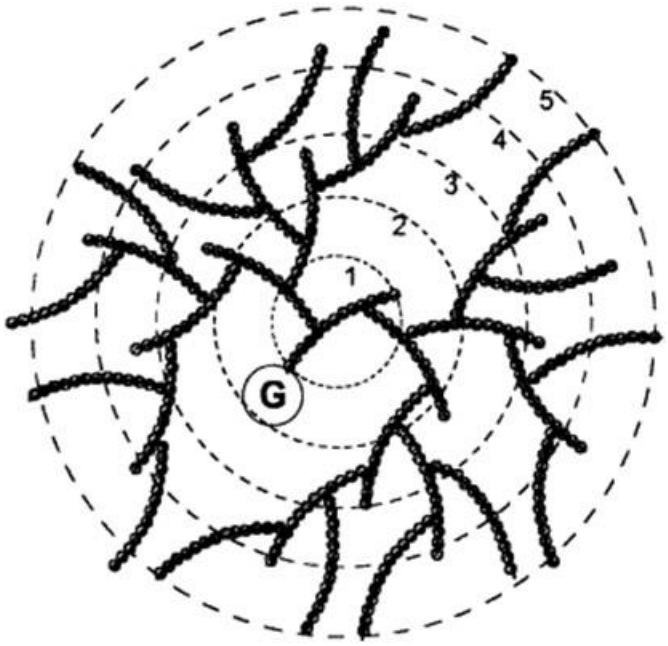

Figure 1.2.2 Schematic representation of the glycogen molecule structure as per Gunja-Smith *et al*. (1970) and Goldsmith *et al*. (1982). The B-chains are branched, each with two branches, which in turn are either branched, or not. The non-branched chains are A-chains. Glycogen possesses a spherical structure with successive branches forming concentric tiers (12 in mature molecule), which become more tightly packed as they move away from the centre. Glycogenin, at the core of the molecule is denoted with G. For ease of representation only 5 tiers are shown (numbered circles). Figure reproduced from Meléndez *et al*. (1998).

1.2.1 Starch and Glycogen Synthesis

The biosynthesis of starch and glycogen includes a number of key enzymes; adenosine 5'-diphosphate glucose (ADP-glucose), or UDP-glucose, pyrophosphorylase (AGPase: E.C. 2.7.7.27, UGPase: E.C. 2.7.7.9), starch and glycogen synthases (SSs: E.C. 2.4.1.21, and GSs: E.C. 2.4.1.11, respectively), and starch and glycogen branching enzymes (SBEs and GBEs, respectively) (James *et al.*, 2003; Preiss, 1984; Myers *et al*.,2000; Tetlow, 2011). AGPase catalyzes the first committed step in starch biosynthesis,

and it (or UGPase) also catalyzes a rate-limiting step in prokaryotic glycogen synthesis (Figure 1.2.1.1 A**)** (Devillers *et al*., 2003; Murakami *et al*., 2006; Tetlow, 2011). Normally, eukaryotes synthesize glycogen from UDP-glucose in the cytosol, while bacteria utilize ADP-glucose, and in some cases UDP-glucose (Lou *et al*., 1997). The formation of ADP-glucose from glucose-1-phosphate (G1P) and adenosine triphosphate (ATP) is established through the action of AGPase (Figure 1.2.1.1 A) (Greenberg and Preiss, 1964; Guan and Keeling, 1998; Tetlow, 2011). SSs/GSs then catalyze glucan chain elongation by transferring glucosyl units of ADP-glucose (or UDP-glucose) to the non-reducing ends of growing polyglucans, connecting them through α-1,4-glycosidic bonds (Figure 1.2.1.1 B) (Ball and Morell, 2003; Guan and Keeling, 1998). Simultaneously, branching of polyglucans is generated by BEs *via* hydrolysis of internal α-1,4-glucosidic linkages within glucans, and transfer of the released reducing ends to C6 hydroxyl groups, of either the original glucan chain or an adjacent one, to form the α-1,6 branch points (Figure 1.2.1.1 C) (Devillers *et al*., 2003; Murakami *et al*., 2006).

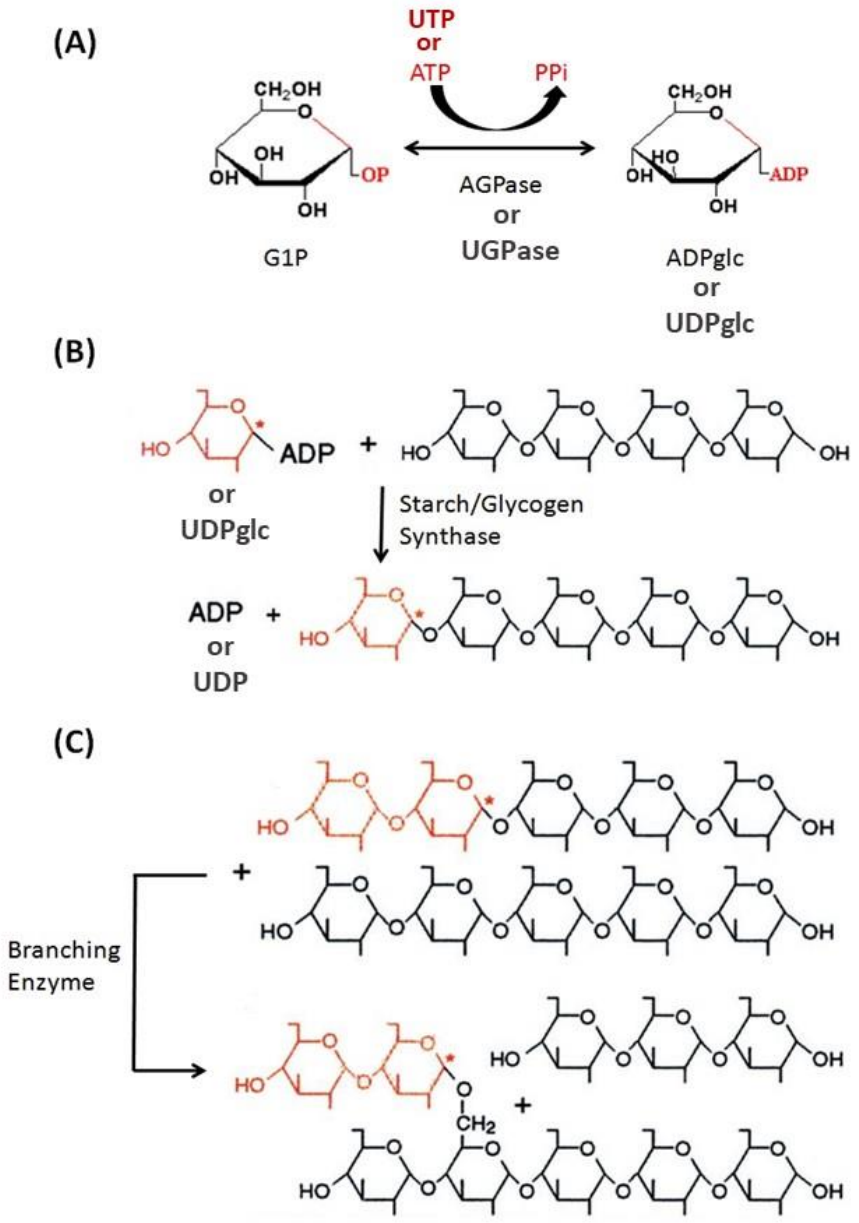

Figure 1.2.1.1 Diagrammatic representation of the chemical reactions catalyzed by enzymes involved in starch and glycogen synthesis. Detailed description of reaction steps is provided in section 1.2.1. Donated glucosyl units are shown in red, and asterisks indicate reducing carbons through which the glucans are transferred. G1P, glucose 1-phosphate; ADP, adenosine 5'-diphosphate; UDP, uridine 5'-diphosphate; ADPglc, ADP-glucose; UDPglc, UDP-glucose; AGPase, ADP-glucose pyrophosphorylase; UGPase, UDP-glucose pyrophosphorylase; ATP, adenosine triphosphate; PPi, pyrophosphate. Figure was adapted from Myers *et al*. (2000) and modified.

BEs are essential for starch and glycogen biosynthesis, and lack of branching activity leads to altered starch and glycogen structure. In higher plants, SBEs are classified into two types, SBEI (also known as SBE B), belonging to class I, and SBEII (SBE A), belonging to class II (Nakamura, 2002; Tetlow, 2011). The SBEII class is further subdivided into SBEIIa and SBEIIb in cereals, each possessing different kinetic characteristics and tissue expression patterns (Rahman *et al*., 2001). It appears that in many plant species, it is the loss of the SBEII class that produces the most prominent effects on starch structure and synthesis, while lack of SBEI seems to have no apparent effect on starch phenotype. Studies of loss of SBEI activity in maize and potato showed no major change in starch structure, including change in chain-length distribution compared to wild-type controls (Blauth *et al*., 2002; Flipse *et al*., 1996). In contrast, lack of both SBEIIb and SBEIIa activity yields an altered starch phenotype and structure. Loss of SBEIIb in maize, referred to as the *amylose-extender* (*ae*$^{-}$) mutation, yielded irregularly shaped starch granules and a 20% reduction in starch synthesis (Boyer *et al*., 1976). In maize and rice, the *ae*$^{-}$ mutation leads to apparent high-amylose starch phenotype, attributed to amylopectin with long internal chain lengths and reduced branching (Kim *et al*., 1998; Tetlow and Emes, 2014). High-amylose starches find a myriad of applications in the food and non-food industries, and are deemed as high-value starches due to their unique properties such as, reduced digestibility, film-forming attributes, and high gelling strength (Jobling, 2004; Richardson *et al*., 2000). In wheat and barley, high-amylose phenotype starch (>70% amylose) has been produced by suppressing the genes encoding both SBEIIb and SBEIIa (Regina *et al*., 2006), while in potato a high-amylose phenotype starch (up to 75%), and altered starch granule

morphology and composition, was induced by inhibiting both SBE A and SBE B to below 1% of wild-type activity (Schwall *et al*., 2000). In Arabidopsis, deletion of either SBE 2.1 or SBE 2.2 produced minimal effects on starch content and structure; however, loss of both SBE 2 isoforms abolished starch synthesis altogether (Dumez *et al*., 2006).

Unlike starch, glycogen synthesis relies on a single BE isoform for α-1,6-branch point formation, imparting a crucial role for GBEs in glycogen structure. Studies using GBE-deficient *Escherichia coli* (*E. coli*), *Saccharomyces cerevisiae*, and cyanobacteria have shown that these mutants accumulate sparsely branched, amylose-like polyglucans, which had iodine-staining properties reminiscent of starch (Damotte *et al*., 1968; Romeo *et al*., 1988; Rowen *et al*., 1992; Yoo *et al*., 2002). In humans, a deficiency in GBE, encoded by the *GBE1* gene, results in accumulation of abnormal glycogen, superficially resembling amylopectin, which contains infrequently branched, long glucan chains (Andersen, 1956; Brown and Brown, 1966). This GBE deficiency leads to glycogen storage disease IV (GSD IV), which clinically manifests widely in severity, ranging from mild adult-onset muscle weakness to neonatal death from liver failure (DiMauro and Lamperti, 2001; Moses and Parvari, 2002). GSD IV has also been reported in horses and cats. In horses, a lack of GBE (caused by a nonsense mutation) produced abnormal globular and crystalline polyglucan, and traces of glycogen, which exhibited iodine staining properties consistent with an unbranched polysaccharide (Valberg *et al*., 2001; Ward *et al*., 2004). The clinical manifestation of GSD IV in horses varies, and has been observed as mid-gestational abortion, stillbirth, or foals surviving from 1 to 18 weeks, with recurring hypoglycemic seizures, persistent weakness, cardiac abnormalities, and sudden death (Render *et al*., 1999; Valberg *et al*., 2001; Ward *et al*., 2004). Deficiency of

GBE activity in cats results in accumulation of abnormal amylopectin-like glycogen (which contains longer chain lengths and fewer branch points than normal glycogen) in skeletal, cardiac, and nervous tissues, and manifests in GSD IV disease, which leads to progressive neuromuscular and cardiac tissue degeneration (Fyfe *et al*., 1992, 2007).

Drawing on the conclusions of the many studies dealing with BE deficiency in various organisms, it is evident that the frequency and the positioning of α-1,6- branch points has a crucial effect on the physicochemical properties of starch and glycogen, and largely contributes to their respective biological functions.

1.2.2 Mode of Action and Properties of Branching Enzymes

BEs act upon glucan chains driving formation of α-1,6 branch points through cleavage of internal α-1,4 bonds, followed by transfer of the reducing ends of the cleaved unit to C6 position on an acceptor chain of either the original glucan chain (intra-chain transfer; Figure 1.2.2.1 A), or an adjacent one (inter-chain transfer; Figure 1.2.2.1 B) (Barker and Bourne, 1951; Devillers, 2003; Murakami *et al*., 2006). Studies of SBEs in potato (*Solanum tuberosum* L.) suggest a preference for inter-chain transfer, and that glucan chains in close proximity, as in a double-helical configuration, promote a more ideal environment for SBE catalytic activity (Borovsky *et al*., 1975; Borovsky *et al*., 1976; Borovsky *et al*., 1979). However, studies with bacterial GBEs suggest the possibility of both reactions occurring, although conditions required for favouring one reaction or the other are not known (Roussel *et al*., 2013; Takata *et al*., 2005). Although the precise branching mechanism, inter- vs. intramolecular branch transfer, has always been hindered by the difficulty to obtain well defined and monodisperse substrates, previous studies with *Rhodothermus obamensis* GBE for instance, showed that this GBE prefers an inter- over intramolecular branching mechanism (Roussel *et al*., 2013). Similarly, studies with *Anaerobranca gottschalkii* GBE showed that this enzyme performs interchain branching in the initial reaction phase (Thiemann *et al*., 2006). By contrast, the *Bacillus stearothermophilus* GBE was found to prefer intrachain branching, producing cyclic glucans from amylose and amylopectin (Takata *et al*., 1996a, 1996b).

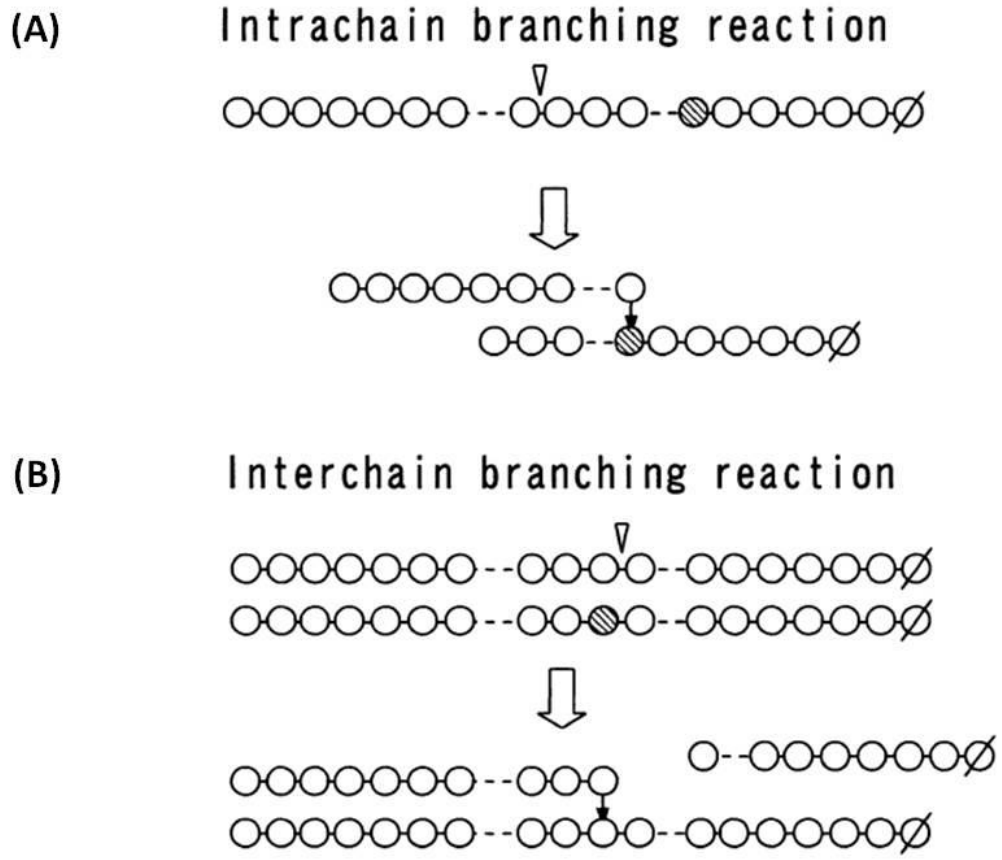

Figure 1.2.2.1 Schematic representation of (A) intra- or (B) inter-chain branching by BEs. Dashes, α-1,4-glucosidic linkage; black arrow, α-1,6-glucosidic linkage; open circles represent glucosyl residues; dashed circles represent glucosyl residues used as acceptors to synthesize α-1,6-linkages; circles with one line represent reducing terminal residues; open triangle, α-1,4-linkage cleaved by BE.

New non-reducing ends are generated with each new branch point addition by BE, creating a platform for reaction by GSs or SSs, which suggests a role for BE in determining polyglucan structure and influencing the amount of polyglucan synthesized, by modifying the rate of α-glucan synthase activity. Past studies have shown that in a number of cases the activities of plant and bacterial α-glucan SSs and GSs, respectively, were induced in the presence of BEs (Fox *et al*., 1973; Hawker *et al*., 1974). Earlier studies suggested that SSs and GSs were able to synthesize α-glucan in the absence of primer (*de novo* synthesis) (Hawker *et al*., 1974; Krisman, 1973). However, it was difficult to obtain SS/GS fractions completely devoid of glucan (traces of endogenous primer were usually present), thereby preventing unequivocal determination of an actual *de novo* synthesis of α-1,4 glucan. In regards to the latter, a more recent study claimed to have purified SS fractions free of any putative carbohydrate primers, which synthesized starch chains *de novo* in the absence of added glucan primers (Mukerjea and Robyt, 2012). Interestingly, parallel studies at the time of the primed versus unprimed GS or SS synthesis debate, showed that bacterial and plant synthase (GS or SS, respectively) preparations were contaminated with BE activity, which stimulated synthesis of α-glucan in absence of added primer (Fox *et al*., 1973; Lavintman and Cardini, 1973; Ozbun *et al*., 1972). It was therefore concluded that the BE stimulated the unprimed SS synthesis reaction by increasing the number of non-reducing ends in the growing glucan chain that can accept glucosyl residues from ADP-glucose (Hawker *et al*., 1974).

The BE enzyme class has a broad specificity with regard to substrate preferences, as well as the length of the glucan chain transferred during the branching process, and these preferences can be largely attributed to the structure of the carboxyl- (C-) and

amino-(NH2-) termini, respectively (see BE protein domains section 1.3) (Devillers *et al*., 2003; Kuriki *et al*., 1997; Van Der Maarel *et al*., 2003; Palomo *et al*., 2009; Takata *et al*., 1994). Amongst the prokaryotic GBEs a wide range of *α*-glucan chain transfer preferences has been observed (for details see Table 4.3.3 in Chapter 4). The number of glucose residues in a transferred glucan chain is also termed degree of polymerization (DP). For instance, previous studies have shown that for *E. coli* and *Aquifex aeolicus* (*A. aeolicus*; Aa) GBEs the preferred DP of chains transferred was between DP 10 and 14 for 40 - 50% of total glucans transferred during branching, while the preferred DP of transferred chains for *Rhodothermus obamensis* GBE was between DP 4 and 12 (Table 4.3.3 in Chapter 4) (Devillers *et al*., 2003; Guan *et al*., 1997; Van Der Maarel *et al*., 2003; Roussel *et al*., 2013). A GBE from *Thermococcus kodakaraensis* KOD1, a member of the GH57 family of enzymes (see section 1.3 for details), appeared to preferentially transfer glucan chains of DP 5 to 15, with transferred chain length optima at DP 6 and 11 (Murakami *et al*., 2006). Partially characterized GBEs from extremophilic species *Deinococcus geothermalis* (*D. geothermalis; Dg*) and *Deinococcus radiodurans* (*D. radiodurans*; Dr) also had a similar preference for transferred chain length, with most transferred chains being between DP 4 and 17 (Palomo *et al*., 2009). However, these two GBEs had a markedly different substrate preference; *D. geothermalis* GBE (DgGBE) preferred amylose, while *D. radiodurans* GBE (DrGBE) preferred amylopectin over amylose as substrate (Palomo *et al*., 2009). In contrast, the GBE from *Bacillus stearothermophilus*, with either amylose or amylopectin as substrate, preferentially transferred longer chains of DP ~22 – 35, with an average glucan chain length of DP ~15.5 (Takata *et al*., 1996a, 1996b, 2003). The *Anaerobranca gottschalkii* GBE also

displayed a broad transferred chain length range, and preferentially transferred short to medium glucan chains of DP 4 – 24 (Thiemann *et al*., 2006).

Another GBE of the GH57 family of enzymes form the thermophilic species *Thermus thermophilus* (*T. thermophilus*; Tt) was recently shown by Palomo *et al*. (2011) to have branching activity with amylose, but not with amylopectin as a substrate, and during branching of amylose it seemed to mainly transfer glucan chains of DP 4 to 16, with a strong preference for DP 6 chains. The substrate preference of *T. thermophilus* GBE (TtGBE) is similar to the *E. coli* GBE, which had a 4-fold increase in activity with amylose compared to amylopectin (Guan *et al*., 1997), as well as to that of *Rhodothermus obamensis* GBE, which showed six times higher specific activity with amylose compared to amylopectin (Shinohara *et al*., 2001), and to that of maize SBEI (mSBEI), which also prefers amylose over amylopectin as substrate (Guan *et al*., 1997). Interestingly, observations from studies with various bacterial GBEs (as stated above) seem to support the notion that prokaryotic GBEs, which tend to transfer on average short to medium glucan chains, also have greater specific activities with amylose compared to amylopectin (Guan *et al*., 1997; Palomo *et al*., 2011; Shinohara *et al*., 2001).

Similar to prokaryotic BEs, plant SBE isoforms also show variation in chain-length transfer characteristics, which in turn influences their glucan substrate preferences (Guan *et al*., 1995; Guan *et al*., 1997; Kuriki *et al*., 1997; Takeda *et al*.,1993). The two plant SBE classes, SBEI and SBEII, differ in their glucan chain length transfer propensity, with SBEI class showing a predisposition to transfer relatively long chains (at times up to DP 30), and a preference for amylose as a substrate (Guan *et al*., 1995, 1997; Kuriki *et al*., 1997; Takeda *et al*., 1993), while the SBEII class (differentiated into tissue

specific SBEIIa and SBEIIb isoforms in cereals) favours transfer of shorter chains (*e.g*. SBEIIb; DP 6 - 14) and has higher activity with amylopectin than amylose (Table 4.3.3 in Chapter 4) (Guan and Preiss, 1993). Various plant species SBEs have been documented to possess similar chain-length transfer preferences, namely in rice (*Oryza sativa* L.) (Nakamura *et al*., 2010), wheat (*Triticum aestivum* L.) (Morell *et al*., 1997), and potato (*Solanum tuberosum*) (Rydberg *et al*., 2001). Studies in plants suggest that the SBEIIb isoform has a more limited range of glucan transfer preference (DP 6-7) than SBEIIa (DP 6-15), and this may lead to the variation in starch fine structure as seen in different plants, which depends on the relative proportions of the two SBEII isoforms (Nakamura *et al*., 2010). In some cereals (*e.g*. mazie), SBEIIa is present ubiquitously throughout the plant tissues (Mizuno *et al*., 1993), while SBEIIb is mainly expressed in the endosperm, and has a key role in starch biosynthesis, contributing to the unique structure and properties of cereal starches (Blauth *et al*., 2001; Sawada *et al*., 2014). In maize endosperm, the level of SBEIIb is about fifty times higher than the level of SBEIIa (Gao *et al*., 1997). However, in other cereals, such as barley and wheat, SBEIIa and SBEIIb are expressed at similar levels in the endosperm (Regina *et al*., 2006, 2010; Sun *et al*., 1998). Although it is difficult to identify the exact function of specific SBE isozymes and their particular contributions to starch structure, due to the effect of other starch biosynthetic enzymes (*e.g*. SSs and starch debranching enzyme), many *in vitro* studies using purified BEs have allowed resolution of some key questions regarding SBE function, such as the chain-length preferences of SBEs, which provide information regarding the extent of BE contribution to the fine structure of amylopectin, a determinant of starch structural and functional properties (Kuriki *et al*., 1997; Nakamura *et al*., 2010; Sawada *et al*., 2014).

Drawing on the conclusions of results of recent biochemical studies with rice SBEs, it has been suggested that SBEI transfers longer chains, which may participate in linking multiple clusters of amylopectin, and medium size chains, which may compose the amylopectin amorphous lamellae, while SBEIIb transfers short chains, which may be at the interphase between the amorphous and the crystalline lamellae of amylopectin (Nakamura, 2002; Nakamura *et al*., 2010; Nishi *et al*., 2001; Satoh *et al*., 2003; Tanaka *et al*., 2004a). Therefore, through their unique chain-length transfer preferences, plant SBEs contribute to the fine structure of starch, playing a distinct role in the biosynthetic process.

1.3 Structure and Function Relationships of Branching Enzymes and Their Protein Domains

Following the publication of the first gene sequence of a GBE by Baecker *et al*. (1986), it was established that BEs and amylolytic enzymes are structurally closely related (Romeo *et al*., 1988). Based on later analyses of various BE gene sequences it was suggested that BEs belong to the α-amylase super-family of enzymes (also termed glycoside hydrolase 13 [GH13] family) (Stam *et al*., 2006). The GH13 family of enzymes comprises many hydrolytic enzymes which act on starch and glycogen, including α-amylases (E.C. 3.2.1.1), isoamylases (E.C. 3.2.1.41), pullulanases (E.C. 3.2.1.68), oligo-1,6-glucosidases (E.C. 3.2.1.10), and cyclodextrin glucanotransferases (E.C. 2.4.1.19) (Baba *et al*., 1991; Jespersen, *et al*., 1993; Jespersen *et al*., 1991; Nakajima *et al*.,1986; Romeo *et al*.,1988). The GH13 family group is divided into a number of subgroups and most GBEs, and all SBEs, belong to subfamily 8 (eukaryotic BEs), or subfamily 9 (prokaryotic BEs), albeit certain GBEs (*e.g*. *Thermococcus* sp., *Thermus* sp., and some

cyanobacteria sp.) have recently been shown to be more similar to members of the GH57 family of enzymes, which are structurally distinct from the GH13-type GBEs (Murakami *et al*., 2006; Palomo *et al*., 2011). The GH57 family of enzymes was defined in 1996 due to a number of α-amylase sequences that lacked the conserved regions characteristic of the GH13 family enzymes (Henrissat and Bairoch, 1996). The main features of enzymes belonging to the GH57 enzyme family are their high sequence diversity and their five conserved sequence regions, which include the two proposed catalytic residues, glutamic acid (Glu; a nucleophile) and aspartic acid (Asp; proton donor) (Zona *et al*., 2004). The suggested catalytic mechanism of the GH57 family enzymes is believed to be α-retaining; *i.e*., acting on α-glycosidic bonds and generating α-linked products (Zona *et al*., 2004). At present the GH57 family contains the following enzyme specificities; α-amylase (EC 3.2.1.1), amylopullulanase (EC 3.2.1.41), α-galactosidase (EC 3.2.1.22), 4-α-glucanotransferase (EC 2.4.1.25), and BE (EC 2.4.1.18) (Janeček, 2005; Murakami *et al*., 2006; Zona *et al*., 2004). The main structural differences between GH57 and GH13 enzyme families are in their catalytic barrel domains; the GH57 N-terminal catalytic domain is a $(\alpha/\beta)_7$ barrel in which seven central parallel β-strands are surrounded by seven α-helices (Imamura *et al*., 2003; Palomo *et al*., 2011), while the GH13 central catalytic domain is formed by eight parallel β-strands flanked by eight α-helices which fold into the $(\alpha/\beta)_8$ barrel, named the TIM-barrel (Janeček, 2005; Matsuura *et al*., 1984).

There are three major domains of secondary structure found in BEs of the GH13 family; the central (α/β) barrel catalytic domain (also termed A-domain), an amino-(NH2-) terminal domain, and a carboxyl-(C-) terminal domain (Abad *et al*., 2002; Buisson *et al*., 1987; MacGregor *et al*., 2001; Matsuura *et al*., 1984). Within the GH13

family of enzymes only isoamylase and BE share the structure of all three domains, and are the only family members that can bind saccharide glucans in the α-1,6 position (Abad *et al*., 2002). The central catalytic domain is conserved amongst the GH13 enzymes, while the amino- and carboxyl- domain sequences show sequence variability, which reflects different substrate preferences and chain length transfer properties (Kuriki *et al*., 1997). Recent studies have shown that the catalytic capacity of BEs is a function of the interaction of all three domains; the individual functionality contribution of each domain has been established through various studies including, amino acid sequence alignments (Romeo *et al*., 1988), X-ray crystallography (Katsuya *et al*., 1998), experiments with domain-mutants (Kuriki *et al*., 1997; Palomo *et al*., 2009), site directed mutagenesis (Libessart and Preiss, 1998; Mikkelsen *et al*., 2001; Palomo *et al*., 2009), and inhibitor binding studies (Binderup *et al*., 2000), as discussed below.

1.3.1 The Central Catalytic Domain

Based on bioinformatic analysis of the catalytic A-domain of GH13 family enzymes, specifically using hydrophobic cluster analysis and structure prediction, it was suggested that this domain consists of a highly symmetrical fold of eight parallel β-strands surrounded by eight α-helices, folded into $(\alpha/\beta)_8$-barrel structure (Brayer *et al*., 1995; Brzozowski and Davies, 1997; Kanai *et al*., 2001; Matsuura *et al*., 1984). The structure was later confirmed through X-ray crystallography of cyclodextrin glucanotransferases (Klein and Schulz, 1991), α-amylases (Boel *et al*., 1990; Buisson *et al*., 1987), isoamylase (Katsuya *et al*., 1998), and BE (Abad *et al*., 2002; Noguchi *et al*., 2011; Pal *et al*., 2010), showing some differences within the structural elements of the

α/β barrel configuration, specifically the absence of an α-helix number five, in the A-domains of GBE and isoamylase from certain species (Abad *et al*., 2002; Katsuya *et al*., 1998). Site directed-mutagenesis experiments have shed light on the identity and importance of specific conserved amino acid residues in the A-domain, which contains four conserved amino acid regions common to BEs and a number of other GH13 family enzymes, termed regions I to IV (Figure 1.3.1 and 1.3.3) (Baba *et al*., 1991; Svensson, 1994). For instance, studies with neopullulanase (E.C. 3.2.1.135), an enzyme that hydrolyzes α-1,4 (and α-1,6)-glycosidic linkages, and catalyzes transglycosylation to form α-1,4 (and α-1,6)-glycosidic linkages, showed through site-directed mutagenesis experiments that a number of amino acids are essential for all four reactions catalyzed by this enzyme (Kuriki *et al*., 1988; Kuriki *et al*., 1991; Takata *et al*., 1992). The catalytic mechanism of neopullulanase is thought to be similar to that of a number of GH13 family enzymes namely, BE, α-amylase, cyclodextrin glucanotransferase, and pullulanase/isoamylase. The amino acid similarities among the aforementioned enzymes of the GH13 family within regions I-IV of the central catalytic domain are shown in Figure 1.3.1 below.

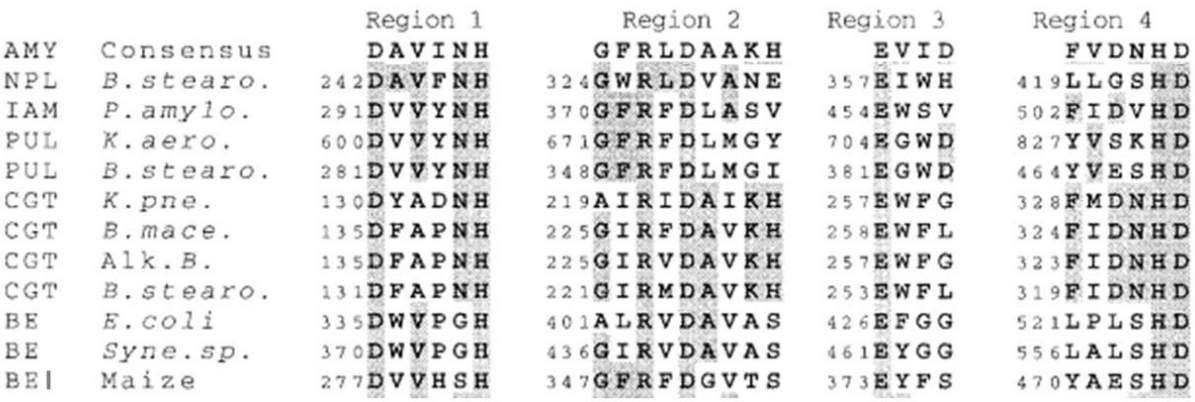

Figure 1.3.1 Amino acid conservation among a number of enzymes of the GH13 family within the highly conserved regions 1 – 4 of the central catalytic domain. The amino acids identical to the consensus sequence (first line) of α-amylase are shaded. AMY, α-amylase; NPL, neopullulanase; IAM, isoamylase; PUL, pullulanase; CGT, cyclodextrin glucanotransferase; BE, branching enzyme; BEI, starch branching enzyme I. The enzyme sources are abbreviated as follows: *B. stearo*., *Bacillus stearothermophilus*; *P. amylo*., *Pseudomonas amyloderamosa*; *K. aero*., *Klebsiella aerogenes*; *K. pne*., *Klebsiella pneumoniae*; *B. mace*., *Bacillus macerans*; Alk. *B*., alkalophilic *Bacillus*; *E. coli*; *Escherichia coli*; *Syne*. sp., *Synechococcus* sp. Figure reproduced from Takata *et al*., (1992).

In BE catalysis specifically, seven amino acids, conserved amongst the GH13 family enzymes, have been shown to be essential to the catalytic mechanism, including Asp^{335}, His^{340}, Arg^{403}, Asp^{405}, Glu^{458}, His^{525} and Asp^{526} (Figure 1.3.3; numbers correspond to *E. coli* sequence) (Abad *et al*., 2002). A number of critical residues, specifically Asp^{405} (region II; Figure 1.3.3), Glu^{458} (region III; Figure 1.3.3), and Asp^{526} (region IV; Figure 1.3.3) were identified as a catalytic triad through comparative sequence analysis, and their importance in BE function was later confirmed by site-directed mutagenesis on *E. coli* and *Bacillus stearothermophilus* GBEs, and maize SBEII (Cao and Preiss, 1996; Kuriki *et al*., 1996; Takata *et al*., 1994). Additionally, in maize SBEIIb (mSBEIIb), a conserved Arg^{384} residue (mSBEIIb numbering), was shown by

mutational analysis and chemical modification to be important for catalysis (Cao and Preiss, 1996; Libessart and Preiss, 1998), while two other conserved residues, His^{320} (mSBEIIb numbering; region I; Figure 1.3.3) and His^{508} (mSBEIIb numbering; region IV; Figure 1.3.3), were suggested to be vital for substrate binding (Funane *et al*., 1998).

A highly conserved tyrosine (Tyr) residue was identified in proximity to the seven conserved amino acids identified in the catalytic A-domain of BEs, and was found to be conserved in all GH13-family enzymes of both prokaryotic and eukaryotic species (Figure 1.3.3; region IV in eukaryotic BEs; or denoted with an asterisk in prokaryotic BEs) (MacGregor and Svensson, 1989). In a study by Matsui *et al*. (1994), using site directed-mutagenesis in *α*-amylase of *Saccharomycopsis* it was found that the enzyme possessing a mutation in the DNA sequence of this highly conserved tyrosine residue had an increase in the ratio of transglycosylation to hydrolysis, suggesting a role for the residue in catalysis. Mikkelsen *et al*. (2001) showed that when the tyrosine residue (Tyr^{300}) was replaced in *E. coli* GBE with a number of other amino acids (*e.g*. Ala, Asp, Leu, Ser, and Trp) the catalytic activity, measured using the quantitative branch-linkage assay, was drastically reduced and resulted in < 1% of wild-type activity. The same group also reported that loss of Tyr^{300} resulted in a more temperature sensitive *E. coli* GBE, with a lower relative activity at elevated temperatures compared to wild type (Mikkelsen *et al*., 2001). The Tyr^{300} residue (*E. coli* numbering) of GH13-family enzymes is thought to be involved in substrate binding, and superimposition analysis of known crystal structures of *α*-amylase, cyclodextrin glucanotransferase, isoamylase and GBE indicate that the Tyr^{300} residue is located near the active site in the *β*2-*α*2 loop of the $(\alpha/\beta)_8$-barrel structure of the A-domain in these enzymes (Katsuya *et al*., 1998). Tyr^{300} may play a role

in structurally stabilizing the catalytic domain through forming a hydrogen bond with Asp^{335} in region I of *E. coli* GBE, which in turn hydrogen bonds with Arg^{403} in region II of *E. coli* GBE, as was suggested by Mikkelsen *et al*. (2001).

Some members of the GH13 family of enzymes contain an extra domain (domain B) composed of loops supporting the elements of secondary structure, present in the $(\alpha/\beta)_8$-barrel between β-strand 3 and α-helix 3 (Abad *et al*., 2002). Although the exact function of domain B is yet to be determined, it is thought to contribute to functional and stability properties of the members of the α-amylase family of enzymes (Conrad *et al*., 1995; Juge *et al*., 1993). The loops of domain B are thought to account for the distinct properties and product specificity of members of the GH13 family of enzymes (Janecek, 1997). Domain B is approximately 60 residues long and is found in α-amylase, cyclodextrin glucanotransferase, and isoamylase, but not in BE (Abad *et al*., 2002; Janecek, 1997). In BE this loop is only 40 residues long, and is thought to be too short to account for the complete B domain structure, although it has not been conclusively determined yet (Abad *et al*., 2002; Baecker *et al*., 1986). Loop structure comparisons between members of the GH13 family showed that BEs tend to have shorter loops, exposing a more open cavity for binding of bulkier structures, such as the branched α-1,6-sugars (Abad *et al*., 2002). GBEs possess a more accessible sugar binding cavity as compared with equivalent structures of other enzymes of the GH13 family namely, isoamylase, cyclodextrin glucanotransferase, and amylase (Abad *et al*., 2002).

As described above, GH13-type BEs possess three domains of secondary structure, a central catalytic domain (domain A), an amino-terminal domain (section 1.3.2), and a carboxyl-terminal domain (section 1.3.3). The evidence from various studies

(described above) confirmed that the central catalytic A-domains of BEs, and some other GH13 family enzymes, share structural and functional similarities. Although the central A domain is deemed as the main catalytic portion of GH13 BEs (containing catalytic sites in region I-IV; Figure 1.3.3), studies suggest that the amino- and carboxy-termini may also contribute to the catalytic capacity of BEs, as well as play a role in substrate specificity and chain-length transfer preferences, potentially through the conformational changes (*e.g*. shielding hydrophobic residues of the catalytic domain) that the amino- and carboxy-termini confer onto the central region (Kuriki *et al*., 1997; MacGregor *et al*., 2001; Palomo *et al*., 2009).

The structure of the catalytic domain of GH57 enzymes adopts an irregular $(\alpha/\beta)_7$ barrel, referred to as a pseudo, or irregular TIM-barrel (Imamura et al., 2003; Zona et al., 2004). The catalytic center of GH57 enzymes contains the catalytic nucleophile (Glu) and the proton donor (Asp) in conserved regions III and IV, respectively (Imamura et al., 2003; Palomo et al., 2011; Zona et al., 2004). A previous study by Imamura *et al*. (2003) with 4-α-glucanotransferase of *Thermococcus litoralis* (*T. litoralis*) showed this enzyme is composed of two domains; the catalytic domain I, which contains the $(\alpha/\beta)_7$ barrel fold, and the C-terminal domain II, consisting entirely of β-strands, which adopts a twisted β-sandwich fold. Another study, which determined the crystal structure of a GH57 α-amylase (AmyC) from *Thermotoga maritima* (*T. maritima*), revealed this enzyme also contains the irregular TIM-barrel formed by seven β-strands and α-helices within its domain A, as characteristic of GH57 enzymes (Dickmanns et al., 2006). AmyC was also shown to have two additional, less conserved domains; domain B, which contains three α-helices and is a protrusion, or insertion, in the TIM-barrel of the catalytic domain after

its β-sheet 2, and domain C, a five-helix region at the C-terminus of the enzyme (Dickmanns et al., 2006). Interestingly, structure comparison revealed a high similarity between AmyC and *T. litoralis* 4-α-glucanotransferase only in the catalytic domain TIM-barrel structure, indicating a similar structural arrangement of the catalytically active residues (Dickmanns et al., 2006). Curiously, AmyC was found to display the higherst structural similarity (~31% sequence identity) with the GBE of *T. thermophilus* (TtGBE) (Dickmanns et al., 2006; Palomo et al., 2011). Similarly to AmyC of *T. maritima*, TtGBE also consists of three domains. The central domain A, which contains the irregular TIM-barrel structure with the characteristic sevenfold (β-sheet/α-helix) motif, and a few additional secondary structure elements compared to *T. maritima* AmyC (Palomo et al., 2011). Domain B of TtGBE also has three α-helices, and is an insertion into domain A after β2, while domain C is composed of a five-helix region, with four tightly bundled α-helices (Palomo et al., 2011), similarly to the *T. maritima* AmyC structure.

An interesting feature of GH57 members is their wide diversity in sequence length, with some enzymes being less than 400 residues in length, while other enzymes being composed of over 1500 resdiues. Therefore, some GH57 members, because of their short sequences, may not contain sequence features like the C-terminal domain. For example, modelling 219 N-terminal resdiues of the total 364-amino acid α-galactosidase of *Pyrococcus furiosus* against the catalytic domain structure of *T. litoralis* 4-α-glucanotransferase, showed sequence homology of 34%, with the catalytic residues of the α-galactosidase interspersed within the modelled region (van Lieshout et al., 2003). The remaining, non-modelled residues, were not calssified as forming part of the C-terminal domain characteristic of GH57 members. Some members of the GH57 family on the

other hand, are extra-long and often contain more than 1500 amino acid residues, and have been shown to contain additional domains. For instance, primary structure analysis of *Thermococcus hydrothermalis* amylopullulanase, consisiting of 1,339 residues, revealed three regions corresponding to a SLH-like domain, a domain bearing S-layer (bacterial surface layer protein motif) homology-like motifs, a threonine-rich region, and a putative transmembrane domain (Erra-Pujada et al., 1999). Interestingly, presence of a SLH motif-bearing domain seems to be restricted only to amylopullulanases of the GH57 family (Zona and Janeček, 2005).

Prior to the availability of the first three-dimensional structure of a GH57 member (*T. litoralis* 4-α-glucanotransferase), efforts were made to join the GH57 family with the main α-amylase family, GH13. However, it was quickly realized that although members of the GH13 and GH57 families employ the same retaining reaction mechanism, fundamental differences between the families are found not only in the differences in the catalytic domain [$(\alpha/\beta)_8$-fold vs. (α/β)7-fold], but also in the differences in the catalytic machineries and conserved sequence regions (Erra-Pujada et al., 1999; Imamura et al., 2003; Zona et al., 2004).

1.3.2 The Amino (NH_2-) Terminal Domain

The BE amino-(NH_2-) terminal domain, common to GH13-family enzymes, is involved in cleaving or forming endo-α-1,6-linkages, such as in pullulanase and isoamylase, although the similarity between the amino-terminal domains in enzymes of GH13-family is low (~20 – 40%) (Jespersen *et al*., 1991). NH_2 –terminal domains of enzymes involved in carbohydrate binding share a common module classified as a family

48 carbohydrate-binding-module (CBM48; Figure 1.3.3) (Koay *et al*., 2007). The CBM48 has the capacity to bind various polyglucans such as, glycogen, cyclodextrin, and various other oligosaccharides (*e.g*. maltoheptaose) (Koay *et al*., 2007; McBride *et al*., 2009; Polekhina *et al*., 2005), and evidence suggest it is essential for glucan binding ability of the enzyme it is present in (Lawson *et al*., 1994). Based on amino acid sequence analysis, there are two major groups into which prokaryotic GBEs are classified, depending on the length of their respective amino-termini (Hilden *et al*., 2000). The first (group 1), and largest group (includes *E. coli*), includes enzymes with NH_2 –terminal domains which contain a module of approximately 150 amino acids encompassing the CBM48, termed the N2 module, which is normally preceded by the N1 module of approximately 100-150 residues (Hilden *et al*., 2000). The N1 module is thought to have been derived from a DNA duplication of the N2 module (Leggio *et al*., 2002). GBEs of prokaryotic species such as *Bacillus* sp., and *Anaerobranca* sp. are classified into group 2, which contain only the N2 module and lack the N1 module extension (Hilden *et al*., 2000). Further investigation into the role of the N1 module using the *E. coli* GBE to produce sequential amino-terminal truncations, revealed that progressive shortening of the N1 module led to an increase in the length of the transferred chains compared to the wild-type GBE (Devillers *et al*., 2003).

The functions of the NH_2 domain of BEs have been examined through truncation and domain-swapping studies with prokaryotic GBEs and plant SBEs. For instance, in one study a 112 amino acid truncation in the *E. coli* GBE N1 module resulted in reduced catalytic activity (~40%) and altered branching pattern, with the truncated GBE transferring fewer short chains of DP 5 - 11, and more chains longer than DP 12, as

compared to the wild-type GBE (Binderup *et al*., 2000; Binderup at al., 2002). Similarly, a later study of sequential deletions of the amino-terminus of *E. coli* GBE, showed that progressive shortening of the N1 module led the enzyme to transfer gradually longer glucan chains (Devillers *et al*., 2003). It has been suggested that one of the roles of the amino-terminal domain is to anchor the glucan substrate during cleavage and transfer of the α-1,4-glucan chains (Devillers *et al*., 2003). Studies with chimeric *Deinococcus* sp. GBEs showed altered substrate specificity as compared to the wild-type counterparts, suggesting that N2 modules of NH_2-domains influence substrate specificity and the product branching pattern (Palomo *et al*., 2009). It was also proposed that the proximity of CBM48 to sugar binding sites in the active cavity of A-domain plays a role in determining the average lengths of transferred side chains (Palomo *et al*., 2009). Plant SBE isoforms also exhibit various biochemical properties and different preferences with regard to chain-length transfer (Guan *et al*., 1997; Kuriki *et al*., 1997; Takeda *et al*., 1993). A study with a SBE chimeric enzyme of low catalytic activity, which was comprised of the amino-terminus of SBEI, and the central catalytic domain as well as the carboxy-terminus of SBEIIb, revealed similar transfer preferences to SBEI, which normally transfers longer glucan chains of DP 11 - 12 (as opposed to SBEIIb which transfers shorter α-glucan chains) (Kuriki *et al*., 1997). Considering that the only part of SBEI present in the chimeric enzyme was its NH_2-domain (Kuriki *et al*., 1997), the data is in agreement with other studies with prokaryotic GBEs, supporting the notion that the NH_2-terminus of SBEs and GBEs plays a role in chain transfer, specifically in determining the size of polyglucan chain transferred.

1.3.3 The Carboxy-Terminal Domain

The chimeric mutants of maize SBEs used to determine the role of the NH_2-domain were also employed to elucidate the role of the carboxy-terminus in BEs. A hybrid maize SBE enzyme was created in which the 229 amino acid residues of the C-terminal domain of SBEIIb were substituted by the corresponding 284 residues of SBEI C-terminus (Kuriki *et al*., 1997). The chimeric enzyme, termed mBE II-I, was more than three-fold more active than the wild-type SBEI and SBEIIb, showing a substrate preference, like that of SBEI, for amylose over amylopectin (Kuriki *et al*., 1997). The mBE II-I chimeric enzyme was shown, through chain transfer experiments, to preferentially transfer shorter chains (DP 6), a preference similar to that of the wild-type SBEIIb enzyme (Kuriki *et al*., 1997). The conclusions from these studies suggested that the C-terminus of SBE is involved in determining enzyme substrate preference and catalytic capacity, and have since been confirmed by other studies using recombinant SBEs form various plant species (Ito *et al*., 2004). The suggested role of C-terminus involvement in catalytic activity was further examined using a truncated version of mBE II-I, in which a total of 145 residues were deleted from the C-terminus of the hybrid enzyme, causing a loss of catalytic activity (Hong and Preiss, 2000). However, loss of catalytic activity was partially rescued (to 25% of the mBE II-I activity), by replacement of some of the deleted residues with 79 amino acid residues from the C-terminus of SBEIIb, without changing substrate preference (Hong and Preiss, 2000). Based on the results from studies of truncated C-termini of chimeric maize SBE enzymes, it was suggested that the C-terminal region is required for catalytic activity, specifically residues Leu^{649} to $Asp^{735}$of mBE II-I, and another C-terminal region, specifically residues Gln^{510}

to Asp^{648} of mBE II-I (which correspond to residues Gln^{476} to Asp^{614} of SBEI) are required in determination of substrate specificity (Hong and Preiss, 2000).

The suggested function of the C-terminus in substrate preference and catalytic activity, and the function of N-terminus in dictating the length of glucan transferred, are consistent with data obtained from experiments with chimeric SBE enzymes. These data also provide evidence that the conserved central catalytic domain of BEs is not the only factor responsible for catalytic activity. In addition to their roles in chain length transfer preference, and substrate binding, the N- and C-termini may also control catalytic activity, potentially through modulating conformational changes induced in the central catalytic A-domain by the two termini, or *via* some vital catalytic residues found in the two termini.

Enzyme		Prokaryote-specific Region		Region I		Region II		Region III		Region IV
Prokaryote						•		■		▼
Bacillus subtilis α-amylase	100	YWL*YQP	138	DA V I NH	213	GFRFDAAKH	245	FQYGE I LQ	302	LVTWVESHD
Bacillus cereus oligo-1,6-glucosidase	9	SVV *YQ I	98	DL VV NH	194	GFRMDVINM	251	MTVGEMPG	321	NSLYWNNHD
Escherichia coli GBE	297	SWG*YQP	335	DWVPGH	401	ALRVDAVAS	454	VTMAEEST	518	NF VLPLSHD
Deinococcus radiodurans GBE	201	SWG*YQV	237	DWVPGH	305	GLRVDAVAS	356	LM IAEEST	419	NYVLAI SHD
Eukaryote										
Maize SBEI			341	DVVHSH	411	GFRFDGVTS	466	TVVAEDVS	531	C I AYAESHD
Maize SBEIIb			376	DVVHSH	443	GFRFDGVTS	498	VT IGEDVS	562	CVTYAESHD
Rice SBEI (RBE1)			335	DVVHSH	405	GFRFDGVTS	460	T I VAEDVS	525	C I AYAESHD
Rice SBEIIb (RBE3)			402	DVVHSH	469	GFRFDGVTS	524	I T I GEDVS	588	CVTYAESHD
Arabidopsis thaliana SBE2.1			415	DI VHSH	482	GFRFDGVTS	537	I VVGEDVS	601	CVVYAESHD
Arabidopsis thaliana SBE2.2			380	DI VHSH	447	GFRFDGVTS	502	I VVGEDVS	566	C I SYAESHD

Figure 1.3.3 Organization of functional domains from prokaryotic and eukaryotic BEs showing the amino-(NH_2) terminal domain (grey), the catalytic A-domain (black), and the carboxy-(C) terminal domain (white). The majority of glycogen branching enzymes (GBEs), and all starch branching enzymes (SBEs), are classed as group 1 BEs, with the NH_2-terminus consisting of both N1 and N2 modules, while a small group of prokaryotes (group 2) possess only the N2 module. All BEs possess a family 48 carbohydrate-binding-module (CBM48) within the N2 module. Within the catalytic A-domain there are four highly conserved regions (I to IV) common to the glycoside hydrolase family 13 (GH13) enzymes. The primary sequences of the conserved regions from a number of prokaryotes and eukaryotes are compared in the table below the domain organization diagram. Key: *****, conserved tyrosine residue within the prokaryotic-specific region, but also conserved in al other GH13 enzymes, including eukaryotic BEs (see region IV); ●, putative catalytic nucleophile; ■, putative acid/base catalyst; ▼, putative transition state stabilizer. The putative functional amino acid residues were assigned by MacGregor *et al*., 2001. Figure and description reproduced from (Tetlow, 2012).

1.4 Post-Harvest Starch Modifications and Applications

Starch is a major dietary constituent of the human diet, and starch-containing crops form a large proportion of the food consumed by the world's population. Aside from consuming starches as a direct food source, starch is also harvested and used directly for industrial applications, or first chemically, physically, and/or enzymatically modified into a variety of products (or as modified starches prior to further use). Depending on its botanic source, starch contains approximately 20 - 25% amylose, a virtually linear α-1,4 polyglucan, and approximately 75 - 80% amylopectin, an α-1,4 polyglucan with recurring α-1,6 branch points (Buléon *et al*., 1998a; Iglesias and Preiss, 1992; Zeeman *et al*., 2010). While the starch granule is insoluble in cold water, heating starch causes it to swell (a process termed gelatinization) and the granule to eventually rupture and break, which leads to leaching out of amylose and formation of a highly viscous slurry (van der Maarel and Leemhuis, 2013; Manners and Matheson, 1981; Vamadevan and Bertoft, 2015). Subsequent cooling of the colloidal starch dispersion results in thick gel formation, a process termed retrogradation. In the process of retrogradation, starch goes from a dissolved and a dissociated polyglucan state to an associated state, wherein the glucan chains within starch attempt to realign and recrystallize (Gidley and Bulpin, 1989; Ring *et al*., 1987). Retrogradation is primarily caused by the amylose component of starch, due to its long polyglucan chains which are more prone to self-assemble, while amylopectin, due to its branched structure and higher solubility is less prone to retrogradation (Gidley and Bulpin, 1989; Ring *et al*., 1987).

In its native form starch has limited uses in the industry (particularly in non-food applications), due to its tendency to retrograde and form undesirable gels, which may

interfere with industrial processing (Kaur *et al*., 2012; van der Maarel and Leemhuis, 2013; Miyazaki *et al*., 2006). Modifications of starch are employed to overcome shortcomings of native starches and increase their usefulness for various industrial applications (Kaur *et al*., 2012; Wurzburg, 1986). Certain starch modifications can combat retrogradation issues, improve paste clarity, sheen and gel texture, and improve film formation and adhesion properties (Bemiller, 1997; Miyazaki *et al*., 2006). Modification of starches brought on an expansion in new processing technologies, and subsequently spurred new market trends (Murphy, 2000). The modified starch derivatives, with new functional and added value properties, have been tailored to create a competitive advantage in emerging new products, thus expanding the market, improving recipes and product aesthetics, lowering production costs, ensuring product consistency and lengthening product shelf-life (Murphy, 2000).

A number of commonly employed starch modification methods exist to improve starch functionalities for various industrial applications; these include, chemical, physical, and enzymatic modifications, and *in planta* genetic modification of starch, and these are outlined below (Bemiller, 1997; Jobling, 2004; Tharanathan, 2005).

1.4.1 Chemical Modification of Starch

Chemical modification of starch is the most common method for improving starch functional properties for food and non-food industrial applications. Chemical modification of starch dates back as far as the 1800s, when starch saccharification was discovered and acid-modified starch was pioneered (Tomasik and Schilling, 2004; Völksen, 1949).

Starch is chemically modified by the introduction of functional groups (*e.g*. hydrophobic, acetylated, ionic groups) into the starch molecule, which results in markedly altered physicochemical properties, imparting changes in retrogradation behaviour, gelatinization capacity, pasting properties and improving freeze-thaw and cold storage stabilities (Alcázar-Alay and Meireles, 2015; Neelam *et al*., 2012; Singh *et al*., 2007). Chemical modification is typically achieved through derivatization reactions, such as etherification, esterification, and crosslinking, or through breakdown reactions by oxidation and hydrolysis (Alcázar-Alay and Meireles, 2015; Kaur *et al*., 2012). Derivatization reactions typically produce cationic starches by esterification and etherification with compounds, amongst others, such as, 2,3-epoxypropyl trimethyl ammonium chloride, and dimethyl/diethyl sulfates, or with food grade compounds such as propylene oxide (Alcázar-Alay and Meireles, 2015; Korma *et al*., 2016). These chemical modifications can disrupt the inter- and intra-molecular hydrogen bonds, weakening the granular starch structure and increasing motional freedom, thereby reducing the amount of energy needed to solubilize the starch in water (Berski *et al*., 2011; Korma *et al*., 2016). Cationic starches are commonly used as additives in textile products, paper, and cosmetics (Alcázar-Alay and Meireles, 2015; Korma *et al*., 2016). Starches modified through esterification or etherification, like hydroxypropyl starches, are widely used in food products, providing viscosity and freeze-thaw stability (Korma *et al*., 2016; Zhang, 2001).

Starch Modification by Cross-linking

Cross-linking treatment of starch reinforces hydrogen bonds in the granule with chemical bonds, creating inter- and intra-molecular connections, thereby covalently interconnecting linear and/or branched starch glucan chains (Singh *et al*., 2007). Common cross-linking reagents used on native starch include, sodium trimetaphosphate, sodium tripolyphosphate, epichlorohydrin, and phosphoryl chloride, among others (Woo and Seib, 2002). This type of chemical modification forms a three-dimensional network and increases the rigidity of the starch polymer, strengthening and stabilizing the granule (Qiu *et al*., 2013; Singh *et al*., 2007). Cross-linking is known to affect starch properties such as paste clarity, swelling capacity, and retrogradation (reduced), and it also minimizes granule rupture (*e.g*. under cooking conditions) and loss of viscosity (Korma *et al*., 2016; Qiu *et al*., 2013; Singh *et al*., 2007). Cross-linked starches find many uses in the food industry, for example, in formulations of frozen products, canned food products, and as thickening and stabilizing agents, imparting resistance to processing conditions such as temperature, acidity, and shear (Alcázar-Alay and Meireles, 2015; Neelam *et al*., 2012).

Starch Modification by Oxidation

Starch modification through oxidation has been in practice since the early 1800s, and is one of the most popular modification methods (Tomasik and Schilling, 2004). Oxidized starch is produced by reaction with an oxidizing agent, under specific reaction conditions (*e.g*. temperature and pH), wherein the hydroxyl groups on starch molecules are first oxidized to carbonyl groups, and then to carboxyl groups (Rutenberg and

Solarek, 1984; Tomasik and Schilling, 2004). In the process, glucan intermolecular bonds loosen and the glucan chains (including the long chains) within starch undergo depolymerisation, resulting in lower dispersion viscosity, better water solubility, and reduced retrogradation rate compared to native unmodified starch (Dias *et al*., 2011; Kuakpetoon and Wang, 2001; Lewicka *et al*., 2015; Rutenberg and Solarek, 1984).

Typically, the reactive oxidants used for starch oxidation include, hydrogen peroxide, hypochlorite, periodate, permanganate, dichromate, ambient oxygen, and ozone, among others (Sánchez-Rivera *et al*., 2005; Sandhu *et al*., 2008; Tomasik and Schilling, 2004; Wang and Wang, 2003). Hypochlorite oxidation is the most common method for production of oxidised starches in the industry; however, a large amount of by-products in the form of salts (often as much as desired product) is produced during the reaction (Kaur *et al*., 2012). Although hydrogen peroxide creates no harmful by-products and is considered more environmentally friendly, as it inevitably decomposes to oxygen and water, it is used to a much lesser extent, as the oxidation of starch by hydrogen peroxide requires a long reaction time, high temperature and pH level (Dias *et al*., 2011). Ozone is a clean and more powerful oxidant than hypochlorite and hydrogen peroxide, and unlike hypochlorite, does not result in harmful by-products, and thus is considered as a safer starch modification agent for both consumers and the environment (Kaur *et al*., 2012; Klein *et al*., 2014; Lawal *et al*., 2005).

The main uses of oxidized starches are in the paper and textile industry, as they improve the mechanical and film-forming properties of paper and textiles by binding the components together (*e. g*. fibers, pigments, and fillers) (Tolvanen *et al*., 2009; Tomasik and Schilling, 2004). Due to their low viscosity, high stability, clarity, and binding

properties, oxidized starches also find uses in the food industry, for instance, in food coatings, sealing agents (*e.g*. in confectionery), and as emulsifiers and thickening agents (Kaur *et al*., 2012; Lawal *et al*., 2005).

Starch Modification by Acid Hydrolysis

One of the oldest methods of chemical modification of starch is by acid hydrolysis, dating back to the 1800s (Tomasik and Schilling, 2004; Völksen, 1949). The historical discovery of starch saccharification by acids paved the way for what became the most practiced method of starch modification before the advent of enzymatic hydrolysis methods (Alcázar-Alay and Meireles, 2015; Tomasik and Schilling, 2004; Völksen, 1949). The mechanism of acid hydrolysis involves the attack of the glycosidic oxygen atom by the hydroxonium ion, which hydrolyzes the glycosidic bond and produces random breaks in the α-1,4- and α-1,6-glycosidic linkages of glucan chains, shortening the starch polyglucan chains (Hoover, 2000; Tomasik and Schilling, 2004).

The resulting polyglucan from a prolonged treatment of native starch granules with strong aqueous acid is referred to as the Naegeli amylodextrin, which is an insoluble residue that maintained much of the starch granule form and crystallinity (Watanabe and French, 1980). Initially, the hydrolysis occurs on the surface of the starch granule, it then gradually enters the inner region of the granule. Studies have shown that in the earlier stages of acid hydrolysis the acid acts on the amorphous regions of granules, and in the later stages the hydrolysis proceeds into the crystalline region (Alcázar-Alay and Meireles, 2015; Tomasik and Schilling, 2004; Wang and Wang, 2001). Modification of starch by acid hydrolysis changes the physicochemical properties of starch, albeit without

destroying its granule structure, and increases solubility and gel strength while decreasing the viscosity due to the depolymerization of the glucans within starch (Hoover, 2000; Lawal *et al*., 2005; Wang and Wang, 2001).

Acid-modified starches can be used at a higher solids concentration, which is of importance in many industrial processes, and thus find uses in the food, paper, textile, and pharmaceutical industries (*e.g*. tableting and cosmetic formulations) (Lawal *et al*., 2005; Wang and Wang, 2001; Wurzburg, 1986). For instance, in the food industry acid-modified starches are used in gum and jelly to provide these products with shorter texture (*i.e*. tender, "pudding-like", spreadable) and flexible properties (Hoover, 2000; Zallie, 1988). Acid hydrolyzed starch is also utilized in the textile industry, for example, as a warp (lengthwise threads within yarn) sizing agent (protective substance) for improving yarn strength and abrasion resistance in the weaving process (Hoover, 2000; Wurzburg, 1986).

The main reason starch is chemically modified before its commercial use is to effectively truncate the long glucan chains of the polymer to reduce the high viscosity of native unmodified starch dispersions, and thereby increase and maximize the volume (solids concentration) of starch that can be processed in technical applications. Through chemical modifications, significant changes in starch behavior, gelatinization capacity, retrogradation and paste properties are generated. Food and non-food industries therefore expand starch properties and improve them through a myriad of chemical modifications as discussed above.

1.4.2 Physical Modifications of Starch

Physical modifications of starches involve physical treatments that do not typically result in modification of the glucosyl units within starch polyglucans, but rather produce changes only in the packing arrangements of amylose and amylopectin polymer molecules within granules, resulting in changes in the overall structure of the starch granule (BeMiller and Huber, 2015). Starch properties are greatly impacted by physical modification, and manifest in changes in the attributes of its pastes and gels, and even its digestibility (Miyazaki *et al*., 2006). Physical modification techniques are simple and inexpensive, and do not require chemical or biological agents, and thus are preferred, especially when the product is intended for human consumption (does not require labelling as modified starch) (BeMiller and Huber, 2015). Currently, the most popular methods of starch physical modification are thermal treatments; however, different combinations of temperature, moisture, pressure, shear, and freeze-thawing are also commonly used (Alcázar-Alay and Meireles, 2015; Ashogbon and Akintayo, 2014; BeMiller and Huber, 2015; Miyazaki *et al*., 2006).

Pre-gelatinization methods involve a cooking process to a point of complete starch gelatinization and a subsequent (or simultaneous) drying process (*e.g*. drum drying, spray drying, and extrusion cooking), resulting in complete destruction of the granular structure (depolymerisation of starch components) (Ashogbon and Akintayo, 2014). Some principal properties of pre-gelatinized starches include an increase in swelling capacity, solubility and improved cold water dispersion properties. Such starches are often used as thickeners in instant food products, such as baby food, soups, and desserts, due to their ability to form pastes and easily dissolve in cold water (Alcázar-

Alay and Meireles, 2015; Ashogbon and Akintayo, 2014; Nakorn *et al*., 2009). In contrast to pre-gelatinization methods, hydrothermal processes involve changes in the physical and chemical properties of the starch without destroying the granule structure (Zavareze and Dias, 2011). Hydrothermal modifications of starch are differentiated into two main methods; annealing (ANN) and heat-moisture treatment (HMT) (Collado and Corke, 1999). The ANN treatment of starch is a physical modification wherein starch is treated in the presence of heat and excess water, at temperatures below the onset of gelatinization, resulting in a physical reorganization of the starch granule and increased molecular mobility (Collado and Corke, 1999; Jacobs and Delcour, 1998; Tester and Debon, 2000). HMT, on the other hand, involves the thermal agitation of starch (below gelatinization temp.) in the presence of a limited amount of water, resulting in reduced starch granular swelling and viscosity, and increased thermal stability (Collado and Corke, 1999; Jacobs and Delcour, 1998). Hydrothermally modified starches have improved thermal stability (Jayakody and Hoover, 2008), decreased granular swelling and amylose leaching (Zhou *et al*., 2003), and increased heat and shear stability (Hormdok and Noomhorm, 2007), and are utilized in canned and frozen food industries, as well as in noodle manufacturing, and as additives to enhance resistant starch levels (Jayakody and Hoover, 2008).

Non-thermal physical modifications of starch are an alternative to traditional methods, in that heat is not intentionally applied in the process. These modifications have been shown to alter the physicochemical properties of starch, and in applications in the food industry they also minimized the loss of taste, color, texture, and nutrients (Ashogbon and Akintayo, 2014). High-pressure technology involves the use of pressure

ranging from 400 to 900 MPa (Stute *et al*., 1996). Generally, high-pressure destroys non-covalent bonds and leads to restricted starch swelling-capacity and consequently reduced paste viscosity (Hu *et al*., 2011; Stolt *et al*., 2000; Stute *et al*., 1996). High-pressure modified starches have been used in the food industry for improving shelf-life of foods, as well as fat-substitute components (Pei-Ling *et al*., 2010; Stute *et al*., 1996).

Mechanical methods (referred to as mechanical activation) of physical modification of starch, such as the use of friction, collision, impingement, and shear, alter the crystalline structures and properties of the starch granule (Che *et al*., 2007; Huang *et al*., 2007; Kaur *et al*., 2012). In the process, large particles crush to form smaller particles, while the tiny particles aggregate and form large particles. The resultant starch has decreased gelatinization temperature and viscosity, and improved cold-water solubility (Che *et al*., 2007; Huang *et al*., 2007; Kaur *et al*., 2012). Mechanical activation of starch as a modification method is simple, accompanied by minimal environmental impact, and subject to convenient operation, compared to other starch modification techniques (Alcázar-Alay and Meireles, 2015; Kaur *et al*., 2012).

Freeze-thaw is a physical treatment often employed in order to modify starch structural and functional characteristics (Szymońska *et al*., 2003; Tao *et al*., 2015). Previous studies have shown that freeze-thawing disrupts the crystalline order of the starch granule (weakening of double helices in amylopectin), and influences the textural and gelatinization characteristics of starch, resulting in gels, formed from frozen starch, that are more viscous and less sensitive to retrogradation (Szymońska *et al*., 2000, 2003). Freeze-thaw treated starches, amongst other applications, are used as gelling agents and in preparation of resistant starch for dietary benefits (Jeong and Lim, 2003; Szymońska *et*

al., 2003; Tao *et al*., 2015). The benefit of this method, as with other starch physical modification methods, is that no chemical agents are involved, thus incurring minimal environmental and safety concerns.

1.4.3 Enzymatic Modifications of Starch

In the past decades, with new emerging commercial enzymes, there has been a shift in starch modification practices from the use of common chemical methods to the use of starch-acting enzymes, where possible. One of the original applications of enzymatic starch modification was for the production of glucose syrup or high fructose corn syrup (Crabb and Mitchinson, 1997; Crabb and Shetty, 1999). In the early 1900s, starch was hydrolyzed into glucose syrup using acid treatment (Völksen, 1949). However, in recent decades the acid hydrolysis method for the production of glucose syrup has been replaced by enzymatic treatment, using starch-converting enzymes of the α-amylase family (Table 1.4.3). Starch-acting enzymes, besides their use in starch hydrolysis/liquification, are also used in other industrial applications, such as for the preparation of viscous, stable starch solutions used for the warp sizing of textile fibers or for paper sizing and coating, for the clarification of haze formed in beer or fruit juices, in preparation of digestive aids or the pre-treatment of animal feed to improve digestibility, in detergent formulations, and even as anti-staling agents (Table 1.4.3) (van der Maarel and Leemhuis, 2013; van der Maarel *et al*., 2002; de Souza and de Oliveira Magalhães, 2010). There is a number of commonly used starch-acting enzymes for the modification of starch in large-scale industrial applications and these include, but not limited to, α-amylase (EC 3.2.1.1), pullulanase (EC 3.2.1.41), cyclodextrin glycosyltransferase

(CGTase; EC 2.4.1.19), *β*-amylase (EC 3.2.1.2), and amyloglucosidase or glucoamylase (EC 3.2.1.3). Starch-acting enzymes that are not yet used in large-scale industrial applications include amylomaltase (4-*α*-glucanotransferase; EC 2.4.1.25) and BE (EC 2.4.1.18).

Table 1.4.3 Some Enzymes of the *α*-Amylase Family and a Number of their Industrial Applications and Products.

Enzyme	Application	Reference
α-Amylase	Starch liquification Starch saccharification Laundry detergents and cleaners Baking and brewing Reduction of haze formation in beer and juices Digestibility of animal feed Textile Pulp and paper	Gupta *et al*., 2003 de Souza and de Oliveira Magalhães, 2010
Pullulnase *Isoamylase* *Amyloglucosidase* *β-Amylase*	Starch saccharification (maltose, high maltose syrup, glucose, high glucose syrup)	van der Maarel *et al*., 2002
Cyclodextrin glycosyltransferase	Cyclodextrin production (mask undesirable flavours, extraction of cholesterol from foods)	Szente and Szejtli, 2004
Amylomaltase	Thermoreversible starch gels (gelling or viscosifying agent; plant alternative to gelatin) Cycloamylose (drug encapsulation, artificial chaperones for heterologously produced proteins)	van der Maarel and Leemhuis, 2013 Tomono *et al*., 2002 Machida *et al*., 2000
Branching Enzyme	Cyclic cluster dextrin (sport drink ingredient) Slow digestible starch	Takata *et al*., 1997 Deremaux *et al*., 2007

The action of *α*-amylases cleaves the *α*-1,4 glycosidic bonds that are present in the inner part of the amylose or amylopectin glucan chains, resulting in end products consisting of oligosaccharides with varying lengths, and *α*-limit dextrins, which

constitute branched oligosaccharides (van der Maarel *et al*., 2002). α-Amylases have the most wide-spread use in industrial applications, and besides their common use in liquefaction or saccharification of starch, they are also widely used in the food and non-food industries, like textile, pulp and paper, and detergent industries (Table 1.4.3) (van der Maarel *et al*., 2002; de Souza and de Oliveira Magalhães, 2010). In the food industry, α-amylases are extensively utilized in the processed-food industry such as baking, brewing, preparation of digestive aids, production of cakes, fruit juices, and starch syrups (Couto and Sanromán, 2006; van der Maarel *et al*., 2002). The most common sources of α-amylases utilized in the industry are bacterial, such as the *Bacillus* genus (*e.g*. *Bacillus subtilis* and *Bacillus amyloliquefaciens*), or fungal, mainly *Aspergillus* species (Gupta *et al*., 2003; de Souza and de Oliveira Magalhães, 2010).

Pullulanase is a starch-modifying enzyme that hydrolyzes α-1,6 glycosidic bonds, and is often utilized in the conversion of dextrin to high glucose or high maltose syrup, in the starch saccharification process (Table 1.4.3) (van der Maarel *et al*., 2002). Additionally, pullulanase is often used in combination with α-amylase to help reduce the gummyness associated with α-amylase-treated bakery products. The gummyness typically arises due to the production of branched maltodextrins resulting from α-amylase action, and can be alleviated by the use of pullulanase to hydrolyze the branched maltodextrins (Carroll *et al*., 1985; van der Maarel *et al*., 2002).

CGTases produce cyclic oligosaccharides and highly-branched high molecular weight dextrins. Thermostable CGTases are utilized in the food industry for liquefaction of starch to cyclodextrins (Table 1.4.3). CGTases are also used as dough additives to

increase the loaf volume of baked products (Van Eijk and Docter, 1993; van der Maarel *et al*., 2002).

β-amylase cleaves *α*-1,4 glycosidic linkages, while amyloglucosidase cleaves both *α*-1,4 and *α*-1,6-glycosidic bonds. These enzymes are used in industrial modification of starch in the saccharification process (Table 1.4.3). *β*-amylase and amyloglucosidase can act on the external side chains of amylopectin to shorten them by cleaving maltose or glucose molecules, respectively. Both enzymes are suggested to have anti-staling properties and can delay bread staling by reducing the tendency of the amylopectin component of starch in bakery products to retrograde (Würsch and Gumy, 1994).

Currently, amylomaltase (catalyzes glucan transfer from one *α*-1,4-glucan to another *α*-1,4- glucan or to glucose) and BE (forms *α*-1,6-glycosidic bonds), do not have large-scale industrial applications. A limited application of amylomaltase in forming thermoreversible starch gels is currently available and marketed under the trade name Etenia^{TM} (by AVEBE of The Netherlands) (Table 1.4.3). Untreated starch can no longer dissolve in water after undergoing retrogradation; however, amylomalatse-treated starch displays thermoreversible gelling characteristics in that it can be dissolved numerous times upon heating (van der Maarel *et al*., 2005). Another application of amylomaltase is for the production of cycloamylose (from amylose), a large cyclic compound, which due to its hydrophobic interior can be used for inclusion of hydrophobic molecules (*e.g*. certain drugs) (Table 1.4.3) (Tomono *et al*., 2002). Applications of BEs are currently limited due to a lack of a widely produced commercial BE. There are several patents, however, describing the potential application of BEs, for instance, in bread as anti-staling agents (Spendler and Jorgensen, 1997), and in production of low-viscosity, high

molecular weight starch that can be used in coating of paper (Bruinenberg *et al*., 1996) or warp sizing of textile fibers (Hendriksen *et al*., 1998) to improve product strength and quality. The following section describes in detail the large-scale potential applications of BEs.

1.5 Biotechnological and Industrial Applications for BEs

Plant species vary in their proportion of amylose and amylopectin within their starch granules, and it is this feature that gives rise to diverse processing characteristics and a multitude of end-uses of starches from various botanic sources (Table 1) (Burrell, 2003; Jobling, 2004; Morell and Myers, 2005). Starches with a high apparent amylose content possess a multitude of useful properties, especially in the food industry, and can for instance be processed into "resistant starches", which are advocated as beneficial for human health, yielding lower glycemic index values upon consumption, as well as promoting colonic health (Annison and Topping, 1994; Cassidy *et al*., 1994; Venn and Mann, 2004). Apparent high-amylose starches contain modified amylopectin with longer internal chain lengths and a reduced branch frequency in outer chains, and thus differ from normal starches (Klucinec and Thompson, 2002; Nishi *et al*., 2001). One means of achieving apparent high-amylose starches is by manipulation of SBE expression in different crop plants (see Chapter 1 for more details).

The availability of various BE mutant crop varieties, such as high-amylose mutants, has shown how the properties of starch from different plant species are altered by changes to composition or structure due to missing BE activity. Differences in amylopectin branching affect granule crystallinity and alter starch thermal, pasting and

biophysical properties, which are key determinants of the commercial suitability of starch. In addition to apparent high-amylose starches, which find a myriad of uses, particularly in the food industry, starches with increased amylopectin branching frequency and shorter chain length also possess improved physicochemical properties, which are commercially beneficial for the food and non-food industries. For example, overexpression of SBEIIb in rice resulted in starch with increased branching frequency, decreased gelatinization temperature, and increased solubility (Tanaka *et al*., 2004b). In potato, overexpression of SBEII resulted in increased ratio of short to long amylopectin branches, producing commercially beneficial changes in the potato starch properties, such as reduced gelatinisation temperature, reduced viscosity and increased swelling volume (Brummell *et al*., 2015). However, mutant crop varieties are typically considerably lower yielding than wild-type crops, and therefore BEs are promising industrial tools for the modification of starches post harvest.

The various studies involving BEs made it abundantly clear that BEs play a distinct role in the starch biosynthesis process, contributing to shaping the fine structure of starch (Bertoft and Seetharaman, 2012; Hizukuri, 1986; Nakamura *et al*., 2010; Ohdan *et al*., 2011; Tetlow and Emes, 2014). The detailed understanding of the structural and functional relationships of SBE enzyme protein domains involved in dictating starch structure and composition presents a potentially useful tool for future manipulation of starch structure in plants and post-harvest, through the use of recombinant BEs (*e.g*. thermostable BEs), or modified BEs, *i.e*. chimeric enzymes and/or BEs altered through site-directed mutagenesis.

Beside the possibility of producing crops with desirable starch properties through manipulating expression of SBEs, BEs, as mentioned above, can also serve as potential industrial tools for post-harvest manipulation of starch (and other polyglucans) properties for a variety of food and non-food applications (Burrell, 2003; van der Maarel and Leemhuis, 2013; Nichols, 2000; Tetlow, 2006; Wu *et al*., 2014). In certain industrial applications, the ability to utilize reactive chemical groups on starch largely depends on the branching frequency and availability of reactive groups during processing (Röper, 2002). Therefore, highly-branched starches with favourable dispersal properties during processing are in high demand, in particular by manufacturers of biopolymers in the paints/inks, adhesives and coatings sectors (Jobling, 2004; Morell and Myers, 2005; Röper, 2002).

Processing of starches for industrial utilization requires aqueous dispersion of the starch granule matrix to allow access to reactive chemical groups (Röper, 2002). Often dispersal requires elevated temperatures as the amylose portion tends to crystallize at lower temperatures (retrograde) and hinder chemical reactions (Abbas *et al*., 2010; Jobling, 2004; van der Maarel and Leemhuis, 2013; Wu *et al*., 2014), and for this reason biopolymer industries often use amylose-free (*Waxy*) starches (see Chapter 1 for more details).

Desirable biopolymers may be created through the use of thermostable BEs as tools for increasing branching frequency of post-harvest starches (van der Maarel and Leemhuis, 2013; Shinohara *et al*., 2001). Thermostable GBEs have recently been isolated and characterized from a number of bacterial species such as, *Bacillus stearothermophilus* (Kiel *et al*., 1991; Takata *et al*., 1994), *Thermus thermophilus*

(Palomo *et al*., 2011), *Aquifex aeolicus* (Van Der Maarel *et al*., 2003), *Rhodothermus obamensis* (Shinohara *et al*., 2001), *Thermococcus kodakaraensis* (KOD1) (Murakami *et al*., 2006) and *Geobacillus mahadia* (Geo-05) (Mohtar *et al*., 2016). An important effect of BEs in post-harvest starch modification, in addition to increasing frequency of branching, which increases non-reducing ends for reactivity, is their ability to overall reduce chain length and essentially remove amylose. Subsequently, the action of BEs reduces retrogradation and increases starch solubility in aqueous solutions (see Chapter 4 for details) (Kawabata *et al*., 2002; Kim *et al*., 2008; Wu *et al*., 2014).

Recently, a commercial GBE (Branchzyme^{TM}; Novozymes) from the thermostable bacterium *Rhodothermus obamensis* has become available (van der Maarel and Leemhuis, 2013). This GBE was the first reported GBE to be active at high temperatures (65°C) (Shinohara *et al*., 2001), which is of utility in processing of gelatinized starch that typically ensues at such temperatures. Although not yet commercialized, the thermostable GBE from the hyperthermophilic bacterium *Aquifex aeolicus*, is used in industrial starch processing, specifically in production of a sport drink ingredient (van der Maarel and Leemhuis, 2013; Takata *et al*., 1997). Recently a slow digestible starch was developed by a BE modification, followed by *β*-amylase treatment, which is unable to bypass branches and thus trims the side-chains by cutting of maltose units from the non-reducing ends (Deremaux *et al*., 2007). The study suggested that the shorter side chains prevent, or reduce, degradation by *α*-amylase, which leads to a slower glucose production and may prevent blood glucose spikes (Deremaux *et al*., 2007; van der Maarel and Leemhuis, 2013).

Industrially useful enzymes must be robust biocatalysts, and possess the ability to withstand harsh processing conditions. Enzymes with favourable properties, such as enhanced thermal stability, tolerance to denaturation, ability to withstand extremes of pH, and a lack of need for co-factors are especially desired for industrial processes. Extremophiles are organisms that have evolved to survive under extreme conditions and their proteins often possess the desired attributes required for industrial applications. *Deinococcus radiodurans* and *Thermus thermophilus* are two examples of extremophilic bacteria. Based on comparative analysis of 16S ribosomal RNA sequences, both belong to a distinct bacterial clade, called the *Deinococcus-Thermus* phylum (Weisburg et al., 1989). However, despite belonging to the same distinct branch of bacteria, the two extremophiles display markedly different phenotypes (Omelchenko *et al*., 2005). *Deinococcus radiodurans* is a mesophile, which is highly radiation- and desiccation-resistant and, generally, can survive diverse types of oxidative stress, whereas *Thermus thermophilus* is a thermophile, which is relatively sensitive to ionizing radiation and desiccation (Omelchenko et al., 2005). The GBEs of these bacteria (DrGBE and TtGBE) may therefore be suitable candidates for use in various industrial applications.

Both DrGBE and TtGBE have previously been characterized to some extent. However, the study involving DrGBE mainly focused on constructing chimeras to investigate the role of enzyme domains in branching preferences (Palomo et al., 2009), while the study with TtGBE focused on deducing its crystal structure (Palomo et al., 2011). The focus of the proposed research aimed to build on previous knowledge established for DrGBE and TtGBE and to further biochemically characterize in detail the activity and branching preferences of these enzymes. Specifically, the activity of DrGBE

and TtGBE under various temperatures and pH levels was assessed using a quantitative assay (assay details in section 4.2.1), which has not previously been used to report these parameters. Additionally, redox-mediated effects on the branching activity of these enzymes were not previously reported (or published), despite past studies showing that the activity of some BEs is affected by redox state (see details in section 4.3.1). Redox-mediated effects on DrGBE and TtGBE activity were quantitatively assessed and are reported below (section 4.3.1). Moreover, kinetic properties of DrGBE and TtGBE have not previously been reported, and therefore were quantitatively determined and reported as part of the work presented in this thesis (section 4.3.2). Previous studies reported the side-chain length distribution of DrGBE products resulting from activity on amylose, but not amylopectin, or other glucan substrates. Similarly, only available reports on TtGBE product side-chain length distribution are from results of TtGBE activity on amylose, not any other glucan substrates (*e.g.* maltodextrins, synthesized medium length maltooligosaccharides). Therefore, branching preferences of DrGBE and TtGBE were further explored by examining the side-chain length distribution of products resulting from the activity of these enzymes with various substrates, like amylopectin, maltodextrins, and maltooligosaccharides, and the results are reported below (section 4.3.3).

Furthermore, the detailed knowledge of the structural organization of BE protein domains from previous studies (see Chapter 1 for details), presented a useful tool for designing chimeric BEs. Such chimeric enzymes could potentially be optimized for particular starch altering applications, producing polyglucans with novel structures, and spurring novel end-uses. Novel chimeric BEs were designed, heterologously expressed,

and purified (section 3.3.2). Prior to chimeric BE design, the thermal stability of DrGBE, TtGBE, as well as plant SBEs, mSBEI and mSBEIIb, was assessed using circular dichroism spectroscopy (section 3.3.1). Thermal stability data were not previously published for these enzymes, and thus constitute an additional novel aspect of the presented research. Preliminary assessment of chimeric BE activities and side-chain length distribution analysis of one chimeric BE were performed.

An additional novel aspect of the presented research is the application of DrGBE, as a proof of concept, to modify a commercial biopolymer to improve its properties (see Chapter 5 for details).

In summary, the research described in this thesis focused on the detailed biochemical characterization of DrGBE and TtGBE using quantitative assay methods for the purpose of implementing these and related enzymes as tools for improving industrial post-harvest starch processing.

1.6 Objectives of the Study

The research project focused on the following objectives;

1) Develop and characterize a number of recombinant BEs under various reaction conditions (*e.g.* temperature, pH, redox state) and with different α-glucan substrates, determine kinetic parameters, and establish suitability to a range of industrial processing conditions in order to create an important new tool and platform technology for bio-product development in non-food and food sectors.
2) Increase branching and improve performance of a commercially successful polyglucan produced by the industrial partner.

As has been discussed above, BEs create products that form viscostable solutions that cannot retrograde as the formed side chains are too short to create strong interactions. As such, BEs have an enormous potential for industrial applications, and as mentioned above BEs are already somewhat utilized in the industry. The outlined project describes in detail the functional characterization of GBEs from *Deinococcus radiodurans* and *Thermus thermophilus*, including their activities under various reaction conditions (*e.g*. temperature, pH, redox state), and with different glucan substrates (*e.g*. amylose, amylopectin, maltooligosaccharides). Additionally, DrGBE was demonstrated to successfully modify an existing commercial starch-derived polyglucan, wherein DrGBE acted rapidly resulting in a branched (12%) product with reduced molecular weight and viscosity that does not gel.

Chapter 2 - Production of Functional Recombinant Glycogen Branching Enzymes from *Deinococcus radiodurans, Thermus Thermophilus* and *E. coli*

2.1 Introduction

In order to characterize the mode of action (*e.g*. preferred substrate, optimum conditions for activity) and enzyme kinetics of *Deinococcus radiodurans* (Dr) GBE and *Thermus thermophilus* (Tt) GBE, sufficient amounts of these GBEs had to be obtained and thus recombinant proteins were generated in *E. coli*. Recombinant *E. coli* GBE (EcGBE) was also generated and had undergone partial characterization of its catalytic activity. Other GBEs, specifically *Aquifex aeolicus* (Aa) GBE and *Deinococcus geothermalis* (Dg) GBE were also cloned and expressed; however, due to various constraints (see discussion; section 2.4) they did not lend themselves to detailed characterization, and thus only DrGBE and TtGBE were fully characterized.

Recombinant protein technology allows for the overexpression of a desired protein product using a prokaryotic or eukaryotic host chosen based on requirements for proper protein expression (Baneyx, 1999). Recombinant proteins are obtained through genetic engineering of a target DNA sequence that is introduced into a DNA vector and then expressed using an appropriate host. A variety of host systems are available for expression of recombinant proteins, including insect cells (Agathos, 1991), mammalian cells (Andersen and Krummen, 2002), yeast (Demain and Vaishnav, 2009), and bacteria (Terpe, 2003). Large quantities (*e.g*. mg amounts) of recombinant protein can be obtained from overexpression (Sørensen and Mortensen, 2005). Recombinant protein is then purified and can serve as a powerful tool for studying enzyme mechanism of action and kinetics.

The basic approach used to produce recombinant protein involves the insertion of a target DNA sequence downstream of an inducible promoter found in a rapidly replicating vector (Baneyx, 1999). The promoter is induced during the host's exponential growth phase allowing for production of recombinant protein. Another important aspect to consider is the addition of a fusion tag, consisting of protein or amino acid sequences added to the N- or C-terminus of the recombinant protein that will facilitate ultimate purification (Sørensen and Mortensen, 2005; Young *et al*., 2012). Fusion tags allow for fast and efficient purification of expressed recombinant proteins from the host cells. Recombinant proteins show large variability in terms of their expression, solubility, and stability and fusion tags can greatly enhance the process, allowing improved purification and solubility (see Table 2.1.1 for some commonly used fusion tags). The downstream application of the recombinant protein will often dictate the choice of host expression cells and the type of fusion tag.

Table 2.1.1 Commonly Used Fusion Tags for Purification and Enhancing the Solubility of Recombinant Proteins.

Tag	Size	Tag Placement	Uses	Reference
His-tag	6 - 8 histidine residues	N- or C-terminal	Purification	(Bornhorst and Falke, 2000)
S-tag	15 residues (KETAAAKFERQHMDS)	N- or C-terminal	Purification	(Raines *et al*., 2000)
Intein tag	28 kDa	N- or C-terminal	Purification	(Chong *et al*., 1997)
GST (Glutathione S-transferase)	26 kDa	N-or C-terminal	Solubility and Purification	(Smith and Johnson, 1988)

E. coli is a widely used host for expression of heterologous proteins, allowing an economical method for production of large amounts of recombinant proteins (Baneyx, 1999; Hannig and Makrides, 1998). *E. coli*'s versatility and ease of manipulation led to its wide use as a model organism around the 1940's, and allowed its exploitation for groundbreaking studies on bacterial physiology, genetics, and viruses (Blount, 2015; Crick *et al*., 1961; Nirenberg *et al*., 1965). Its use in many foundational studies made it the organism of choice at the onset of the molecular biology revolution in the 1950's (Blount, 2015), and subsequently it became a prominent organism for studies in genetic engineering and heterologous protein expression (Blount, 2015; Shiloach and Fass, 2005; Studier and Moffatt, 1986). *E. coli* is a "workhorse" organism, meaning that the wealth of knowledge concerning its physiology has led to its frequent use for recombinant protein expression (Rosano and Ceccarelli, 2014). *E. coli* has a number of properties that make it an attractive host organism such as its fast growth, which can also be fine-tuned and reduced to avoid potential recombinant protein imparted metabolic burden, typically without a negative impact on heterologous protein concentrations (Bentley *et al*., 1990; Rosano and Ceccarelli, 2014). Additionally, ability to reach high cell densities, and its ease of transformation with exogenous DNA, make *E. coli* one of the preferred organisms for heterologous protein expression (Lee, 1996; Pope and Kent, 1996; Rosano and Ceccarelli, 2014).

An array of inducible bacterial expression vectors is available for recombinant protein expression. In the present project, two such vectors were used; pET28a (Novagen) and pTXB1 (New England BioLabs). Expression vectors allow for fusion of various epitope tags to the recombinant protein, such as the N-terminal hexa-histidine

(6His) tag of pET28a, and the C-terminal self-cleavable intein chitin-binding domain (CBD) tag of pTXB1. Due to its relatively small size and the charge it possesses, the polyhistidine affinity tag rarely interferes with protein activity and structure and is thus amongst the preferred tag types (Wu and Filutowicz, 1999). The His-tag can be cleaved from the recombinant protein by digestion with a site-specific protease, thrombin (LVPR↓GS), and therefore the risk of potential interference with the catalytic activity of the recombinant protein is reduced (Figure 2.2.3.1). Also, commercial antibodies against the His-tag are available and can be used to monitor fusion protein expression during trials, which is especially useful for low-level expressing recombinant proteins (Rosano and Ceccarelli, 2014). Finally, the His-tag allows for a one-step affinity purification wherein the fusion protein is recovered from a cell lysate by immobilized metal ion affinity chromatography using Co^{2+}, Ni^{2+} or Cu^{2+} ions bound to an agarose resin (Terpe, 2003).

Another vector expression system used in this project is the intein-CBD affinity tag. This system takes advantage of a protein splicing element, termed intein, that can be induced to undergo self-cleavage activity and in the process separates the target protein from the affinity tag (Figure 2.2.5.1) (Chong *et al*., 1997). The protein of interest is cloned in-frame with the intein-CBD tag and the fusion protein can be purified by adsorption onto a chitin resin (Chong *et al*., 1997). Once the fusion protein is immobilized, the intein portion of the tag is induced to undergo self-cleavage, by addition of a thiol reagent (*e.g*. dithiothreitol), releasing the target protein while the intein-CBD fusion remains bound to the chitin beads (Chong *et al*., 1997). The advantages of this system include the ability to purify recombinant protein in a single chromatographic step

without the use of a protease, and the ability to produce a native recombinant protein without any additional amino acids derived from the vector (Chong *et al*., 1996, 1997).

Target recombinant protein sequences are cloned under the control of a strong bacteriophage T7 promoter within the vector, and expression is induced by supplying the host cells with T7 RNA polymerase (Figure 2.2.4.2). RNA T7 polymerase is selective for its own promoters and directs high-level transcription from the T7 promoter, employing almost all of the host's resources for target gene expression (Studier and Moffatt, 1986). T7 polymerase expression is induced by the addition of isopropyl *β*-D-1-thiogalactopyranoside (IPTG) to the medium, which consequently induces the expression of the gene of interest (Figure 2.2.4.2). IPTG is a molecular mimic of allolactose, a lactose metabolite that triggers transcription of the *lac* operon, it binds to the *lac* repressor and releases the tetrameric repressor, thereby allowing expression of genes in the *lac* operon, specifically T7 RNA polymerase (Jobe and Bourgeois, 1972).

Two *E. coli* strains were employed for the expression of recombinant DrGBE and TtGBE, namely BL21 (DE3) and ArcticExpress (DE3). BL21 (DE3) is an all-purpose strain for high-level protein expression and easy induction, and is compatible with many commercially available vectors, including the pET vectors. This host strain contains the bacteriophage T7 gene 1, under the control of IPTG-inducible *lac*UV5 promoter, which encodes the bacteriophage T7 RNA polymerase (Figure 2.2.4.2). High-level expression of a heterologous protein can often impair the cell's ability to properly process the recombinant protein, generating aggregates of inactive protein known as inclusion bodies (Baneyx, 1999). Low-temperature cultivation and use of *E. coli* chaperonins, involved in facilitating proper protein folding, represent some of the strategies for increasing the

recovery of soluble, functional recombinant protein. ArcticExpress cells have the capacity for improved protein processing at low temperatures (4–12 °C) as they express the cold-adapted chaperonins Cpn10 and Cpn 60 from the psychrophilic bacterium, *Oleispira antarctica* (Strocchi *et al*., 2006). Chaperonins are able to bind and stabilize unfolded or partially folded proteins, thereby facilitating proper protein folding.

Previously, purification of maize SBEs typically involved a number of conventional biochemical purification steps such as, ammonium sulphate precipitation, ion exchange, and affinity chromatography (Guan *et al*., 1994a, 1994b; Liu *et al*., 2012), which is lengthy and laborious. In contrast, studies involving GBEs, such as TtGBE and DrGBE, typically employed the use of affinity tags, specifically the His-tag, due to the simplicity of the purification method and the one-step chromatographic purification (Palomo *et al*., 2009, 2011). In this project, a similar approach was undertaken wherein GBE sequences were cloned in frame with His- and intein-CBD affinity tag sequences. The intein tagged recombinant GBEs yielded the best expression and purification results (see section 2.3), and were thus subsequently used throughout the project.

This chapter describes the expression of functional, recombinant DrGBE, TtGBE and EcGBE, using the pET28a vector with N-terminal His-tag and the pTXB1 vector with C-terminal intein-CBD tag, in BL21 (DE3) and ArcticExpress (DE3) *E. coli* strains. The use of two vector systems and two types of expression systems served as a fail-proof mechanism in case one vector or expression system produced insufficient amounts of recombinant protein. Additionally, the presented work aimed to produce functional recombinant AaGBE and DgGBE, albeit without success. Recombinant GBE proteins were produced for the purpose of characterizing their respective catalytic activities under

various reaction conditions *in vitro*, and with different α-glucan substrates. The GBEs were overexpressed, and recombinant proteins were then purified using the intein-CBD affinity tag to yield purified protein without vector derived amino acids and to achieve highest purity and functionality. The success of the IMPACT protein purification system, eliminated the need for use of the His-tag purification method.

Production of recombinant DrGBE and TtGBE proteins provides a useful tool to address questions regarding their activity under different temperature points, pH levels, redox conditions, and with various glucan substrates (see Chapter 4). Transferred branch chain length preference of recombinant DrGBE and TtGBE, as well as their formed products, were also analyzed (see Chapter 4). AaGBE and DgGBE, did not undergo functional characterization due to expression and/or purification difficulties (see discussion; section 2.4).

2.2 Methods

2.2.1 Polymerase Chain Reaction (PCR) – Amplification of GBE cDNAs

cDNA clones of GBEs from *Deinococcus radiodurans* (DrGBE), *Deinococcus geothermalis* (DgGBE), *Thermus thermophilus* (TtGBE), and *Aquifex aeolicus* (AaGBE) were kindly provided by Dr. Lubbert Dijkhuizen (University of Groningen, Netherlands). *E. coli* purified genomic DNA (strain 1/1/43), which was kindly provided by Dr. Emma Allen-Vercoe, was used to amplify the *E. coli* glycogen branching enzyme sequence.

Primers were designed (using PrimerQuest® program, IDT, Coralville, USA) to amplify GBE cDNA sequences from the above clones for subsequent cloning into expression vectors, pET28a and pTXB1. A summary of the primers used, their nucleotide

sequence, restriction sites, and predicted product size is shown in table 2.2.1.1. The PCR reaction performed was a modification of the method developed by Mullis *et al*. (1986). The PCR reaction mixture contained the following components: 5 µL of 10X PCR Buffer (-Mg) (EMD Millipore catalog no. 71085), 1.5 mM magnesium sulfate, 0.2 mM of each deoxyribonucleotide triphosphate, 0.3 µM of each oligonucleotide primer (Table 2.2.1.1), 100 ng template DNA (either purified genomic or plasmid DNA) and 1-2 units of *Thermococcus kodakaraensis* KOD1 (KOD) DNA polymerase (EMD Millipore catalog no. 71085) in a total volume of 50 µL. PCR amplification was performed in a programmable thermocycler (Techne model TC-412) using 35 reaction cycles. The PCR reaction cycle consisted of a 1 min. denaturation step at 94 °C, 1 min. annealing step at 70 °C and 1 min. elongation step at 72 °C. Additionally, an initial 5 min. denaturation step at 94 °C and a final 5 min. elongation step at 72 °C were also included. Amplification products (for sizes see Table 2.2.1.1) were then used to construct recombinant expression plasmids (see section 2.2.3).

Table 2.2.1.1 Summary of Primers Used for Amplifying BE Sequences for Cloning into pET28a and pTXB1 Expression Vectors. FW, forward primer; RV, reverse primer.

Name	Primer	Cloning vector	Oligo Sequence	Restriction Site	Predicted Product size (bp)
TtGBE	TtBE-*Nde*I-**FW**	pET28a	TATAATCATATGGCGCGCTTCGCCCTGGTCCTCCAC	*Nde*I	~1563
	TtBE-*Sal*I-**RV**		ATATTAGTCGACTCACGCCTCCCGGAAAAGGTAGAG	*Sal*I	
TtGBE	TtBE-*Nde*I-**FW**	pTXB1	TATAATCATATGGCGCGCTTCGCCCTGGTCCTCCAC	*Nde*I	~1587
	TtBE-*Spe*I/intein-**RV**		TATAATAACTAGTGCATCTCCCGTGATGCACGCCTCCCGGAAAAGGTAGAG	*Spe*I	
AaGBE	AaBE-*Nde*I-**FW**	pET28a	CGCCACCATATGAAGAAGTTCAGTCTCATCAGTG	*Nde*I	~1893
	AaBE-*Sal*I-**RV**		GGCTGCGTCGACTCATCCTTCGTGCTTTAAATAGATC	*Sal*I	
AaGBE	AaBE-*Nde*I-**FW**	pTXB1	CGCCACCATATGAAGAAGTTCAGTCTCATCAGTG	*Nde*I	~1917
	AaBE-*Spe*I/intein-**RV**		GGGTGCAACTAGTGCATCTCCCGTGATGCATCCTTCGTGCTTTAAATAGATC	*Spe*I	
DgGBE	DgBE-*Nde*I-**FW**	pET28a	AATATACATATGCTTGACCCGTTGCGGGCGTCCTC	*Nde*I	~1959
	DgBE-*Sal*I-**RV**		TAATATAGTCGACTCACCGGTCCTCGCTGCGGGGC	*Sal*I	
DgGBE	DgBE-*Nde*I-**FW**	pTXB1	AATATACATATGCTTGACCCGTTGCGGGCGTCCTC	*Nde*I	~1983
	DgBE-*Spe*I/intein-**RV**		TATAATAACTAGTGCATCTCCCGTGATGCACCGGTCCTCGCTGCGGG	*Spe*I	
DrGBE	DrBE-*Nde*I-**FW**	pET28a	AATCATCATATGACGTTTCCCTTGCCCCTCGACCACG	*Nde*I	~2118
	DrBE-*Sal*I-**RV**		ATTTCAGTCGACTCAAGCCTTCTTCCCGCCTTTCTG	*Sal*I	
DrGBE	DrBE-*Nde*I-**FW**	pTXB1	AATCATCATATGACGTTTCCCTTGCCCCTCGACCACG	*Nde*I	~2142
	DrBE-*Spe*I/intein-**RV**		TATAATAACTAGTGCATCTCCCGTGATGCAAGCCTTCTTCCCGCCTTTCTG	*Spe*I	
EcGBE	EcBE-*Nde*I **FW**	pET28a	GAGCGCATATGTCCGATCGTATCGATAGAG	*Nde*I	~2187
	EcBE-*Xho*I-**RV**		TACGCTCTCGAGTCATTCTGCCTCCCGAAC	*Xho*I	
EcGBE	EcBE-*Nde*I **FW**	pTXB1	GAGCGCATATGTCCGATCGTATCGATAGAG	*Nde*I	~2220
	EcBE-*Spe*I/intein-**RV**		TATAATAACTAGTGCATCTCCCGTGATGCATTCTGCCTCCCGAACCAG	*Spe*I	

2.2.2 Agarose Gel Electrophoresis

DNA fragments produced by PCR were separated by electrophoresis using a 0.8%-1% (w/v) agarose gel. Agarose powder was added to 1X TAE buffer (40 mM Tris-acetate, 1 mM [ethylenediaminetetraacetic acid] EDTA; pH 8.0) and boiled in a microwave oven to completely dissolve. The boiled solution was allowed to cool to room temperature and ethidium bromide was added to a final concentration of 0.2 µg/mL. The resulting solution was poured into an agarose gel electrophoresis unit to solidify, and TAE buffer was then overlaid on the cooled gel to prevent drying. DNA samples were mixed with 6X DNA loading buffer (Thermo Scientific catalog no. R0611) and loaded onto the gel (sample volumes ranged between 10-100 µL). Electrophoresis was carried out at 100V for 30-60 min. DNA separated in agarose gels was visualized using a gel documentation system (ChemiDoc™ XRS BioRad#170-8265) under UV light.

2.2.3 Cloning of GBE cDNAs

PCR amplification products (TtGBE, DrGBE, DgGBE, AaGBE, and EcGBE coding DNA sequences) were purified using a QIAquick® PCR purification kit (Qiagen). The purified amplicons were used as inserts and cloned into pET28a (Novagen) and pTXB1 (New England BioLabs) expression vectors. Target GBE sequences were cloned into the pET28a vector in frame with the N-terminal His-tag (Figure 2.2.3.1). Target GBE sequences were also cloned into the pTXB1 vector in frame with the C-terminal intein-CBD tag, which allowed purification of recombinant protein through immobilization on chitin resin (Figure 2.2.3.2; see section 2.2.5) (Chong *et al*., 1996; Chong *et al*., 1997). Prior to cloning, both insert and vector DNA were digested at 37 °C

for 1.5 h with 40 units *Nde*I (New England BioLabs) and 40 units *Sal*I (New England BioLabs) or 40 units *Xho*I restriction enzymes for cloning into pET28a, and 40 units *Nde*I and 40 units *Spe*I (New England BioLabs) for cloning into pTXB1. GBE cDNA inserts were ligated (Rapid DNA Ligation Kit, Fermentas) at 16 °C overnight with pET28a or pTXB1 vector DNA and directly fused to the His-tag sequence (N-terminus) of pET28a, or the intein-CBD tag sequence (C-terminus) of pTXB1. Ligated plasmid/insert preparations were transformed (by heat shock, and allowed 45 min. recovery in Super Optimal broth with Catabolite repression [SOC]) into BL21-CodonPlus (DE3)-RIPL (Stratagene) and ArcticExpress (DE3) *E. coli* strains and grown overnight on Luria-Bertani (LB) agar plates supplemented with ampicillin (100 µg/mL; pTXB1 selection) or kanamycin (50 mg/mL; pET28a selection), as well as chloramphenicol (50 mg/mL) for host strain plasmid selection. Successful clones were picked from the overnight plate and used to separately inoculate aliquots (5 mL) of fresh LB media containing 5 µL ampicillin (100 mg/mL stock) or 5 µL kanamycin (50 mg/mL) and grown overnight at 37 °C with constant shaking at 250 rpm. The overnight cultures were then used to isolate plasmid DNA and prepare 40% (v/v) glycerol stocks. Plasmid DNA was purified using a plasmid purification Miniprep Kit (Qiagen) according to the manufacturer's instructions. Purified plasmid DNA was sequenced (at Laboratory Services, University of Guelph) to verify the presence of the complete coding sequence of the different GBE proteins (TtGBE, DrGBE, DgGBE, AaGBE, and EcGBE).

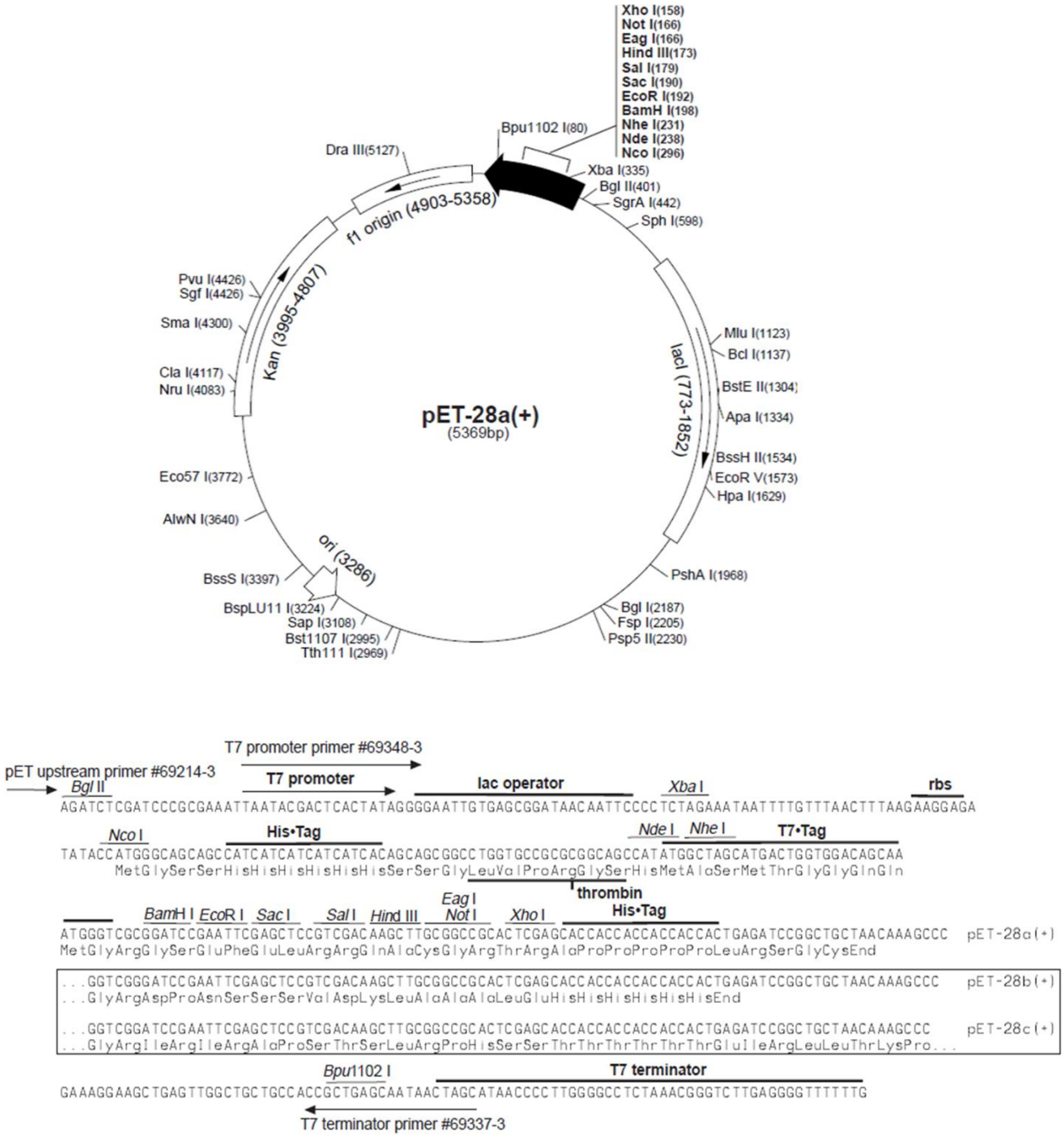

Figure 2.2.3.1 Schematic of Novagen's pET28a expression vector and its polylinker sequence unique sites. The pET28a expression vector carries N- and C-terminal His-tag sequences with the N-terminal sequence followed by a thrombin cleavage site, for His-tag removal, and a number of cloning sites. Target protein sequence was cloned under the control of the T7 promoter, in frame with the N-terminal His-tag. RBS, ribosomal binding site. Figure reproduced from Novagen pET system manual.

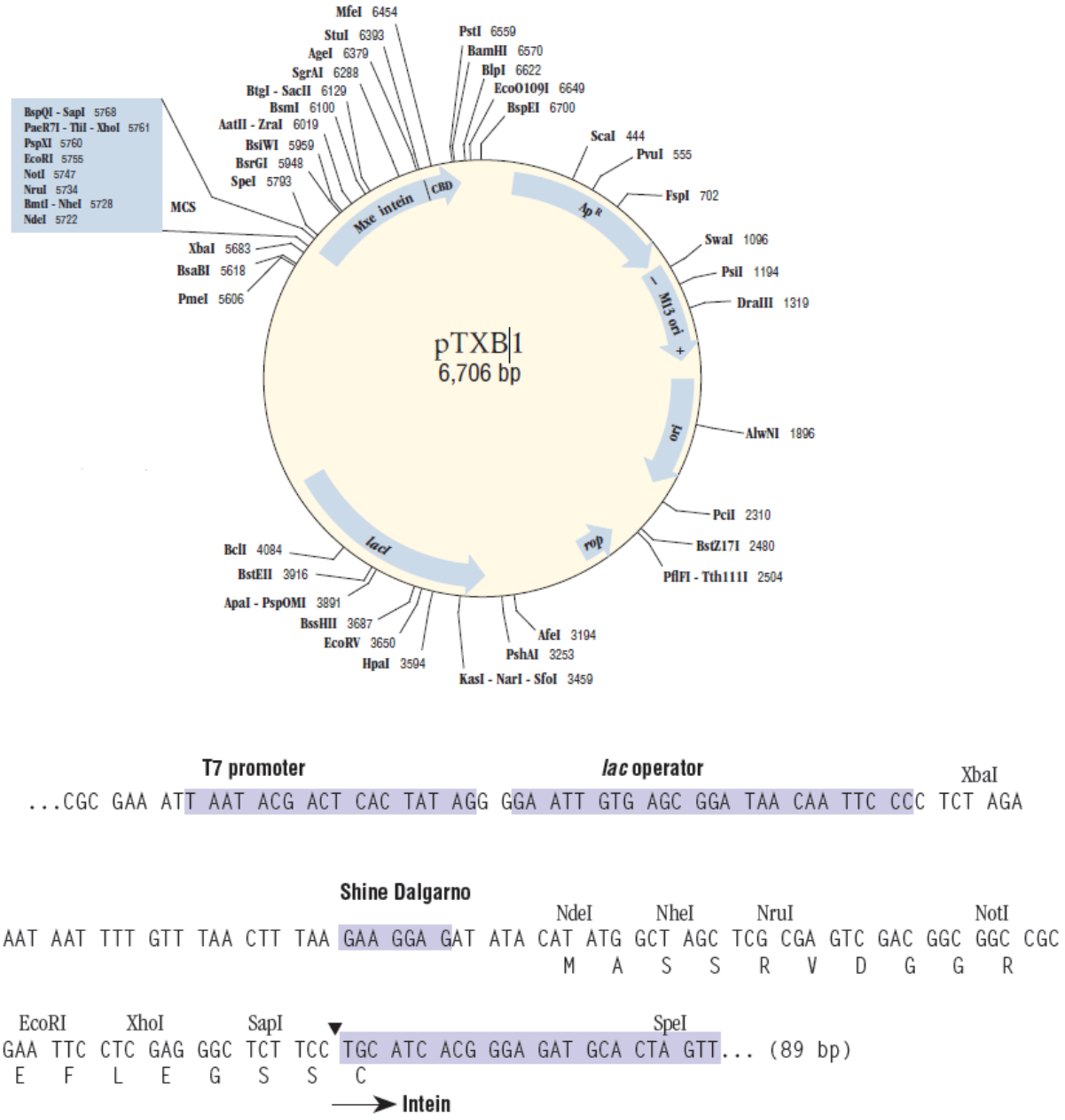

Figure 2.2.3.2 Schematic of pTXB1 expression vector and its polylinker sequence unique sites. The pTXB1 vector carries a C-terminal intein-CBD tag. Target protein sequence is cloned under the control of the T7 promoter, in frame with the intein-CBD tag. Figure reproduced from IMPACT™ kit Instruction Manual, New England Biolabs.

2.2.4 Expression of Recombinant GBEs in BL21 and ArcticExpress *E. coli* Strains

The recombinant pET28a and pTXB1 plasmids containing the different GBE cDNA sequences were transformed into various strains of *E. coli* (Table 2.2.4.1). For recombinant protein overexpression, a single colony of transformants was inoculated, using a sterile loop, into 5 mL of LB media containing 5 µL ampicillin (100 mg/mL) for expression from pTXB1 or 5 µL kanamycin (50 mg/mL) for expression from pET28a, and an additional antibiotic, corresponding to each specific bacterial strain requirement (Table 2.2.4.1), and grown at 37 °C overnight. Next, 2 mL of the overnight culture was used to inoculate 100 mL of fresh LB media (containing no antibiotics) and grown at a strain dependent temperature (Table 2.2.4.1) for approximately 3 h until the culture reached an optical density between 0.6-0.8 at 600 nm. At this point, an aliquot of the culture was taken to serve as pre-induction control. Recombinant protein overexpression was then induced by adding IPTG (Figure 2.2.4.2), to a final concentration of 0.4 mM, to the culture and incubating for 3 h or overnight at strain dependent temperature (Table 2.2.4.1) in a shaking incubator (New Brunswick Scientific model Innova® 44) set to 250 rpm. An aliquot of the culture was taken to serve as post-induction control. The culture was then centrifuged at 4 °C for 20 min. at 3900 g. The supernatant was discarded and the cell pellet was lysed, by resuspending in approximately 2-5 mL BugBuster Protein Extraction Reagent (Novagen catalog no. 70584), and incubated on a rotator (Stuart, model SB2) at room temperature for 40-60 min. The cell lysates were then centrifuged in a microcentrifuge (Beckman Coulter Microfuge® 22R) at 4 °C for 20 min. at 14,000 g. Following centrifugation, the supernatant (soluble protein fraction) and pellet fractions were separated by decanting the supernatant into a fresh tube, while the pellet was

extensively washed with BugBuster Protein Extraction Reagent to remove contaminating proteins and cell debris. The supernatant and the pellet were both analyzed for presence of recombinant protein by Coomassie Blue R250 protein staining (section 2.2.8), and His-tagged recombinant BEs were also western blotted and probed with anti-His-tag antibodies (section 2.2.9).

Table 2.2.4.1 Host Strain Features and Overexpression Conditions.

Host Strain	Recombinant plasmid	Host Strain Plasmids	Selection Antibiotics	Temperature prior to Induction	Temperature post Induction
BL21-CodonPlus (DE3)RIPL	pET28a-BE or pTXB1-BE	pACYC	Chloramphenicol Kanamycin Ampicillin	37°C	34°C
ArcticExpress (DE3)	pET28a-BE or pTXB1-BE	*Cpn10/cpn60* chaperonin plasmid	Gentamycin Kanamycin Ampicillin	30°C	12°C

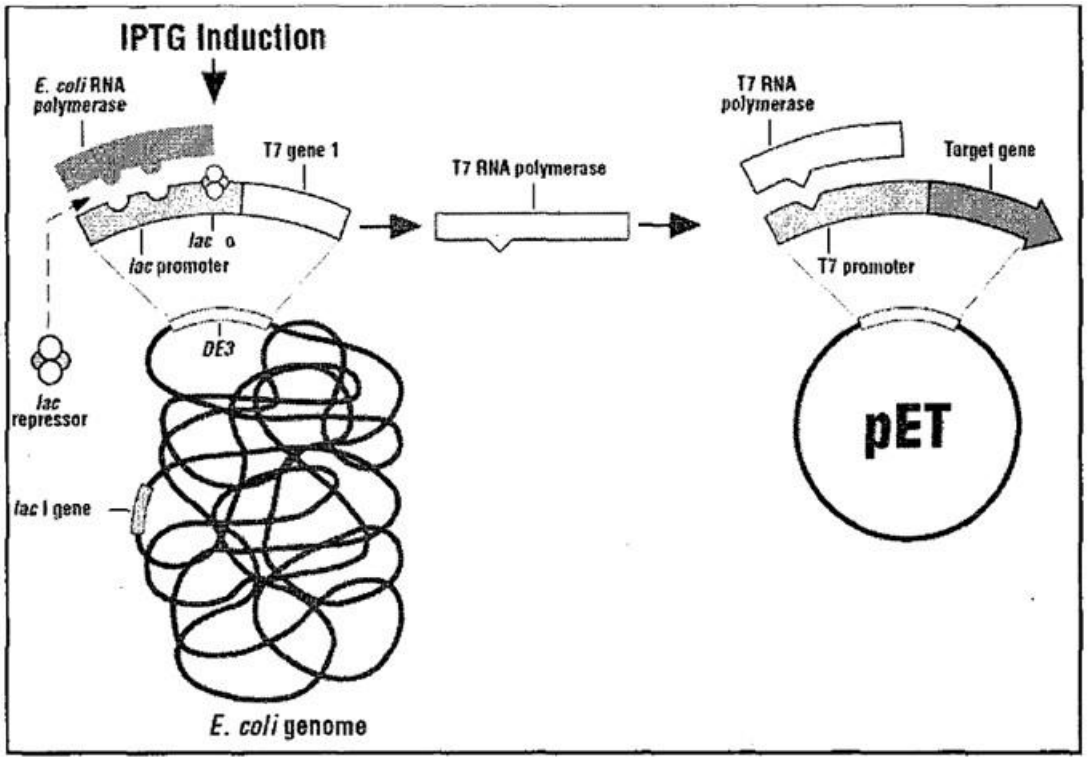

Figure 2.2.4.2 Control elements of the pET system. Host and vector elements controlling T7 RNA polymerase levels and subsequent transcription of a target gene cloned in a pET vector. Recombinant protein expression is induced by the addition of IPTG. Figure reproduced from Novagen pET system manual.

2.2.5 Recombinant Protein Purification

Although GBE sequences were cloned into, and expressed from, both pET28a and pTXB1 vectors, purification was initiated (and used throughout the project) using the intein-CBD tagged recombinant GBEs as it allows recovery of recombinant protein without any additional vector derived amino acids.

Recombinant protein was purified (Figure 2.2.5.1) according to the method outlined in Intein Mediated Purification with an Affinity Chitin-binding Tag (IMPACT) manual (New England BioLabs catalogue no. E6901S). Following expression and cell lysis, 5 mL (approximately 25 mg total protein) of the supernatant (soluble protein) fraction was applied to chitin resin (New England BioLabs catalogue no. S6651S) for immobilization and subsequent purification of recombinant protein. Chitin resin was prepared by pipetting 2-5 mL of chitin bead slurry into a 20 mL Poly-Prep chromatography column (Bio-Rad) and washed with five to seven column volumes of column buffer (20 mM Tris-HCl pH 8.5, 500 mM NaCl). Prior to application to chitin resin, 5 mL of soluble recombinant protein fraction was mixed with 5 mL column buffer and filtered through a 0.45 μm filter. The filtered soluble protein fraction was applied to chitin resin column which was capped and allowed to incubate overnight on a rotator (Stuart, model SB2) at 4°C to improve recombinant protein binding efficiency. Next, the column was uncapped and the soluble fraction was collected and saved for analysis on sodium-dodecyl-sulfate-polyacrylamide gel electrophoresis (SDS-PAGE). The column was then washed with 250-500 mL washing buffer (20 mM Tris-HCl pH 8.5, 500 mM NaCl, 1% (v/v) Triton X-100), 20 mL at a time. After washing, the flow to the column was stopped, 5 mL cleavage buffer (20 mM Tris-HCl pH 8.5, 500 mM NaCl, 50 mM dithiothreitol (DTT)) was applied and the column was

left to incubate for 24-72 h at 23 °C. Finally, recombinant protein was eluted from the column using 2-3 column volumes of column buffer. The eluate fraction then underwent buffer-exchange (50 mM 3-morpholinopropane-1-sulfonic acid [MOPS] pH 7) and was concentrated through a 50K (expected size of all recombinant proteins was >60 kDa) molecular weight cut-off spin column (EMD Millipore catalog no. UFC905024). This step also allowed removal of DTT. The concentrated eluted recombinant protein samples were checked for protein concentration and stored at -80 °C (in 50 mM MOPS pH 7). Purification results were analyzed by SDS-PAGE and protein concentration was determined using the Bradford assay (section 2.2.6). Purified recombinant GBEs were subjected to mass spectrometric analysis to confirm their identity (section 2.2.11). Protein yield is approximately equivalent to that produced with the pET28a system.

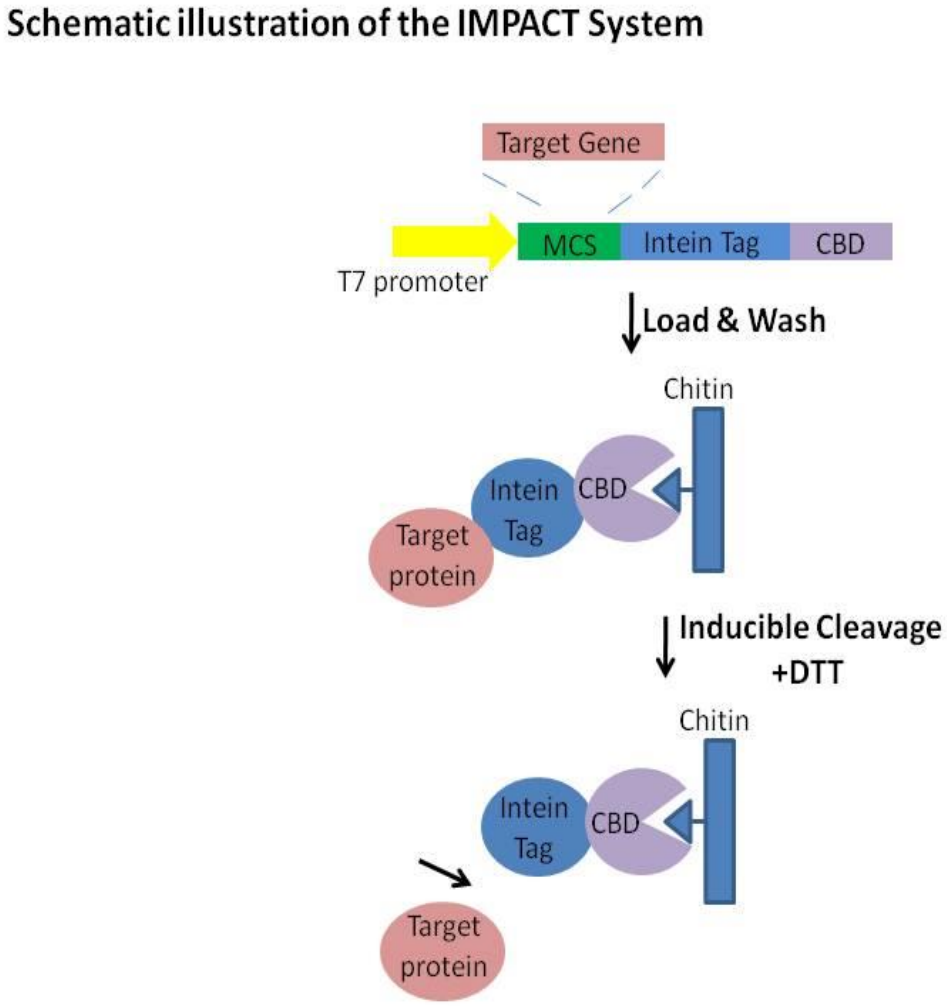

Figure 2.2.5.1 Schematic illustration of the IMPACT protein purification system. Target protein sequence is cloned under the control of the T7 promoter, in frame with the intein-CBD tag. Expressed fusion protein is applied to a chitin resin, and following washing intein self cleavage is induced with a thiol reagent (*e.g.* DTT) and the target protein is released from the intein-CBD tag. MCS, multiple cloning site; CBD, chitin-binding domain; DTT, 1,4-dithiothreitol.

2.2.6 Protein Concentration Determination

Protein content was determined by using the Bio-Rad Quick Start™ Bradford reagent (Bio-Rad Laboratories, Canada) based on a modification of the technique used by Bradford (1976). Protein concentration assays were performed in a 1 mL volume containing 5 µL protein sample, 795 µL milliQ water, and 200 µL protein dye reagent. The blank sample contained 800 µL of milliQ water plus 200 µL dye reagent. The samples were incubated at 25 °C for 5-10 min. and protein concentration was determined by measuring the absorbance at a wavelength of 595 nm in a Shimadzu UV-Visible Spectrophotometer UV-1601. A standard curve for determination of protein concentration was generated using known amounts of bovine serum albumin (BSA) protein (Figure 2.2.6.1).

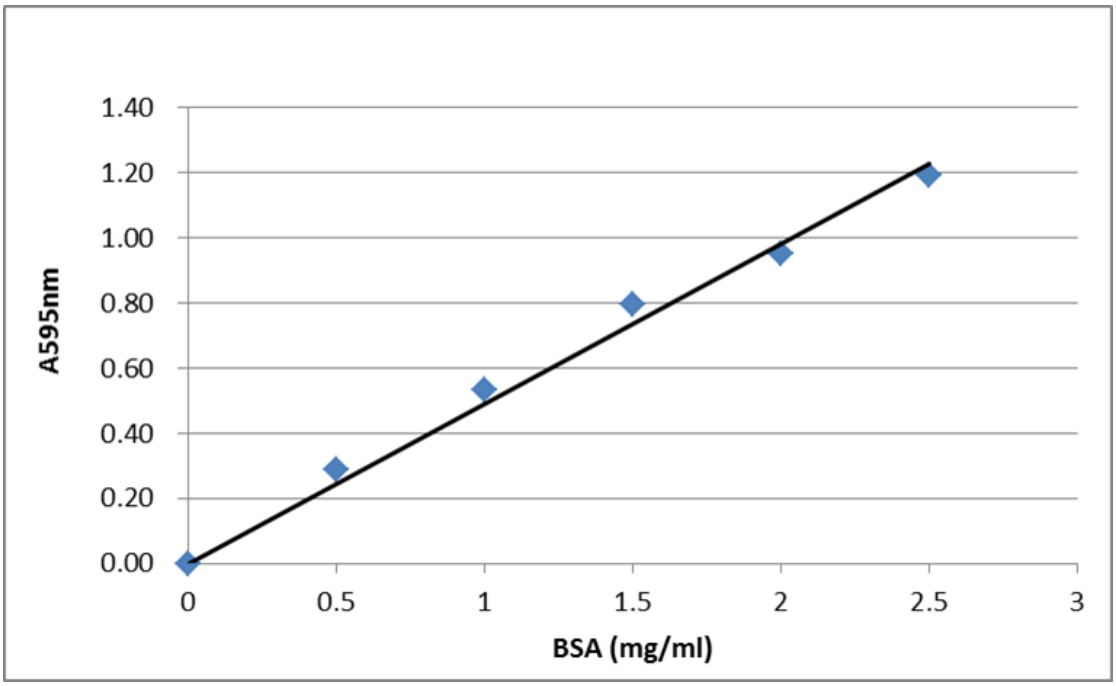

Figure 2.2.6.1 Standard curve for protein concentration determination using the Bradford assay. The dye binding assay was used to determine the absorbance (A) at 595 nm for known amounts of BSA protein.

2.2.7 Sodium-Dodecyl-Sulfate-Polyacrylamide Gel Electrophoresis (SDS-PAGE)

Proteins were separated based on their molecular mass using a modification of the method developed by Laemmli (1970). Prior to electrophoresis, protein samples were boiled in 5X-SDS loading buffer (0.31 M Tris-HCl pH 6.75, 25% (v/v) 2-mercaptoethanol, 10% (w/v) SDS, 50% (v/v) glycerol, 0.005% (w/v) Bromophenol Blue) at a ratio of 4:1 (sample: buffer) for 5 min. at 95 °C. After cooling, 30-50 µL protein (~5-25 µg) sample was loaded into wells of a 10% polyacrylamide gel. Proteins were separated according to molecular weight by SDS-PAGE made up with a 10% resolving gel (0.5 M Tris pH 8.8, 10% (w/v) acrylamide, 0.1% (w/v) SDS, 0.1% (w/v) ammonium persulfate (APS), 0.01% (v/v) TEMED) and a 5% stacking gel (0.128 M Tris pH 6.8, 5% (v/v) acrylamide, 0.1% (w/v) SDS, 0.1% (w/v) APS, 0.01% (v/v) TEMED). Electrophoresis was performed at room temperature for approximately 2 h at 120V in a 1X SDS-running buffer (0.25 M Tris, 1.92 M glycine, 1% (w/v) SDS).

2.2.8 Coomassie Blue Protein Staining

Following SDS-PAGE, proteins separated by molecular mass were visualized using Coomassie Blue R250 protein stain. The Coomassie Blue staining procedure was a modification of the method developed by Meyer and Lamberts (1965). Gels were incubated in Coomassie Brilliant Blue stain (40% (v/v) methanol, 0.1% (w/v) Brilliant Blue R-250 crystals, 10% (v/v) acetic acid) for 1-1.5 h at room temperature on a shaker (New Brunswick Scientific Gyrotory Shaker Model G2). Following staining, gels were incubated in destaining buffer (8% (v/v) acetic acid, 25% (v/v) methanol) for

approximately 3 h at room temperature on a shaker (New Brunswick Scientific Gyrotory Shaker Model G2).

2.2.9 Immunodetection of Proteins - Western Blotting

A variation of the method developed by Towbin *et al*. (1979) was employed for immunochemical protein identification. Proteins were first separated based on their molecular weight by SDS-PAGE, and then transferred from the gel onto a nitrocellulose membrane in an XCell™ II Blot Module (Invitrogen) for 90 min. at 28V in transfer buffer (1X running buffer (25 mM Tris, 192 mM glycine), 20% (v/v) methanol, 70% (v/v) dH_2O). Following transfer, the nitrocellulose blot was blocked with 1.5% (w/v) BSA in 1X TBS buffer (10 mM Tris-HCl pH 7.5, 250 mM NaCl) at room temperature for 15 min. followed by incubation for approximately 2-4 h at room temperature with anti-His-tag primary antibody (New England BioLabs catalog no. 23655) diluted with 1.5% (w/v) BSA in 1X TBS buffer to 1:1000. The blot was then washed 3 times for 15 min. with a total of 1 L of Tween 20 Tris buffered saline solution (TTBS) (10 mM Tris-HCl pH 7.5, 250 mM NaCl, 0.1% (v/v) Tween 20) followed by incubation in secondary antibody (anti-rabbit IgG conjugated with alkaline phosphatase) used at a dilution of 1: 30,000 for 2 h. The blot was then washed again 3 times for 15 min. with a total of 1 L of TTBS, it was then developed with approximately 10 mL of 5-Bromo-4-Chloro-3-Indonyl Phosphate/Nitro Blue Tetrazolium (BCIP/NBT) liquid substrate solution (Sigma-Aldrich).

2.2.10 GBE Zymogram Assay

Zymogram analysis was used as a non-quantitative means of visualizing BE catalytic activity, and was performed according to a method previously modified by Tetlow *et al*. (2004). In-gel zymogram assays were performed using non-denaturing 5% (w/v) polyacrylamide gels which contained 375 mM Tris-HCl (pH 8.8), 0.2% (w/v) maltoheptaose (Sigma-M7755), 1.4 units rabbit-muscle phosphorylase *a* (Sigma-Aldrich, catalog no. P-1261), and 10 mg of the α-amylase inhibitor Acarbose (Prandase®, Bayer). The protein samples were mixed with 6X native loading buffer (0.32 M Tris-HCl pH 6.8, 40% (v/v) glycerol, 20% (w/v) β-mercaptoethanol, and 1.2 mM Bromophenol Blue) and loaded onto the zymogram gel. Proteins were electrophoresed at 90V in 1X running buffer (0.25 M Tris, 1.92 M glycine) at 4 °C for 3 h, or until the dye front reached the gel bottom. After electrophoresis, gels were washed 3 times for 15 min. in BE zymogram washing buffer (100 mM Na-citrate and 20 mM 2-(N-morpholino)-ethanesulfonic acid [MES], pH6.6). The washed gels were then incubated in the incubation buffer (20 mM MES-NaOH, pH 6.6, 100 mM Na-citrate, 45 mM glucose-1-phosphate (G1P), 2.5 mM AMP, 1 mM DTT, and 1 mM Na_2-EDTA) for 1.5 - 4.5 h at 30 °C, with shaking at 50 rpm. After washing the native gel with distilled water, Lugol's solution (0.2% (w/v) iodine and 2% (w/v) potassium iodide) was used to stain the gel and the BE catalytic activity, in the form of bands on the gel, were visualized immediately.

2.2.11 Mass Spectrometry

Mass spectrometric analysis was performed at the University of Guelph Advanced Analysis Centre. Protein samples were subjected to an in-gel trypsin digest (according to

a method described by Shevchenko *et al*., 1996), and resulting tryptic peptides were extracted and separated on a Waters nano-Acquity Q-TOF (micro instrument). Nano-UPLC-MS/MS analyses were performed using a nanoAcquity UPLC System (Waters, Milford, MA) in combination with a QTOF (quadrupole time-of-flight) micro mass spectrometer (Waters Micromass, Manchester, U.K.). The column used was a 75 μm × 150 mm Atlantis™ dC18 column packed with 3 μm particles with an initial Symmetry® C18 trapping column of 180 μm x 20 mm with 5 μm particles. The liquid chromatography (LC) was coupled with the mass spectrometer using a Universal Nanoflow Sprayer (Waters, Manchester, U.K) operated with a PicoTip Emitter (New Objective, Woburn, MA) with an inner diameter of 10 μm. UPLC-MS/MS analyses were carried out at a flow rate of 400 nL/min. and a column temperature of 35 °C. Samples were loaded onto the trapping column and washed for 3 min. with 2% B (acetonitrile with 0.1% formic acid). Peptides were separated using a linear gradient from 90% A (water with 0.1% formic acid), 2%B to 60% A, 40% B in 40 min. The mass spectrometer was operated in positive ion mode with a capillary voltage of 3600 V and a cone voltage of 35 V. Data were acquired in DDA (data dependent acquisition) mode, one survey scan of 2 s was carried out followed by up to three MS/MS scans (of 2 s) of each of the three most intense precursor ions. MS/MS spectra were processed using Peaks Studio 8 (Bioinformatics Solutions Inc. Waterloo, ON, Canada) and searched against the protein database NCBI (Ma *et al.*, 2003). These searches were performed using trypsin specificity with the possibility of one missed cleavage at a MS tolerance of 100 ppm and a MS/MS tolerance of 0.1 Da and included the following variable modifications, carbamidomethyl-Cys and oxidized Met.

2.3 Results

2.3.1 Expression and Purification of Recombinant GBEs in BL21 and ArcticExpress Cells

In order to determine the best possible expression vector and host for production of sufficient amounts of recombinant protein for characterization, two different expression vectors and expression cell lines were tested. GBE sequences were successfully amplified by PCR (section 2.2.1) and cloned into both pET28a and pTXB1 vectors. N-terminal His-tag (pET28a) and C-terminal intein-CBD (pTXB1) tag constructs were created. Recombinant protein constructs were transformed into BL21 (DE3) and ArcticExpress (DE3) cells. Prior to expression experiments, recombinant plasmids were purified and used for insert sequencing. The obtained insert sequences were then aligned against available cDNA sequences for corresponding GBE proteins found in the National Center for Biotechnology Information (NCBI) database. Alignment results confirmed a complete match between NCBI sequences for the GBEs and the respective insert sequences. Recombinant GBEs were then expressed in BL21 (DE3) and ArcticExpress (DE3) cells. Expressed recombinant proteins were visualized *via* Coomassie Blue staining (Figures 2.3.1.1 and 2.3.1.2 A and B) and the presence of His-tagged GBE proteins was confirmed by immunoblotting with an anti-His-tag antibody (Figure 2.3.1.2 C).

2.3.1.1 EcGBE Expressed from pET28a and pTXB1 Vectors

The expected size of recombinant His-tagged EcGBE (in pET28a) is approximately 86 kDa (see Table 2.3.1.1 for recombinant protein and affinity tag sizes). Figure 2.3.1.1 A illustrates the expression results of BL21 (DE3) and ArcticExpress (DE3) cultures, harbouring the pET28a-EcGBE construct, post induction with IPTG. As anticipated, the Coomassie Blue stained gels showed no polypeptide bands of the expected size (~86 kDa) in the pre-induction controls (C) of BL21 (DE3) and ArcticExpress (DE3) cells. However, unexpectedly, anticipated polypeptide bands corresponding to EcGBE were also not observed in the soluble fractions and the inclusion bodies fractions, suggesting lack of expression of recombinant His-tagged EcGBE (Figure 2.3.1.1 A). Indeed, the soluble fraction of BL21 (DE3) and ArcticExpress (DE3) cells containing the pET28a-EcGBE construct immunodetected with anti-His-tag antibody showed no polypeptide bands of the expected size (Figure 2.3.1.2 C).

By contrast, expression results of recombinant EcGBE cloned into pTXB1 vector and transformed into BL21 (DE3) and ArcticExpress (DE3) cells showed distinct polypeptide bands of expected size in both the soluble and inclusion bodies fractions (Table 2.3.1.1; Figure 2.3.1.1 B). The pre-induction control and soluble fraction of BL21 (DE3) culture showed faint polypeptide bands in the expected position of approximately 118 kDa, the expected size of intein-CBD-tagged EcGBE (Figure 2.3.1.1 B). The inclusion body fraction showed a thicker, darker stained polypeptide band in the same position (black arrow), indicating that majority of the expressed recombinant EcGBE was aggregated. Expression of EcGBE in ArcticExpress (DE3) cells showed a faint polypeptide band of approximately 118 kDa in the pre-induction control. A larger and

more intensely stained polypeptide band of a similar size was observed in the soluble fraction (black arrow), indicating a higher quantity of soluble recombinant protein as compared to that in the soluble fraction of BL21 (DE3) culture. The inclusion bodies fraction showed the presence of a thicker and darker polypeptide band of expected size (black arrow), although smaller and less intensely stained than that of the BL21 (DE3) inclusion bodies fraction. Recombinant EcGBE was purified by means of its intein-CBD tag (see section 2.2.5) and was subjected to zymogram analysis for preliminary determination of catalytic activity (section 2.3.3).

Table 2.3.1.1 Estimated Sizes of Recombinant GBEs, Affinity Tags, and Resulting Fusion Proteins as Determined Based on Available GBE Sequences in the NCBI Database.

Target protein	Size (kDa)	Affinity tag used and its size (kDa)	Fusion protein size (kDa)
EcGBE (728 aa)	84.36	His-tag (6 aa) – 0.84	~86
		Intein-CBD tag – 34	~118
TtGBE (520 aa)	59.18	His-tag (6 aa)) – 0.84	~60
		Intein-CBD tag– 34	~93
AaGBE (630 aa)	74.17	His-tag (6 aa)) – 0.84	~75
		Intein-CBD tag– 34	~108
DgGBE (637aa)	74.45	His-tag (6 aa)) – 0.84	~76
		Intein-CBD tag– 34	N/D
DrGBE (705 aa)	80.02	His-tag (6 aa)) – 0.84	~81
		Intein-CBD tag– 34	~114

aa – amino acid
N/D – was not determined; transformation unsuccessful

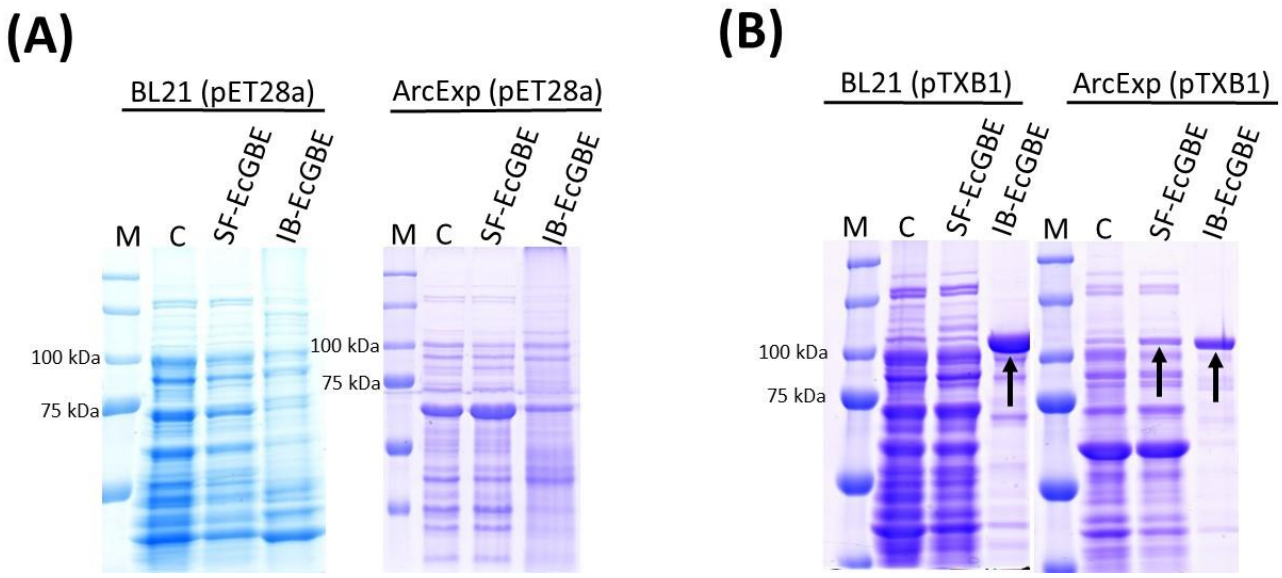

Figure 2.3.1.1 Expression of pET28a-EcGBE (A) and pTXB1-EcGBE (B) constructs in BL21 (DE3) and ArcticExpress (DE3) cells as detected by Coomassie Blue staining. Cultures were induced with 0.4 mM IPTG and BL21 cells were grown for 3 h at 34 °C, and ArcticExpress cells were grown overnight at 12 °C. Cells were harvested by centrifugation at 3900 g for 20 min. at 4 °C and lysed using Novagen BugBuster Protein Reagent. Cell lysates were centrifuged at 14,000 g and the supernatant (SF fraction) was separated from the pellet (IB fraction). Approximately 20 µg total protein was loaded per lane and separated by SDS-PAGE. Lanes: M, protein marker; C, pre-induction control; SF-EcGBE, soluble fraction; IB-EcGBE, inclusion bodies fraction.

2.3.1.2 TtGBE, DrGBE, AaGBE and DgGBE Expressed from pET28a

GBEs from the extremophilic bacteria, *Deinococcus radiodurans* (DrGBE), *Deinococcus geothermalis* (DgGBE), *Thermus thermophilus* (TtGBE), and *Aquifex aeolicus* (AaGBE), were also cloned into pET28a and expressed in BL21 and ArcticExpress cells (see Table 2.3.1.1 for recombinant protein and affinity tag sizes).

TtGBE expression

As illustrated in Figure 2.3.1.2 A, a thick polypeptide band of approximately 60 kDa, the expected size of His-tagged TtGBE (Table 2.3.1.1), was observed in both the soluble and inclusion bodies fractions of BL21 cells (black arrows). By contrast, expression of His-tagged TtGBE in ArcticExpress cells failed to produce polypeptide bands in the expected position in soluble and inclusion bodies fractions (Figure 2.3.1.2 B). Immunodetection with anti-His-tag antibody of soluble fractions of BL21 and ArcticExpress cells expressing His-tagged TtGBE revealed a polypeptide band of expected size (~60 kDa) in the soluble fraction of BL21 cells, but not in the soluble fraction of ArcticExpress cells (Figure 2.3.1.2 C). These experiments confirmed expression of TtGBE in BL21 but not in ArcticExpress cells.

AaGBE expression

His-tagged AaGBE was not successfully expressed in BL21 cells, as a polypeptide band of expected size of approximately 75 kDa was not observed in either the soluble or the inclusion bodies fractions (Figure 2.3.1.2 A). Indeed, immunodetection with anti-His-tag antibody of the soluble fraction of BL21 cells did not show presence of a polypeptide band that would correspond to the size of AaGBE (Figure 2.3.1.2 C). Expression of AaGBE seemed evident in ArcticExpress cells showing a very thin

polypeptide band of approximately 75 kDa within the inclusion bodies fraction, and a faint polypeptide band in the soluble fraction (green arrows; Figure 2.3.1.2 B). However, immunodetection with anti-His-tag antibody of the soluble fraction of ArcticExpress cells expressing His-tagged AaGBE did not reveal a polypeptide band that would indicate AaGBE was present (*i.e.* a protein band at ~75 kDa; Figure 2.3.1.2 C).

DgGBE expression

The expected size of His-tagged DgGBE is approximately 76 kDa. Expression of DgGBE was evident in both BL21 and ArcticExpress cells, with light bands in the soluble fractions of both cell types and very thick, dark bands in the inclusion bodies fractions of both cell types (brown arrows; Figure 2.3.1.2 A and B). Immunodetection with anti-His-tag antibody of soluble fractions of BL21 and ArcticExpress cells, expressing His-tagged DgGBE, confirmed expression showing a polypeptide band of expected size (~76 kDa) in the soluble fractions of both cell types (Figure 2.3.1.2 C).

DrGBE expression

Expression results of DrGBE showed a thick, dark polypeptide band of approximately 81 kDa in the soluble fraction of BL21 cells, and an even thicker, darker polypeptide band in the inclusion bodies fraction (pink arrows; Figure 2.3.1.2 A). ArcticExpress expression of DrGBE showed a thin polypeptide band of expected size (~81 kDa) in the soluble fraction, and a rather thin band in the inclusion bodies fraction (pink arrows; Figure 2.3.1.2 B). Soluble fractions of BL21 and ArcticExpress cells, expressing DrGBE, immunodetected with anti-His-tag antibody confirmed presence of DrGBE showing a polypeptide band in the expected position (at ~81 kDa; Figure 2.3.1.2 C).

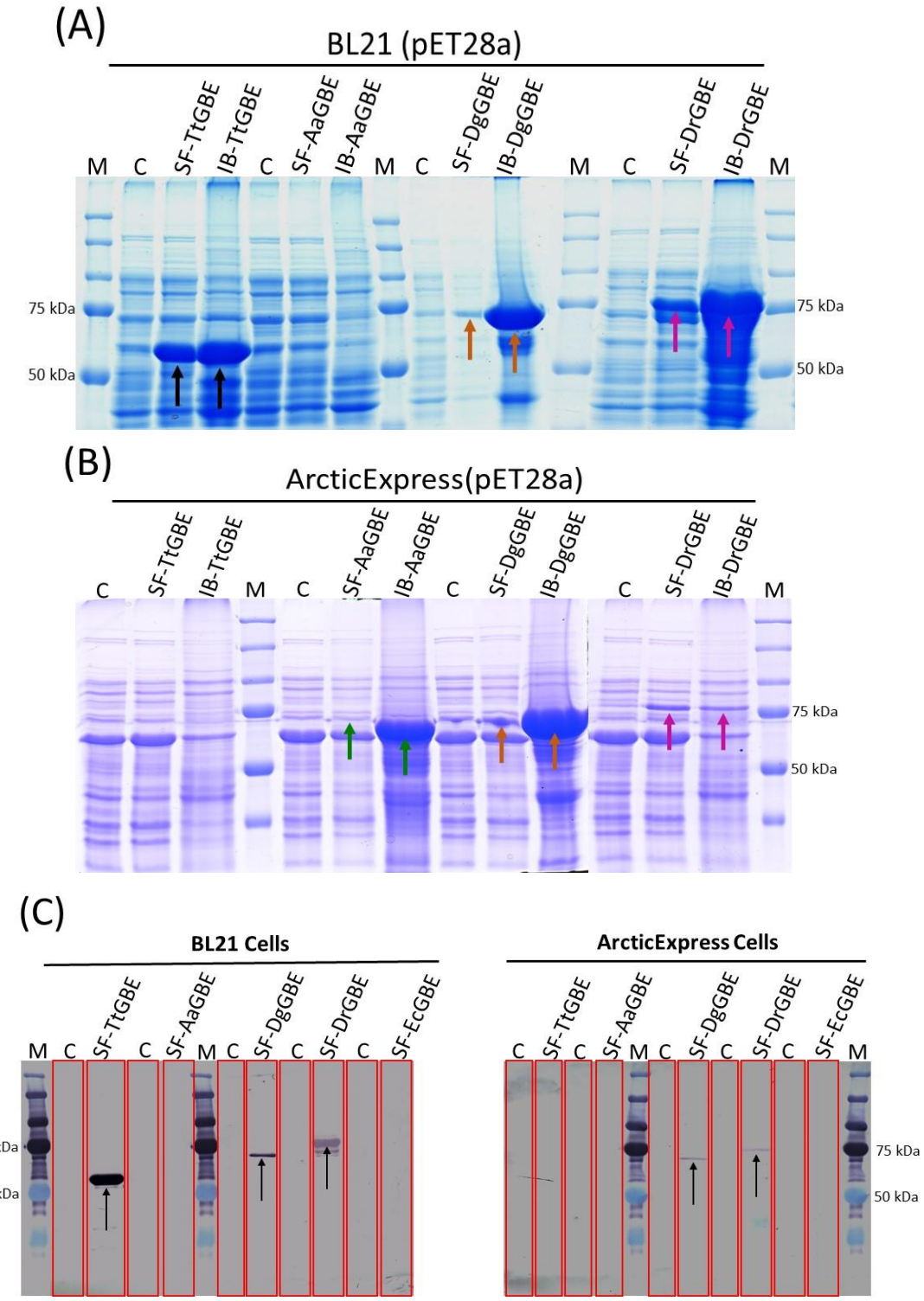

Figure 2.3.1.2 Expression of His-tagged TtGBE, AaGBE, DgGBE and DrGBE in BL21 cells (A) and ArcticExpress cells (B) as detected by Coomassie Blue staining of protein extracts. Approximately 25 µg total protein was loaded per lane. Expression of GBEs in soluble fractions of BL21 and ArcticExpress cells was also detected using western blotting (C) with anti-His-tag antibody. Lanes: M, protein marker; C, pre-induction control; SF, soluble fraction of the expressing cells of the respective GBE; IB, inclusion bodies fraction of the expressing cells of the respective recombinant GBE.

2.3.1.3 TtGBE, DrGBE, AaGBE and DgGBE Expressed from pTXB1

All GBEs described in this chapter were also cloned into the pTXB1 vector and transformed into BL21 and ArcticExpress cells (for expression of recombinant protein) in order to ensure sufficient amounts of recombinant protein (~mg quantities) are produced for subsequent biochemical characterization (see Table 2.3.1.1 for recombinant protein and affinity tag sizes). However, not all transformations were successful. Despite many attempts, the pTXB1-DgGBE construct was never successfully transformed into either cell line. pTXB1-TtGBE and pTXB1-DrGBE constructs were only successfully transformed into BL21 cells, while pTXB1-AaGBE was successfully transformed into both BL21 and ArcticExpress cells. Recombinant intein-CBD tagged TtGBE was successfully expressed in BL21 cells with thick polypeptide bands of approximately 93 kDa, the expected size, observed in both the soluble and inclusion bodies fractions (black arrows; Figure 2.3.1.3). AaGBE expression in BL21 and ArcticExpress cells was only observed in the inclusion bodies fractions of these cell types (green arrows, Figure 2.3.1.3). However, the size of the observed polypeptide band is smaller (<100 kDa) than the expected size of approximately 108 kDa for intein-CBD tagged AaGBE. No further attempts were made to identify AaGBE via mass spectrometry. Expression results of DrGBE in BL21 yielded thick, dark polypeptide bands of approximately 114 kDa, the expected size of intein-CBD tagged recombinant DrGBE, in both the soluble and inclusion bodies fractions (pink arrows; Figure 2.3.1.3). Hereafter, recombinant DrGBE and TtGBE proteins were the focus of subsequent experimental work. These recombinant proteins were purified by means of their intein-CBD tag (see section 2.2.5) and their catalytic activities and respective products characterized (see Chapter 4). Purified TtGBE

and DrGBE were first subjected to zymogram analysis for preliminary determination of catalytic activity (section 2.3.3).

Chapter 4 describes the detailed characterization of catalytic activities of TtGBE and DrGBE assessed using a variety of standard branching enzyme activity assays, namely the iodine binding assay and the branch-linkage assay. The products of TtGBE and DrGBE activity with various substrates are also analyzed in detail and described in Chapter 4.

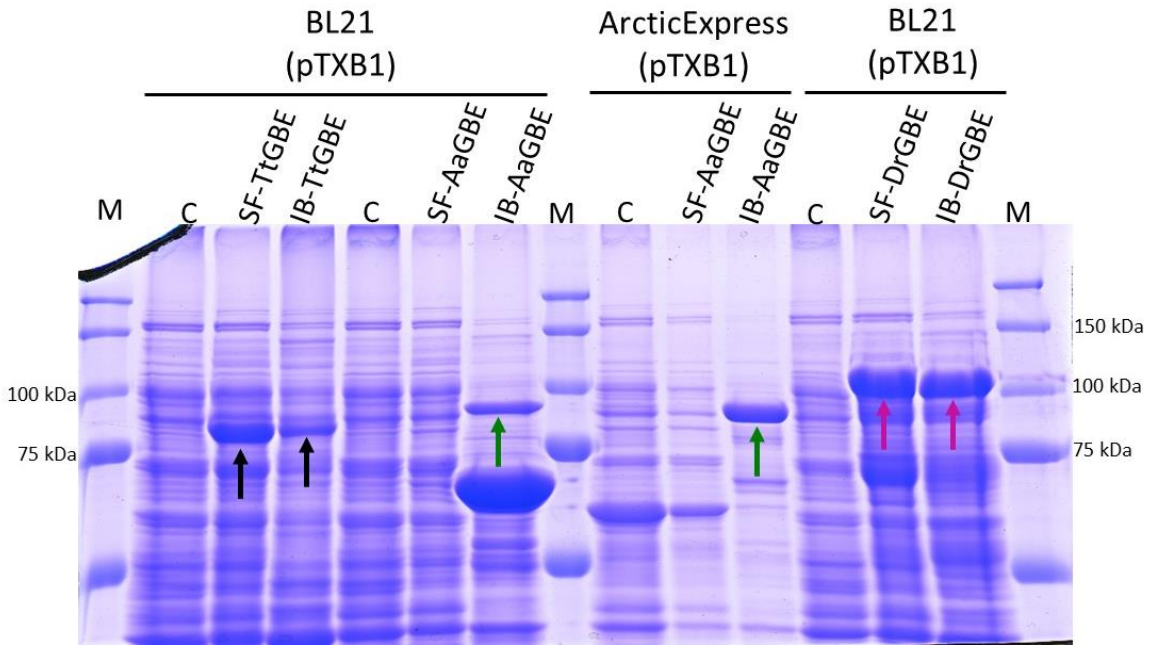

Figure 2.3.1.3 Expression of intein-CBD-tagged TtGBE, AaGBE, and DrGBE in BL21 and ArcticExpress cells as detected by Coomassie Blue staining. Approximately 25 µg total protein was loaded per lane. Lanes: M, protein marker; C, pre-induction control; SF, soluble fraction of the expressing cells of the respective recombinant GBE; IB, inclusion bodies fraction of the expressing cells of the respective recombinant GBE.

2.3.2 Purification of Recombinant GBEs from *E. coli*

The initial purification strategy took advantage of the intein-CBD tag system, as cleavage of this tag yields purified recombinant protein without any additional amino acids derived from the vector. This strategy was successful (see results below) and was hereafter used for purification of DrGBE, TtGBE, and EcGBE (see section 2.2.5).

Affinity purification of chitin-CBD-tagged recombinant EcGBE, TtGBE, and DrGBE was performed by application of the soluble protein fraction (~25 mg total protein in ~5-10 mL), from IPTG induced-host cells, to chitin agarose resin, as previously described (section 2.2.5). Proteins bound to the resin were then thoroughly washed and an on-column cleavage reaction, to remove the intein-CBD tag from the recombinant protein, was induced by incubating the resin in cleavage buffer containing 50 mM DTT. Purified recombinant GBEs were eluted from chitin resin and underwent buffer-exchange through a filter spin column to remove DTT. High yields of recombinant GBEs, purified to near homogeneity, were obtained using this procedure. Purification results were visualized by Coomassie Blue staining and purified TtGBE and DrGBE were subjected to mass spectrometric analysis to confirm identity (Figure 2.3.2.2) prior to further biochemical characterization.

Figure 2.3.2.1 A illustrates the purification results of recombinant EcGBE expressed in ArcticExpress (DE3) cells. During each step of the purification procedure, fractions were taken and proteins were separated on SDS-PAGE, and stained with Coomassie Blue R250 to check for presence of polypeptide bands of expected size (~118 kDa; Table 2.3.1.1). Intein-CBD tagged recombinant EcGBE was detected bound to chitin resin as is observed in chitin resin after wash (AW) lane, showing a polypeptide

band around 118 kDa, the expected size of intein-CBD tagged EcGBE (Figure 2.3.2.1 A). The intein-CBD tag was cleaved from recombinant EcGBE, and purified EcGBE was eluted from the chitin resin as detected by Coomassie Blue staining, which revealed a polypeptide band of approximately 84 kDa (Table 2.3.1.1), the expected size of native EcGBE (black arrow; Figure 2.3.2.1 A).

Recombinant, intein-CBD tagged DrGBE was also successfully purified, to near homogeneity, from the soluble fraction of BL21 cell lysates. During each step of the purification procedure, fractions were taken and proteins separated on SDS-PAGE, and stained with Coomassie Blue R250 to check for presence of polypeptide bands of expected size. A polypeptide band, corresponding to the size of intein-CBD tagged DrGBE (~114 kDa), was observed in the soluble fraction chitin column flow through (lane: SF; Figure 2.3.2.1 B), suggesting that not all of the tagged recombinant protein successfully bound to chitin beads. Chitin resin after wash fraction (lane: AW; Figure 2.3.2.1 B) revealed a major polypeptide band of approximately 114 kDa, the expected size of tagged DrGBE (see Table 2.3.1.1). The eluate fraction showed a major polypeptide band of approximately 80 kDa (black arrow; Figure 2.3.2.1 B), the expected size of native DrGBE (NCBI; see Table 2.3.1.1), suggesting successful purification and tag cleavage as was also confirmed by mass spectrometric analysis (Figure 2.3.2.2 A). A faint polypeptide band of approximately 114 kDa was also observed in the eluate fraction (lane: E; Figure 2.3.2.1 B), this most likely corresponds to uncleaved intein CBD-tagged DrGBE. Following elution an aliquot of chitin resin was analyzed for remaining proteins on the beads (lane: AE; Figure 2.3.2.1 B). This sample showed presence of a polypeptide

band of approximately 114 kDa, suggesting that most likely some intein-CBD tagged DrGBE remained bound to the resin after cleavage and elution.

Intein-CBD tagged recombinant TtGBE was also successfully purified using the chitin resin as is illustrated in Figure 2.3.2.1 C. During each step of the purification procedure, fractions were taken and proteins were separated on SDS-PAGE, and stained with Coomassie Blue R250 to check for presence of polypeptide bands of expected size. The major polypeptide band observed in chitin resin after wash fraction (lane: AW; Figure 2.3.2.1 C) is of approximately 93 kDa, the expected size of intein-CBD tagged TtGBE (see Table 2.3.1.1). Purification and subsequent intein tag cleavage was successful as the eluate fraction revealed a major polypeptide band of approximately 59 kDa, the expected size of native TtGBE (black arrow; Figure 2.3.2.1 C), which was also confirmed by mass spectrometric analysis (Figure 2.3.2.2 B). Another minor polypeptide band (~93 kDa) was observed in the eluate fraction, which most likely corresponds to intein-CBD tagged TtGBE (lane: E; Figure 2.3.2.1 C). Following elution an aliquot of chitin resin was analyzed for remaining proteins on the beads (lane: AE; Figure 2.3.2.1 C). The resin showed the presence of a polypeptide band of approximately 93 kDa, most likely indicating that some intein-CBD tagged TtGBE remained bound to the chitin resin.

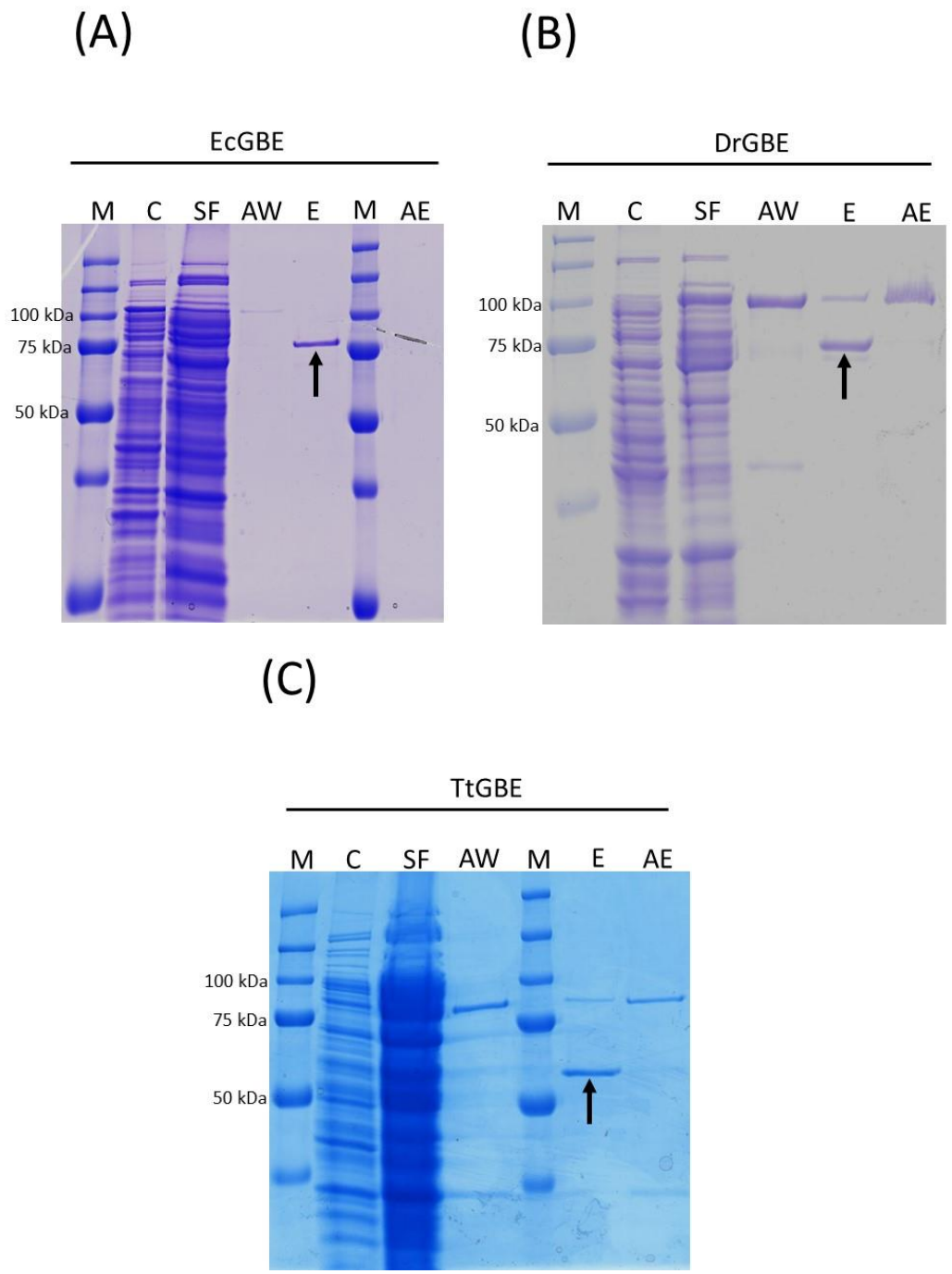

Figure 2.3.2.1 Affinity purification of recombinant intein-CBD tagged EcGBE (A), DrGBE (B) and TtGBE (C). Cells were lysed and centrifuged in order to separate the soluble fraction from inclusion bodies. The soluble fraction was applied to chitin resin column, which was then washed. The intein-CBD tag on the corresponding recombinant GBEs was cleaved with 50 mM DTT, and the recombinant protein eluted from the resin and detected by Coomassie Blue staining. Approximately 10 µg total protein was loaded. Lanes: M, protein marker; C, pre-induction control; SF, soluble fraction flow through; AW, chitin resin after wash; E, eluate of purified tag-free recombinant protein; AE, chitin resin after elution.

(A)

```
  1 MTFPLPLDHE HLQKLVTADL VRPDHLLGAH PTTEHGVQGV RFAVWAPNAQ HVSVVGDFND
 61 WNGFDHPLQR LDFGFWGAFV PAAQPGQRYK FRVTGAGGQT VDKTDPYGTF FEVRPNNASI
121 IWQQDFEWTD AGWLEQRARR GQALEDPISI YECHVGSWAR RDDGWFLNYR DLAHRLGEYV
181 TYMGYTHVEL LGVMEHPFDG SWGYQVTGYY APTSRLGSPE DFKYLVNHLH SLGIGVLLDW
241 VPGHFPTDEF ALAHFDGSPL YEYADPRKGY HYDWNTYIFD YGRNEVVMFL IGSALKWVQD
301 YHVDGLRVDA VASMLYLDFS RTEWVPNIYG GRENLEAIAF LKRLNEVAHH MAPGCLMIAE
361 ESTSFPGVTT PTPEGLGFDY KWAMGWMNDS LAYFEQDPIY RKYDHHKLTF FNVYRTSENY
421 VLAISHDEVV HLKKPMVLKH PGDWYAQRAD YRAFLAMMWT TPGKKLLFMG QDFAQGSEWN
481 HDAPLPWFHA DQPDHRGVMN LVRRLNELYR ERPDWHTGDA REEGMAWISA DDTDNSVYAY
541 ARRDTYSGAW SLVIANLTPV YREDYVIGVP QGGEYRVLLS TDDGEFGGFG TQQPDLSARD
601 EAAHGQAHAL HLNLPPSSVL VLEPVAAAPV KGLVSRQELT PELREVARQS AQAVQVERAA
661 DPRPNEQQRL VAETPAHEGG RSAPADAAES AEQKPDDEQK GGKKA
```

(B)

```
  1 MARFALVLHA HLPYVRAHGM WPFGEETLYE AMAETYLPLI RVLERLRAEG VEAPFTLGIT
 61 PILAEQLADA RIKEGFWAYA KDRLERAQGD YQRYRGTALE ASARHQVAFW ELTLDHFQRL
121 SGDLVAAFRK AEEGGQVELI TSNATHGYSP LLGYDEALWA QIKTGVSTYR RHFAKDPTGF
181 WLPEMAYRPK GPWKPPVEGP PEGVRPGVDE LLMRAGIRYT FVDAHLVQGG EPLSPYGEAA
241 LGPVESQEAT YHVHELESGL RVLARNPETT LQVWSADYGY PGEGLYREFH RKDPLSGLHH
301 WRVTHRKADL AEKAPYDPEA AFAKTEEHAR HFVGLLERLA GRHPEGVILS PYDAELFGHW
361 WYEGVAWLEA VLRLLAQNPK VRPVTAREAV QGPAVRTALP EGSWGRGGDH RVWLNEKTLD
421 YWEKVYRAEG AMREAARRGV LPEGVLRQAM RELLLLEASD WPFLMETGQA EAYARERYEE
481 HARAFFHLLK GASPEELRAL EERDNPFPEA DPRLYLFREA
```

Figure 2.3.2.2 Identification of purified recombinant DrGBE (A) and TtGBE (B) by mass spectrometry. Purified recombinant proteins were trypsin digested and the resulting peptides were subjected to LC-MS-MS for identification using Peaks 8 software (Bioinformatics solutions) and the NCBI protein database. Highlighted in grey are areas of the sequence identified by mass spectrometry.

2.3.3 Determination of Catalytic Activity of Purified GBEs by Zymogram Analysis

Recombinant EcGBE, DrGBE, and TtGBE were purified to near homogeneity (Figure 2.3.2.1 A, B, and C) and their catalytic activities detected using an in gel zymogram assay (methods section 2.2.10). The catalytic activity of the GBEs was visualized by loading 1-3 µg of each GBE onto a non-denaturing polyacrylamide gel containing maltoheptaose as a substrate and rabbit muscle phosphorylase *a* for glucan chain elongation. Following electrophoresis, the gel was incubated with a buffer containing G1P, which is necessary for glucan chain elongation by phosphorylase *a*. The presence of branched glucan within the gel is indicative of GBE catalytic activity and can be visualized by staining with Lugol's solution (I_2/KI) (Figure 2.3.3.1). A blue-black band is indicative of the presence of long linear glucan chains, while a brown-clear yellow colour band indicates the presence of branched glucan or shorter glucan chains (Bailey and Whelan, 1961).

Figure 2.3.3.1 illustrates the presence of catalytically active TtGBE, DrGBE and EcGBE. A large clear-yellow zone indicated by a pink arrow (Figure 2.3.3.1 B) corresponds to the catalytic activity area of DrGBE which forms short branches of DP ~4 – 12 (Palomo *et al*., 2009). Both TtGBE and EcGBE showed formation of longer branches compared to DrGBE, as illustrated by the presence of brown bands on the zymogram gels (blue arrows, Figure 2.3.3.1 A and C, respectively). Maize endosperm crude extract and maize endosperm amyloplast preparations served as positive control for SBE activity, showing the catalytic activities of native SBEI, SBEIIa, and SBEIIb (Liu *et al*., 2012). Zymogram analysis was used as a preliminary determination of GBE catalytic activity and crude estimate of different glucan product formation by the different GBEs.

In Chapter 4, GBE activities were characterized in detail under varying assay conditions using a number of methods, including the quantitative branch-linkage assay (section 4.2.1).

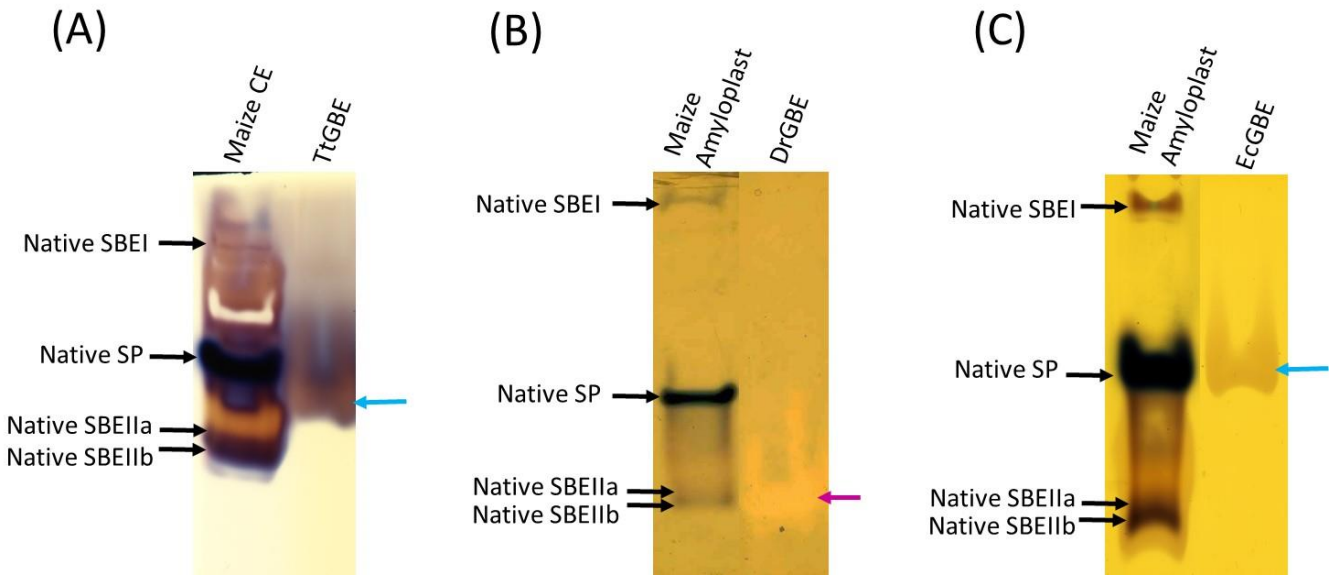

Figure 2.3.3.1 Zymogram analysis of purified recombinant TtGBE (A), DrGBE (B), and EcGBE (C). GBE catalytic activities were assayed indirectly by stimulation of G1P incorporation into glucan by phosphorylase *a*. Purified recombinant TtGBE (A), purified recombinant DrGBE (B), and purified recombinant EcGBE (C) were separated on non-denaturing 10% (w/v) gels containing 0.2% (w/v) maltoheptaose as primer, and incubated with 45 mM G1P as substrate for 4.5 h at 30 º C. Arrows indicate bands of BE catalytic activities. Catalytic activities of native maize endosperm SBEs are marked as according to Liu *et al*. (2012). Lanes: Maize CE, maize crude extract (15-25 µg protein per lane); TtGBE, purified recombinant TtGBE (3 µg protein per lane); DrGBE, purified recombinant DrGBE (1 µg protein per lane); EcGBE, purified recombinant EcGBE (3 µg); SBE, starch branching enzyme; SP, starch phosphorylase.

2.4 Discussion

Previous studies have reported the expression of recombinant SBEs and GBEs using *E. coli* expression systems (Guan *et al*., 1995, 1997, 1994a, 1994b; Liu *et al*., 2012; Makhmoudova *et al*., 2014; Palomo *et al*., 2009, 2011). In the present work, EcGBE, TtGBE, DrGBE, AaGBE, and DgGBE were overexpressed using different strategies to increase the yield of recombinant protein. Recombinant GBE proteins were then purified using the intein-CBD affinity tag.

Expression of His-tagged AaGBE was not evident as was confirmed by immunoblotting (Figure 2.3.1.2 C). Expression of intein-CBD tagged AaGBE yielded aggregated protein, which was most likely slightly truncated (observed polypeptide band was of smaller molecular weight (~90 kDa) than expected (~108 kDa); green arrows, Figure 2.3.1.3). The pTXB1-DgGBE (in frame with intein-CDB tag) construct was not successfully transformed into BL21 and ArcticExpress cells and therefore expression could not be attempted. Thus, due to the various hurdles encountered with these proteins, such as aggregation and inability to transform cell lines, work with AaGBE and DgGBE was discontinued. The project was carried on using recombinant EcGBE, DrGBE and TtGBE, which were successfully expressed and purified in high yields and were catalytically active.

EcGBE was cloned into pET28a and pTXB1 vectors and subsequently transformed into BL21 and ArcticExpress cells. Recombinant plasmids were sequenced to confirm insert presence, and the sequences were also aligned against the cDNA sequence for EcGBE found in the NCBI database. Sequence alignment results confirmed a complete match between the NCBI sequence for EcGBE and the insert sequences.

Despite the presence of the insert, expression of EcGBE from pET28a vector yielded no protein in either cell line (Figure 2.3.1.1 A), as was confirmed by immunoblotting (Figure 2.3.1.2 C). Inability to detect expression of recombinant protein may result from a harmful effect that the heterologous protein can exert on the host cell (Dumon-Seignovert *et al*., 2004; Rosano and Ceccarelli, 2014). Occasionally, low expression can also result from toxic effects produced by the expression plasmid on the host cell (Miroux and Walker, 1996). Since EcGBE is a native *E. coli* protein perhaps it is more likely that lack of expression is due to toxicity of the expression vector. It has been previously demonstrated that vectors of the pET family can produce inhibitory effects on host expression cells, such as BL21 (Miroux and Walker, 1996). In other studies with recombinant EcGBE, the pET plasmid was modified to change the origin of replication to achieve a lower plasmid copy number, which can help alleviate plasmid toxic effects and improve expression of the recombinant protein (Abad *et al*., 2002; Binderup *et al*., 2002; Guan *et al*., 1997). The origin of replication element determines the number of plasmids produced in a cell (Camps, 2010). Thus, regulating and modifying the plasmid copy number in recombinant gene expression can achieve a high gene dosage while maintaining the stability of the expression system (Camps, 2010; Kittleson *et al*., 2011).

In the present study, the use of the pTXB1 vector helped abolish EcGBE expression issues and yielded highly purified recombinant EcGBE. The pTXB1 vector codes for the intein-CBD affinity tag, composed of ~198 amino acid intein element and a ~51 amino acid CBD portion (Chong *et al*., 1996; Terpe, 2003). The intein-CBD affinity tag is commonly used for purification of recombinant protein as it allows single step chromatographic purification of the recombinant protein (Chong *et al*., 1997; Sharma *et*

al., 2006). Additionally, this affinity tag does not require a protease for its cleavage, and thus eliminates an extra purification step and prevents complications associated with protease use, such as poor specificity and inefficient tag cleavage (Chong *et al*., 1997; Sharma *et al*., 2006; Terpe, 2003). Moreover, high salt and non-ionic detergent concentrations can be used to reduce non-specific protein binding, thus increasing recombinant protein purity (Cantor and Chong, 2001; Chong *et al*., 1997; Sharma *et al*., 2006). Many previous studies have engaged the use of the intein-CBD affinity tag, reporting high yields of highly purified, catalytically active recombinant proteins such as, the bacteriophage P1 Cre recombinase (Cantor and Chong, 2001), *Staphylococcus simulans* lysostaphin enzyme (Szweda *et al*., 2001), and the human pituitary adenylate cyclase (Yu *et al*., 2004). In the present study, EcGBE cloned into pTXB1 vector was successfully expressed in BL21 and ArcticExpress cells (Figure 2.3.1.1 B). Heterologous expression in BL21 cells yielded mostly aggregated recombinant protein (black arrow, Figure 2.3.1.1 B), while expression in ArcticExpress cells produced sufficient amounts of soluble protein (black arrow, Figure 2.3.1.1 B), which was then used for affinity purification of EcGBE through its intein-CBD tag. The tag was cleaved during the purification procedure yielding pure (near homogeneity) recombinant EcGBE (Figure 2.3.2.1 A).

Recombinant DrGBE and TtGBE were also produced and purified through intein-CBD tag affinity purification, which allowed high yields of soluble recombinant DrGBE (approximately 40 mg per litre) and TtGBE (approximately 30 mg per litre) (Figure 2.3.1.3). During affinity purification, the intein-CBD tag was successfully cleaved and DrGBE (Figure 2.3.2.1 B) and TtGBE (Figure 2.3.2.1 C) were purified to near

homogeneity. EcGBE expression and purification also yielded soluble recombinant protein (Figure 2.3.1.1 A), however, at lower amounts than that of DrGBE and TtGBE.

Preliminary testing of activity of purified recombinant TtGBE, DrGBE, and EcGBE was accomplished by zymogram analysis. The in-gel zymogram assay is a common non-quantitative technique used to assess BE catalytic activity (Tetlow *et al*., 2004). Other studies have previously reported assessing the catalytic activities of maize SBE isoforms using the zymogram assay (Dumez *et al*., 2006; Liu *et al*., 2004; Makhmoudova *et al*., 2014). BE catalytic activity detection through the use of in-gel zymogram assay has also been previously described for GBEs, including EcGBE (Boyer *et al*., 2016), *Rhodothermus obamensis* GBE (Roussel *et al*., 2013), and *Mycobacterium tuberculosis* GBE (Garg *et al*., 2007). The three GBEs described in this chapter, EcGBE, TtGBE, and DrGBE, were shown to be catalytically active (Figure 2.3.3.1 A, B, and C). One of the objectives of the present project is the detailed functional characterization of recombinant GBEs, which is described in detail in Chapter 4.

Chapter 3 - BE Thermal Stability and Chimeric Protein Design, Expression, and Purification

3.1 Introduction

Traditional starch-acting enzymes are often utilized in the industry; however, requirements for optimally performing starch-acting enzymes are quite specific for each industry, mainly concerning pH, oxidative stability, and temperature behaviors (Chi *et al*., 2010). Therefore, new starch-acting enzymes (*e.g*. α-amylases, BEs) with optimized properties, such as enhanced thermal stability, acid tolerance, and ability to function under oxidative conditions, are being developed using strategies such as (but not limited to), site-directed mutagenesis, and design of chimeric enzymes (Bisgaard-Frantzen *et al*., 1999; Chi *et al*., 2010; Declerck *et al*., 2000; Shaw *et al*., 1999).

One of the main priorities of protein engineering from an industrial perspective is thermostabilization of enzymes in order to make them fit candidates for the harsh conditions of post-harvest starch processing. Currently, however, in spite of increasing knowledge and understanding of protein domain architecture, no convincing general rules for enzyme stabilization have emerged, and elucidation of the molecular processes that occur in proteins when exposed to high temperatures is still heavily debated. Recent research suggests that stabilizing interactions contributing to the structural integrity of the active site region may be reinforced through hydrophobic and/or conformational effects (Declerck *et al*., 2000). One way to investigate protein folding and stability is through assessment of secondary structure under thermal denaturation conditions using, for example, circular dichroism spectroscopy.

The detailed understanding of the structural and functional relationships of BE enzyme protein domains presents a useful tool for modifying BE protein characteristics

through, for example, protein engineering, to produce BEs with improved characteristics (*e.g.* thermostability, improved pH profile, and unique substrate and branching preferences) that can be applied to generate polyglucans with unique and novel properties. Chimeric BEs can be designed by using computational sequence analysis, as well as by taking advantage of known three-dimensional structure of various BEs. Such designed chimeric BEs could potentially be optimized for particular starch altering applications, producing polyglucans with novel structures, and spurring novel end-uses.

The following sections of this chapter describe the design of chimeric BEs, estimation of their activity, and assessment of branch chain length distribution of their products, which are all novel aspect of the presented research. The designed chimeric enzymes were composed of TtGBE, mSBEI, and mSBEIIb sequence elements (Figure 3.3.2.1).

3.2 Methods

3.2.1 Circular Dichroism (CD) Spectroscopy for Protein Folding Clues

CD spectroscopy was used to evaluate recombinant protein secondary structure, folding properties, and thermal stability. Both, CD-wavelength scans as well as CD-monitored thermal denaturation experiments were carried out on wild-type recombinant TtGBE, DrGBE, mSBEI and mSBEIIb (both recombinant mSBEs kindly provided by Amina Makhmoudova). These experiments were performed with a Jasco J-815 spectropolarimeter (Japan Spectroscopic, Tokyo, Japan) using a quartz cuvette with a 1-mm path length. Recombinant proteins were in 10 mM potassium phosphate buffer pH 7. In CD-wavelength scans, minimally four scans were collected and averaged; the corresponding buffer blank (containing no protein sample) scans were subtracted from all

sample scans. In thermal-melt experiments, the change in α-helical content was monitored at a single wavelength (at which maximum peak signal was obtained [see Figure 3.3.1.2 in section 3.3.1]; 208 nm for mSBEI, mSBEIIb and DrGBE, and 222 nm for TtGBE), as the temperature was increased at a scan rate of 1°C/min. using a Jasco PTC-424S/15 Peltier temperature controller (Japan Spectroscopic, Tokyo, Japan). Buffer blank thermal denaturation experiments were carried out under the same experimental conditions, and these buffer data were subtracted from protein data prior to analysis. In order to estimate the mid-point of thermal unfolding, the CD-monitored thermal denaturation traces were fit to a two state model described by the following equation (Greenfield, 2006):

$$Y_{\text{obs}} = \frac{(Y_N + S_N[T]) + (Y_U + S_U[T])e^{\frac{-(\Delta H_m * (1-T/T_m) - \Delta Cp * ((T_m - T) + T * \ln(T/T_m)))}{RT}}}{1 + e^{\frac{-(\Delta H_m * (1-T/T_m) - \Delta Cp * ((T_m - T) + T * \ln(T/T_m)))}{RT}}}$$

where Y_{obs} is the observed CD signal at temperature T; Y_N and Y_U are the y-intercepts of the pre-transition (native) and post-transition (denatured) baselines, respectively; and S_N and S_U are their respective slopes. Further, T_m is the temperature at which the protein unfolding reaction is half-completed, ΔH_m is the van 't Hoff enthalpy at the T_m, ΔC_p is the change in specific heat capacity of unfolding, and R is the universal gas constant. Fitting to the equation was kindly done by Kenrick A. Vassall using Microcal OriginPro version 8.0 (OriginLab, Northampton, MA). In fitting, the values of ΔC_p, as well as of S_N and S_U, were fixed to zero. All collected data were normalized to mean residue ellipticity

units ([deg*cm^2/dmol] x 10^{-3}) as it reports the molar CD for individual protein residues instead of whole protein molecules, and thus allows convenient comparison of different proteins with different molecular weights (Greenfield, 2006). CD spectra data was analyzed to predict BE secondary structure α-helix and β-strand fractions using the web server K2D3 (Louis-Jeune *et al*., 2012). Prediction of the content of helices and strands in the tested BEs was also done based on their respective primary amino acid sequences using the secondary structure prediction web tools GOR4 (Garnier *et al*., 1996) and PredictProtein (Rost *et al*., 2004).

3.2.2 Chimeric Branching Enzyme Constructs, Expression, Purification, and Analysis of Activity and Products

Chimeric branching enzyme DNA sequences were assembled based on DNA sequences of TtGBE (NC_006461.1), mSBEI (NM_001111900.1), and mSBEIIb (L08065.1) available through GenBank. Each chimeric branching enzyme sequence contained the domain A (including domain B; an insertion into domain A) of TtGBE (Palomo *et al*., 2011), and either domain C or N of mSBEI or mSBEIIb (Kuriki *et al*., 1997) (Figure 3.3.5.1). The chimeric DNA sequences were commercially synthesized (Life Technologies). To enhance the heterologous expression of chimeric branching enzymes, the sequences encoding chimeric BEs were codon optimized for expression in *E. coli*. prior to synthesis. Synthesized chimeric sequences were subcloned into pTXB1 vector in frame with the C-terminal intein chitin-binding tag, using *Nde*I and *Spe*I restriction sites (as described previously; section 3.2.2). Recombinant constructs were then expressed in *E. coli* BL21 or ArcticExpress cells, and subsequently purified *via* the intein chitin-binding tag (method in section 2.2.5). Chimeric BE activity was tested using

the iodine binding assay (method in section 3.2.3). Cimeric BE reaction product analysis was performed using HPAEC (method in section 3.2.4).

3.2.3 Iodine-Binding Assay for Detection of Recombinant BE Activity

The iodine-binding assay is based on the decrease in absorbance of the iodine-glucan complex (Bailey and Whelan, 1961; Cori and Cori, 1943) that results from BE branching activity on amylose, amylopectin, or other MOS. The reaction mixture contained, in a final volume of 100 µL, 50 mM MOPS (pH 7) and 0.025 mg amylose (Sigma catalogue no. A0512), or 0.1 mg amylopectin (Sigma catalogue no. 10120). The reaction was initiated by the addition of an appropriate amount of recombinant GBE (see Table 3.2.1). Optimal assay conditions (*e.g*. temperature, pH, enzyme concentration) were determined and used thereafter (Table 3.2.3). The reaction was terminated by heating at 95 ºC for 5 min. and cooled to room temperature. Next, 400 µL of 10 mM hydrochloric acid and 400 µL of 1X iodine solution (0.0125% (w/v) iodine and 0.04% (w/v) potassium iodide) were added to the reaction mixture. The absorbance of the reaction mixture was determined by measuring at a wavelength of 660 nm, or 520 nm (Shimadzu UV-Visible Spectrophotometer UV-1601) for amylose, or amylopectin and MOS, respectively. One unit (U) of enzyme activity is defined as the decrease in absorbance of 1.0 per min. at 660 nm for amylose, and 520 nm for amylopectin and MOS.

Table 3.2.3 Iodine Binding Assay Conditions.

Branching Enzyme	Substrate	Reaction Temperature	Typical BE Amount in Reaction (µg)
TtGBE	Amylose Amylopectin MOS	65 °C	0.13 - 1
DrGBE	Amylose Amylopectin MOS	35 °C	0.12 – 0.3
Maize SBEI	Amylose	30 °C	1 - 10
Maize SBEIIb	Amylopectin	20 °C	1 - 10

3.2.4 Analysis of Products of BE Reactions – HPAEC

The branch chain size distribution of branching enzyme reaction products was determined by hydrolyzing the α-1,6-glucosidic linkages in the resultant glucan with a debranching enzyme (isoamylase), and analysis by HPAEC. The assay was performed according to a method previously described by Annor *et al.* (2014). The branching enzyme substrate was prepared by dissolving 10-15 mg amylopectin, or *in vitro* synthesized MOS (section 4.2.2), in 90% (v/v) DMSO (50 µL) with gentle stirring for 30-60 min. Once dissolved, the solution was diluted by adding 50 mM MOPS (pH 7; 80°C) to a final volume of 1 mL. An aliquot (0.5 - 1.5 mg) was then taken for the BE reaction, which contained 50 mM MOPS (pH 7) and an appropriate amount of BE in a final volume of 450 µL. The BE reaction was incubated at a temperature appropriate for each enzyme (Table 3.2.3) for 5 h, and then terminated by heating at 95°C for 5 min. Next, 0.1 M sodium acetate buffer (50 µL; pH 4.5), and 1-2 µL isoamylase were added to the mixture and incubated at 37 °C overnight as per a standard protocol (Annor *et al*., 2014). After debranching, the reaction was terminated by boiling for 5 min., the volume adjusted

to obtain a final concentration of 1 mg/mL glucan, and the sample filtered through a 0.45 μm nylon filter (Fisher Scientific). The filtered sample (25-100 μL) was injected into the Dionex ICS 3000 HPAEC system (Dionex Corporation, Sunnyvale, CA, U.S.A.) equipped with a pulsed amperometric detector, CarboPac PA-100 ion-exchange column (4 × 250 mm), and a similar guard column (4 × 50 mm). The samples were then eluted with a flow rate of 1 mL/min. The two eluents used were 150 mM sodium hydroxide (A) and 150 mM sodium hydroxide containing 500 mM sodium acetate (B). An elution gradient was made by mixing eluent B into eluent A as follows: 0–9 min., 15–36% B; 9–18 min., 36–45% B; 18–110 min., 45–100% B; 100–112 min., 100–15% B; and 112–130 min., 15% B. The system was stabilized by elution at 15% B for 60 min. between runs. The areas under the chromatograms were corrected to carbohydrate concentration following the method of Koch *et al*. (1998). Average chain length of glucan chains separated by HPAEC was calculated using a previously established formula (Annor et al., 2014; Bertoft et al., 2008); wherein the average chain length equals sum of weight % of glucan in sample divided by sum of glucan moles in the sample.

3.3 Results and Discussion

3.3.1 CD Spectroscopy for Assessing DrGBE, TtGBE, mSBEI, and mSBEIIb Secondary Structure Stability

In preparation for chimeric BE design, the conformational stability of purified recombinant DrGBE, TtGBE, mSBEI, and mSBEIIb was investigated at 20 °C and 95 °C (or 110 °C for TtGBE), as well as in response to gradual thermal denaturation (20 °C to 95 °C, or 110 °C) using CD spectroscopy. Such data would allow estimation of the apparent melting temperature (which has not previously been reported) of these enzymes,

and thus speculation on their potential as sequence donors for designing thermostable chimeric BEs.

The purified recombinant BE solutions were prepared in 10 mM potassium phosphate buffer (pH 7), and far-UV (190 – 250 nm) data scans were collected at 20 °C and 95 °C (or 110 °C), and for thermal denaturation from 20 °C to 95 °C (or 110 °C) at a rate of 1 °C/min. at 208nm or 222 nm (method in section 3.2.1). CD was used to rapidly assess the overall secondary structure of the BEs, as the CD spectrum of a protein provides information about the content of secondary structure elements (Greenfield, 2006). The well defined different forms of secondary structure found in peptides and proteins exhibit distinct spectra (Figure 3.3.1.1) (Greenfield and Fasman, 1969; Kelly and Price, 2000). As demonstrated in Figure 3.3.1.1 the α-helical structure has three characteristic bands between 190 and 240 nm; a strong double minimum at around 222 nm and 208 – 210 nm and a strong maximum near 190 – 193 nm (Greenfield and Fasman, 1969; Sreerama and Woody, 2003; Wu *et al*., 1992). Far-UV CD spectra of β-sheet structure on the other hand, usually has a negative band in the 210 – 220 nm region and a strong positive band around 190 nm (Figure 3.3.1.1) (Greenfield and Fasman, 1969; Sreerama and Woody, 2003; Wu *et al*., 1992). The unordered protein form (random coil) tends to have a strong negative band around 195 nm and a weak positive or negative band around 218 - 220 nm (Figure 3.3.1.1) (Greenfield and Fasman, 1969; Sreerama and Woody, 2003; Wu *et al*., 1992).

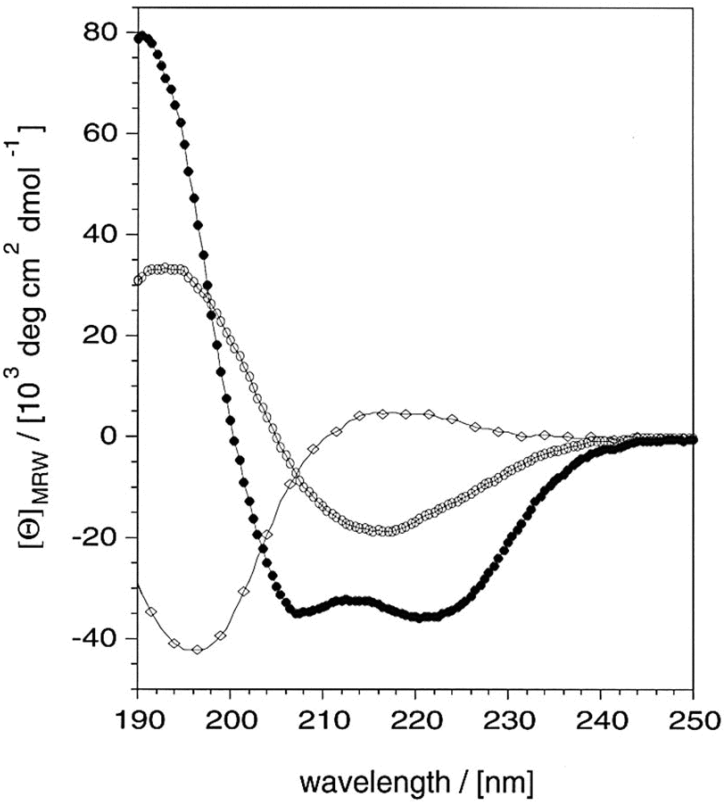

Figure 3.3.1.1 Far-UV CD spectra of different conformations of poly-L-lysine. The far-UV CD spectra of poly-L-lysine in an α-helical (black filled circles), β-sheet (open circles) and random coil (diamonds) conformation. Figure reproduced from (Greenfield and Fasman, 1969).

CD spectroscopy of the four BEs yielded spectra consistent with well-folded proteins, with a high degree of α-helical structure for TtGBE, mSBEI, and mSBEIIb, and spectra typical of a mixture of α-helical, β-sheet, and random coil structure for DrGBE (Figure 3.3.1.2; black dotted curves) (Greenfield and Fasman, 1969). Analysis of CD spectra results to predict BE secondary structure α-helix and β-strand fractions was done using a web server K2D3 (Louis-Jeune *et al*., 2012). Additionally, secondary structure prediction web tools, such as GOR4 (Garnier *et al*., 1996) and PredictProtein (Rost *et al*., 2004), which predict the backbone conformation of amino acid residues from the primary amino acid sequence, was used to predict the content of helices and strands in the tested BEs. Table 3.3.1 shows the percentage secondary structure content predicted from CD spectra and from amino acid sequence analysis. Overall, the analysis indicates that while the β-structure is present in TtGBE, mSBEI, and mSBEIIb, the α-helical structure is the dominant element. By contrast, prediction results suggest that the obtained DrGBE spectra is due to contributions from α-helical, β-sheet, and random coil structures. Similar results were previously obtained for *Mycobacterium tuberculosis* GBE and *Thermococcus kodakaraensis* KOD1 GBE (GH57 family), the far-UV CD spectra of which suggested they were rich in α-helices (Garg *et al*., 2007; Santos *et al*., 2011), while *Solanum tuberosum* SBEI spectra suggested that the dominant secondary-structural elements were β-sheets, and to a lesser extent α-helices (Khoshnoodi *et al*., 1996). The CD spectra measured at 95 °C (Figure 3.3.1.2; red dotted curves) showed some alterations to the protein secondary structure when compared to that observed at 20 °C for all four BEs. Thus, thermal denaturation studies were performed to deduce the apparent melting temperature for DrGBE, TtGBE, mSBEI, and mSBEIIb (see blow). Moreover,

the thermal stability of the secondary structure of the tested BEs determined the candidate BE sequences for chimeric BE enzyme design (see section 3.3.2 below).

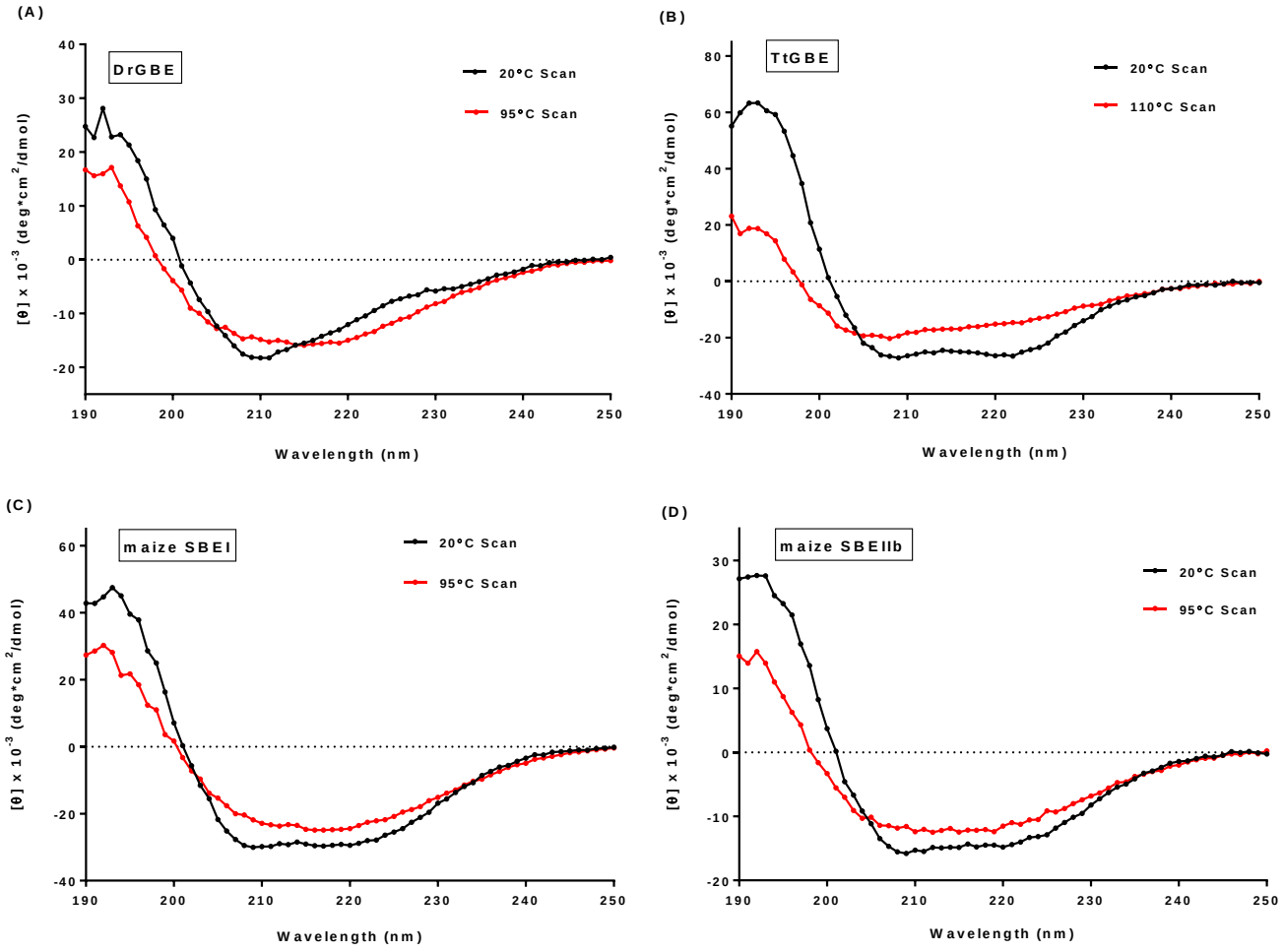

Figure 3.3.1.2 Far-UV CD spectra of DrGBE (A), TtGBE (B), mSBEI (C), and mSBEIIb (D). Variation in secondary structure was monitored in response to increase in temperature (red dotted line), and the resulting spectra were compared to ambient temperature spectra (black dotted line). Purified recombinant BEs were scanned in 10 mM potassium phosphate buffer (pH 7), and data were collected at 20 °C (black dotted line) and 95 °C (red dotted line), or 110 °C (only TtGBE; red dotted line). The presented data are an average of a minimum of 4 scans with buffer scans subtracted. The data were normalized to mean residue ellipticity (y-axis units).

Table 3.3.1 Predicted Secondary Structure Content based on CD Spectra and Amino Acid Sequence.

Branching Enzyme	CD spectra analysis[a]		Amino acid sequence analysis[b]		
	α-helix	β-sheet	α-helix	β-sheet	Random coil
DrGBE	31%	20%	22-27%	15-23%	~50%
TtGBE	44%	14%	44-48%	7-13%	~39%
Maize SBEI	58%	22%	30 - 35%	16 - 20%	~51%
Maize SBEIIb	42%	21%	29 – 31%	21 – 23%	~49%

***a** – analysis done using the obtained CD spectra data (see section 3.2.1 for details)*
***b** – analysis done using BE primary amino acid sequence (see section 3.2.1 for details)*

In order to compare structural stability under high temperature, CD thermal denaturation curves were obtained for DrGBE, TtGBE, mSBEI, and mSBEIIb (Figure 3.3.1.3). The change in structure was CD-monitored (at 208 nm for DrGBE, mSBEI, mSBEIIb, and at 222 nm for TtGBE) as the temperature was increased at a scan rate of 1 °C/min. Fitting of the denaturation curves to a 2-state model equation (Greenfield, 2006) (described in section 3.2.1) to obtain the apparent melting temperature, the temperature at which 50% of the protein is unfolded, was kindly done by Dr. Kenrick Vassall. The fitting yielded apparent melting temperatures of 61 °C ± 3.5 °C for DrGBE, 96 °C ± 1.3 °C for TtGBE, 49 °C ± 1.6 °C for mSBEI, and 59 °C ± 2.1 °C for mSBEIIb. The results suggest that the secondary structure of the tested BEs was quite resistant to thermal denaturation, in particular that of TtGBE, which exhibited ultra thermal tolerance. These

results are expected for TtGBE, which was shown to retain over 90% of activity after heating at 80 ºC for 1 h (see section 4.3.2 below; also reported by Palomo *et al*., 2011), and is an enzyme of the extreme thermophile, *Thermus thermophilus*, which is capable of proliferating at high temperatures (≥ 80 °C) (Kagawa *et al*., 1984). The derived apparent melting temperature of 61 °C for DrGBE comes as no surprise as it was previously shown to remain fully active at 50 °C after a 1 h incubation (Palomo *et al*., 2009). Therefore, it is plausible that DrGBE secondary structure contributes to its activity at elevated temperatures (≤55 °C) and remains stable at relatively high temperatures as demonstrated by its thermal denaturation curve (Figure 3.3.1.3). By contrast, the apparent melting temperature results obtained for mSBEI and mSBEIIb were not expected, as maize thrives at moderate temperatures (~15-30 °C) (Hardacre and Turnbull, 1986). Moreover, the reported optimum temperature for mSBEI and mSBEIIb activity was 33 °C and 15 – 20 °C, respectively (Takeda *et al*., 1993). It is therefore unclear why the thermal denaturation curves exhibited higher than expected melting temperatures for mSBEI and mSBEIIb. However, maintenance of secondary structure does not necessarily guarantee maintenance of activity (Dong *et al*., 1996; Garg *et al*., 2007), meaning that although the mSBEI and mSBEIIb mid-point denaturing temperatures were found to be quite high (49 °C and 59 °C, respectively), this finding does not guarantee activity at high temperatures.

The BE batches assessed in far-UV CD analysis were also checked for activity using the iodine binding assay and standard reaction conditions (section 3.2.3) (Figure 3.3.1.4). All four tested BEs (DrGBE, TtGBE, mSBEI, and mSBEIIb) were active,

implying that these enzymes were in a native conformation conducive to their activity at the time of far-UV CD and CD-monitored thermal denaturation assessment.

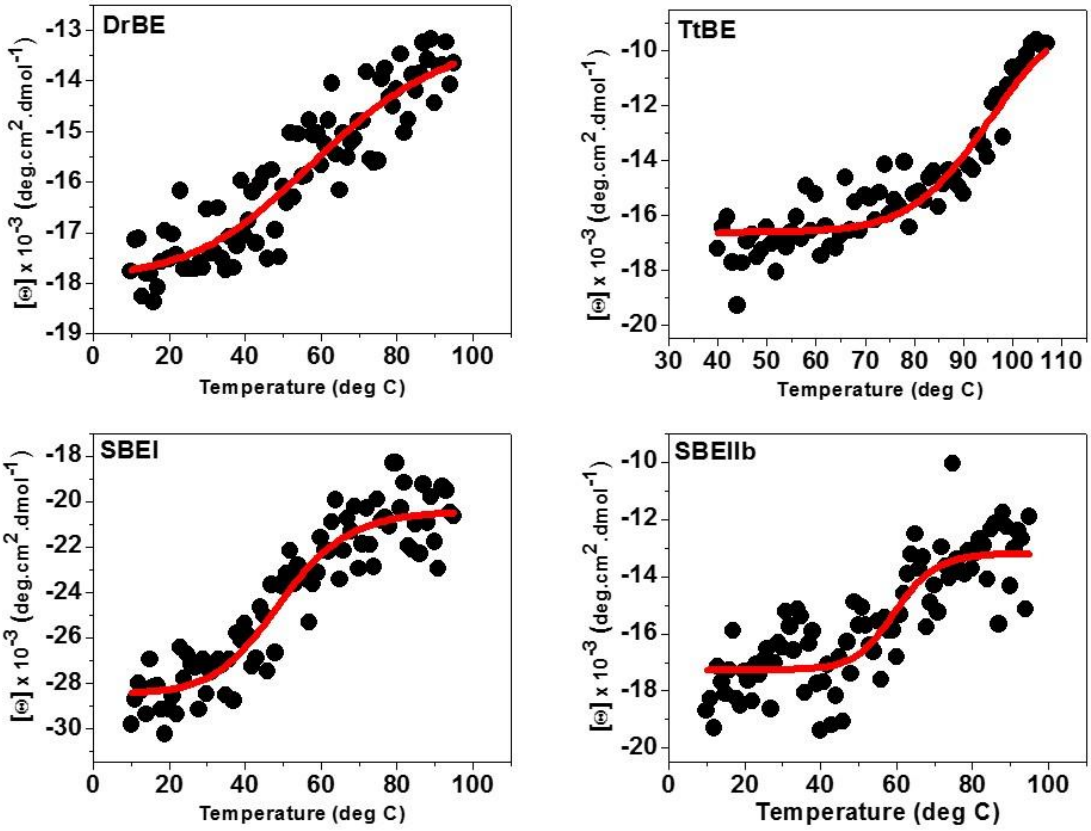

Figure 3.3.1.3 Representative full-length DrGBE, TtGBE, mSBEI, and mSBEIIb thermal-melt data. BEs were suspended 10 mM potassium phosphate buffer (pH 7) and the CD-monitored change in secondary structure (208 nm for DrGBE, SBEI, SBEIIb, and at 222 nm for TtGBE) was recorded as the temperature was increased at a scan rate of 1 °C/min. The effects of buffer were subtracted from the data before fitting to a 2-state model (folded ↔ unfolded; solid red line) in order to obtain the apparent mid-point temperature of the unfolding transition. These fitted apparent mid-points were 61 °C ± 3.5 °C for DrGBE, 96 °C ± 1.3 °C for TtGBE, 49 °C ± 1.6 °C for SBEI, and 59 °C ± 2.1 °C for SBEIIb. The presented data were normalized to mean residue ellipticity (see section 3.2.1 for unit explanation).

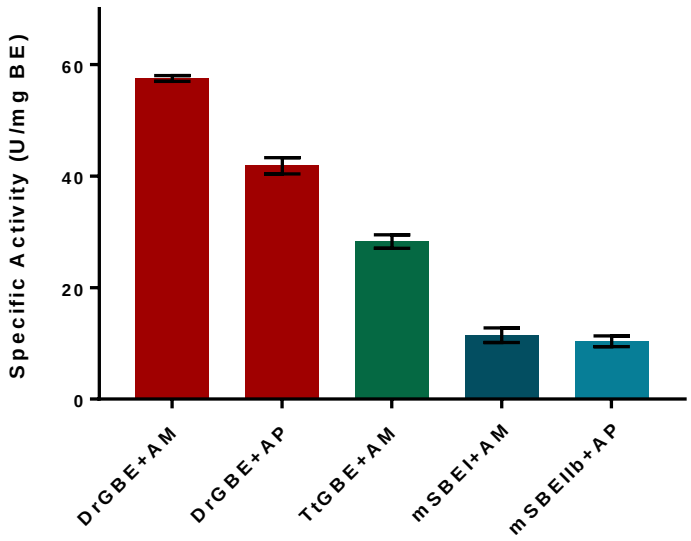

Figure 3.3.1.4 Activity of DrGBE, TtGBE, mSBEI, and mSBEIIb used for far-UV CD assessment and for CD-monitored thermal denaturation studies. Activity was assessed using the iodine binding assay and standard reaction conditions (see section 3.2.3 for method details). Each BE was tested with its appropriate substrate (either amylose – AM; or amylopectin – AP). Results are the average of three different experiments, and the error bars represent the SD of the replicas.

3.3.2 Chimeric Branching Enzymes

The observed thermal stability of TtGBE, as well as mSBEI and mSBEIIb, secondary structure made the sequences of these BEs choice candidates for chimeric branching enzyme design. The detailed understanding of the structural and functional relationships of BE enzyme protein domains presents a potentially useful tool for modifying post-harvest starch structure through the use of chimeric enzymes designed for particular starch altering applications. Chimeric branching enzyme design took a number of elements into account, such as thermostability, branching specificity, and substrate preference. The TtGBE sequence was exploited for its potential to conform thermostability, while the N- and C-terminal domain sequences of mSBEI and mSBEIIb were exploited for their potential to contribute to branching specificity and substrate preference. The designed chimeric BE constructs, Tt-SBEI-C, Tt-SBEI-N, Tt-SBEIIb-C, and Tt-SBEIIb-N are demonstrated in Figure 3.3.2.1 below.

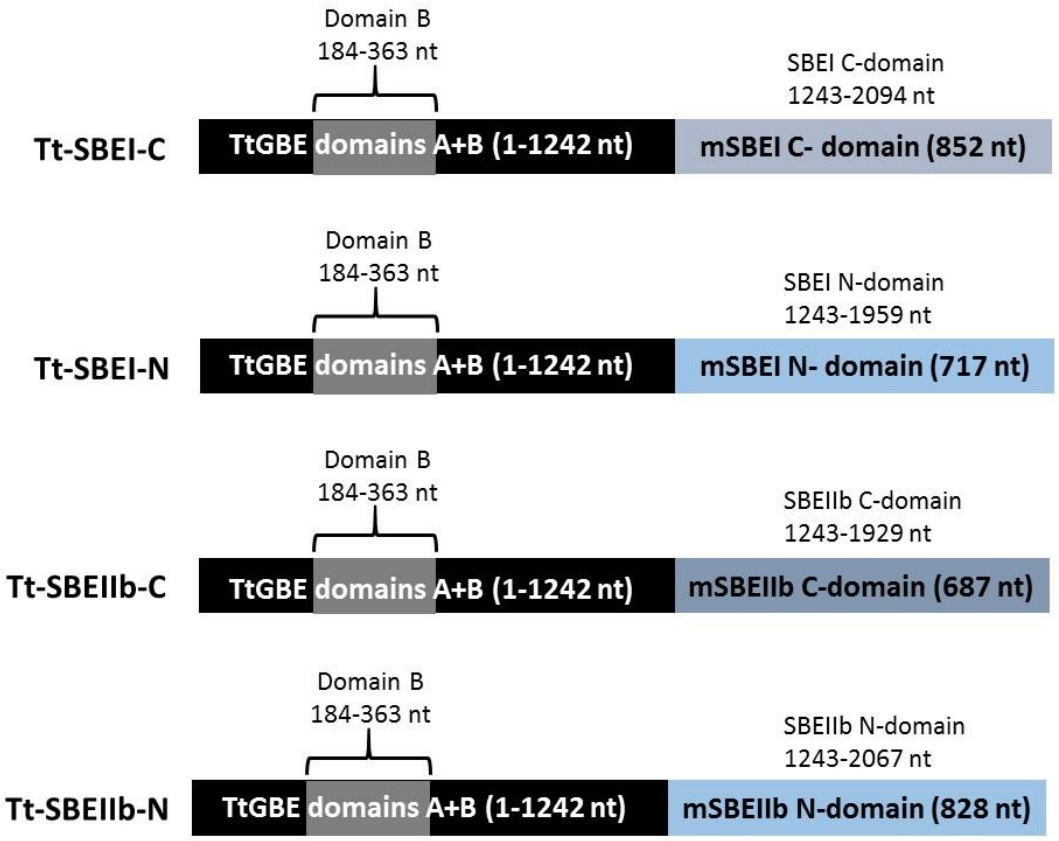

Figure 3.3.2.1 Schematic representation of the chimeric enzyme constructs. The chimeric enzymes consisted of the A and B domains of TtGBE ligated to either a C- or N- terminal domain of mSBE or mSBEIIb. Lengths of the domains are indicated and correspond to the nucleotide numbering of the respective native BE. The name of each chimeric construct is indicated to the left of the schematic.

Chimeric BE sequences were cloned into the pTXB1 vector and fused directly to the intein-CBD tag at its amino terminus (section 3.2.2 for cloning details). The recombinant chimeric BE constructs were transformed into BL21 (DE3) and ArcticExpress (DE3) cells. Prior to expression experiments, recombinant plasmids were purified and used for insert sequencing. Sequencing results confirmed presence of full length chimeric sequences of Tt-SBEI-C, Tt-SBEI-N, and Tt-SBEIIb-N, while the sequence of Tt-SBEIIb-C was incomplete. Tt-SBEIIb-C was not further characterized due to inability to clone the full chimeric sequence. Chimeric BEs were expressed and purified as previously described (see sections 2.2.4 and 2.2.5 for method details). Expression results yielded a large portion of aggregated protein for all three chimeric BEs post purification. Figure 3.3.2.2 depicts the purification results of chimeric Tt-SBEI-C, Tt-SBEI-N, and Tt-SBEIIb-N with the expected native sizes of 77 kDa, 72 kDa, and 76 kDa, respectively. Elution (from chitin beads; method in section 2.2.5) of purified tag-free chimeric BEs yielded low amounts of all three recombinant proteins (in particular Tt-SBEIIb-N) as indicated by the black arrows in Figure 3.3.2.2 (lanes: E). Additionally, in the case of all three chimeric BEs, some tag-free protein remained on chitin beads post elution (lane AE, red arrow; Figure 3.3.2.2), which indicates that the protein was insoluble and aggregated (Chong *et al*., 1997). Although the eluate fraction showed presence of purified tag-free chimeric proteins, it does not mean that the recombinant proteins were properly folded, and a portion may very well have been aggregated. The low observed activity of chimeric Tt-SBEI-C, Tt-SBEI-N, and Tt-SBEIIb-N (Figure 3.3.2.3 below) may be due to the presence of aggregates in the purified protein fraction, which may lead to protein conformational deformity and prevent activity.

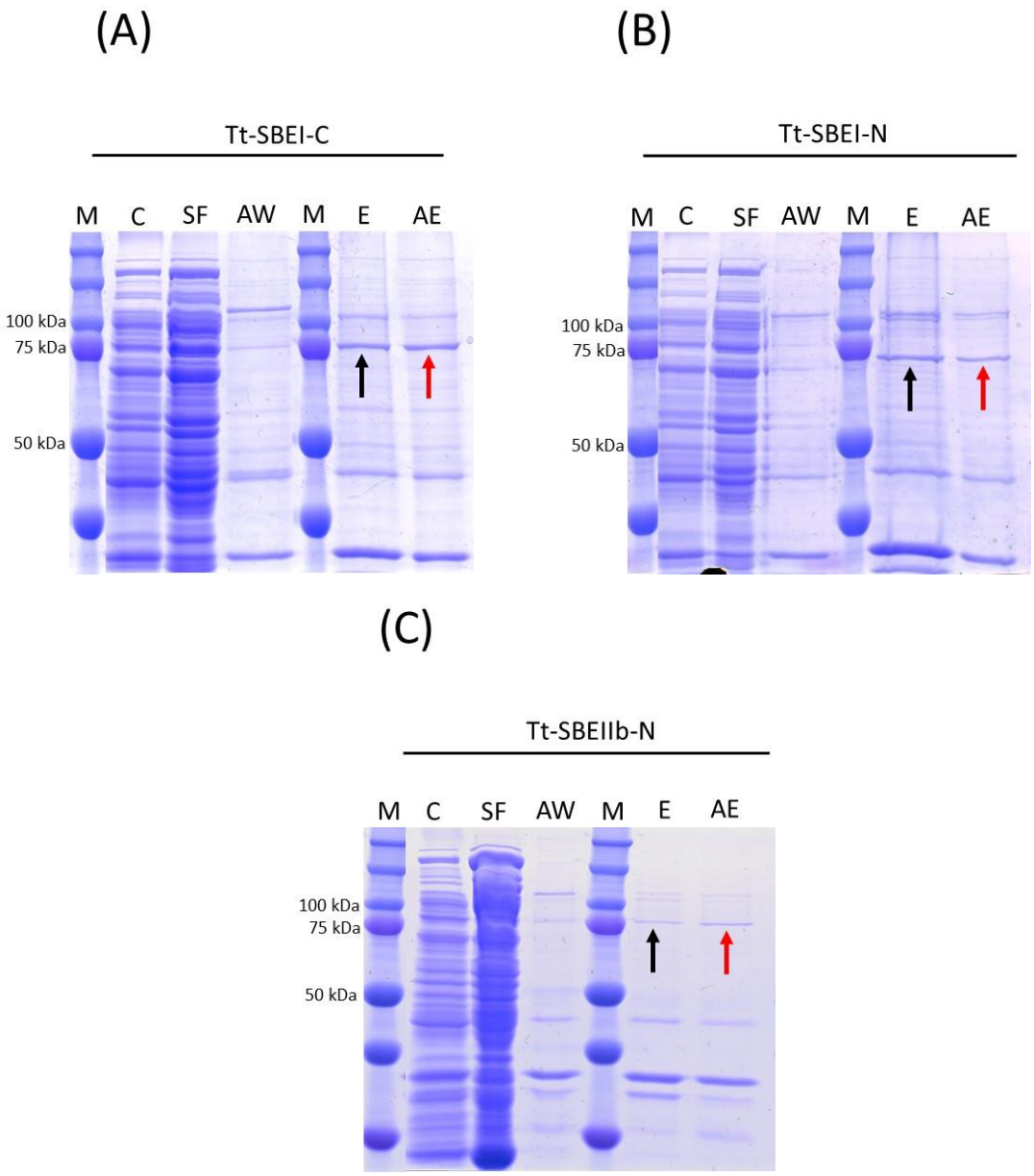

Figure 3.3.2.2 Affinity purification of recombinant intein-CBD tagged chimeric BEs, Tt-SBEI-C (A), Tt-SBEI-N (B) and Tt-SBEIIb-N (C). Cells were lysed and centrifuged in order to separate the soluble fraction from inclusion bodies. The soluble fraction was applied to chitin resin column, which was then washed. The intein-CBD tag on the corresponding recombinant chimeric BEs was cleaved with 50 mM DTT, and the recombinant protein eluted from the resin and detected by Coomassie Blue staining. Approximately 0.5-10 µg total protein was loaded per lane. Black arrows, eluted tag-free protein; red arrows, tag-free protein remaining on chitin beads post elution. Lanes: M, protein marker; C, pre-induction control; SF, soluble fraction flow through; AW, chitin resin after wash; E, eluate of purified tag-free recombinant protein; AE, chitin resin after elution.

Efforts were undertaken to optimize expression and purification to obtain a larger portion of soluble chimeric protein with potentially proper structural conformation which would facilitate chimeric BE activity (data not shown). Optimization efforts included expression and purification (from soluble fraction and inclusion bodies) of recombinant chimeric enzymes in the presence of arginine, which has been suggested to have suppressive effects on protein aggregation, although the mechanism of action is yet to be elucidated (Chen *et al*., 2008; Schäffner *et al*., 2001; Tsumoto *et al*., 2004). Additionally, optimization methods included chimeric protein purification in the presence of detergent (*e.g*. 0.5 - 1% Triton X-100), which has been suggested to improve the yield of bioactive proteins (Chen *et al*., 2008; Privé, 2007; Singh and Panda, 2005), and use of glycerol in storage buffer to enhance stability of the recombinant protein as glycerol has been shown to act as an amphiphilic interface between hydrophobic patches of the protein and the polar solvent, thereby preventing protein aggregation (Vagenende *et al*., 2009). Optimization efforts did not yield sufficient amounts of soluble and active recombinant chimeric proteins, which hindered comprehensive characterization. However, preliminary assessment of chimeric BE activity was performed with the available purified recombinant chimeric BEs, despite a large portion of it being aggregated protein. Chain length distribution analysis of products of one chimeric BE (Tt-SBEI-C) was also performed.

The branching activity of purified recombinant chimeric enzymes was assayed using the iodine-binding assay and standard reaction conditions (see section 3.2.3) at 30 °C and 60 °C with amylose as substrate (Figure 3.3.2.3). The chimeric enzymes exhibited branching activity; however, it was much lower compared to their native counterparts,

TtGBE and mSBEI (Figure 3.3.2.3). Tt-SBEI-C exhibited the highest activity of all three chimeric BEs, with a specific activity of approximately 2.1 U/mg chimeric BE at 30 °C. By comparison, the specific activities of TtGBE and mSBEI were 28.3 U/mg and 11.5 U/mg, respectively. Due to the low activity of Tt-SBEI-C, a thorough characterization under different reaction conditions (*e.g.* temperature and pH) and with various substrates could not be carried out, although useful information was gained on chain length transfer preferences (see below).

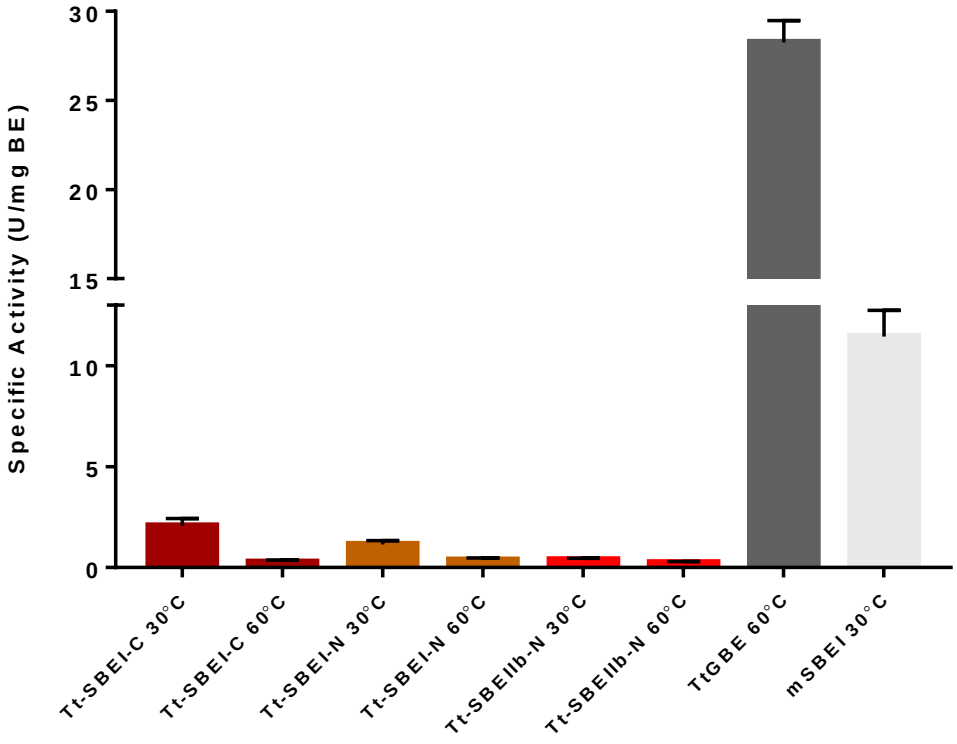

Figure 3.3.2.3 Comparison of specific activities of chimeric BEs with activities of TtGBE and mSBEI. Activities of chimeric BEs (10 µg), TtGBE (0.3 µg; ~0.15 mU), and mSBEI (1 µg) were assayed using the iodine binding assay with 0.1 mg amylose as substrate at various temperatures as indicated in the figure. Specific activity is expressed as U/mg protein and the results are an average of at least three different experiments with the error bars representing the standard deviation.

Chain length distribution analysis of Tt-SBEI-C, TtGBE, and mSBEI was performed using HPAEC (see section 3.2.4 for method details). BEs were incubated overnight with short MDs (DP 4 – 43) to assess chain length transfer preferences with short linear α-1,4-glucans. Preliminary results of HPAEC analysis of Tt-SBEI-C products showed a decrease of chains of DP 4 – 7 and DP 20 – 42, and an increase in chains of DP 8 – 19 (Figure 3.3.2.4 C). Similarly, HPAEC results of TtGBE products showed a decrease of chains of DP 4 – 5 and DP 17 – 37, and an increase in chains of DP 6 – 16 (Figure 3.3.2.4 A). mSBEI HPAEC results were also similar, showing a decrease in chains of DP 4 – 9 and DP 26 – 43, and an increase in chains of DP 10 – 25 (Figure 3.3.2.4 B).

The observed decrease in short chains in products of all three enzymes most likely indicates hydrolytic activity. TtGBE has been previously shown to possess hydrolytic activity (this thesis; section 4.3.2), wherein the cleaved donor segment is not reattached to create a branch (Palomo *et al*., 2011). Specifically, it has been demonstrated that TtGBE hydrolyzed chains of DP 3 – 13 (Palomo *et al*., 2011). It is therefore plausible, that the decrease in the number of chains of DP 4 – 7 in the products of Tt-SBEI-C, which is partly composed of domains A and B of TtGBE, is due to hydrolytic activity, like that of TtGBE.

Previous studies have shown mSBEI (with amylose as substrate) preferentially transfers longer chains with a broad distribution of lengths and a high frequency of chains of DP 11 – 12 (Kuriki *et al*., 1997; Takeda *et al*., 1993). Similarly, this study found that with MDs as substrate, mSBEI transferred longer chains with a broad distribution of chain lengths (DP 10 – 25), with a high frequency of chains of DP 10 – 12 (Figure 3.3.2.4

B). TtGBE has also been previously shown to transfer a range of chain lengths with amylose as substrate, however, the chains tended to be shorter, specifically chains of DP 4 – 16, with a preference for DP 6 chains (Palomo *et al*., 2011). The results obtained here for TtGBE with MDs as substrate, corroborated previous findings, and suggest that TtGBE abundantly transfers chains of DP 6 – 16 with MDs as substrate (Figure 3.3.2.4 A).

The results obtained through HPAEC analysis suggest that Tt-SBEI-C also transfers shorter to medium length chains, with a relatively broad distribution of lengths, specifically chains of DP 8 – 19 (Figure 3.3.2.4 C). Therefore, the overall results suggest that chain length transfer preferences of Tt-SBEI-C resemble more that of TtGBE, rather than mSBEI. However, unlike TtGBE products, Tt-SBEI-C and mSBEI products showed persistence of longer chains (DP ≥ 37). Therefore, the preliminary analysis of Tt-SBEI-C chain length transfer preferences suggests that Tt-SBEI-C combines branching preference elements of both TtGBE and mSBEI.

The differential plots in Figure 3.3.2.5 suggest that the minimum CL required for branching MDs by Tt-SBEI-C is 20 (Figure 3.3.2.5 C), while the minimum CL required for branching by TtGBE and mSBEI, is 17 and 26, respectively (Figure 3.3.2.5 A and B). Therefore, the results suggest that the minimum CL required for branching MDs by Tt-SBEI-C is intermediate between those of TtGBE and mSBEI, the native counterparts of the chimeric enzyme. Allowing the branching reaction to proceed longer (>12 h) may have reduced the minimum CL required for branching MDs by all three tested enzymes.

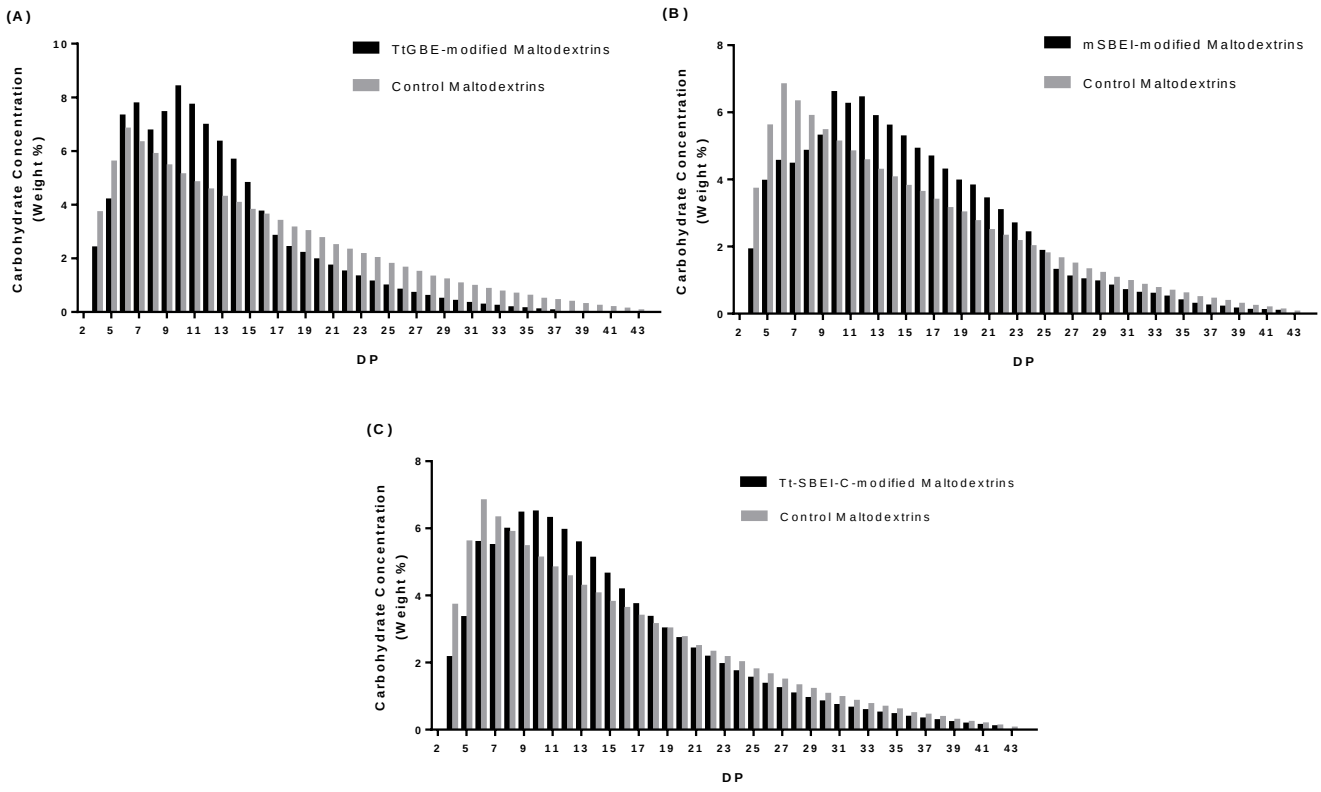

Figure 3.3.2.4 HPAEC analysis of debranched products formed from Tt-SBEI-C (A), TtGBE (B), and mSBEI (C) activity with MDs (DP 4-43). MDs (0.5 mg) were treated with Tt-SBEI-C (22 µg), TtGBE (2.6 µg; ~1.3 mU), and mSBEI (10 µg) under standard reaction conditions in 50 mM MOPS-NaOH (pH 6.5) overnight. The reaction products were debranched by isoamylase (in 100 mM sodium acetate pH 4, 37 °C) overnight.

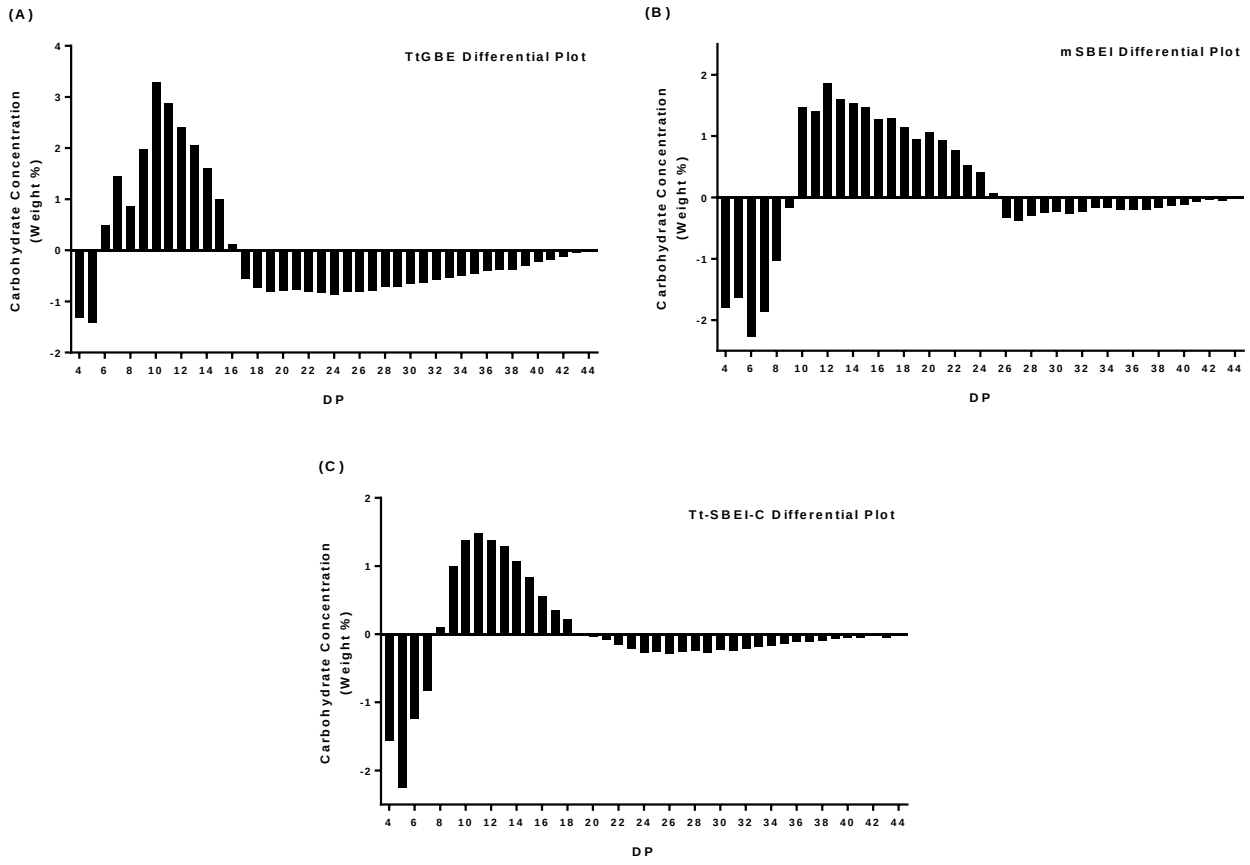

Figure 3.3.2.5 Differential plots of Tt-SBEI-C (A), TtGBE (B), and mSBEI (C) activity with MDs. Reaction conditions were as described above for Figure 3.3.5.4. The differential plots reflect the difference between CLD profiles of MDs before and after modification by the chimeric enzyme and BEs (CLD profile of BE-modified polyglucans minus CLD profile of untreated polyglucans).

3.3.3 Concluding Remarks

CD-monitored thermal denaturation studies of DrGBE and TtGBE secondary structure stability showed that both GBEs had high melting temperatures, especially TtGBE (~96 °C). Chimeric enzymes, composed of sequence elements of TtGBE, mSBEI, and mSBEIIb were designed. However, due to low exhibited branching activity, only one chimeric enzyme (Tt-SBEI-C) was characterized to a limited degree. The Tt-SBEI-C chimeric sequence was composed of A and B domains of TtGBE, and of the C-terminal domain of mSBEI. Tt-SBEI-C showed branching preferences intermediate between those of TtGBE and mSBEI.

Chimeric BE sequences were designed with the rationale in mind of their potential to be suited for a range of industrial processing conditions and to potentially create unique glucan polymers with distinct structures that may exhibit novel properties. Future efforts will include further optimization of chimeric BE expression and purification, as well as designing novel chimeric BE variants, in order to attempt more thorough biochemical characterization to reveal potential utility in industrial processing of post-harvest starch.

Chapter 4 – Characterization of Activity and Product Analysis of DrGBE and TtGBE

4.1 Introduction

GBEs can be distinguished in terms of their reactivity with different substrates, temperature responses, and the nature of the formed products (van der Maarel *et al*., 2002; Nakamura *et al*., 2010). In order to unveil the characteristics of GBE reactions, it is crucial to separate and quantify the various unit glucan chains with different DP values in the glucan substrate (linear or branched) for GBE and its reaction products. In earlier studies on the BE reaction mechanism, the products of the reactions were debranched and separated by conventional gel permeation chromatography (GPC), although the resolution of this technique did not always allow an accurate representation of all the present glucan chains (Borovsky *et al*., 1975b, 1976, 1979). In more recent years, BE reaction products were mainly quantified by high-performance anion-exchange chromatography equipped with a pulsed amperometric detector (HPAEC-PAD), which provides more detail, such as the amount of the individual unit glucan chains (Koch *et al*., 1998; Roussel *et al*., 2013). Continued improvement of the HPAEC column materials are making it possible to separate individual maltooligosaccharides (MOS) with a degree of polymerization up to 80 with high resolution (Koch *et al*., 1998).

To characterize GBEs, it is important to determine the kinetic parameters, and the appropriate glucan substrates (Nakamura *et al*., 2010). In addition to amylose and amylopectin, synthetic MOS, which were enzymatically synthesized *in vitro* by rabbit-muscle phosphorylase *a* from maltoheptaose and G1P, were used. The MOS were linear glucans free from *α*-1,6-glucosidic linkages, which possessed varied molecular masses and allowed determination of GBE glucan chain transfer preferences. Additionally,

maltodextrins were also used as substrate for determining TtGBE glucan chain transfer preferences. Maltodextrins are produced commercially through enzymatic hydrolysis of starch using amylolytic enzymes, which degrade starch and convert it into low-molecular weight maltodextrins (de Souza and de Oliveira Magalhães, 2010).

GBE activity is typically assayed by three methods; the phosphorylase *a* stimulation assay, the iodine binding assay, and the branch linkage assay (Guan and Preiss, 1993; Hawker *et al*., 1974). The semi-quantitative phosphorylase *a* stimulation assay is based on the principal of measuring the BE stimulation of synthesis of *a*-D-glucan catalyzed by phosphorylase *a* (Hawker *et al*., 1974). The non-quantitative iodine binding method is based on monitoring the decrease in absorbance of the glucan-iodine complex as a consequence of branching (and reduced chain length) catalyzed by BE (Borovsky *et al*., 1975b). The quantitative branch-linkage assay is based on the direct measurement of the number of branch linkages (generated reducing ends) introduced into a glucan substrate by BE (Guan and Preiss, 1993; Takeda *et al*., 1993). Although the phosphorylase *a* stimulation assay and the iodine binding assay are amongst the most frequently used methods for determining BE activity, they are both semi-quantitative. The branch linkage assay, on the other hand, allows for the quantitative determination of the number of α-1,6 branch points introduced by the BE following debranching and assay of reducing ends by Cu(II) to Cu(I) reduction using bicinchoninic acid (Utsumi *et al*., 2009). The branch linkage assay is useful not only to determine the BE enzymatic activity on the molar basis, but also to determine the kinetic parameters (Utsumi *et al*., 2009). In the presented work, the iodine binding assay and the branch linkage assay were utilized to characterize the activity of GBEs.

In this chapter, a detailed biochemical and functional characterization of overexpressed recombinant DrGBE and TtGBE is reported. The biochemical assessment of the activity and kinetics of these GBEs was examined using the quantitative branch linkage assay (section 4.2.1) as well as the iodine binding assay (section 3.2.3). Additionally, products of GBE reactions, specifically their branch chain length distribution, were analyzed using HPAEC-PAD (section 3.2.4).

4.2 Methods

4.2.1 Branch Linkage Assay for Detection of Recombinant BE Activity

The branch-linkage assay is a direct and quantitative method for assaying BE activity, and is based upon the principle of measuring the actual number of branch points introduced by BE into a substrate (Takeda *et al*., 1993). The assay was performed according to the technique developed by Waffenschmidt and Jaenicke (1987) with a modification as outlined by Utsumi *et al*. (2009). Total assay volume was 100 μL, containing 50 mM MOPS pH 7, 0.033-0.1 mg of gelatinized amylose (Sigma catalogue no. A0512) or 0.017 mg amylopectin (Sigma catalogue no. 10120), and 1-2 μL purified recombinant BE (approximately 0.12 - 2 μg recombinant protein). The mixture was incubated for 20 min. at 35°C or 65-70°C for DrGBE and TtGBE, respectively, and terminated by heating at 100 °C for 5 min. 100 μL of 0.1 M sodium-acetate (pH 3.5) and 2 μL of isoamylase (1000 U/mL; Megazyme, catalogue no. E-ISAMY) were added into the mixture and incubated at 37°C for 90 min. to debranch the α-1,6-glucosidic linkages. The debranching treatment was stopped by boiling at 100°C for 5 min. Reactions were then briefly centrifuged to collect all liquid (approximately 200 μL), and 100 μL of

solution A (97.1 mg of disodium 2.2-bicinchoninate, 3.2 g of sodium carbonate monohydrate and 1.2 g of sodium bicarbonate in a total volume of 50 mL) and 100 μL of solution B (62 mg of copper sulphate pentahydrate and 63 mg of L-serine in a total volume of 50 mL) were added to the mixture. The resulting mixture was incubated at 100°C for 15 min. After cooling to room temperature, 200 μL of the resulting solution was transferred to a 96 well-plate and the absorbance measured using a microplate spectrophotometer (ThermoScientific Multiskan GO) at 560 nm. The BE activity was calculated from the difference in absorbance of samples containing substrate only (boiled BE, or no BE) subtracted from samples with added BE. A standard curve was generated using known amounts of glucose and the absorbance at 560 nm was found to be proportional to the concentration of glucose in the range of 0 - 25 μM (Figure 3.2.2.1). One U of branching activity was defined as 1 μmol of α-1,6 linkages synthesized per min. For the determination of the pH profile, amylose was used as substrate in the following buffers; 100 mM sodium acetate (pH 5 to 6), 50 mM MES-NaOH (pH 6 to 7), 50 mM MOPS-NaOH (pH 7 to 8), 50 mM Tricine (pH 8 to 9), or 250 mM sodium carbonate (pH 9 to 10). For redox modulation studies, GBEs were treated with 10 mM DTT for reduction, or with 10 mM sodium tetrathionate for oxidation. Reduced or oxidized GBE was then incubated with amylose in a standard reaction mixture (as described above) for 5, 10, 20, or 40 min. After the branching reaction ran its course, it was boiled for 5 min. to inactivate the GBE. All assay mixtures (control and samples) were then subjected to filtration through a Sephadex™ G-25 gravity column (GE Healthcare illustra™ NAP-5 columns) to remove excess reducing (DTT) and oxidizing (sodium tetrathionate) agents.

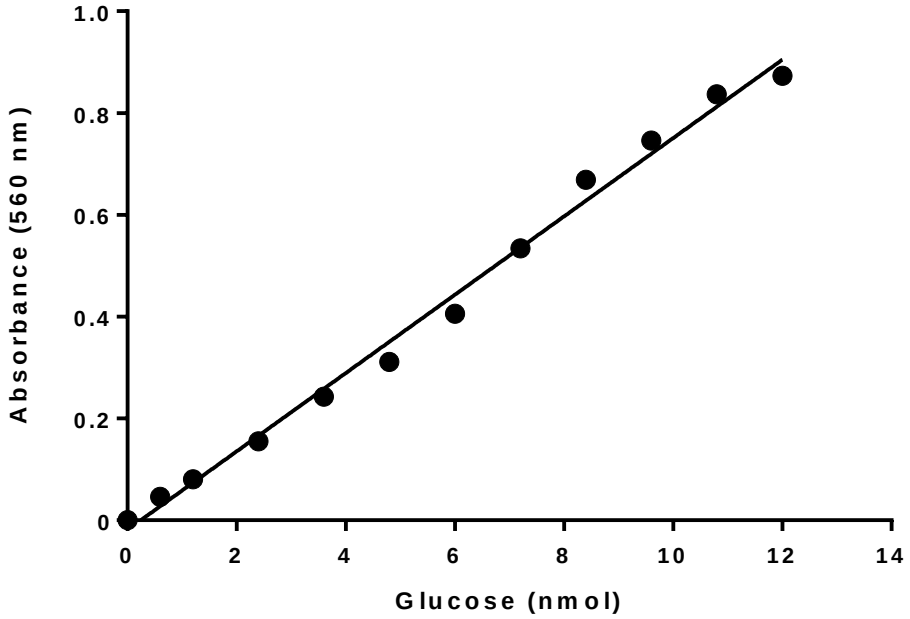

Figure 4.2.1 A glucose standard curve depicting the relationship between glucose concentration and absorbance at 560 nm as measured by the branch linkage assay using the bicinchoninic acid reagent.

4.2.2 Phosphorylase *a*-Catalyzed MOS Synthesis

In vitro synthesized MOS were used as substrate in BE activity assays and for BE reaction product analysis. *In vitro* synthesis of MOS was performed *via* phosphorylase *a* catalyzed polycondensation using a modification of the method developed by van der Vlist *et al*. (2012). Phosphorylase *a* catalyzed the formation of linear polysaccharides from G1P, the donor substrate, and maltoheptaose, the acceptor substrate. The reaction mixture contained, in a final volume of 1 mL, 100 mM Tris-HCl buffer (pH 6.8), 700 mM G1P, 3.5 mM maltoheptaose, 1 mM DTT, 3 mM adenosine monophosphate (AMP), and 3, 6, or 9 U rabbit-muscle phosphorylase *a* (Sigma-Aldrich, catalogue no. P-123). The reaction mixture was incubated at 30 °C, with gentle agitation, for 2-5 h. Reactions were then terminated by boiling for 5 min., cooled to room temperature, and denatured

enzyme removed by means of centrifugation (14,000 g, 5 min.). The reaction mixture was then dialyzed (MWCO 0.5 - 1 K; Float-A-Lyzer G2, Spectrum Laboratories) against buffer (20 mM Tris-HCl pH 6.8) to remove excess G1P, AMP, and DTT for 15 or 40 h. The resulting mixture was then vacuum dried and stored at -20 °C until analysis by HPAEC column, or used as substrate for BE activity assays.

4.2.3 Determination of Kinetic Parameters

Kinetics studies were performed using the branch linkage assay as described for specific activity determination (section 4.2.1). The Km and Vmax parameters were determined for TtGBE over a range of amylose concentrations; specifically, 0.08, 0.17, 0.33, 0.50, 0.67, and 0.83mg/mL. The Km and Vmax parameters were also determined for DrGBE over a range of amylose concentrations; specifically, 0.07, 0.14, 0.29, 0.49, 0.69, and 0.89 mg/mL, as well as over a range of amylopectin concentrations; specifically, 0.024, 0.049, 0.069, 0.089, 0.109, and 0.129 mg/mL. The reactions were followed for 20 min., which is within the linear portion of the reaction as determined from the progress curves for DrGBE and TtGBE. Data was fitted to irreversible single substrate Michaelis-Menten model (rectangular hyperbola) by non-linear regression using Prism 7.0 (GraphPad Software Inc., San Diego, CA).

4.3 Results and Discussion

4.3.1 Assessment of Effect of Temperature, pH, and Redox State on GBE Activity

Effect of Temperature on Activity

To understand the nature of DrGBE and TtGBE enzymatic activity, some of their biochemical properties were studied, these included the effect of temperature, pH, and redox state.

The effect of temperature on DrGBE and TtGBE activity was examined using the iodine binding assay and standard reaction conditions (section 3.2.3; Figure 4.3.1.1). DrGBE activity was determined over a temperature range of 25 ºC to 85 ºC (Figure 4.3.1.1 A). DrGBE was quite active in the temperature range of 25 ºC to 55 ºC, with maximal activity between 25 ºC and 35 ºC (Figure 4.3.1.1 A; Table 4.3.1). The activity of DrGBE dropped sharply at temperatures above 55 ºC. Palomo *et al*. (2009) reported a similar trend for DrGBE activity in a range of temperature spanning between 30-40 ºC, with maximal activity at 34 ºC (Table 4.3.1). TtGBE activity was determined over a temperature range of 25 ºC to 80 ºC (Figure 4.3.1.1 B; Table 4.3.1). TtGBE exhibited activity in the temperature range of 55 ºC to 80 ºC, with maximal activity at 70 ºC. It seems that TtGBE showed more variability in its stability over a broader range of temperature than DrGBE, exhibiting activity (at least some) at 25 ºC to 80 ºC, while DrGBE activity dropped drastically above 55 ºC.

Thermostable enzymes are often desired in the starch processing industry, as the gelatinization temperature of starch is 60–75 °C (Jobling, 2004; Röper, 2002). Therefore, the temperature stability of TtGBE was tested to determine whether TtGBE would have a potential application in starch processing. Over 90% of TtGBE activity was retained after heating the enzyme at 80 ºC for 1 h. A previous publication had reported a similar

observation wherein TtGBE remained fully active after an incubation for 1 h at 80 ºC (Palomo *et al*., 2011). A comparison of optimum temperatures for activity of various GBEs and SBEs is shown in Table 4.3.1.

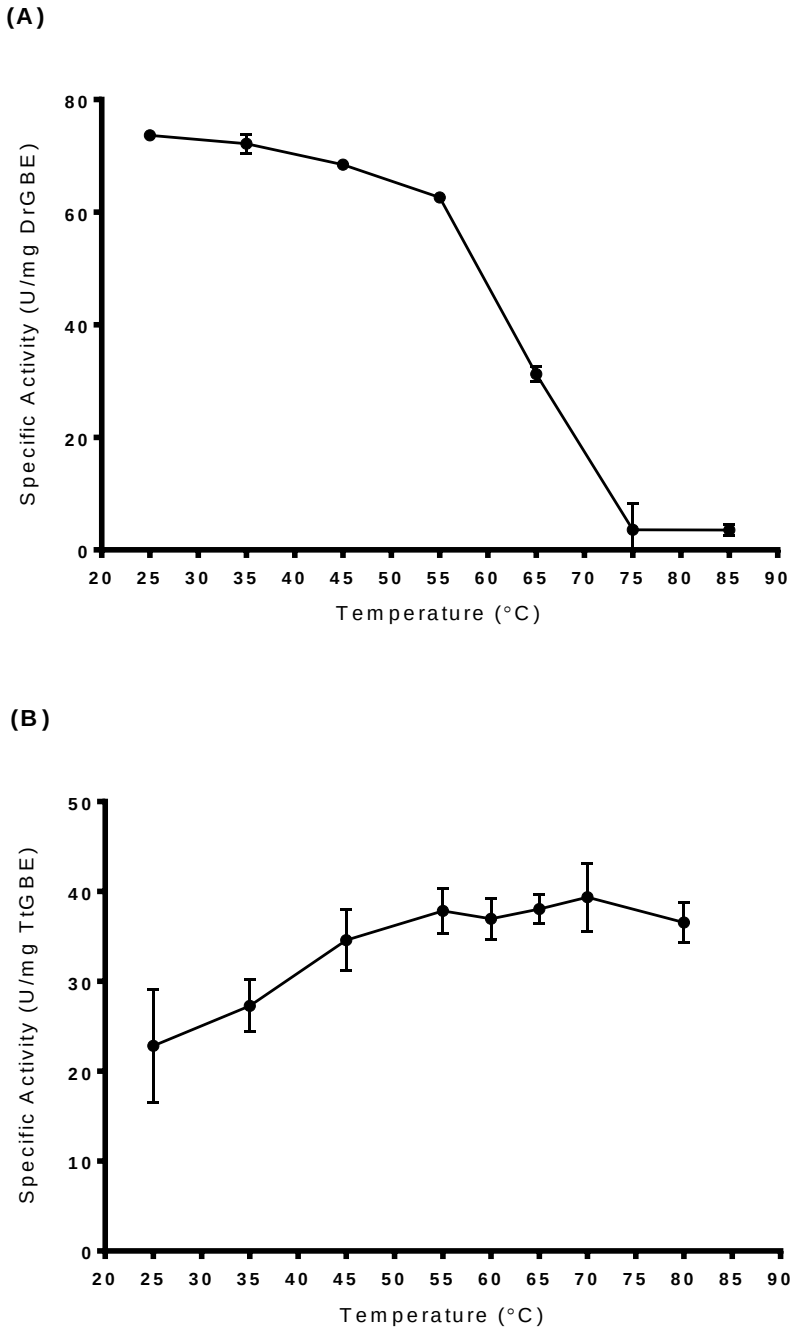

Figure 4.3.1.1 Effect of temperature on the activity of DrGBE (A) and TtGBE (B). Optimal temperature was determined by measuring enzyme activity at different temperatures (as indicated in figure) using the iodine binding assay. Activity was assayed in 50 mM MOPS-NaOH (pH 7) with amylose as substrate under standard reaction conditions as described in section 3.2.3. Values are the mean ± SD of three replicates.

Table 4.3.1 Temperature and pH Stability of Various Branching Enzymes.

Branching Enzyme	Optimum Temperature for Activity	Optimum pH for Activity	Reference
TtGBE	70 ºC	6 - 7	Nasanovsky, 2017 (this thesis)
	65 ºC	6.5	Palomo *et al*., 2011
DrGBE	25 – 35 ºC	7	Nasanovsky, 2017 (this thesis)
	34 ºC	8	Palomo *et al*., 2009
AaGBE	75 ºC	7.5 – 8	Takata *et al*., 2003
	80 ºC	7.5	Van Der Maarel *et al*., 2003
***Bacillus stearothermophilus* GBE**	50 ºC	7.5	Takata *et al*., 1994
***Rhodothermus obamensis* GBE**	65 ºC	6 - 6.5	Shinohara *et al*., 2001
***Mycobacterium tuberculosis* GBE**	30 ºC	7	Garg *et al*., 2007
***Ec*GBE**	30 ºC	7.7	Guan *et al*., 1997
Mazie SBEI	33 ºC	7.5	Takeda *et al*., 1993
Maize SBEIIb	15-20 ºC	7.5	Takeda *et al*., 1993

pH Stability

The effect of pH on DrGBE and TtGBE activity was examined using the quantitative branch linkage assay, standard reaction conditions (section 4.2.1), and the following buffers; 100 mM sodium acetate (pH 5 to 6), 50 mM MES-NaOH (pH 6 to 7), 50 mM MOPS-NaOH (pH 7 to 8), 50 mM Tricine (pH 8 to 9), or 250 mM sodium carbonate (pH 9 to 10) (Figure 4.3.1.2). DrGBE was quite active in the range of pH 6 to 8, and the optimum pH for activity was 7 (Figure 4.3.1.2). A previous study had reported similar results of pH effects on DrGBE activity wherein DrGBE was active in a relatively broad range of pH 7 to 9, with maximal activity at pH 8 (Table 4.3.1) (Palomo *et al*., 2009). TtGBE was active in the range of pH 6 to 7, with maximum activity at pH 6

(Figure 4.3.1.2). Palomo *et al*. (2011) observed maximal TtGBE activity at pH 6.5 (Table 4.3.1), which was corroborated by the optimum pH for TtGBE activity obtained through this study. Table 4.3.1 above displays values of optimum pH for activity of various GBEs and SBEs for comparison purposes.

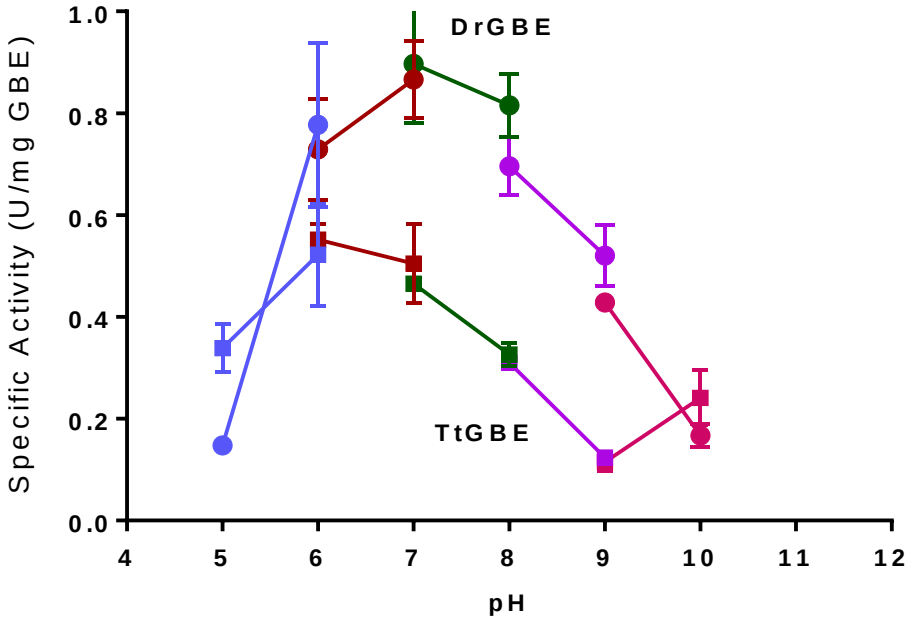

Figure 4.3.1.2 Effect of pH on the activity of DrGBE and TtGBE. Optimum pH was assessed by measuring enzyme activity at the indicated pH using the branch linkage assay (section 4.2.1). Activity was assayed with amylose as substrate and the pH range was determined in 100 mM sodium acetate (pH 5 to 6; blue), 50 mM MES-NaOH (pH 6 to 7; red), 50 mM MOPS-NaOH (pH 7 to 8; green), 50 mM Tricine (pH 8 to 9; purple), or 250 mM sodium carbonate (pH 9 to 10; pink) buffer. Values are the mean ± SD of three replicates. Squares, TtGBE activity; Circles, DrGBE activity.

Effects of Reducing and Oxidizing Conditions on Activity

Previous studies have shown that the activity of some BEs is affected by redox state. Redox modulation is based on breaking and re-forming of specific disulfide bonds between cysteine residues in the polypeptide chain of the BE in response to the redox state. For example, Arabidopsis SBE 2 showed reductive activation under reducing conditions (Glaring *et al*., 2012), while although mSBEIIb (Makhmoudova, 2014 unpublished) and *Anaerobranca gottschalkii* (Ag) GBE (Thiemann *et al*., 2006) were active in non-reducing conditions, addition of a reducing agent resulted in an increase in mSBEIIb activity, and a 2.4-fold spike in the activity of AgGBE. Additionally, a study using an immuno-proteomics approach in wheat indicated that wheat SBEIIa is also redox-regulated (Balmer *et al*., 2006). As part of characterizing the nature of DrGBE and TtGBE activity, redox mediated effects on branching activity were assessed. As this may have implications for their future use in industrial applications.This has not previously been published, and thus constitutes a novel aspect of the presented work.

In order to quantitatively analyze the effect of modulating the redox conditions *in vitro*, DrGBE and TtGBE enzymatic activity was assessed using the branch linkage assay and amylose as substrate, after treatment with reductant (10 mM DTT) or oxidant (10 mM sodium tetrathionate) to obtain a fully reduced or oxidized GBE, respectively. Manipulation of redox potentials revealed that neither DrGBE, nor TtGBE activity was affected by the reduction or oxidation treatment (Figure 4.3.1.3), suggesting that their involvement in glycogen biosynthesis is most likely not regulated by redox modulation. However, conformational changes, in response to reducing or oxidizing conditions, of DrGBE and TtGBE enzyme structure have not been monitored, and thus lack of

regulation by redox modulation of these GBEs can not be firmly concluded as redox-dependent conformational changes can affect interactions with other cellular components (Garg *et al*., 2007). Similarly, Garg *et al*. (2007) showed that *Mycobacterium tuberculosis* GBE (MtGBE) activity was not affected by the redox state, although redox-dependent conformational changes were observed using near-UV CD spectroscopy. Redox-dependent conformational states of MtGBE have different surface hydrophobicities, which may play a role in MtGBE regulation during glycogen synthesis by influencing the interaction or dissociation of different cellular proteins with MtGBE in response to different physiological redox states (Garg *et al*., 2007). Lack of redox state effect on DrGBE and TtGBE activity may be beneficial for their potential use as tools in industrial starch processing, as processing conditions often include oxidizing and/or reducing agents (Dias *et al*., 2011).

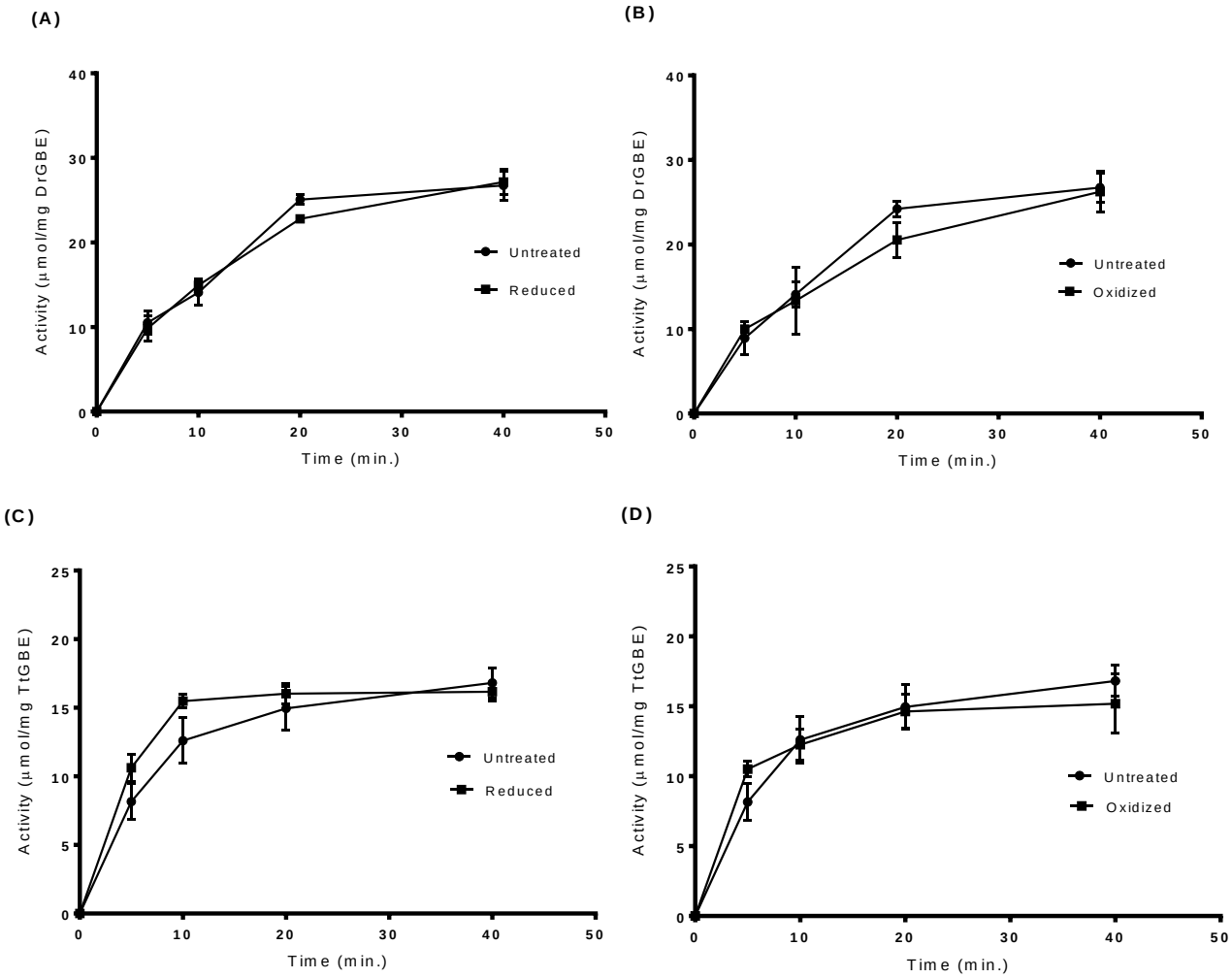

Figure 4.3.1.3 Redox mediated effects on DrGBE and TtGBE activity. Enzymatic activity was assayed using the branch linkage assay, and standard reactions contained 0.3 mU DrGBE, 0.5 mU TtGBE and 0.1 mg amylose as substrate. Prior to assaying branching activity, DrGBE and TtGBE were either reduced with 10 mM DTT (A or C, respectively), or oxidized with 10 mM sodium tetrathionate (B or D, respectively). The determined DrGBE and TtGBE specific activities (with amylose) were used to calculate the units of GBE used, and correspond to 1.64 U/mg and 0.5 U/mg, respectively (section 4.3.2).

4.3.2 Assessment of Activity and Kinetic Parameter Determination for DrGBE and TtGBE

Time Course Experiments

Time course experiments were performed to investigate the activity of DrGBE and TtGBE with amylose and amylopectin as substrates. Progress curve data describe the activity of an enzyme with a substrate, and show the period of linear enzymatic activity. Progress curve results have not previously been determined (or published) for DrGBE and TtGBE, and therefore constitute a novel aspect of the presented research.

The branch linkage assay was utilized to determine product formation (generation of α-1,6 glycosidic linkages), wherein standard reaction mixtures were incubated under optimal conditions for each GBE (see section 4.2.1). To determine branching activity, the amount of branches originally existing in the substrate was measured by the same procedure, but without addition of GBE (or with added boiled GBE), and was subtracted from the amount of branches in samples with GBE added. Product formation was monitored over 75 min., and the resulting progress curves of the reactions catalyzed by DrGBE and TtGBE exhibited typical hyperbolic shapes (Figure 4.3.2.1), indicating an initial increase in product formation ultimately followed by leveling off possibly due to various factors such as, substrate depletion, product inhibition, and enzyme denaturation (Stenesh, 1998). Product formation appears to increase linearly for approximately 20 min. in the DrGBE catalyzed reaction with amylose, or amylopectin, as substrate (Figure 4.3.2.1 A and B). By contrast, the TtGBE catalyzed reaction with amylose as substrate shows a linear reaction rate within approximately the first 40 min. of the reaction. TtGBE showed no branching activity with amylopectin (Figure 4.3.2.1 C), and this finding is in agreement with previous studies (Palomo *et al*., 2011).

The specific activities of DrGBE and TtGBE with amylose and amylopectin as substrates were determined under standard reaction conditions (section 4.2.1) and within the linear range of enzymatic activity. The specific activity of DrGBE with amylose and amylopectin, as determined by the branch linkage assay, was ~1.64 U/mg and ~1.15 U/mg, respectively. The resulting specific activity of DrGBE with amylose is somewhat lower than the specific activity of 4.70 U/mg reported by Palomo *et al*., (2009) (Table 4.3.2). The discrepancy in the values could be due to different standard reaction conditions. The specific activity of TtGBE with amylose was 0.50 U/mg, which is similar to the specific activity value of 0.29 U/mg reported by Palomo *et al*., (2011) (Table 4.3.2). The specific activities of other GBEs and SBEs, as determined by the branch linkage assay, have been previously reported and are listed in Table 4.3.2 for comparison purposes.

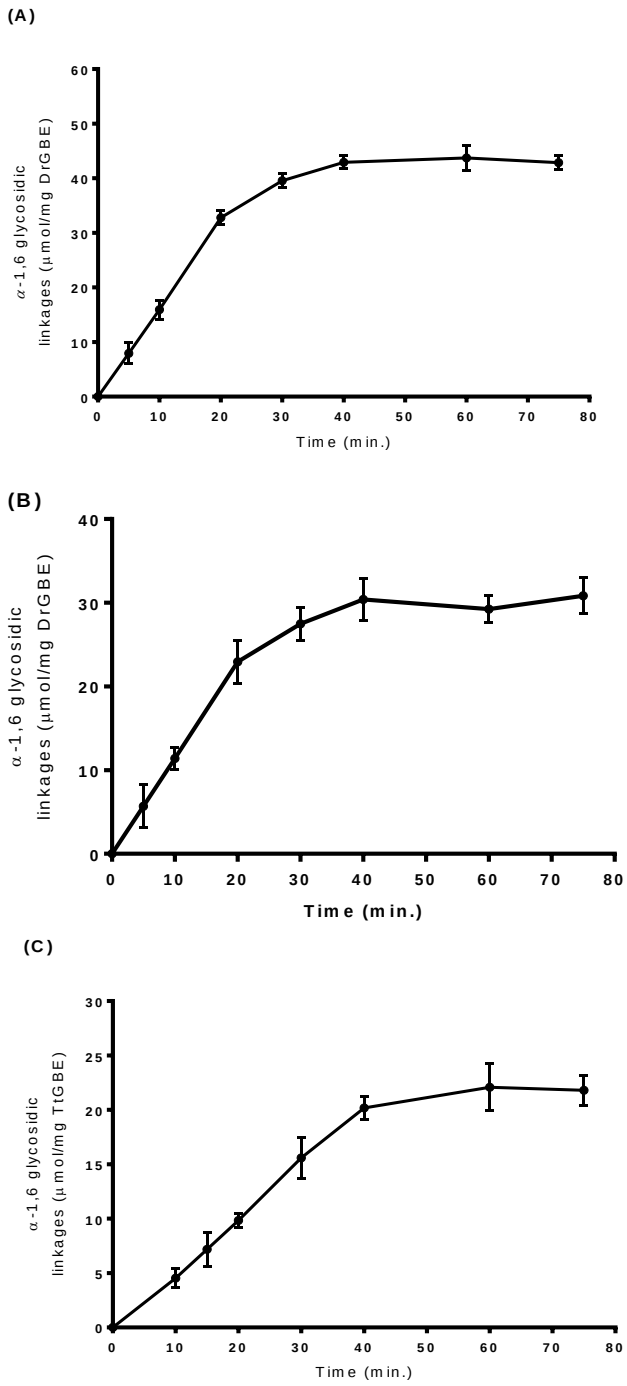

Figure 4.3.2.1 Progress curves of reactions catalyzed by DrGBE with amylose (A) and amylopectin (B) as substrates, and TtGBE with amylose (C) as substrate, measured by the branch linkage assay. Standard reactions contained either 120 - 300 ng DrGBE with 0.14 mg amylose, or 0.017 mg amylopectin, or 130 ng TtGBE and 0.14 mg amylose in 50 mM MOPS-NaOH (pH 7). Reactions were performed from 0 to 75 min. and subsequently terminated by boiling. Values are the mean ± standard deviation (SD) of three replicates.

The branch linkage assay allows discrimination between the branching activity and the hydrolytic activity of GBEs. The GBE is incubated with a glucan substrate and the amount of α-1,6 branch points introduced is determined by measuring the difference in the amount of reducing ends before (hydrolytic activity) and after debranching (total activity) of the product by isoamylase (Takeda *et al*., 1993).

The hydrolytic activity of DrGBE and TtGBE on amylose and amylopectin was determined (Figure 4.3.2.2). DrGBE displayed less than 2% hydrolytic activity of total activity with amylose as a substrate (Figure 4.3.2.2 A), which is similar to the DrGBE hydrolytic activity with amylose (less than 1% of total activity) reported by Palomo *et al*. (2009). The hydrolytic activity of DrGBE with amylopectin as a substrate was less than 0.5% of total activity (data not shown). In contrast, TtGBE displayed a relatively high hydrolytic activity, considering it is a branching enzyme, of approximately 10% of total activity with amylose as a substrate (Figure 4.3.2.2 B). A hydrolytic activity of approximately 10% of total activity was also observed by Palomo *et al*. (2011) for TtGBE with amylose as a substrate. Similarly, a previous study involving the characterization of *Anaerobranca gottschalkii* GBE, had also shown that this enzyme possesses hydrolytic activity when incubated with dextrins, but not when incubated with amylose (Thiemann *et al*., 2006).

TtGBE did not show branching activity with amylopectin, it did, however, show hydrolytic activity when incubated with amylopectin (Figure 4.3.2.2 C). A similar pattern was observed by Palomo *et al*. (2011) who reported presence of hydrolytic activity, and a lack of branching activity, of TtGBE on amylopectin. Note that in Figure 4.3.2.2 C, the number of reducing ends at t = 0 is not equal zero, and that is because the amylose

substrate inherently contains a certain amount of α-1,6 branch points in it, which are released following a debranching treatment. TtGBE did not further branch the amylopectin substrate, and thus the number of reducing ends does not vary much between time points.

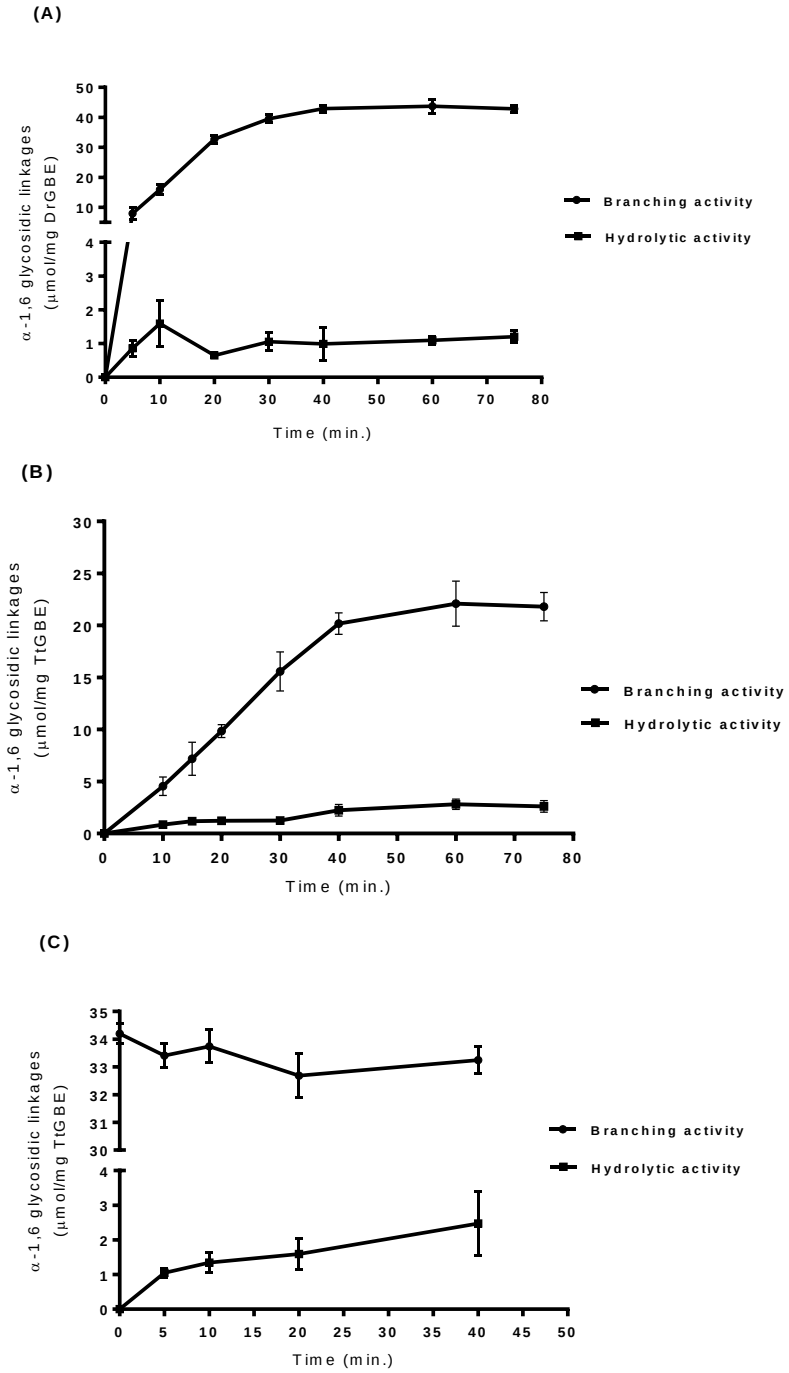

Figure 4.3.2.2 Branching versus hydrolytic activity displayed by DrGBE with amylose as substrate (A), and TtGBE with amylose (B) and amylopectin (C) as substrate, measured by the branch linkage assay. Standard reactions contained either 120 - 300 ng DrGBE with 0.14 mg amylose or 0.017 mg amylopectin, or 130 ng TtGBE and 0.14 mg amylose in 50 mM MOPS-NaOH (pH 7). Reactions were performed from 0 to 75 min. and subsequently terminated by boiling. Values are the mean ± SD of three replicates. In (C), value at time zero in the branching activity curve represents branches present in the substrate (amylose).

Kinetic Analysis

The kinetic properties of DrGBE and TtGBE have not been previously reported. The kinetic parameters of purified recombinant DrGBE and TtGBE were investigated using the branch linkage assay with amylose and amylopectin (only for DrGBE) as substrates. The velocity (enzyme activity) was obtained at various substrate concentrations, and product formation was monitored for 20 min. (within the linear range of enzyme activity). Plots of velocity (enzyme activity; U/mg GBE) against various amylose or amylopectin concentrations (mg/mL; Figure 4.3.2.3) revealed a rectangular hyperbola that fit the Michaelis–Menten equation by non-linear regression. For ease of presentation of these data, double-reciprocal plots (1/V vs. 1/[S]) were also established (Figure 4.3.2.3 inset). The apparent kinetic parameters, K_m and V_{max}, for DrGBE with amylose or amylopectin as substrate, and for TtGBE with amylose as substrate, were obtained by fitting velocity (V) versus substrate concentration ([S]) data to the Michaelis-Menten equation (non-linear regression), and from linear transformation of the data by the Lineweaver-Burk double reciprocal plot using GraphPad Prism 7.0 software. A disadvantage of the double-reciprocal plot is that it tends to be distorted by experimental errors, especially by data obtained at low substrate concentrations (Belitz and Grosch, 1999; Dowd and Riggs, 1965). However, despite its shortcomings, the double-reciprocal plot is still widely used, and typically if the data fit a rectangular hyperbola fairly closely, they can be readily analyzed using the Lineweaver-Burk plot (Dowd and Riggs, 1965).

The apparent K_m values obtained by hyperbolic regression (non-linear regression) for DrGBE with amylose and amylopectin as substrates were ~0.27 mg/mL, and ~0.07 mg/mL, respectively (Figure 4.3.2.3 A and B). The K_m values obtained from the double

reciprocal plot (linear regression) were very similar, with 0.32 mg/mL and 0.071 mg/mL for DrGBE with amylose and amylopectin, respectively. The Michaelis-Menten constant, K_m, is defined as the substrate concentration required to attain half of the maximum enzyme velocity, and a lower K_m value represents a stronger affinity of the enzyme towards the substrate (Counotte and Prins, 1979; Dowd and Riggs, 1965; Michaelis and Menten, 1913). Based on the preliminary kinetic analysis presented here, a lower K_m value was obtained for DrGBE with amylopectin as substrate (compared to amylose as substrate), suggesting a higher affinity of DrGBE towards amylopectin, and thus a preference for amylopectin over amylose as substrate. A similar substrate preference trend was suggested by Palomo et al. (2009), although it was based on a semi-quantitative activity assay (iodine-binding) results, rather than on kinetic parameters.

Hyperbolic regression analysis of data of TtGBE with amylose as substrate gave an apparent K_m value of 0.11 mg/mL, and linear regression by a double-reciprocal plot yielded a similar K_m value of 0.15 mg/mL(Figure 4.3.2.3 C). The kinetic parameter that represents the maximal enzymatic activity, or velocity, when the enzyme is fully saturated with substrate, is referred to as V_{max} (Counotte and Prins, 1979; Dowd and Riggs, 1965; Michaelis and Menten, 1913). V_{max} values were reported in units (µmol/min.) per milligram of BE protein as they are comparable with previously published values (see Table 4.3.2)

The apparent V_{max} values determined from non-linear regression analysis for DrGBE were ~1.7 U/mg and ~1.2 U/mg with amylose and amylopectin, respectively (Figure 4.3.2.3 A and B). Linear regression analysis yielded similar V_{max} values corresponding to DrGBE activity of ~1.73 U/mg with amylose, and ~1.20 U/mg with

amylopectin. The apparent V_{max} value for TtGBE with amylose as substrate, calculated using non-linear regression, was 0.38 U/mg (Figure 4.3.2.3 C). A similar V_{max} value of 0.42 U/mg was also obtained by non-linear regression. Similar kinetic parameters were previously reported for other GBEs and SBEs and are summarized in Table 4.3.2.

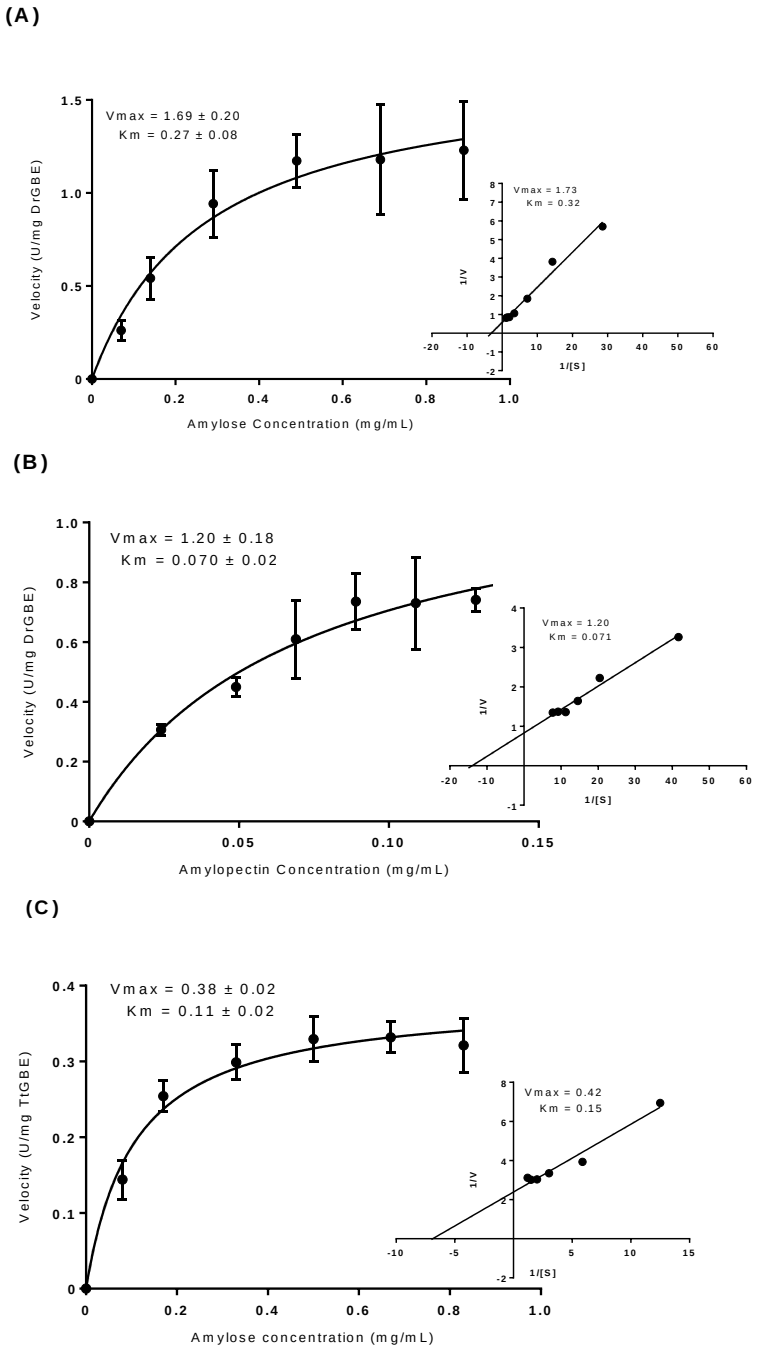

Figure 4.3.2.3 Michaelis–Menten enzyme kinetics plots of the DrGBE activity with amylose (A) and amylopectin (B), and of the TtGBE activity with amylose (C). The Lineweaver–Burk plots are shown as insets. Velocity is expressed as U (μmol $min.^{-1}$)/mg GBE, and substrate concentration as mg/mL. Reaction conditions and substrate concentrations used are as described in sections 4.2.1 and 4.2.3. Values are the mean ± SD of three replicates.

Table 4.3.2 Kinetic Parameters and Specific Activities of Various Branching Enzymes.

Branching Enzyme	K_m	V_{max}	Specific Activity	Reference
TtGBE	0.11 mg/mL	0.38 U/mg	0.5 U/mg (current study)	Nasanovsky, 2017 (this thesis)
	N/D	N/D	0.29 U/mg	Palomo *et al*., 2011
DrGBE	0.27 mg/mL	1.69 U/mg	1.64 U/mg (current study)	Nasanovsky, 2017 (this thesis)
	N/D	N/D	4.70 U/mg	Palomo *et al*., 2009
AaGBE	4.0 µM	4.90 U/mg	N/D	Van Der Maarel *et al*., 2003
***E. coli* GBE**	11.7 µM	3.70 U/mg	1.10 U/mg	Binderup and Preiss, 1998
			0.59 U/mg	Guan *et al*., 1997
mSBEI	8.4 µM	3.30 U/mg	2.10 U/mg	Binderup and Preiss, 1998; Kuriki *et al*., 1997
			3.2 U/mg	Guan *et al*., 1997
mSBEIIb	8.4 µM	0.62 U/mg	0.40 U/mg	Binderup and Preiss, 1998
			0.2 U/mg	Guan *et al*., 1997

Determined by the branch linkage assay with amylose as substrate
U; µmol/min.
N/D; was not determined

4.3.3 Analysis of DrGBE and TtGBE Products

The products of DrGBE and TtGBE branching reactions were subjected to HPAEC analysis to characterize the *in vitro* branching properties of the GBEs. The length of the branches introduced by DrGBE and TtGBE into a glucan substrate was determined by incubating the purified recombinant GBEs with either MOS (see section 4.2.2 for synthesis method), or maltodextrins (MDs) (only TtGBE), or amylopectin (DrGBE only), followed by analysis of the side-chain distribution by HPAEC after debranching with isoamylase (see section 3.2.4 for method details). TtGBE was not assessed with amylopectin as it does not show branching activity with amylopectin, and is only able to hydrolyze this polyglucan (see section 4.3.2; Figure 4.3.2.2 C). Amylose is often used as

substrate for analysis of BE reaction product chain-length distribution by HPAEC. However, this study (side-chain distribution analysis) did not employ the use of amylose as substrate due to the limitation of the used HPAEC column, which is not suitable for separating polyglucans of > DP 85.

GBEs differ in their preferences for the sizes of chains transferred and the minimum required chain length for branching (Guan *et al*., 1997; Kuriki *et al*., 1997; Sawada *et al*., 2014; Takata *et al*., 2003; Thiemann *et al*., 2006), and therefore it was important to examine the branching specificities of DrGBE and TtGBE. As a branching reaction proceeds, the number of longer chains decreases, as long as the size of the chain is sufficiently long to serve as a donor substrate for the BE (Guan *et al*., 1997; Roussel *et al*., 2013). Simultaneously, shorter chains formed from the longer donor chains accumulate as they are now too short to serve as a donor substrate (Guan *et al*., 1997; Roussel *et al*., 2013). Monitoring the changes in chain length distribution (CLD) by HPAEC, and differential plotting of CLD profiles of the substrate glucan before and after modification by BE, allows to define the minimum chain length required for branching (the minimum preferred donor substrate chain length), and the preferred transferred chain length.

Generally, it is accepted that if some chains increased post GBE reaction, it means that these chains were the transferred chains (donor segments), or residual chains or segments of donor chains (Borovsky *et al*., 1976). The results obtained from HPAEC analysis of DrGBE action on amylopectin showed a substantial increase in chains of DP 6-8 and a moderate increase in chains of DP 9-12, while chains of DP≥13 decreased (Figure 4.3.3.1 A and B). These results suggest that DrGBE preferentially transfers

(branches) short chains of DP 6-8 by attacking chains of DP≥13, and the increase in chains of DP 9-12 is most likely due to the formation of residual segments from the donor chains (DP≥13). However, it is important to note that a portion of the shorter chains (DP 6-8) may also be composed of residual segments formed from the longer donor chains (DP≥13). Additionally, chains of DP 4-5 were observed post DrGBE reaction with amylopectin, which were not present in the untreated amylopectin substrate (Figure 4.3.3.1 A). These chains can be assumed to be the residual segments of longer glucan chains that were used as donor substrate, as chains of DP 4 - 5 would be too short to be accommodated in the active site of DrGBE and thus could not have served as donor segments (transferred chain) (Nakamura *et al*., 2010; Palomo *et al*., 2009). This is consistent with the results reported below showing the inability of DrGBE to use maltoheptaose (DP 7) as a substrate for branching (Figure 4.3.3.2). The HPAEC results also indicate that products made by DrGBE action on amylopectin showed optima at side-chains containing 10 glucosyl residues, and an average chain length (CL) of 10 glucosyl units (Figure 4.3.3.1 A).

The differential plot in Figure 4.3.3.1 B shows the difference between the CLD profiles of amylopectin before and after modification by DrGBE. The negative values in the differential plot indicate that the corresponding glucans were consumed by DrGBE during the reaction and therefore acted as donor substrate. On the other hand, the positive values represent the glucans that increased after DrGBE action, suggesting that these glucans were produced from the cleavage of longer glucans and the transfer of the cleaved chain to create an α-1,6 branch point. The results obtained from HPAEC analysis suggest that the minimum CL required for branching by DrGBE is 13, when amylopectin

was the substrate (Figure 4.3.3.1 B). The results thus indicate that DP≥13 linear segments of amylopectin are suitable donor-substrates for DrGBE. The minimum chain length (DP) required for branching amylopectin by *Rhodothermus obamensis* GBE and by mSBEIIb was 12 (Guan *et al*., 1997; Roussel *et al*., 2013), and is similar to the minimum CL (of DP 13) required for branching of amylopectin by DrGBE (Table 4.3.3). The optima of 10 glucose residues in the side-chain profile of DrGBE-modified amylopectin is similar to the optima of the side-chain profile of AaGBE-modified amylopectin (DP 12) (Takata *et al*., 2003). However, the side-chain CL optima observed for amylopectin modified by other GBEs is quite different; DP 7 for *Rhodothermus obamensis* GBE, and DP 6-7 for mSBEIIb (Guan *et al*., 1997; Van Der Maarel *et al*., 2003; Roussel *et al*., 2013; Takata *et al*., 2003). The average CL of the DrGBE-modified amylopectin side-chain profile was 10, and is quite different from the average CL obtained for amylopectin modification by AaGBE and *Bacillus stearothermophilus* GBE of 16 and 15.5 glucosyl residues, respectively (Takata *et al*., 2003). It is plausible to speculate that the differences in the side-chain distribution of branched glucan products formed by various BEs are likely due to the subtle differences in their active site architecture.

As indicated by Figure 4.3.3.2, maltoheptaose was not a suitable substrate for DrGBE (not previously empirically established). Incubation of DrGBE with maltoheptaose did not yield branched products, and there was no overall change in chain-length distribution between the untreated and DrGBE-treated maltoheptaose profiles. These results suggest that maltoheptaose is too short to be efficiently accommodated in the DrGBE active site, and therefore cannot be used as substrate for cleavage and generation of a donor substrate (branch to be transferred). Palomo *et al*. (2009)

hypothesized, based on their findings, that the substrate glucan chain is accommodated in part in the DrGBE N2 module (of the N-terminal domain; Figure 1.3.3 in Chapter 1) glucan binding subsites, while the donor segment to be transferred is in the donor subsites of the active site, and that substrates longer than 7 glucosyl residues are accommodated (Palomo *et al*., 2009). Recently, the N2 module was annotated as a carbohydrate binding module (CBM48) (Palomo *et al*., 2009). It is therefore likely that the N2 module may play a role in the branching preferences of DrGBE, and the distance between the glucan binding subsites in the active site and the CBM48 subdomain may affect the average lengths of side chains transferred (Palomo *et al*., 2009).

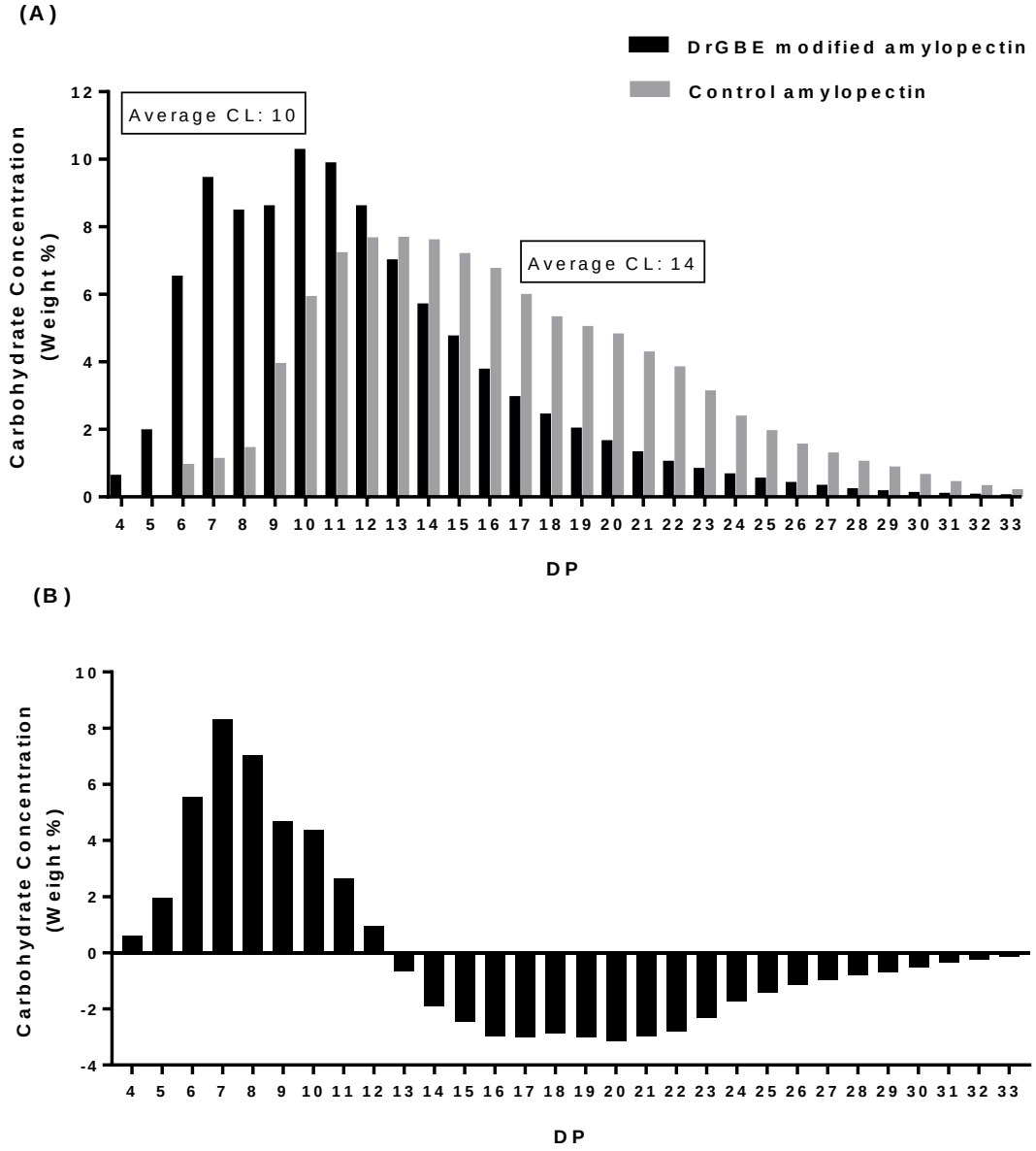

Figure 4.3.3.1 HPAEC analysis of debranched products formed from DrGBE activity with amylopectin. (A) Side-chain distribution resulting from DrGBE (1.7 µg; ~2 mU based on specific activity with amylopectin) treatment of amylopectin (1 mg) under standard reaction conditions in 50 mM MOPS-NaOH (pH 7) at 35 °C for 5 h. The reaction products were debranched by isoamylase (in 100 mM sodium acetate pH 4, 37 °C) overnight. (B) The differential plot between CLD profiles of amylopectin before and after modification by DrGBE (CLD profile of DrGBE-modified amylopectin minus CLD profile of untreated amylopectin). Average CL values were calculated using a previously established formula (Annor *et al*., 2014; Bertoft *et al*., 2008).

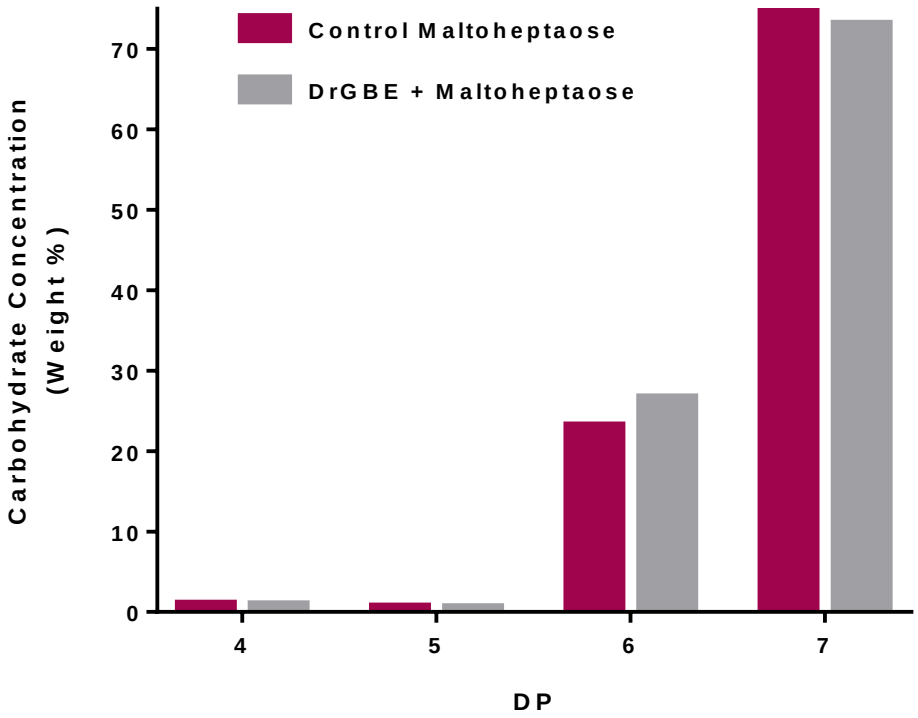

Figure 4.3.3.2 HPAEC analysis of DrGBE-treated maltoheptaose. 1.5 mg maltoheptaose was incubated with DrGBE (1.7 µg; ~2.8 mU based on specific activity with amylose) under standard reaction conditions in 50 mM MOPS-NaOH (pH 7) at 35 °C for 5 h.

DrGBE was incubated with linear *α*-1,4 glucan chains synthesized *in vitro* by phosphorylase *a* from G1P and maltoheptaose (see section 4.2.2 for synthesis method). The synthesized MOS batches were highly polydisperse and contained chains of DP either ranging from 23 - 62 (batch 1), or 36 - 76 (batch 2) (Figure 4.3.3.3 A and C). After MOS branching by DrGBE, and debranching by isoamylase, the formed products were analyzed by HPAEC.

The results of batch 1 MOS branching by DrGBE showed a significant reduction in the amount of long chains of DP 29 – 62, and a formation of shorter chains of DP 6 –

28 (Figure 4.3.3.3 A and B). In particular, an abundant accumulation of short chains of DP 7 – 11 (~40% of the total), and a moderate accumulation of chains of DP 12 – 21 was observed, as well as an increase in chains of DP 23 – 28 (Figure 4.3.3.3 A). The observed short glucan chains of DP 7 – 11 were most likely a combination of both transferred chains and residual chains resulting from DrGBE action. By contrast, chains of DP≥12 are most likely the residual chains or segments of the donor chains, the glucan chains that served as a substrate. Therefore, it can be concluded that DrGBE action on batch 1 MOS (DP 23-62) yielded short side chains (branches) of 7 to 11 glucosyl residues predominantly, which constituted ~40% of the total chain-length distribution profile. The observed chains of DP 6 are most likely the residual segments of longer glucan chains that served as donor substrate, as DrGBE uses substrates longer than DP 7 and therefore chains of DP 6 would be too short to be accommodated in the active site (Palomo *et al*., 2009) (Figure 4.3.3.2).

It seems then that the branching preference of DrGBE with linear MOS is similar to the branching preference of DrGBE with amylopectin (Figure 4.3.3.1 A), and that this GBE preferentially transfers (branches) short chains of DP 6 - 8 (with amylopectin as substrate) and chains of DP 7 - 11 with linear MOS, suggesting that the branched or linear status of the substrate may not significantly affect the DrGBE preference for the size of the transferred chain. Additionally, DrGBE seems to have a preference for initially using the longest available chains as substrate and once these are used up, it moves on to attacking the shorter chains next (Figure 4.3.3.3 A and C). In other words, DrGBE initially transfers longer glucan chains to acceptor molecules, and as the reaction proceeds these newly formed longer chains seem to become the donor substrate, and thus

are shortened. This conclusion is based on the observation that the longest chains (DP 56 – 62) have almost entirely disappeared, while chains of DP 32 – 55 are still present, but have drastically decreased (Figure 4.3.3.3 A). In a previous study, when DrGBE was incubated with amylose a similar trend was observed wherein the long glucan chains were consumed entirely to form short chains, with most of the formed side chains being between DP 4 – 17, and predominantly side chains of DP 6 and 7 (~35% of total chains) were preferentially transferred by DrGBE (Palomo *et al*., 2009). Similarly, AaGBE has been shown to behave in the same fashion, initially using the longer glucan chains as substrate (until too short), thus transferring longer chains, and later proceeding to use the shorter chains (newly formed) as substrate, effectively eliminating long chains from the CLD profile (Van Der Maarel *et al*., 2003).

The differential plot in Figure 4.3.3.3 B suggests that the minimum CL required for branching by DrGBE, under the employed conditions, is 29, when batch 1 MOS was the substrate. This minimum CL for DrGBE branching of batch 1 MOS is drastically different than the minimum CL required for branching amylopectin by DrGBE (DP≥13). However, the chain-length distribution of untreated amylopectin varies drastically from that of batch 1 MOS, with relatively short chains over the range of DP ~6 – 33, compared to the much longer chains of MOS (batch 1) spanning a range of DP 23 – 62. Therefore, the difference in the chain length distribution of MOS (batch 1) and amylopectin could be responsible for the observed difference in the minimum required CL for branching by DrGBE. However, allowing the reaction of DrGBE with MOS to proceed longer than 5 h may have resulted in further disappearance of the longer chains (DP≥13) and a reduction in the minimum CL required for branching activity.

DrGBE was also incubated with longer MOS chains of DP 36 - 76 (batch 2) to assess whether the chain length of the linear substrate affects its branching preferences. The results of batch 2 MOS branching by DrGBE showed a reduction in the amount of long chains of DP 44 – 68, a complete disappearance of long chains of DP≥69, a formation of shorter chains of DP 5 – 35, and an increase in chains of DP 36 – 43 (Figure 4.3.3.3 C and D). In particular, a large accumulation of short chains of DP 6 – 10 (~45% of the total), and a moderate accumulation of chains of DP 11 – 35 was observed (Figure 4.3.3.3 C). The branching preference of DrGBE did not vary much between batch 1 MOS and batch 2 MOS. Regardless of the chain-length distribution of the MOS substrate, DrGBE preferentially transferred short DP chains, of either DP 7 – 11 (~40% of the total) with batch 1 MOS, or of DP 6 – 10 (~45% of the total) with batch 2 MOS.

As with DrGBE-treated batch 1 MOS, the observed short glucan chains of DP 6 – 10 in DrGBE-treated batch 2 MOS were most likely a combination of both transferred chains and residual chains resulting from DrGBE action, while chains of DP≥11 were most likely the residual chains or segments of the longer glucan chains that served as donor substrate. The minimum CL required for branching batch 2 MOS by DrGBE, under the employed conditions, is 44 (Figure 4.3.3.3 D). The relatively large minimum CL observed is most likely due to the presence of very long chains in batch 2 MOS compared with batch 1 MOS. Allowing the DrGBE reaction to proceed longer than 5 h may have resulted in disappearance of the longer chains and subsequently a reduction in the minimum CL required for branching activity. The overall results indicate that although untreated batch 1 MOS had shorter glucan chains on average than batch 2 MOS, DrGBE preferentially transferred short side chains (DP 6 - 7 until DP 10 - 11) with both

MOS batches, and attacked the longest chains first, followed by consumption of shorter glucan chains. Similar results have been observed with other GBEs using MOS substrates; when *Rhodothermus obamensis* GBE was incubated with MOS (DP 2 – 60) it produced abundant short chains of DP 4 - 12, with an optima at DP 7 (Roussel *et al*., 2013), while *Anaerobranca gottschalkiin* GBE produced short chains of DP 6 - 15 (Thiemann *et al*., 2006). For ease of comparison, Table 4.3.3 summarizes HPAEC results of a number of BEs acting on amylose (a mostly linear polyglucan), amylopectin, and linear MOS, including the DP of chains transferred at highest frequency, the side chain profile optima, and the minimum required CL for branching.

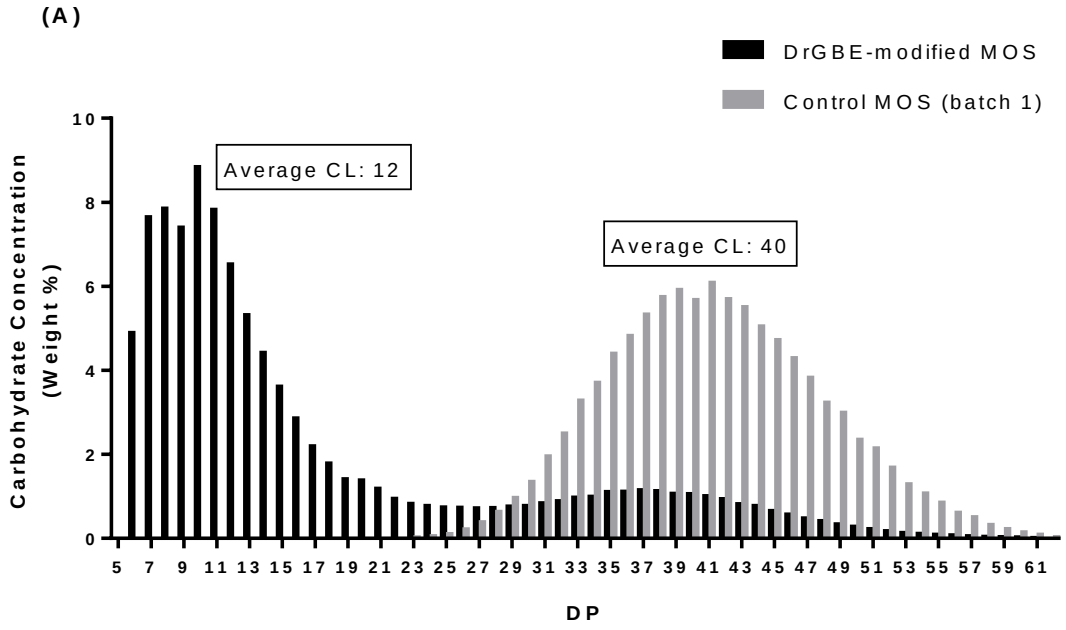

(B)

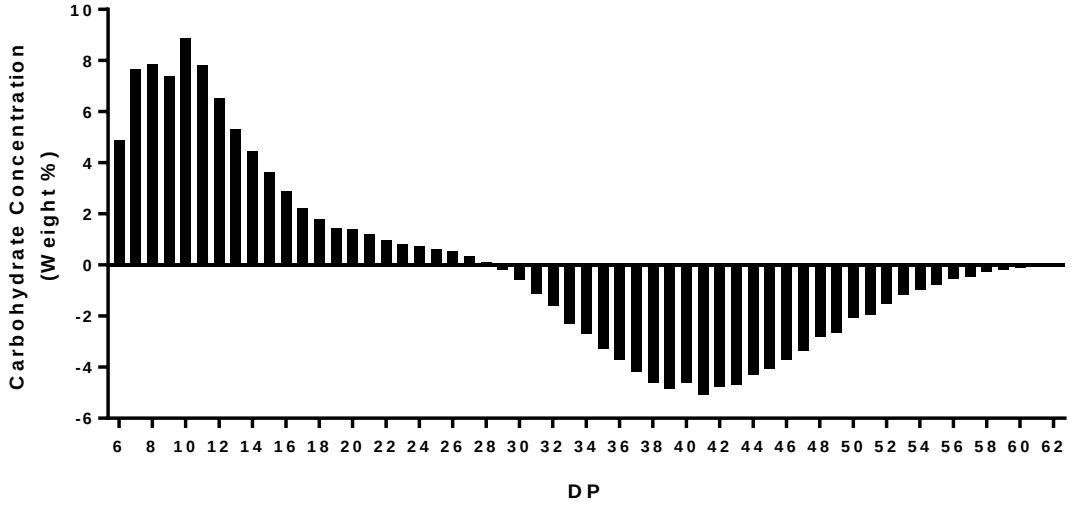
Carbohydrate Concentration (Weight %)
10
8
6
4
2
0
-2
-4
-6
6 8 10 12 14 16 18 20 22 24 26 28 30 32 34 36 38 40 42 44 46 48 50 52 54 56 58 60 62
DP

(C)

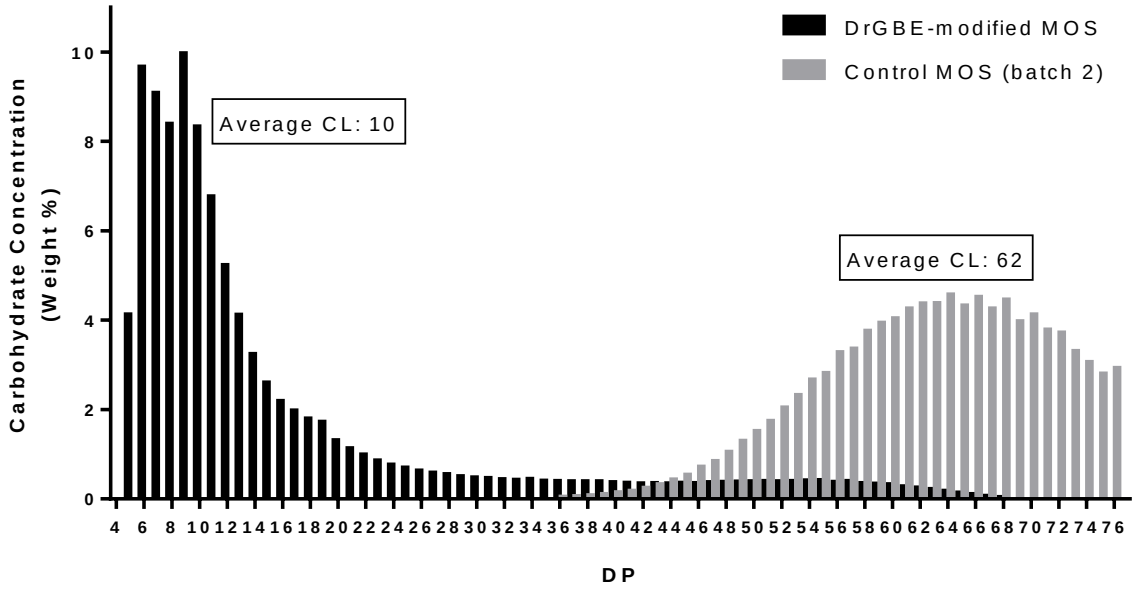
DrGBE-modified MOS
Control MOS (batch 2)
Average CL: 10
Average CL: 62
Carbohydrate Concentration (Weight %)
10
8
6
4
2
0
4 6 8 10 12 14 16 18 20 22 24 26 28 30 32 34 36 38 40 42 44 46 48 50 52 54 56 58 60 62 64 66 68 70 72 74 76
DP

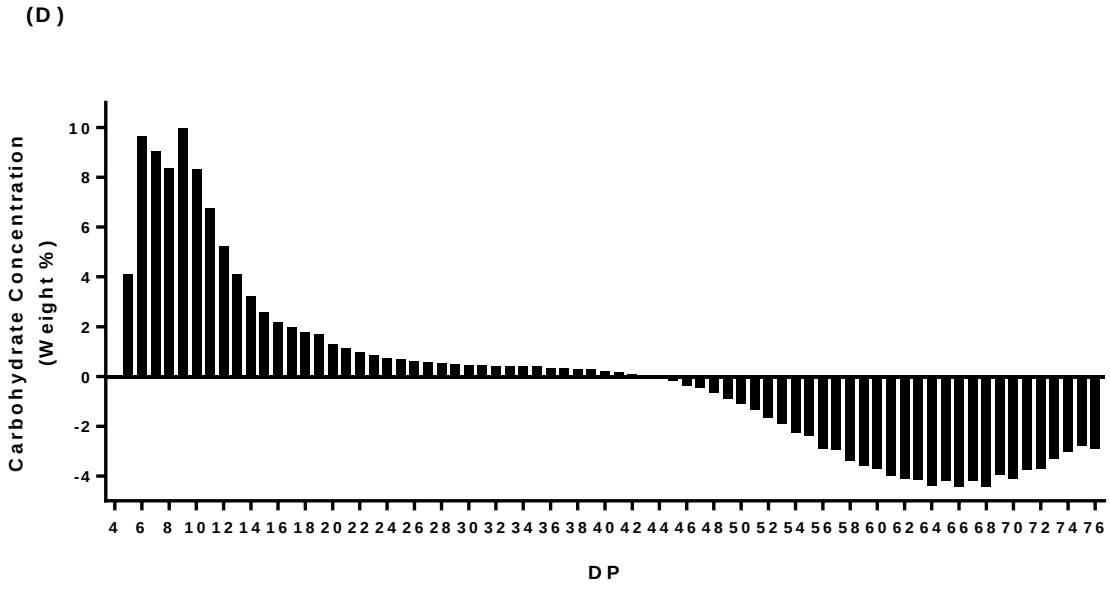

Figure 4.3.3.3 HPAEC analysis of products formed from DrGBE activity with various size *in vitro* synthesized MOS following debranching treatment (A and C), and their corresponding differential plots (B and D). Phosphorylase *a* synthesized MOS (0.5 mg) were treated with DrGBE (1.7 µg; ~2.8 mU) under standard reaction conditions in 50 mM MOPS-NaOH (pH 7) at 35 °C for 5 h. The reaction products were debranched by isoamylase (in 100 mM sodium acetate pH 4, 37 °C) overight. The side-chain distribution plots show the products of DrGBE treatment of MOS (batch 1) with an average CL of 40 (A), or MOS (batch 2) with an average CL of 62 (C). The differential plots (B and D) reflect the difference between CLD profiles of MOS before and after modification by DrGBE (CLD profile of DrGBE-modified MOS minus CLD profile of untreated MOS). Average CL values were calculated using a previously established formula (Annor *et al*., 2014; Bertoft *et al*., 2008).

TtGBE was incubated with linear *α*-1,4 MOS glucan chains synthesized *in vitro* by phosphorylase *a* from G1P and maltoheptaose (DP 7) (see section 4.2.2 for synthesis method), which had a DP range of 19 – 58. After branching of MOS by TtGBE, and debranching by isoamylase, the formed products were analyzed by HPAEC. The results showed a reduction in the amount of long chains of DP 27 – 40, a complete disappearance of long chains of DP≥41, increase in chains of DP 19 – 26, and formation of shorter chains of DP 3 – 18 (Figure 4.3.3.4 A and B). In particular, a large accumulation of short chains of DP 6 - 13 (~58% of the total), and a moderate accumulation of chains of DP 14 - 18 was observed (Figure 4.3.3.4 A). The CL distribution profile of TtGBE-treated MOS had optima of DP 8 and 11.

TtGBE has been shown to have hydrolytic activity of ~ 10% (Figure 4.3.2.2 B), wherein it cleaves *α*-1,4 glycosidic bonds but does not reattach the donor segment. Similar rates of TtGBE hydrolytic activity (with amylose) have previously been reported by Palomo *et al*. (2011). Therefore, the observed short glucan chains of DP 3-18 were most likely a combination of transferred chains (branching activity), residual chains or segments resulting from TtGBE activity on longer donor glucans, and chains formed from the hydrolytic action of TtGBE. To examine the root cause (branching or hydrolysis) of the formed short chains, products of TtGBE activity with MOS should be assessed prior to debranching as well as post-debranching, which would allow one to distinguish between the amount of chains formed from TtGBE hydrolytic activity versus TtGBE branching activity. However, due to the limitation of the available HPAEC column, which is not suitable for separating branched glucans, pre-debranching products could not be analyzed.

Palomo *et al*. (2011) have previously reported that TtGBE activity with amylose yielded hydrolysis products of DP 3 – 13, and branching products of DP 4 – 16, with a preference for TtGBE to transfer chains of DP 6. The transferred chain distribution profile attained through the analysis reported here (abundant chains of DP 6 – 13) was similar to that observed by Palomo *et al*. (2011). The CL optima, however, varied slightly, with DP 8 and 11 obtained through this analysis compared to DP 6 obtained by Palomo *et al*. (2011). The differences may be due to the types of substrate and the details of the methods used (*e.g*. type of HPAEC separating column and instrument) in the different studies. Previous studies with *Thermococcus kodakaraensi*s GBE (TkGBE), another GH57 family enzyme, showed that this GBE (with amylose as substrate) also preferentially transferred short chains with DP 5 – 15, with two CL distribution profile optima at DP 6 and 11 (Table 3.3.3) (Murakami *et al*., 2006). The results obtained with TkGBE closely resemble those reported here for TtGBE activity with MOS (Table 4.3.3).

The differential plot in Figure 4.3.3.4 B suggests that the minimum CL required for branching MOS by TtGBE, under the employed conditions, is 27. The relatively large minimum CL observed is most likely due to the presence of very long chains in the MOS substrate. These results indicate that the minimum CL required for branching is not fixed, but rather, in part, depends on the substrate. Allowing the TtGBE reaction to proceed longer than 5 h may have resulted in disappearance of the longer chains and subsequently a reduction in the minimum CL required for branching activity.

TtGBE was also reacted with short MDs (DP 4 – 43) to examine whether the chain length of the linear substrate affects its branching preferences. The HPAEC results showed a decrease of chains of DP 4 – 5 and DP 17 – 37, a disappearance of chains of

DP 38 – 43, and an increase in chains of DP 6 – 16 (Figure 4.3.3.4 C and D). The observed decrease in chains of DP 4 – 5 most likely indicates that TtGBE hydrolyzed these chains to smaller glucan moieties. In a previous study with TtGBE, it was found the enzyme tends to hydrolyze chains of DP 3 – 13 (Palomo *et al*., 2011) and therefore it is plausible that chains of DP 4-5 that were present in the MD substrate prior to TtGBE action were cleaved by TtGBE at their α-1,4 glycosidic linkages. The most abundantly observed chains of DP 6 – 16 were most likely composed of a combination of donor segments (transferred chain), residual segments of donor substrate, and potentially hydrolysis products. The optima of the CLD profile was found at DP 10, and is similar to the optima found for TtGBE modified MOS (DP 11), as well as to the optima found for TkGBE action with amylose (DP 11) (Murakami *et al*., 2006).

The differential plot in Figure 4.3.3.4 D suggests that the minimum CL required for branching MDs by TtGBE, under the employed conditions, is 17. Allowing the reaction to proceed longer (>12 h) may have reduced the minimum CL required for branching MDs, however, previous research has shown other GBEs possess a similar minimum CL for branching, such as that of *Anaerobranca gottschalkii* GBE with MOS (DP 16) (Thiemann *et al*., 2006), and that of mSBEI with amylose (DP 16) (Guan *et al*., 1997). The overall results suggest that the CLD of the substrate most likely has some effect on the branching specificity of TtGBE, as the obtained CLD profiles for TtGBE-modified MDs and TtGBE-modified MOS somewhat differ (Table 4.3.3). These findings are in accord and further complement previous research wherein Palomo *et al*. (2011) also reported that TtGBE branching specificity differed when incubated with amylose alone, compared to TtGBE reaction in the presence of potato phosphorylase, and G1P

and maltoheptaose as donor substrate and primer, respectively. The resultant products of the two reactions differed, with an over 3-fold increase in branching in the tandem reaction (Palomo *et al*., 2011). Palomo *et al*. (2011) therefore concluded that the substrate characteristics and incubation conditions heavily influence TtGBE branching specificity and the resulting product properties. The presented results indicate that TtGBE seemed to follow a similar pattern with both substrates (MDs and MOS), wherein during the process of branching consumption of the longest glucan chains occurred first, contributing to their decrease or entire elimination, followed by consumption of the next longest available glucan donor chains (Figure 4.3.3.4 A and C). A similar branching pattern was observed for DrGBE (reported here) and for AaGBE (Van Der Maarel *et al*., 2003).

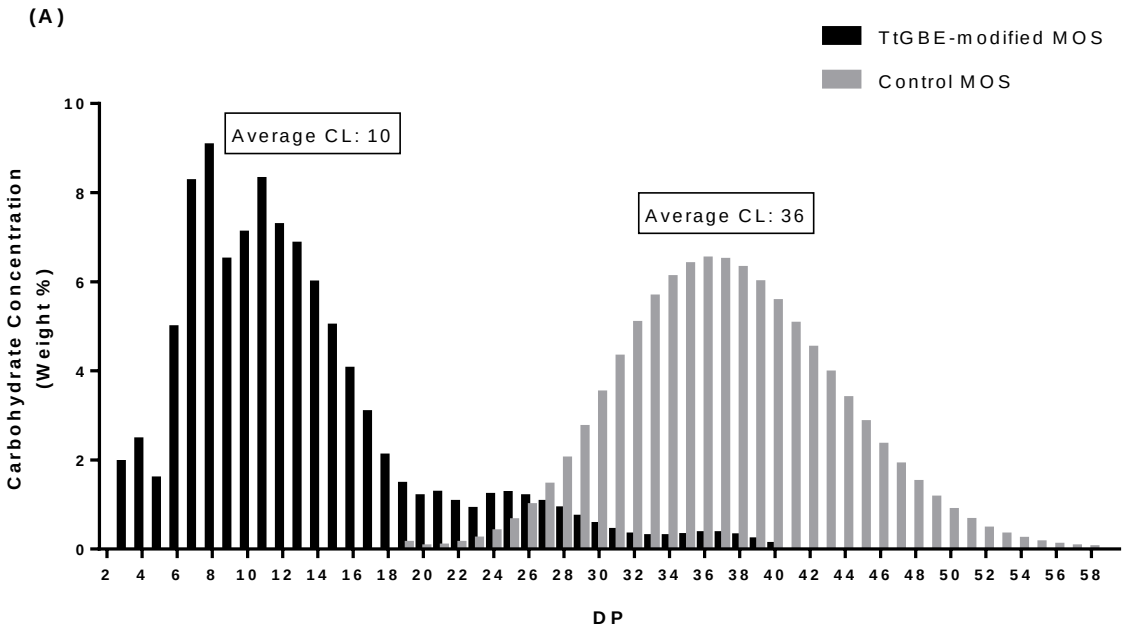

(B)

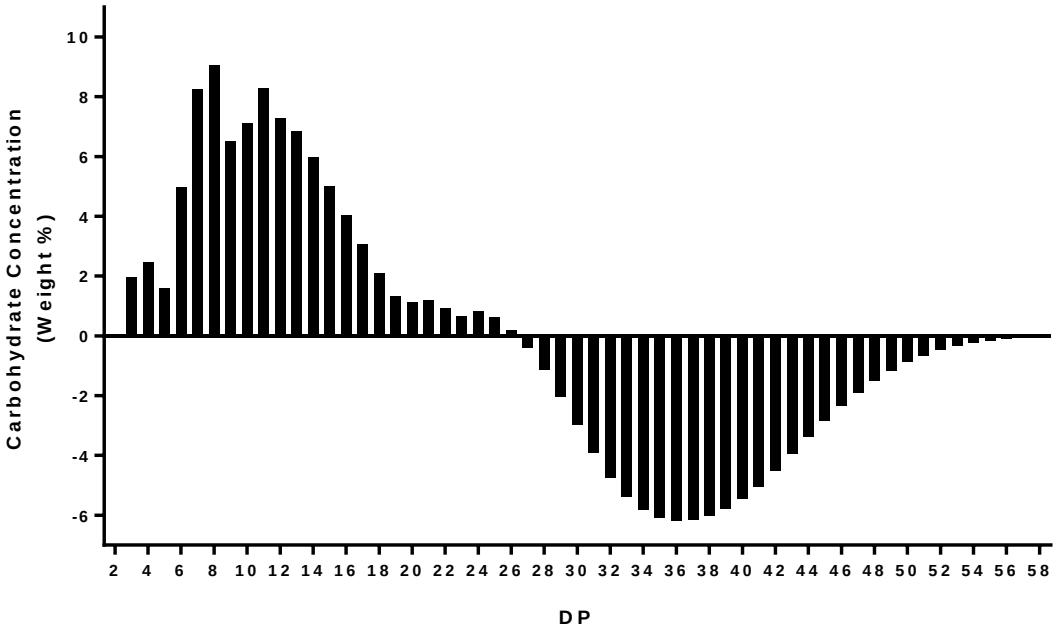
Carbohydrate Concentration (Weight %)
10
8
6
4
2
0
-2
-4
-6
2 4 6 8 10 12 14 16 18 20 22 24 26 28 30 32 34 36 38 40 42 44 46 48 50 52 54 56 58
DP

(C)

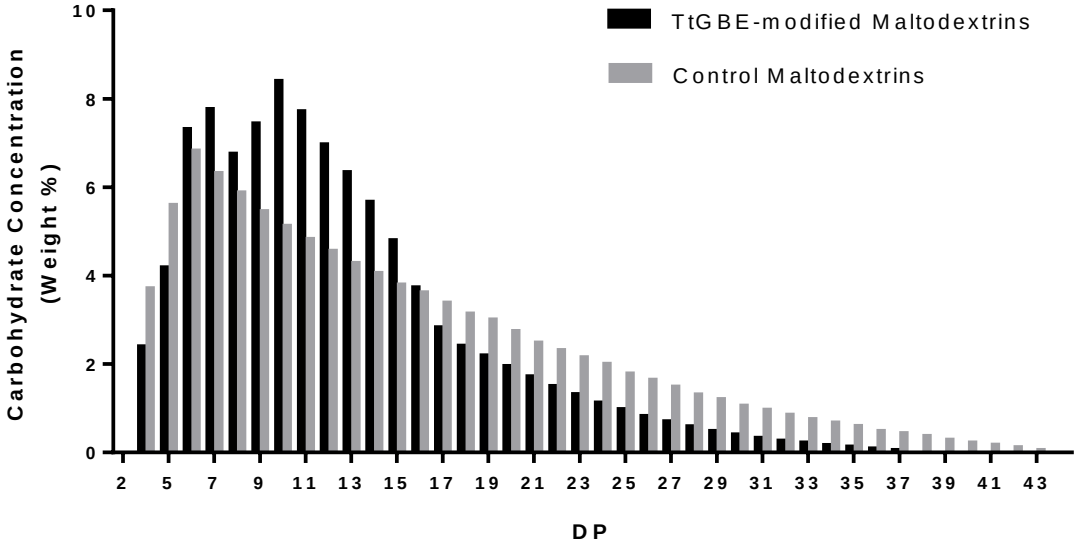
TtGBE-modified Maltodextrins
Control Maltodextrins
Carbohydrate Concentration (Weight %)
10
8
6
4
2
0
2 5 7 9 11 13 15 17 19 21 23 25 27 29 31 33 35 37 39 41 43
DP

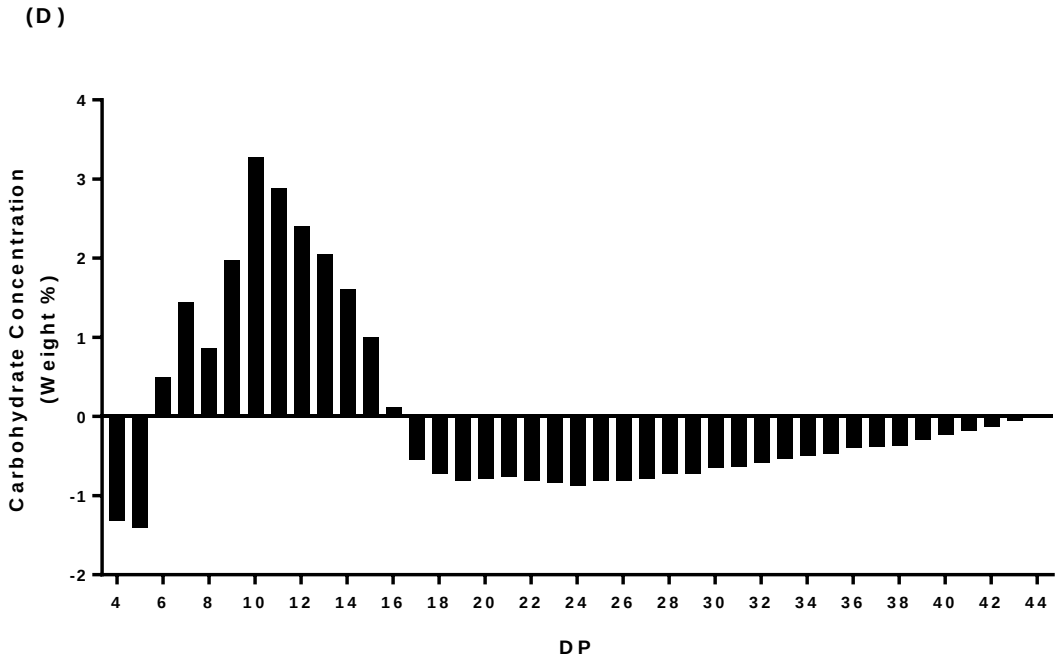

Figure 4.3.3.4 HPAEC analysis of debranched products formed from TtGBE activity with *in vitro* synthesized MOS (A), or maltodextrins (C), and their corresponding differential plots (B and D). The differential plots (B and D) reflect the difference between CLD profiles of MOS, or maltodextrins, before and after modification by TtGBE (CLD profile of TtGBE-modified polyglucans minus CLD profile of untreated polyglucans). Phosphorylase *a* synthesized MOS (0.5 mg), or maltodextrins (0.5 mg), were treated with TtGBE (2.6 µg; ~ 1.3 mU) under standard reaction conditions in 50 mM MOPS-NaOH (pH 6.5) at 65 °C for 5 h or overnight, respectively. The reaction products were debranched by isoamylase (in 100 mM sodium acetate pH 4, 37 °C) overnight. Average CL values were calculated using a previously established formula (Annor *et al*., 2014; Bertoft *et al*., 2008).

Table 4.3.3 Preferred Lengths of Transferred Chains, CLD Profile Optima, and Minimum CL Required for Branching by Various BEs with Different Substrates.

Branching Enzyme	Substrate	Optimal chain transfer range (DP)	Optima DP (most frequent CL)	Minimum CL for branching (DP)	Reference
TtGBE	Amylose	4 – 16	6	N/D	Palomo *et al*., 2011
	MOS	6 – 13	8 and 11	27	Nasanovsky, 2017 (this thesis)
	MDs	6 - 16	10	17	
DrGBE	amylopectin	6 - 12	10	13	Nasanovsky, 2017 (this thesis)
	amylose	4 - 11	6 and 7	N/D	Palomo *et al*., 2009
	MOS	6 - 11	9 and 10	29 or 44 (depending on MOS DP range)	Nasanovsky, 2017 (this thesis)
AaGBE	amylopectin	8 - 25	12	N/D	Takata *et al*., 2003
	amylose	8 - 15	10	N/D	Van Der Maarel *et al*., 2003; Takata *et al*., 2003
***Bacillus stearothermophilus* GBE**	amylopectin	22 - 35	N/D	N/D	Takata *et al*., 1996a
***Rhodothermus obamensis* GBE**	amylopectin	4 – 10	7	12	Roussel *et al*., 2013
	MOS (DP 2 to 60)	4 - 12	7	14	
Anaerobranca gottschalkii	amylose	4 – 24	6	N/D	Thiemann *et al*., 2006
	MOS	6 - 15	N/D	16	
***E. coli* GBE**	amylose	5 - 16	10	12	Guan *et al*., 1997
TkGBE	amylose	5 - 15	6 and 11	N/D	Murakami *et al*., 2006
mSBEIIb	amylopectin	3 - 12	6 and 7	12	Guan *et al*., 1997
	amylose	3 - 9	6 and 7	12	
mSBEI	amylose	6 - 14	11	16	Guan *et al*., 1997

4.3.4 Concluding Remarks

This chapter describes the thorough biochemical characterization of two recombinant GBEs, DrGBE and TtGBE, from the extremophilic bacteria *Deinococcus radiodurans* and *Thermus thermophilus*, respectively. The substrate preference and kinetics of both GBEs were assessed and showed that DrGBE is able to branch both amylose and amylopectin (and starch – data not shown), while TtGBE branched amylose and was only able to hydrolyze amylopectin. DrGBE was optimally active at 25 – 35 °C and pH 7, while TtGBE had an optimum temperature of 70 °C and was optimally active at pH 6 – 7. The products of DrGBE and TtGBE activity varied in their side chain distribution. DrGBE activity with amylopectin yielded products with a CL optima of 10 and a high frequency of chains of DP 6 – 12, while with MOS the CL optima was 9 – 10, and a high abundance of chains of DP 6 – 11. TtGBE on the other hand, when reacted with MOS, had a CL optima of 8 and 11, and preferentially transferred chains of DP 6 – 13, while its activity with MDs yielded products with a CL optima of 10, and a high frequency of chains of DP 6 – 16. These GBEs possess similar branching preferences based on the chain length distribution of their products, and both act by α-retaining mechanism (see Introduction for details).

It is possible that the minimum required chain length for branching is an intrinsic property of the BE. However, assay and method conditions may contribute to the variation in the minimum required chain length for branching obtained for DrGBE and TtGBE with different substrates. If insufficient time for branching elapsed, accumulation of longer chains would be observed, and these would most likely represent the residual chains from branching activity, not the branches. If sufficient time is allowed for

branching to reach completion, these longer chains would be used up as substrate, resulting in shorter products which most likely reflect the branch chains created by the GBE. In support of this speculation, Roussel *et al*. (2013) saw that amount of longer glucan chains reduced with longer reaction times (*e.g*. 5 h vs. 24 h). Furthermore, the observed variation in minimum required chain length between the action of DrGBE and TtGBE on different substrates, may potentially stem from maximum chain length of the substrate, wherein the GBE would use longer glucan chains as donors and some as acceptors. Therefore, persistence of the long glucan chains (as reflected by the relatively high minimum required CL – DrGBE or TtGBE with MOS) in products could be due to some long chains being acceptors, thus no longer accessible to the GBEs as substrate, resulting in accumulation of longer DP chains contributing to the relatively high minimum CL for branching observed with MOS (Table 4.3.3).

GBEs are promising tools for industrial modification of post-harvest starch to improve starch properties in food and non-food applications. The use of BEs can potentially be introduced during post-harvest starch processing for reducing starch retrogradation and high viscosity, and yielding high stability dispersions, as BEs will increase the branching frequency of the original polymer and thus alter its properties (see Chapter 5 for details). BEs can also act on the amylose component of starch, a chief contributor to retrogradation during post-harvest starch processing, to effectively reduce chain length, which results in a decrease in retrogradation and gelling of the starch product. Therefore, the thorough biochemical characterization of DrGBE and TtGBE was necessary to assess their potential utility in industrial application for post-harvest starch modification.

Chapter 5 - Industrial Application of Recombinant DrGBE

5.1 Introduction

Owing to their unique α-1,6 transglycosylation activity, which results in glucan branching, GBEs and SBEs can be explored for their potential for modification of post-harvest starch in several industrial applications (Kasprzak *et al*., 2012; van der Maarel *et al*., 2002; Wu *et al*., 2014). Normal plant starches contain approximately 25% amylose, and in certain industries this can limit processing and end uses. Due to the low solubility of the long amylose chains within starch, the maximum concentration of starch in starch-degrading procedures in the industry is limited, as at higher concentrations amylose tends to retrograde leading to lower product quality (gelling) (Alcázar-Alay and Meireles, 2015; Jobling, 2004; Thiemann *et al*., 2006; Wu *et al*., 2014). In order to prevent retrogradation, processing must occur at high temperatures which ultimately means increased costs. The ability of bacterial GBEs to break α-1,4-glycosidic linkages and form α-1,6-branches yields products devoid or reduced in long linear chains. Therefore, GBEs can potentially form products that create visco-stable solutions that do not retrograde as the side chains are too short to form strong glucan chain interactions (van der Maarel and Leemhuis, 2013). Furthermore, GBE treated starches possess higher degree of branching, approximately 8% as was demonstrated by Gunja *et al*. (1960) and ~12% as shown through the work in this chapter (see section 5.3.3), compared to the ~4-5% branching frequency of normal starches (Gunja *et al*., 1960; Hizukuri, 1986). Higher degree of branching can potentially improve starch properties by reducing retrogradation and gelling, and allow the use of higher concentrations of starch in starch-degrading procedures in industrial processing at lower processing temperatures (Nichols, 2000). For

instance, in paper manufacturing, wherein starch is used as an ingredient for paper coating, process speed is of primary importance (Nichols, 2000). The processing speed is limited by the need to remove water accumulated during the coating procedure (Nichols, 2000; Roberts, 1996). Using a higher starch concentration would lead to reduced water accumulation throughout the process and allow higher processing speeds (Roberts, 1996). However, higher concentrations of starch cause rapid starch retrogradation and the undesirable deposition of gelled starch onto the paper (Roberts, 1996). Increasing branching of post-harvest starch can improve starch functionality by preventing retrogradation, as glucan chains become shorter, unable to realign and retrograde, thus allowing use of higher starch concentrations during processing in paper manufacturing (Nichols, 2000). Indeed, GBE-modified starch has previously been applied in the paper coating step of paper manufacturing (Nichols, 2000). Other research demonstrated that GBE from *Neurospora crassa* altered the molecular structure of starch, producing highly-branched starch with improved solubility and stability properties (Kawabata *et al*., 2002). GBEs have also been implicated as effective anti-staling agents (preventing retrogradation), shown to improve quality and shelf life of food products such as cookies, cakes and breads (van der Maarel and Leemhuis, 2013; Wu *et al*., 2014).

Studies have recently shown that long-term consumption of foods with a high glycemic index (GI), which describes the level of postprandial glucose rise in the blood as compared to a reference food or glucose, is associated with obesity, and metabolic and cardiovascular diseases (Ao *et al*., 2007; Zhang *et al*., 2006). Slow digestible starches are considered to have a low GI and promote slow glucose release into the blood (Zhang and Hamaker, 2009; Zhang *et al*., 2006). Recently, the use of GBEs has been suggested to

convert normal starches into slowly digestible starches in order to mediate the glucose spike in the blood and the insulin response, and in the long run, potentially help reduce the incidence of common chronic diseases, such as obesity and diabetes (Kasprzak *et al*., 2012; Lee *et al*., 2013; Zhang *et al*., 2006). Studies have shown that highly-branched *α*-glucans, resulting from GBE treatment of starch, reduce the rate of *α*-amylolysis in the digestive tract, resulting in a slower release of glucose into the blood, which in turn reduces the insulin response (Kasprzak *et al*., 2012; Lee *et al*., 2013, 2008; van der Maarel and Leemhuis, 2013).

GBEs are promising tools for industrial modification of post-harvest starch to improve starch properties in food and non-food applications. This chapter describes the novel application of recombinant DrGBE to modify a commercial proprietary polyglucan produced from maize starch by chemical modification in order to reduce gelling properties, improve stability and solubility, and produce a more visco-stable product. One of the obstacles of processed post-harvest starch is the reduced "shelf-life", a consequence of retrogradation of the polyglucans within starch caused by the amylose component (or long glucan chains). This impedes the manufacturer's ability to transport dispersed starch solutions, especially at high starch concentrations (>35% (w/v) solids), as they tend to harden and form gels. The investigation of properties of starch dispersions in water attracts much research attention due to the wide array of uses in industrial applications (Christianson and Bagley, 1983). Depending on the application, higher starch concentrations (~35% w/v) may be of particular interest, as is in the paper coating process (Christianson and Bagley, 1983; Nichols, 2000). However, dispersions or solutions with a higher starch concentration tend to retrograde and hinder further

processing of starch. Therefore, the objective of the study presented in this chapter was to treat a dispersed commercial starch preparation with DrGBE in order to obtain a product less prone to retrogradation and gelling. DrGBE acted rapidly, reducing the molecular weight and polyglucan size distribution in the resultant product, and prevented gelling. Additionally, the branching frequency of the resultant polymer was significantly higher compared to the original polyglucan.

The following experiments were performed in collaboration with Dr. Julien Mesnager (Senior Scientist, EcoSynthetix) and with the help of our lab member Jessica White (MSc candidate).

5.2 Methods

5.2.1 Sample Preparation

A commercial proprietary starch-derived polyglucan was dispersed in warm (~40 ºC) 50 mM MOPS-NaOH (pH 7) at a concentration of 15.75% (w/v) solids in a final volume of 500 mL. The reaction took place in a temperature controlled double jacketed glass reactor with a mechanical stirrer set to 250 rpm. Prior to the addition of 20 mg DrGBE (corresponding to a catalytic activity of 1.15 µmol α-1,6 linkages/min./mg DrGBE; 23 U), a control sample (~10-15 mL) was taken and kept at room temperature. The reaction was initiated by the addition of DrGBE (20 mg; 23 U) and proceeded at 35 ºC for 22 h. Samples were taken at multiple time points throughout the reaction to observe the change in properties of the product polyglucan over time. Two samples (~10 mL) were taken at each time point, after 2 h, 4 h, and 22 h, and immediately heated to 95 ºC for 20 min. in order to inactivate DrGBE. Subsequently, the samples from each time

point were kept at either room temperature, or 4 ºC. A ~2 mL aliquot from a sample at each time point was spread on a small Teflon bar and dried in an oven at 80 ºC for approximately 30 min. For GPC analysis (for method see section 5.2.2), 25 mg of the dried sample was dissolved in 10 mL DMSO (>99.9%; Anachemia) at 80 ºC with constant stirring. A 1 mL aliquot was then filtered through a 0.2 µm nylon filter (Sigma, catalogue no. Z259942) into a small glass vial (VWR, catalogue no. 46610-722) prior to loading onto the GPC column. For nuclear magnetic resonance (NMR) analysis (for method see section 5.2.3), ~10 mg of the dried sample was dissolved in 1 mL of deuterated water (D_2O).

5.2.2 GPC - Triple Detection

Triple detection gel-permeation chromatography, equipped with a refractive index (RI), intrinsic viscosity, and light scattering (LALS, RALS) detectors, was performed on a Malvern Viscotek GPCmax instrument (Malvern, USA) equipped with a Malvern Viscotek triple detector assembly (TDA). For data collection, the Viscotek TDA was outfitted with refractive index (RI; polymer concentration), intrinsic viscosity, and light scattering (low and right angle light scattering) detectors. For separation of glucans produced by DrGBE treatment, a Polyanalytik size exclusion chromatography column (PAA-206M, London, ON, Canada) was used, measuring 8 x 300 mm, packed with a polyhydroxymethacrylate-based gel and possessing an estimated exclusion limit of 2 x 107 g/mol. A guard column was also used, measuring 6 x 50 mm (PAA-G; Polyanalytik, London, ON, Canada). An in-line post-column 0.2µm nylon filter (Malvern, GPC1210), which protects the light scattering detectors, was used. Pullulan 50K (Mw:46,001g/mol, PDI: 1.069; Polyanalytik, London, ON, Canada) was used for calibration, and

confirmation was achieved with PolyCAL^{TM} Dextran standard (Mw:71,747g/mol, Mn=53,956g/mol; Polyanalytik, London, ON, Canada). All samples were analyzed under a flow rate of 0.5 mL/min., 50 °C column temperature, and a mobile phase consisting of DMSO (>99.9%; Anachemia, Montreal, QC, Canada) with 0.05 M LiBr (99+%; Sigma-Aldrich, Oakville, ON, Canada). Sample concentration was 2.5 mg/mL, and injection volume was 100µL. Data acquisition and processing were carried out by use of OmniSEC software (Viscotek Corporation, USA).

5.2.3 ^{1}H-NMR Spectroscopy

The NMR measurements were performed with a Bruker AVANCE II 400 MHz spectrometer operating at 400.32 MHz for ^{1}H. All samples, 10 mg (+/- 2 mg) were solubilized in 1 mL of solvent, deuterium oxide (D_2O, 99.9 atom % D, Aldrich). Spectra were accumulated at 60 °C with 32 scans and a repetition time of 4.8 seconds (recycle delay = 1 second, acquisition time = 3.8 seconds) at a 30° excitation pulse. A ^{1}H selective 5mm probe was employed for quantitative measurements. The probe was tuned to each sample to ensure optimal signal-to-noise ratio (S/N) and consistency throughout the experimental series. The raw 1D data were Fourier transformed and the resulting spectra were baseline corrected by subtraction of a matched polynomial using SpinWorks 4.2 software. Chemical shifts were assigned relative to the water peak (4.378 ppm), which was relative to the internal standard DSS (4,4-dimethyl-4-silapentane-1-sulfonic acid) at 0 ppm. Integration of the peak areas of α-(1,4) and of α-(1,6) was performed at fixed ppm values on the spectrum at 5.23-5.53 and 4.89-4.99, respectively, using SpinWorks 4.2. The aforementioned raw data manipulations were kindly performed by Dr. Julien

Mesnager (Senior Scientist, EcoSynthetix). The % branching (using data collected by NMR) was calculated by taking the ratio of the integral of the α-(1,6) peak area to the α-(1,4) peak area (multiplied by 100).

5.3 Results and Discussion

5.3.1 Examining the Viscosity and Gelling Properties of a DrGBE-Modified Commercial, Proprietary Polyglucan

One of the objectives of the presented work was to alleviate gelling (retrogradation) of a commercial proprietary starch-based polyglucan, which is routinely used in industrial applications.

A commercial starch-based polyglucan (proprietary) was dispersed in warm (~40 ºC) 50 mM MOPS-NaOH (pH 7) at a concentration of 15.75% (w/v) solids and treated with 20 mg DrGBE (23 U) for a period of 2 h, 4 h, and 22 h. A 15.75% (w/v) solids polyglucan concentration was used to accommodate for the relatively low temperature (35 ºC) required for DrGBE activity. Higher solids concentration of the polyglucan dispersion would have led to almost immediate retrogradation upon cooling, even if the initial dispersion temperature was higher (typically 60 ºC; data not shown). Samples were taken at each time point (2 h, 4 h, and 22 h) and kept either at room temperature (Figure 5.3.1.1 B), or 4 ºC (Figure 5.3.1.1 C) for viscosity observations for the duration of the experiment (~48 h). The gelling properties of the resultant products were assessed visually and compared to the control, the untreated commercial polyglucan (no DrGBE added; Figure 5.3.1.1 A). The untreated polyglucan became visibly viscous within minutes (~10-20 min.), and fully gelled in less than an hour at room temperature (Figure 5.3.1.1 A). The samples that were taken out of the stock reaction containing DrGBE at 2

h, 4 h, and 22 h were modified by DrGBE and thus did not form a gel and remained liquid, even after long periods at room temperature (Figure 5.3.1.1 B) and 4 ºC (Figure 5.3.1.1 C). Therefore, a proof of concept was demonstrated, showing that treatment of a starch-derived commercial polyglucan (proprietary) with DrGBE abolished gel formation and retrogradation of the polyglucan at a dispersal concentration of 15.75% (w/v) solids. It is of particular interest for industrial use that gelling is avoided and that higher concentrations of the polyglucan (preferably ~35% (w/v)) are used, as it is more beneficial for the end application. However, higher solids concentration of the polyglucan dispersion lead to almost immediate retrogradation upon cooling, and therefore are not practical to use for initial optimization and proof of concept experiments. Further experiments are needed to determine the required amount of DrGBE to treat this commercial polyglucan at higher dispersion concentrations (*e.g.* ~35% (w/v) solids) to achieve similar effects as were observed for a 15.75% (w/v) solids concentration dispersion.

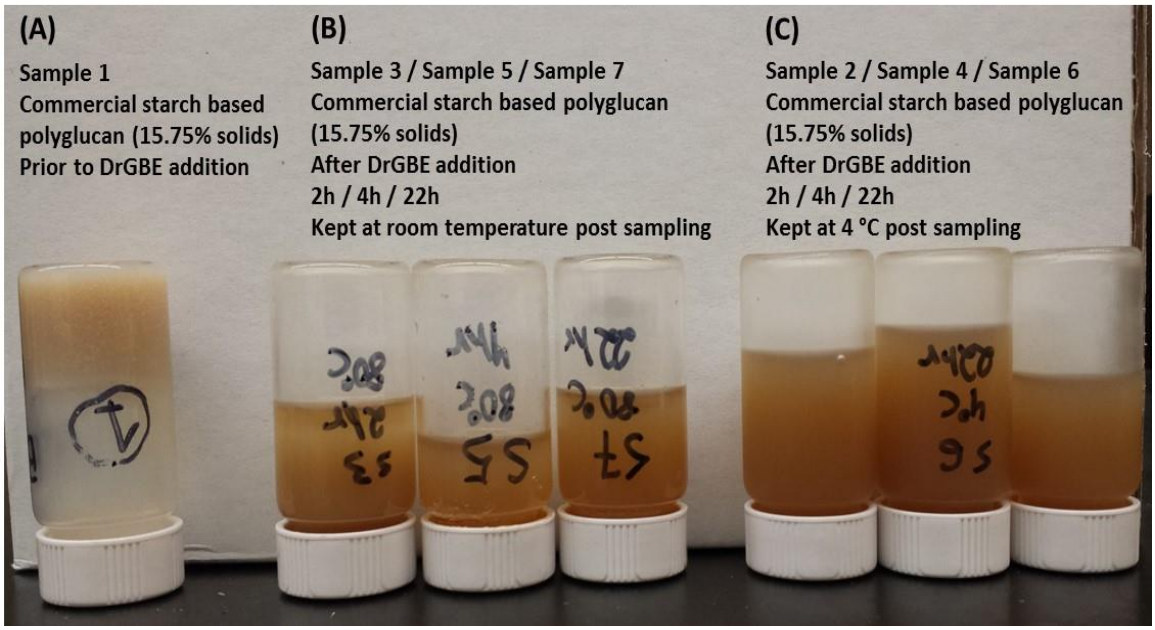

Figure 5.3.1.1 Observed viscosity and gelling properties of a DrGBE-treated commercial starch-derived polyglucan (proprietary) compared to the untreated control polyglucan (A). The proprietary polyglucan was dispersed in warm MOPS-NaOH buffer (50 mM, pH 7) and incubated with 20 mg DrGBE (23 U) at 35 °C for 2 h, 4h, or 22 h. The samples taken at each time point were boiled to heat-inactivate DrGBE and subsequently stored at either room temperature (B), or 4 ºC (C). The control sample (A) was stored at room temperature.

5.3.2 GPC– Triple Detection

Triple detection GPC was used to examine the physicochemical properties of DrGBE-modified commercial proprietary polyglucan. The principle of GPC is the separation of macromolecules by size as they elute from a column filled with a porous gel of various size cut-off. Triple detection GPC involves the use of light scattering, viscometry and concentration detectors to measure absolute molecular weight, molecular size and intrinsic viscosity, generating information on macromolecular structure, conformation, aggregation and branching. Samples of DrGBE-treated commercial polyglucan (proprietary) from each time point (2 h, 4 h, and 22 h) and the untreated

commercial polyglucan (control) were subjected to triple detection GPC analysis for characterization. The molecular weights of the resultant polyglucans were determined (Table 5.3.2). The weight average (Mw) and number average (Mn) molecular weight were acquired for each sample. Mn and Mw are the most commonly used average molecular weights; in industry they are usually sufficient to provide a working estimate of the main features of a molecular weight distribution of a polymer (Neira-Velázquez *et al*., 2013). Number average molecular weight (Mn) is the statistical average molecular weight of all the polymer chains in the sample (sum molecular weight of all the polymer molecules, divided by the total number of polymer molecules in a sample), while the weight average molecular weight (Mw) takes into account the molecular weight of a chain in determining contributions to the molecular weight average (the bigger the chain, the more it contributes to Mw). The equations (Eq.) for Mn (Eq. 1) and Mw (Eq. 2) are outlined below, where Mi is the molecular weight of a chain and Ni is the number of chains of that molecular weight:

Equation 1:

$$Mn = \frac{\sum NiMi}{\sum Ni}$$

Equation 2:

$$Mw = \frac{\sum NiMi^2}{\sum Ni\,Mi}$$

Table 5.3.2 shows the data obtained from GPC analysis of the polyglucans resulting from treatment of the commercial polyglucan (proprietary) with DrGBE, at each time point (2 h, 4h and 22 h), including Mw, Mn, molecular weight dispersity, and intrinsic viscosity. The Mw values of the resulting DrGBE-modified product showed a reduction in molecular weight over time with approximately a 54% reduction in molecular weight between the 2 h (407,147 g/mol; Table 4.3.2) and the 4 h (185,695 g/mol: Table 4.3.2) treatment, and a further 34% reduction between the 4 h and the 22 h (121,346 g/mol: Table 4.3.2) treatment. The observed reduction in molecular weight may be the result of the branching action of DrGBE, which modified the polyglucan structure leading to a reduction in long, high molecular weight glucan chains as branching proceeded, resulting in a decrease in molecular weight of the tested polyglucan due to a change in structure (Figure 5.3.2.1). The resulting Mn values also decreased (Table 5.3.2) between each time point, however, these reductions were not as great as the Mw values. In general, it is also evident that the resulting Mw values are larger than the Mn values. This is expected, and is accounted for in the equation for Mw, wherein there is an additional *"Mi"* term which consequently places greater emphasis on the highest molecular weight molecules within the polymer sample (see Eq. 2 above and Figure 5.3.2.2 below). The Mn, therefore, provides information about the specific molecular weight classes which are present at the greatest frequency in the sample, while Mw is a weighted average which favours higher molecular weight molecules, and appears on the higher side of the molecular weight distribution (Figure 5.3.2.2). Therefore, the observed reduction in Mw of the DrGBE-treated polyglucan suggests a change in the polyglucan structure and a decline in the numbers of longer (high molecular weight) glucan chains,

shifting the molecular weight of the treated polyglucan sample downward (Figure 5.3.2.1).

Table 5.3.2 Physicochemical Properties of the Resultant Products of a Commercial Proprietary Polyglucan Treated with DrGBE.

Sample	Mw (g/mol)	Mn (g/mol)	Dispersity (Mw/Mn)	Intrinsic Viscosity (dL/g)
2h treatment	407,147	101,395	4.0	0.093
4h treatment	185,695	89,621	2.07	0.095
22h treatment	121,346	84,461	1.44	0.097

-Control (0 h) results were not reported due to confidentiality. Starting material MW was higher than 600,000 g/mol.

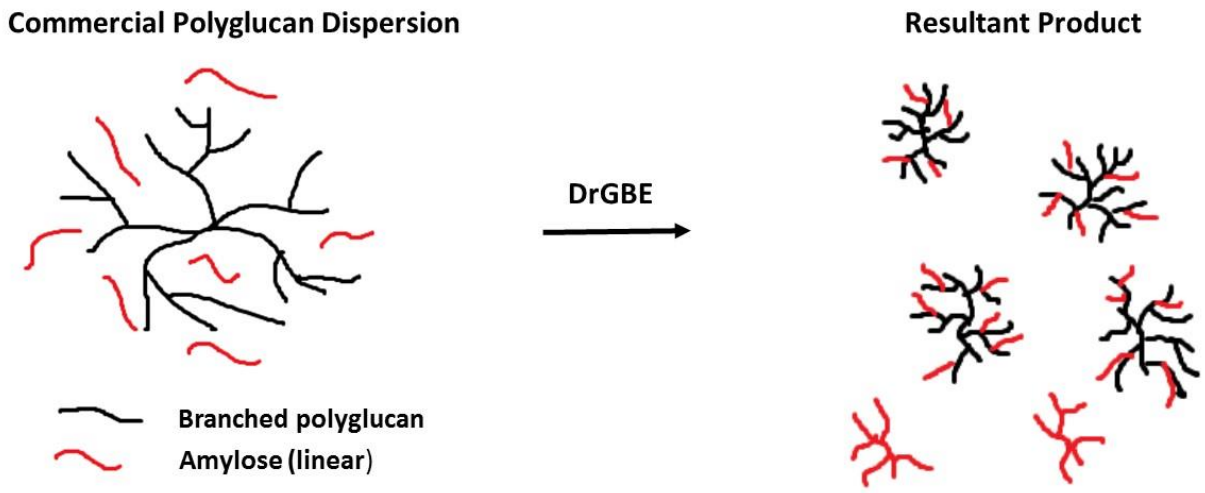

Figure 5.3.2.1 A schematic representation of the commercial polyglucan (proprietary) dispersion and the potential resultant products post DrGBE treatment. A commercial proprietary polyglucan was incubated with 20 mg DrGBE (23 U) for 2 h, 4 h, or 22 h and an aliquot of the resultant samples was loaded onto a GPC column. The obtained GPC results suggest that DrGBE modified the polyglucan structure leading to increased branching and a reduction in molecular weight and viscosity compared to the untreated commercial polyglucan control. Amylose segments were most likely utilized by DrGBE and some were potentially incorporated as branches into the new, unique polyglucan structure formed by DrGBE.

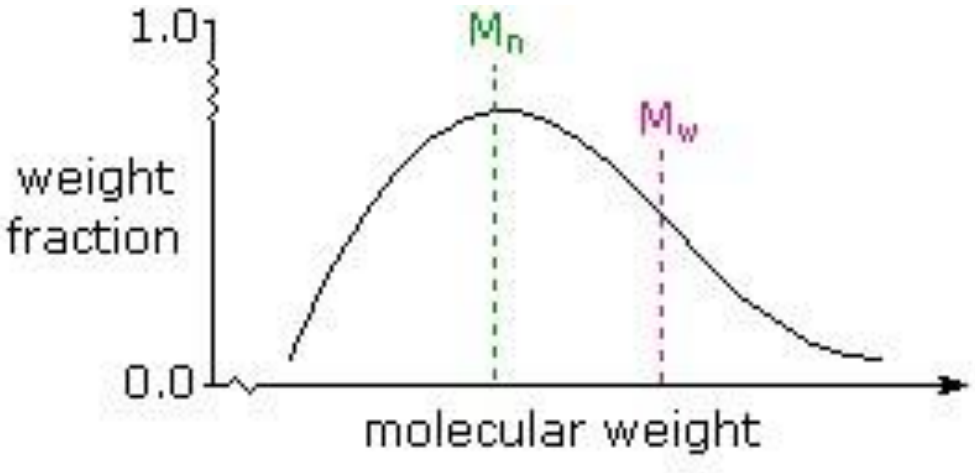

Figure 5.3.2.2 Mn and Mw in a typical sample of polydispersed macromolecules. As larger molecules in a sample weigh more than smaller molecules, the weight average, Mw, is necessarily skewed to higher values, and is always greater than Mn. Figure reproduced from https://www2.chemistry.msu.edu/faculty/reusch/virttxtjml/polymers.htm

Due to confidentiality reasons the exact molecular weight value of the untreated (control) commercial proprietary polyglucan cannot be reported. However, the molecular weight (Mw) of the commercial polyglucan is greater than that of the resulting DrGBE-modified products, and is higher than 600,000 g/mol. It is evident then, that a substantial reduction in molecular weight was observed post treatment of the commercial polyglucan with DrGBE within 2 h incubation (Table 5.3.2). A reduction in polymer molecular weight typically also means a reduction in viscosity (Neira-Velázquez *et al*., 2013; Su, 2013). Indeed, the viscosity of the untreated polyglucan (value not shown due to confidentiality reasons) is greater than that of the resulting DrGBE-modified product. The reported intrinsic viscosity value for regular dent corn starch is ~1.53 dL/g, the values for maize amylose and amylopectin are ~1.24 dL/g and ~1.54 dL/g, respectively, while the values for potato amylose and amylopectin are ~1.67 dL/g and 1.78 dL/g, respectively (BeMiller and Whistler, 2009; Yu *et al*., 2014). The intrinsic viscosity values obtained by GPC analysis of the DrGBE-modified commercial polyglucan were 0.093 dL/g for the 2 h sample, 0.095 dL/g for the 4 h sample, and 0.097 dL/g for the 22 h sample (Table 5.3.2).

The intrinsic viscosity values for the 3-time point samples were very similar to each other. However, all are significantly lower than the intrinsic viscosity value of the untreated commercial polyglucan (not reported), and are over 90% lower than the reported intrinsic viscosity values for starch, amylose and amylopectin from maize and potato (see above). The difference in intrinsic viscosity between the values of the DrGBE-treated polyglucan and the control, the untreated polyglucan (as well as the reported values; see above), may be due to the branching action of DrGBE, which results

in reduction in the presence of long glucan chains and a more branched ("dense") polymer, contributing to lower molecular weight, a narrower molecular weight dispersity, and a reduced intrinsic viscosity (Figure 5.3.2.1). From an industrial processing point of view, specifically the adhesives and paper manufacturing sectors, polymers with a lower molecular weight and lower viscosity are easier to process as they dissolve more rapidly (higher solubility) and have favourable dispersion properties, and thus require lower temperatures for processing (Giles *et al*., 2005). The ability to control the molecular weight and viscosity is often used to obtain and improve certain desired physical properties in a polymer product (Giles *et al*., 2005; Su, 2013). Native starches tend to form pastes when processed, and generally these pastes are too viscous to permit formulation of desired high solids coating compositions, which can be readily used and applied, particularly in the adhesives sectors (Giles *et al*., 2005; Schwalbe, 1966). The data obtained for molecular weight and viscosity through GPC analysis of the DrGBE-modified polyglucan, suggests that the use of branching enzymes, such as DrGBE, may be beneficial for controlling the molecular weight and viscosity of starch-based polymers, thereby improving polymer properties and making it more suitable for specific end applications.

The distribution chromatogram obtained from GPC typically displays a molecular weight distribution within a polymer sample describing the proportion of the various molecular weight fractions present (Figure 5.3.2.3). For a perfectly uniform, or monodisperse sample, consisting of exactly one molecular weight, both the Mw and the Mn would be the same value (Nichetti and Manas-Zloczower, 1998). However, for most samples the two numbers are not the same, and the ratio of Mw and Mn (molecular

weight dispersity) can be used to describe how far away the observed distribution is from a uniform distribution. The molecular weight dispersity of a monodisperse polymer sample, where all the chain lengths are the same, is equal to one (Nichetti and Manas-Zloczower, 1998). The larger the dispersity, the broader the molecular weight distribution.

The molecular weight dispersity was calculated for each time point sample (2 h, 4 h, and 22 h) by taking the ratio of Mw to Mn (Table 5.3.2). The molecular weight dispersity decreased from 4.00 to 2.07 between the 2 h and 4 h treatment, and further decreased to 1.44 between the 4 h and the 22 h treatment. The decrease in molecular weight dispersity indicates that the molecular weight of the molecules within each resulting product after treatment with DrGBE is tending towards uniformity, or consisting of a smaller range of molecular weights compared to the untreated commercial polyglucan control (dispersity value not reported due to confidentiality). The resulting GPC chromatogram also supports this conclusion, showing that the molecular weight distribution has drastically reduced, and even changed shape from a somewhat bimodal distribution shaped-curve observed for the untreated commercial polyglucan (control; data not shown due to confidentiality) to a normal distribution, bell-shaped curve observed for post DrGBE treatment products (2 h, 4 h, and 22 h samples; Figure 5.3.2.3). One can observe in a normal distribution curve the same number of long high-molecular-weight chains as short low-molecular-weight chains, and majority of chains with a common molecular weight range in the center of the graph (Figure 5.3.2.3; 2 h, 4 h and 22 h). On the other hand, in a bimodal distribution there are two molecular weight ranges. It is also known that the untreated commercial polyglucan forms a gel within about an

hour at room temperature (Figure 5.3.1.1), which is most likely due to the presence of the high-molecular-weight hump and tail (long glucan chains) in the higher end of its bimodal molecular weight distribution (Giles *et al*., 2005). Although the exact starch source is unknown (due to confidentiality reasons), the high-molecular-weight hump and tail in the commercial polyglucan may be due to the presence of long amylose chains (*e.g*. if source is normal starch), or high molecular weight amylopectin (*e.g*. if source is *waxy* maize starch). The products of the DrGBE treatment of the commercial polyglucan (proprietary), however, do not form a gel (even after long periods), most likely due to their normal molecular weight distribution, characterized by the lower molecular weight and smaller molecular weight dispersity compared to the untreated commercial polyglucan control (Figure 5.3.2.3; control data not shown due to confidentiality) (Giles *et al*., 2005). Overall, GPC results suggest a change in polyglucan structure post treatment with DrGBE, most likely resulting from increased branching and a reduction in high molecular weight glucan chains (see schematic in Figure 5.3.2.1).

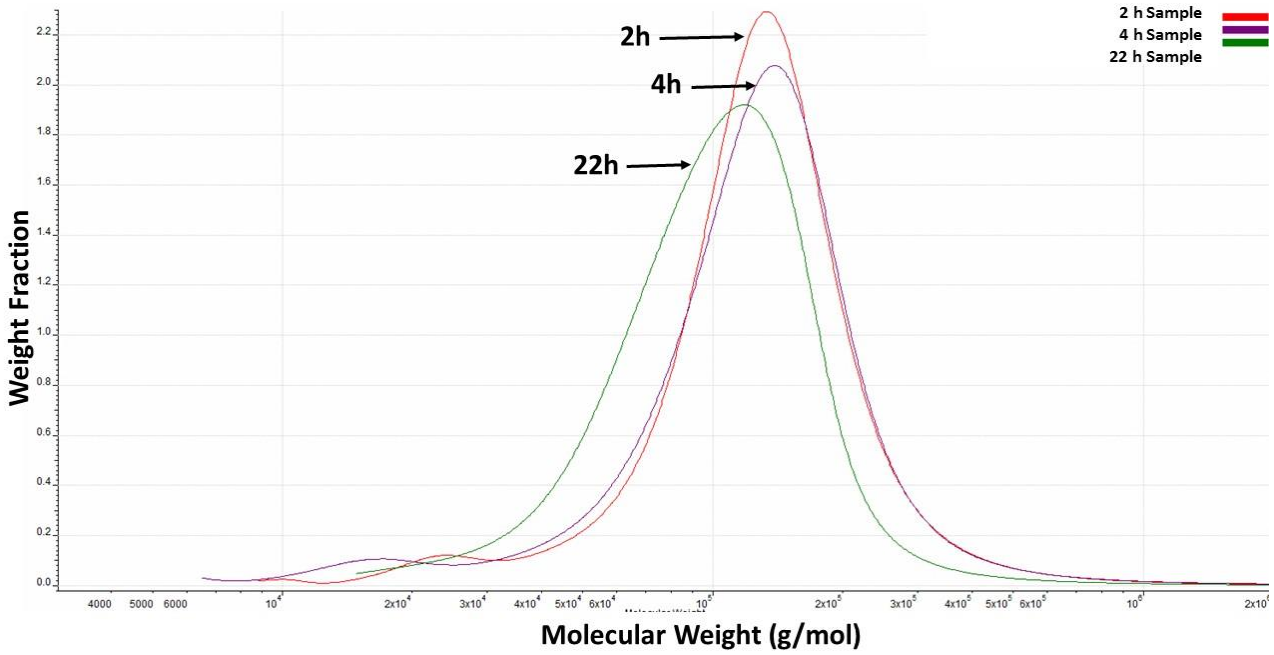

Figure 5.3.2.3 Molecular weight distribution plot of the DrGBE-treated commercial polyglucan (proprietary) generated by GPC triple detection. Commercial proprietary polyglucan was incubated with 20 mg DrGBE (23 U) for 2 h, 4 h, or 22 h. DrGBE was heat-inactivated and an aliquot (~2mL) of each reaction was dried in an oven at 80 ºC. For GPC analysis, 25 mg of the dried sample was dissolved in 10 mL DMSO and a 1 mL aliquot was then filtered and injected into the GPC column.

5.3.3 Determination of Branching Frequency Using ^{1}H-NMR Spectroscopy

The degree of branching of the untreated commercial, proprietary starch-based polyglucan, and the resulting products from the treatment of the polyglucan with DrGBE, were assessed by ^{1}H-NMR spectroscopy. NMR spectroscopy is a technique that exploits the magnetic properties of certain atomic nuclei to assess the physical and chemical properties of molecules of interest (McIntyre *et al*., 1990; Morris, 1986). NMR active nuclei, such as ^{1}H, can absorb electromagnetic radiation and possess a property known as nuclear spin; they act as tiny magnets which can orient themselves in an applied external magnetic field producing a nuclear magnetic resonance response, or a chemical shift (Bharti and Roy, 2012; Morris, 1986). The use of ^{1}H-NMR spectroscopy, amongst other structural features, allows for the determination of degree of branching without prior chemical or enzymatic treatment of the polyglucan (Gidley, 1985; Nilsson *et al*., 1996). Due to the high sensitivity of ^{1}H-NMR spectroscopy, the resonances of the anomeric protons involved in α-(1,4) and α-(1,6) linkages can be distinguished and used to calculate the degree of branching in the polyglucan of interest (Blake *et al*., 1985; Gidley, 1985; Kasprzak *et al*., 2012; McIntyre *et al*., 1990; Nilsson *et al*., 1996). A number of previous studies have reported the use of ^{1}H-NMR spectroscopy to determine the degree of branching (in applicable polyglucans) and characterize structural properties of various polysaccharides including starch, amylopectin, glycogen, maltopheptaose, maltodextrin, pullulan, and inulin (Blake *et al*., 1985; Gidley, 1985; McIntyre and Vogel, 1990, 1991; McIntyre *et al*., 1990; Nilsson *et al*., 1996; Zang *et al*., 1991).

The effect of DrGBE on the proportion of α-1,6-glycosidic linkages in the commercial polyglucan was examined by ^{1}H-NMR spectroscopy. The untreated

commercial polyglucan was also analyzed by ^{1}H-NMR spectroscopy. Samples of the DrGBE-treated commercial polyglucan were taken after 2 h, 4 h, and 22 h and dissolved (~10 mg) in 1 mL of deuterium oxide (D_2O). The untreated commercial polyglucan (~10 mg) was also dissolved in 1 mL D_2O. Distilled water protons give rise to a strong signal in NMR spectroscopy and therefore D_2O is routinely used as NMR sample solvent instead (McIntyre *et al*., 1990; Nilsson *et al*., 1996). D_2O is also the solvent of choice for NMR samples of starch and starch-based polysaccharides (Blake *et al*., 1985; Gidley, 1985; McIntyre *et al*., 1990; Zang *et al*., 1991). The ^{1}H-NMR spectra in figures 5.3.3.1 A, B, C, and D show an intense signal (peak) at a chemical shift of 5.34 ppm (parts per million), which is due to the anomeric proton associated with the α-1,4 linkages of the tested polyglucans. A smaller signal can also be observed at 4.94 ppm which arises from the anomeric proton at sites of α-1,6 branch points. Similar chemical shift values were previously reported for potato starch (5.35 ppm for H-1[α-1,4] and 4.94 ppm for H-1[α-1,6]) (Nilsson *et al*., 1996), glycogen (5.38 ppm for H-1[α-1,4] and 4.98 ppm for H-1[α-1,6]) (McIntyre and Vogel, 1990; Zang *et al*., 1991), and maltodextrin (5.40 ppm for H-1[α-1,4] and 5.00 ppm for H-1[α-1,6]) (McIntyre and Vogel, 1990; McIntyre *et al*., 1990). Other resonances corresponding to poorly resolved and overlapping peaks were also observed (not shown in the presented spectra). The presence of overlapping peaks is a drawback of conventional one-dimensional proton spectra, and it is one of the reasons why proton NMR spectroscopy has been utilized to a limited extent in starch characterization (McIntyre *et al*., 1990). The overlapping peaks would require further investigation, and complete assignment of the proton NMR spectra (all chemical shifts)

would require the use of two-dimensional NMR techniques (McIntyre *et al*., 1990; Nilsson *et al*., 1996).

Application of DrGBE caused hydrolysis of α-1,4 glycosidic linkages within the commercial polyglucan and subsequent transfer and reattachment of the cleaved fragments to a hydroxide oxygen on the C6 in a glucose unit of the same, or another chain, creating a branch point. The DrGBE-induced modification of branching within the commercial polyglucan was detected and measured by ^{1}H-NMR spectroscopy and expressed as a peak (signal) at a particular chemical shift (ppm). Integration of the signal (peak) at a chemical shift of 4.94 ppm provides information regarding the degree of branching of the analyzed polyglucan when compared to the area of the signal (peak) at 5.34 ppm, corresponding to the α-1,4 linkages. The integral peak of the anomeric proton on units linked by α-1,4 glycosidic linkages (peak at 5.34 ppm) was fixed at 1, and the integral peak of the anomeric proton on units linked by α-1,6 glycosidic linkages was determined by electronic integration after appropriate baseline correction as necessary (Table 5.3.3). The percent branching of the analyzed polyglucans was calculated as the ratio of (Kasprzak *et al*., 2012; Nilsson *et al*., 1996):

$$\%\, Branching = \frac{Integral\ H^1\ (\alpha - 1{,}6)}{[Integral\ H^1\ (\alpha - 1{,}4) + Integral\ H^1\ (\alpha - 1{,}6)]}\ x\ 100$$

Branching in amylopectin of normal starches occurs regularly with different size branch points organized in a periodic manner and occurring at a rate of approximately 3-5% (Gunja *et al*., 1960; Hizukuri, 1986; Kasprzak *et al*., 2012; Nilsson *et al*., 1996). The untreated commercial polyglucan has approximately 5.7% branching (Table 5.3.3).

Figure 5.3.3.2 depicts the change in the signal (peak) of the anomeric proton associated with the α-1,6 glycosidic linkages of the tested polyglucans (red arrows). The peak at a chemical shift of 4.94 ppm (anomeric proton of α-1,6 linkages) in the spectra of the DrGBE-treated commercial polyglucan (Figure 5.3.3.2 b, c, and d) appears larger compared to the peak (at 4.94 ppm) of the untreated commercial polyglucan (Figure 5.3.3.2 a). Indeed, the degree of branching within the treated commercial polyglucan increased by approximately 42% after 2 h of incubation with DrGBE, 50% after 4 h, and 53% after 22 h of incubation (at a constant temperature of 35 ºC) compared to the untreated commercial polyglucan control (Table 5.3.3). The data suggests that the most dramatic increase in branch content occurred within the first 2 h of incubation and tapered off thereafter. This implies that the degree of branching of the product may depend on the time of incubation and likely the amount of enzyme in the reaction (was not determined in this set of experiments). However, it is possible that not only time and amount of enzyme are responsible for the observed change in reaction rate, but also the structure of the product. A plausible explanation is that the change in branching, and thus structure, of the commercial polyglucan throughout the reaction is affecting the activity of DrGBE and possibly slowing the rate of branching. In other words, the highly-branched product (~10%; Table 5.3.2) produced in the first 2 h of incubation may impede further branching by DrGBE. Moreover, it is possible that some enzyme degradation is occurring over time and thus contributing to the reduced reaction rate. One way to test the effect of the changing substrate structure on DrGBE activity, is by adding fresh enzyme to the ongoing reaction and recording the rate of change in branching. The change in compound structure can be further characterized and fine-tuned by not only varying the

time of incubation, but also by varying the enzyme dose and adding additional enzyme throughout the reaction to assess the change in branching rate.

Proton NMR analysis of DrGBE products did not show any sign of hydrolysis, as the anomeric proton of reductive ends (in both conformational anomers – *alpha* and *beta*; Figure 5.3.3.3) was observed in equilibrium and was comparable to the anomeric reductive ends proton of the untreated polyglucan control (data not shown). The reducing end glucose can exist in two conformational anomers, *alpha* and *beta*, (Figure 5.3.3.3), and these two forms interconvert and can be distinguished by ^{1}H-NMR spectroscopy since the *alpha* form resonates further downfield (>5 ppm) from the *beta* form (<5 ppm) (Drake and Brown, 1977). If branching was inefficient, hydrolysis would be observed as it would result in generation of terminal reducing units contributing to a larger signal (peak) compared to that of the control (data not shown) (Drake and Brown, 1977; Nilsson *et al*., 1996; Zang *et al*., 1991). The two anomeric populations of the terminal reducing units, *alpha* and *beta*, were observed in equilibrium in the ^{1}H-NMR spectra and their signals (peaks) closely resembled those of the untreated control polyglucan (data not shown due to confidentiality), indicating lack (or insignificant levels) of hydrolysis and implying efficient branching activity. The hydrolytic activity of DrGBE (on amylose) was previously assessed by the quantitative branch linkage assay (Chapter 4), and determined to be less than 2% of the total activity of DrGBE (see Chapter 4; Palomo *et al*., 2009), which is in agreement with the ^{1}H-NMR results reported here.

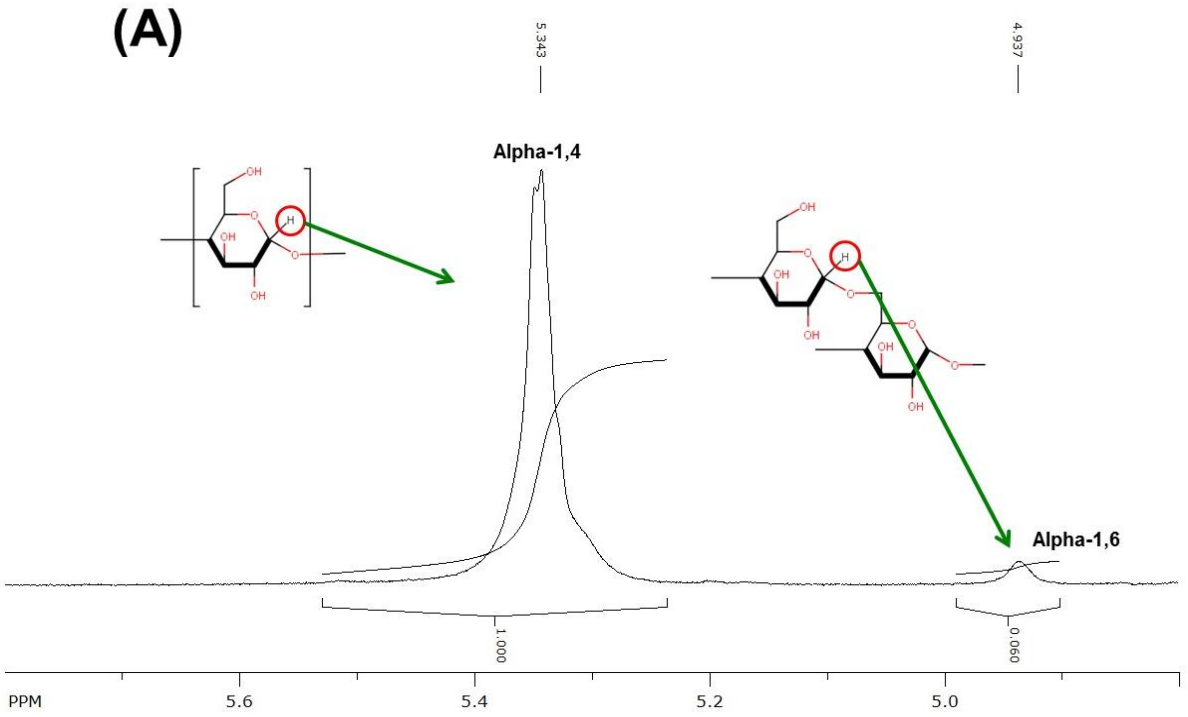
(A)
5.343
4.937
Alpha-1,4
Alpha-1,6
1.000
0.060
PPM
5.6
5.4
5.2
5.0

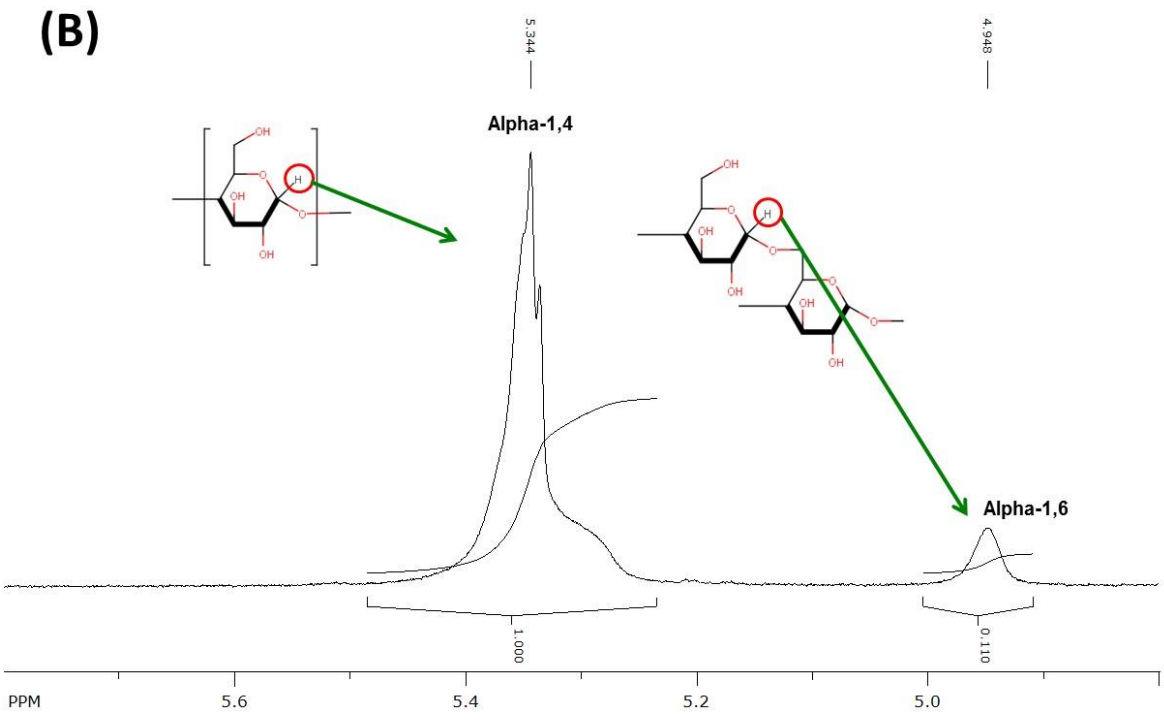
(B)
5.344
4.948
Alpha-1,4
Alpha-1,6
1.000
0.110
PPM
5.6
5.4
5.2
5.0

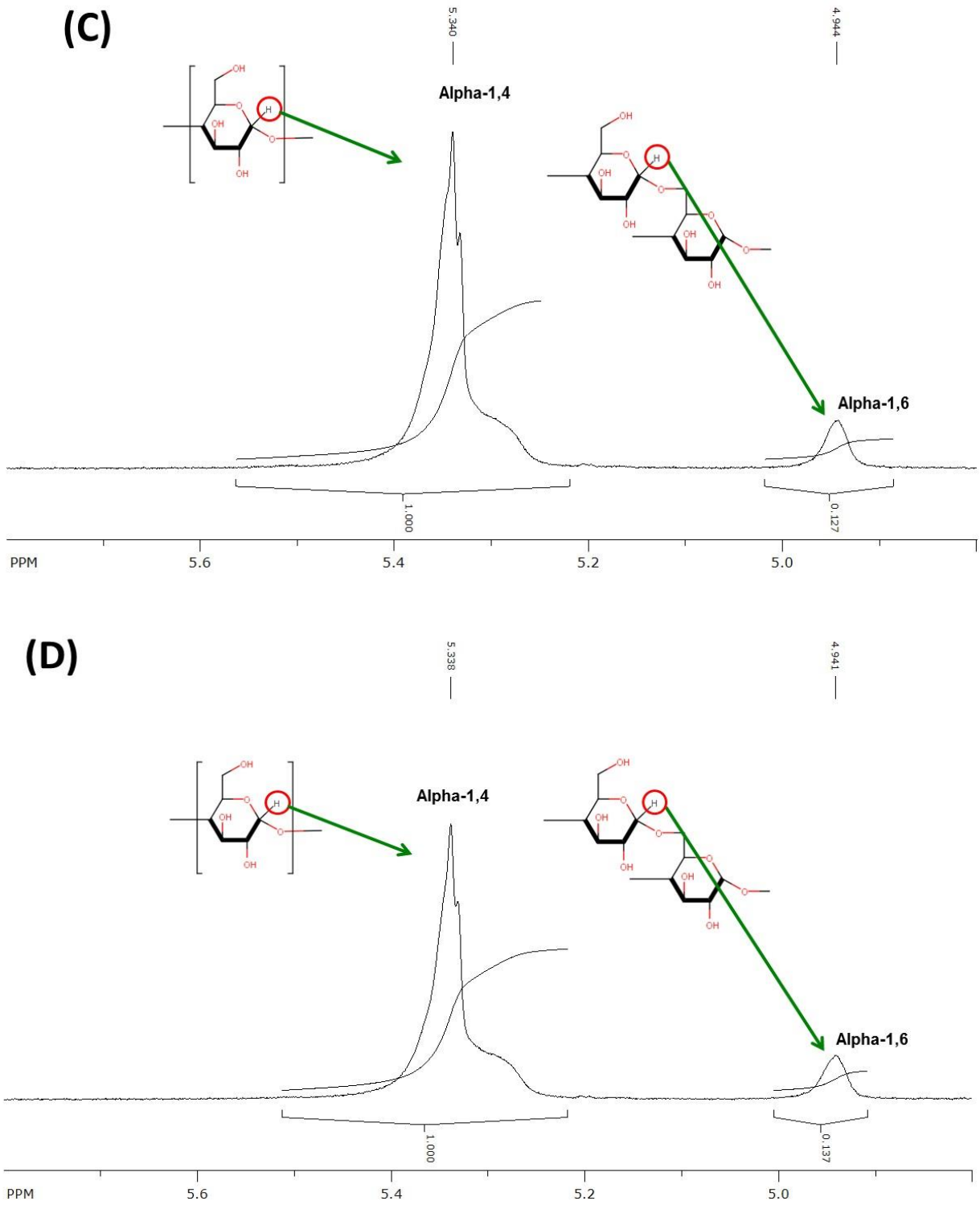

Figure 5.3.3.1 ^{1}H-NMR spectra (D_2O, 60 ºC) of the untreated commercial starch-based polyglucan (A) and the resulting products from treatment of the commercial polyglucan with DrGBE for 2 h (B), 4 h (C), and 22 h (D). Resonances of anomeric hydrogens (chemical shift and peaks) in α-1,4 and α-1,6 glucose linkages are indicated.

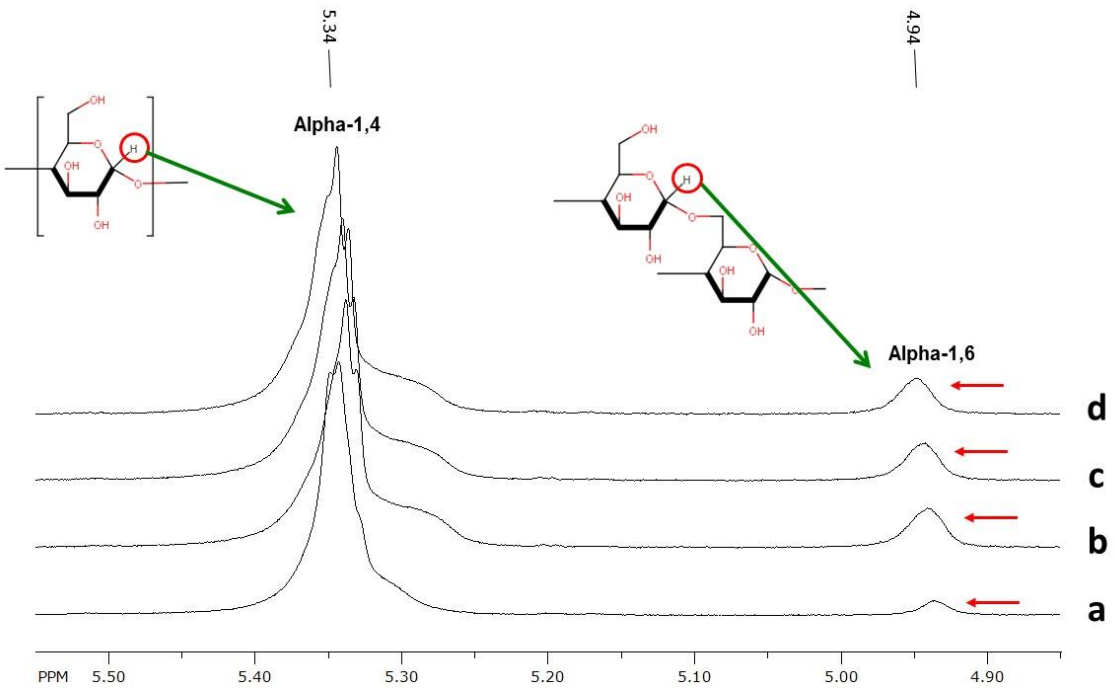

Figure 5.3.3.2 ^{1}H-NMR spectral sections depicting the change in the signal (peaks) of the anomeric hydrogens in α-1,4 and α-1,6 glucose linkages of the untreated commercial polyglucan (a), and DrGBE-treated commercial polyglucan after 2 h (b), 4 h (c), and 22 h (d). The peak of the anomeric hydrogen associated with the α-1,6 glucose linkages in the DrGBE-modified commercial polyglucan increases with time as compared to the untreated commercial polyglucan (depicted with red arrows).

Table 5.3.3 The Effect of DrGBE on the Branch Content (%) of a Commercial Polyglucan as Calculated Using the Integral (^{1}H) Peak Values Obtained by ^{1}H-NMR Spectroscopy.

Sample	Integral (^{1}H) peak at 4.94 ppm	% Branching
Control	0.060	5.7
2h treatment	0.110	9.9
4h treatment	0.127	11.3
22h treatment	0.137	12.0

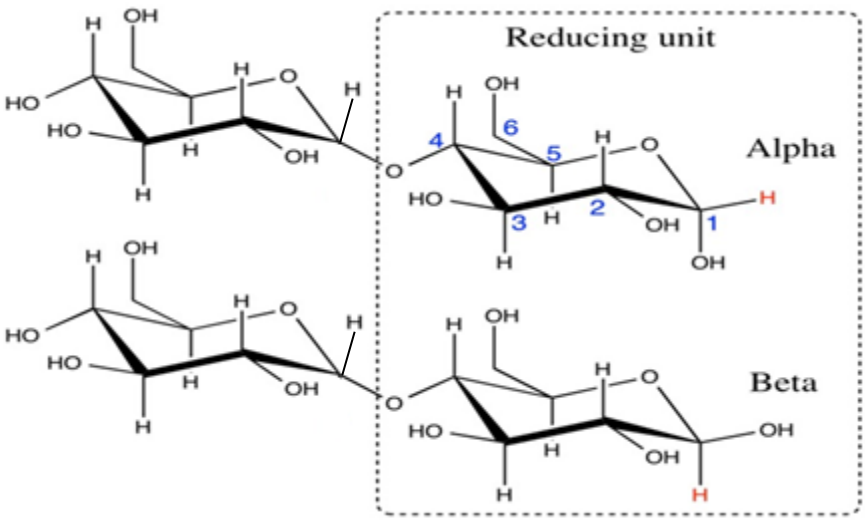

Figure 5.3.3.3 The *alpha* and *beta* anomeric conformations of maltose with the anomeric protons shown in red. Figure adapted from Magritek Spinsolve™ application note and modified.

5.3.4 Concluding Remarks

Overall, the results of this study, wherein a commercial proprietary polyglucan was subjected to enzymatic modification by DrGBE, suggest that DrGBE acts rapidly (within 2 h) to reduce the molecular weight and viscosity, producing a non-gelling product. ^{1}H-NMR spectroscopy showed a significant increase in branching after only a 2 h treatment and no sign of hydrolysis, which indicates that DrGBE has efficient branching activity. It can be further concluded that through the branching action of DrGBE, which significantly increases the branching frequency of the treated polyglucan (~12% vs. 3-5% in native starch), it effectively reduces the abundance of long glucan chains and leads to a reduction in the molecular weight and molecular weight distribution of the tested polyglucan (see Figure 5.3.2.2 and schematic in Figure 5.3.2.1). The

resultant polyglucan also possess a much lower intrinsic viscosity compared to the control, most likely due to the contraction of the polymer in terms of the hydrodynamic volume, attributed to the increased branching frequency. The approach of using DrGBE to modify this specific commercial polyglucan is promising as it produced a unique polymer structure which is not obtainable by the manufacturer's current extrusion process and processing conditions. Although the treatment is efficient at producing new polymer structures, it should be further optimized to suit manufacturer's processing conditions (*e.g.* piloted and scaled up). In order to obtain a product with desirable properties - non-gelling with a minimum shift in molecular weight - the optimization should be conducted at a higher polyglucan solid content (30-35% (w/v) solids), higher temperature (60-80 °C), at least in the beginning of the run, and varied enzyme dose and time of treatment. However, higher concentration dispersions of this commercial polyglucan lead to almost imminent retrogradation and gelling. We wanted to be able to keep the polyglucan in solution so the added GBE can have a chance to act on its glucan chains prior to gelling occurring. Higher concentrations therefore, would hinder some of the basic characterization we wanted to establish with this polyglucan. A proof of concept was shown at the dispersed concentration (~16% solids), and in the future higher concentrations could be attempted (part of the post-doc research).

Starches from various botanic sources are widely commercially exploited (Alcázar-Alay and Meireles, 2015). However, native starches are structurally and functionally too restrictive for the vast range of industrial applications (see Chapter 1 for details). Therefore, post-harvest starch is modified in various ways such as physical, chemical, or enzymatic, to enhance the functionality of starch (Kasprzak *et al.*, 2012;

Kraak, 1992; van der Maarel and Leemhuis, 2013). The use of enzymes has a number of advantages over the chemical and physical methods, including high substrate selectivity and substrate specificity, and tighter control of the biochemical reaction. Additionally, the enzymatic method for starch modification is safer for the consumer and the environment, and produces less unexpected and hazardous chemical side products (Kasprzak *et al*., 2012; Le *et al*., 2009; Lee *et al*., 2008). As illustrated in this chapter, the use of branching enzymes offers a valuable tool for post-harvest starch modification for various industrial applications, in particular for applications in paints, coatings and adhesives industries where highly-branched, non-gelling starches with favourable dispersion properties are desired (Kiel *et al*., 1991; Röper, 2002).

Chapter 6 – General Discussion

In the research outlined in this thesis, a thermostable GBE from *Thermus thermophilus*, and a GBE from *Deinococcus radiodurans*, were biochemically characterized. As discussed in Chapter 2, these recombinant GBEs were heterologously expressed, purified to near homogeneity (Figure 2.3.2.1 B and C), and their identity confirmed through mass spectrometric analysis (Figure 2.3.2.2).

A detailed biochemical and functional characterization of recombinant TtGBE and DrGBE revealed their optimum activity conditions (*e.g*. temperature, pH), kinetic parameters (K_m and V_{max}) with amylose and amylopectin, and their substrate and branching chain length preferences (Table 4.3.3). These GBEs were characterized in detail in order to gain insight into the intricacies of their activities for potential future applications in post-harvest starch modification.

TtGBE exhibited branching activity with amylose corresponding to a specific activity of 0.5 U/mg (and a K_m of 0.11 mg/mL), which closely resembled a previously reported specific activity value for TtGBE with amylose of 0.29 U/mg (Palomo *et al*., 2011). Interestingly, TtGBE did not show branching activity with amylopectin as a substrate, although it did tend to hydrolyze it, but did not further branch it. Similar preference for amylose as substrate has also been previously reported for *Thermococcus kodakaraensis* (KOD1) GBE. Surprisingly, TtGBE also displayed a relatively high hydrolytic activity, considering it is a branching enzyme, of approximately 10% of total activity with amylose as a substrate (as reported in Chapter 4, and also observed by Palomo *et al*. (2011)). A previous study with AgGBE had also shown that this enzyme possesses hydrolytic activity when incubated with dextrins, but not when incubated with

amylose (Thiemann *et al*., 2006). Interestingly, plant SBEs have not been previously reported to show hydrolytic activity, and seem to possess high fidelity transglycosylation activity. It is unknown why some GBEs have promiscuous hydrolytic activity, despite their major activity being transglycosylation. However, it may be possible that it has something to do with the length of the substrate and the enzyme's active cleft substrate accommodation preferences, wherein certain substrates may promote the GBE to hydrolyze the α-glucan, while also causing it to occasionally fail to reattach the cleaved portion. Moreover, the length (DP) and structure of the acceptor molecule may also be a determinant of the total transglycosylation activity of a BE. For instance, the required DP of an acceptor molecule for a certain GBE may be higher than the DP of the substrate used (*e.g*. shorter dextrins), resulting in hydrolysis without transfer of fragmentation products to an acceptor glucan.

DrGBE exhibited branching activity with both amylose and amylopectin corresponding to 1.64 U/mg (and a K_m of 0.27 mg/mL) and 1.15 U/mg (and a K_m of 0.07 mg/mL), respectively. In contrast to TtGBE, the hydrolytic activity of DrGBE with either substrate was negligible.

To understand the nature of their enzymatic activity, the effect of temperature, pH, and redox state on TtGBE and DrGBE activity was also examined, and is summarized in Table 4.3.1 along with the temperature and pH preferences of other characterized BEs. Thermostability and the pH response of starch-acting enzymes are critical properties for industrial use (Kandra, 2003; de Souza and de Oliveira Magalhães, 2010). The optimum temperature for activity of TtGBE (70 ºC) and DrGBE (25 - 35 ºC) differed markedly (Table 4.3.1), which is not surprising as TtGBE is an enzyme of the

extreme thermophile, *Thermus thermophilus*, which thrives at high temperatures (≥80 ºC) (Kagawa *et al*., 1984), whereas DrGBE is from the extremophile *Deinococcus radiodurans*, which has a much lower optimal growth temperature of 25 – 35 ºC (Brooks and Murray, 1981). The structural thermostability of these GBEs was confirmed by CD spectroscopy, yielding apparent melting temperatures of ~96 ºC and ~61 ºC for TtGBE and DrGBE, respectively (Figure 3.3.1.3). The CD-obtained thermal denaturation curves suggest that despite their differences in optimum temperature for activity, the secondary structure of both GBEs was quite resistant to thermal denaturation, and as expected, particularly that of TtGBE, which exhibited ultra thermal tolerance. The CD thermal denaturation analysis further attests to the true thermostable nature of TtGBE, which also retained over 90% of activity after heating at 80 ºC for 1 h (determined in this study; for more detail see section 4.3.1), a result that was corroborated by a previous study which reported that TtGBE remained fully active following incubation at 80 ºC for 1 h (Palomo *et al*., 2011). The thermostable nature of TtGBE can lend itself useful in applications of this GBE for industrial post-harvest starch processing. As mentioned previously, the industrial utilization of starch requires dispersal of starch polyglucans (crystalline granule matrix) in an aqueous environment at high temperatures (to prevent retrogradation of the amylose component) in order to access the functional reactive groups on starch. Therefore, thermostable GBEs may come in useful in this process, increasing branching frequency, removing amylose by hydrolyzing long glucan chains, and simultaneously creating novel polyglucan structures with improved, and commercially beneficial physicochemical properties. For example, an important application of thermostable BEs in the food industry can be in the modification of starches to produce nutritional-grade

carbohydrates with low digestibility, which have an increased resistance to pancreatic α-amylase degradation. Recent studies by Le *et al*. (2009) using a thermostable *Bacillus subtilis* GBE in combination with a maltogenic amylase (from *Bacillus stearothermophilus*), generated highly-branched (~10% vs. ~5% in wild type) tapioca (*Manihot esculenta* L.) starch with reduced susceptibility to α-amylase digestion.

The optimum pH for activity of TtGBE and DrGBE was 6 and 7, respectively (Table 4.3.1). The range of optimum pH for activity of both GBEs is quite narrow, and may limit their uses in certain industries, in particular in applications wherein pH levels vary. However, most post-harvest processing procedures involve the aqueous dispersal of the starch granule crystalline matrix and thus typically pH levels do not vary drastically, unless certain applications require the addition of pH altering compounds. For instance, in the detergent industry starch-acting enzymes active at alkaline pH are preferred, in order to maintain stability under detergent conditions (Kirk *et al*., 2002). In contrast, the initial steps in a typical high-fructose syrup production process, involve the aqueous dispersal of starch (final solution concentration ~35%) at a pH of ~6.5 (Hobbs, 2009).

Some plant SBEs, and at least one GBE, have previously been shown to be affected by redox modulation. For instance, Arabidopsis SBE 2 showed reductive activation under reducing conditions (Glaring *et al*., 2012), while mSBEIIb (Makhmoudova, 2014 unpublished) and AgGBE had increased activities in the presence of a reducing agent (Thiemann *et al*., 2006), and wheat SBEIIa was indicated to be redox-regulated through an immuno-proteomics approach (Balmer *et al*., 2006). No redox state effect was observed for TtGBE and DrGBE, meaning both enzymes functioned well under either oxidative or reductive reaction conditions (Figure 4.3.1.3). Lack of visible

effect on activity of changing redox state may be beneficial for the potential use of TtGBE and DrGBE as tools in industrial starch processing. Indeed, the oxidative stability of starch-acting enzymes is one of the most important criteria for their use in certain industries, especially in the detergent industry (Chi *et al*., 2010). Although traditional starch-acting enzymes are still utilized in the industry, requirements for optimally performing starch-acting enzymes are quite specific for each industry, mainly concerning pH, oxidative stability, and temperature behaviors (Chi *et al*., 2010). Therefore, new starch-acting enzymes (*e.g*. *α*-amylases) with optimized properties, such as enhanced thermal stability, acid tolerance, and ability to function under oxidative conditions, are being developed using strategies such as (but not limited to), site-directed mutagenesis, and design of chimeric enzymes (Bisgaard-Frantzen *et al*., 1999; Chi *et al*., 2010; Declerck *et al*., 2000; Shaw *et al*., 1999).

The detailed understanding of the structural and functional relationships of BE enzyme protein domains presents a useful tool for modifying BE protein characteristics through, for example, protein engineering, to produce BEs with improved characteristics (*e.g*. thermostability, improved pH profile, and unique substrate and branching preferences) that can be applied to generate polyglucans with unique and novel properties. With that in mind, chimeric BEs were designed (Figure 3.3.2.1), and incorporated part of the TtGBE sequence, for its potential to impart thermostability, and part of either mSBEI, or mSBEIIb sequence, for their potential to contribute to branching specificity and substrate preference. Chimeric BEs were heterologously expressed, purified (through an affinity-tag), and tested for activity. The chimeric BEs exhibited much lower specific branching activity (>50%) compared to their native counterparts

(Figure 3.3.2.3), and only one chimeric BE, Tt-SBEI-C (with the highest specific branching activity), was partially characterized (section 3.3.2). Tt-SBEI-C activity resulted in novel polyglucan products with chain lengths intermediate between those of TtGBE and mSBEI (Figure 3.3.2.4 and 3.3.2.5), and therefore it was concluded that Tt-SBEI-C potentially combines branching preference elements of both TtGBE and mSBEI. The work with chimeric BEs showed a proof of concept, demonstrating that chimeric BE sequences can potentially be used to generate unique α-glucan polymers with distinct structures that may exhibit novel properties and could potentially be suited (through optimization and testing) to a variety of industrial applications.

The substrate and branching preferences of recombinant DrGBE and TtGBE were analyzed in detail, and showed that DrGBE efficiently branches both amylose and amylopectin (as well as starch), while TtGBE preferentially branches amylose, but not amylopectin (although it is able to hydrolyze amylopectin). The products of DrGBE and TtGBE activity were analyzed and determined to differ in their side-chain length distribution profile (section 4.3.3; details outlined in Table 4.3.3). DrGBE activity with amylopectin yielded products with a CL optima of 10 and a high frequency of chains of DP 6 – 12, while with MOS the CL optima was 9 – 10, and a high abundance of chains of DP 6 – 11 (Table 4.3.3). TtGBE on the other hand, when reacted with MOS, had a CL optima of 8 and 11, and preferentially transferred chains of DP 6 – 13, while its activity with MDs yielded products with a CL optima of 10, and a high frequency of chains of DP 6 – 16 (Table 4.3.3). The BE enzyme class has a broad specificity with regard to substrate preferences, as well as the length of the glucan chain transferred during the branching process, as is summarized in Table 4.3.3 for a number of GBEs and SBEs, including

TtGBE and DrGBE. Therefore, owing to their unique α-1,6 transglycosylation activity, substrate specificities, and branching preferences, BEs may find new applications in starch-related industries (as has been reviewed in Chapter 1).

The work presented in this thesis also described the novel application of recombinant DrGBE to modify a commercial starch-based polyglucan in order to reduce gelling, improve stability (*e.g.* "shelf-life") and solubility, and produce a visco-stable product. A common obstacle of processed post-harvest starch is the reduced "shelf-life", resulting from retrogradation of the polyglucans within the starch dispersion, caused chiefly by long glucan chains (*i.e.* amylose component). This phenomenon impedes manufacturer's ability to transport and store dispersed starch solutions, especially at high starch concentrations (>35% solids), as they tend to harden and form undesirable gels. BEs can be applied as effective industrial tools to increase the branching frequency of post-harvest starch, and to reduce chain length (thus remove amylose), thereby reducing retrogradation, and improving solubility and visco-stability properties. A proof of this concept was demonstrated (in this thesis) by treating a dispersed commercial starch preparation with recombinant DrGBE (Chapter 5). DrGBE acted rapidly, reducing the molecular weight and polyglucan size distribution in the resultant product (Figure 5.3.2.3), and prevented gelling (Figure 5.3.1.1). Not surprisingly, DrGBE activity also resulted in an increased branching frequency within the resultant polymer product, which was much higher (>50%) compared to the branching frequency of the original polyglucan (Figure 5.3.3.1; Table 5.3.3).

To summarize, the branching action of DrGBE resulted in reduction in the presence of long glucan chains and a more branched ("dense") polymer, contributing to

lower molecular weight, a narrower molecular weight dispersity, and a reduced intrinsic viscosity (see Figure 5.3.2.1 showing proposed structure of the resulting novel polyglucan). Based on these results, the action of DrGBE produced a polyglucan with a novel structure (Figure 5.3.2.1), which may have commercial benefits due to improved physicochemical properties (*e.g.* improved solubility and visco-stability). It is therefore clear, that the use of BEs offers a valuable tool for post-harvest starch modification, and in the future, industrial-grade BEs may find uses in various industrial applications.

REFERENCES

Abad, M.C., Binderup, K., Rios-Steiner, J., Arni, R.K., Preiss, J., and Geiger, J.H. (2002). The X-ray crystallographic structure of Escherichia coli branching enzyme. J. Biol. Chem. *277*, 42164–42170.

Abbas, K.A., K. Khalil, S., and Meor Hussin, A.S. (2010). Modified Starches and Their Usages in Selected Food Products: A Review Study. J. Agric. Sci. *2*, 90.

Agathos, S.N. (1991). Production scale insect cell culture. Biotechnol. Adv. *9*, 51–68.

Ahmed, Z., Tetlow, I.J., Ahmed, R., Morell, M.K., and Emes, M.J. (2015). Protein–protein interactions among enzymes of starch biosynthesis in high-amylose barley genotypes reveal differential roles of heteromeric enzyme complexes in the synthesis of A and B granules. Plant Sci. *233*, 95–106.

Alcázar-Alay, S.C., and Meireles, M.A.A. (2015). Physicochemical properties, modifications and applications of starches from different botanical sources. Food Sci. Technol. *35*, 215–236.

Andersen, D.H. (1956). Familial cirrhosis of the liver with storage of abnormal glycogen. Lab. Invest. *5*, 11–20.

Andersen, D.C., and Krummen, L. (2002). Recombinant protein expression for therapeutic applications. Curr. Opin. Biotechnol. *13*, 117–123.

Annison, G., and Topping, D.L. (1994). Nutritional role of resistant starch: chemical structure vs physiological function. Annu. Rev. Nutr. *14*, 297–320.

Annor, G.A., Marcone, M., Bertoft, E., and Seetharaman, K. (2014). Unit and Internal Chain Profile of Millet Amylopectin. Cereal Chem. *91*, 29–34.

Ao, Z., Simsek, S., Zhang, G., Venkatachalam, M., Reuhs, B.L., and Hamaker, B.R. (2007). Starch with a Slow Digestion Property Produced by Altering Its Chain Length, Branch Density, and Crystalline Structure. J. Agric. Food Chem. *55*, 4540–4547.

Ashogbon, A.O., and Akintayo, E.T. (2014). Recent trend in the physical and chemical modification of starches from different botanical sources: A review. Starch - Stärke *66*, 41–57.

Baba, T., Kimura, K., Mizuno, K., Etoh, H., Ishida, Y., Shida, O., and Arai, Y. (1991). Sequence conservation of the catalytic regions of amylolytic enzymes in maize branching enzyme-I. Biochem. Biophys. Res. Commun. *181*, 87–94.

Baecker, P.A., Greenberg, E., and Preiss, J. (1986). Biosynthesis of bacterial glycogen. Primary structure of Escherichia coli 1,4-alpha-D-glucan:1,4-alpha-D-glucan 6-alpha-D-(1, 4-alpha-D-glucano)-transferase as deduced from the nucleotide sequence of the glg B gene. J. Biol. Chem. *261*, 8738–8743.

Bailey, J.M., and Whelan, W.J. (1961). Physical properties of starch. I. Relationship

between iodine stain and chain length. J. Biol. Chem. *236*, 969–973.

Ball, S.G., and Morell, M.K. (2003). From bacterial glycogen to starch: understanding the biogenesis of the plant starch granule. Annu. Rev. Plant Biol. *54*, 207–233.

Ball, S., Guan, H.-P., James, M., Myers, A., Keeling, P., Mouille, G., Buléon, A., Colonna, P., and Preiss, J. (1996). From Glycogen to Amylopectin: A Model for the Biogenesis of the Plant Starch Granule. Cell *86*, 349–352.

Balmer, Y., Vensel, W.H., Cai, N., Manieri, W., Schurmann, P., Hurkman, W.J., and Buchanan, B.B. (2006). A complete ferredoxin/thioredoxin system regulates fundamental processes in amyloplasts. Proc. Natl. Acad. Sci. *103*, 2988–2993.

Baneyx, F. (1999). Recombinant protein expression in Escherichia coli. Curr. Opin. Biotechnol. *10*, 411–421.

Barker, S.A., and Bourne, E.J. (1951). The oligosaccharides synthesized by Escherichia coli from maltose. Biochem. J. *49*, lxi.

Belitz, H.-D., and Grosch, W. (1999). Food chemistry (Springer).

Bell, D.J. (1948). The structure of glycogens. Biol. Rev. Camb. Philos. Soc. *23*, 256–266.

Bemiller, J.N. (1997). Starch Modification: Challenges and Prospects. Starch - Stärke *49*, 127–131.

BeMiller, J.N., and Huber, K.C. (2015). Physical Modification of Food Starch Functionalities. Annu. Rev. Food Sci. Technol. *6*, 19–69.

BeMiller, J.N., and Whistler, R.L. (2009). Starch : chemistry and technology (Academic).

Bentley, W.E., Mirjalili, N., Andersen, D.C., Davis, R.H., and Kompala, D.S. (1990). Plasmid-encoded protein: the principal factor in the “metabolic burden” associated with recombinant bacteria. Biotechnol. Bioeng. *35*, 668–681.

Berski, W., Ptaszek, A., Ptaszek, P., Ziobro, R., Kowalski, G., Grzesik, M., and Achremowicz, B. (2011). Pasting and rheological properties of oat starch and its derivatives. Carbohydr. Polym. *83*, 665–671.

Bertoft, E. (2007). Composition of building blocks in clusters from potato amylopectin. Carbohydr. Polym. *70*, 123–136.

Bertoft, E., and Seetharaman, K. (2012). Starch Structure. In Starch : origins, structure and metabolism (Society for Experimental Biology).

Bertoft, E., Piyachomkwan, K., Chatakanonda, P., and Sriroth, K. (2008). Internal unit chain composition in amylopectins. Carbohydr. Polym. *74*, 527–543.

Bharti, S.K., and Roy, R. (2012). Quantitative 1H NMR spectroscopy. TrAC Trends Anal. Chem. *35*, 5–26.

Binderup, K., and Preiss, J. (1998). Glutamate-459 Is Important for *Escherichia coli* Branching Enzyme Activity †. Biochemistry *37*, 9033–9037.

Binderup, K., Libessart, N., and Preiss, J. (2000). Slow-binding inhibition of branching enzyme by the pseudooligosaccharide BAY e4609. Arch. Biochem. Biophys. *374*, 73–78.

Binderup, K., Mikkelsen, R., and Preiss, J. (2002). Truncation of the amino terminus of branching enzyme changes its chain transfer pattern. Arch. Biochem. Biophys. *397*, 279–285.

Bisgaard-Frantzen, H., Svendsen, A., Norman, B., Pedersen, S., Kjaerulff, S., Outtrup, H., and Borchert, T. V. (1999). Development of Industrially Important α-Amylases. J. Appl. Glycosci. *46*, 199–206.

Blake, J.D., Clarke, M.L., and Littlemore, J. (1985). Some structural properties of amylopectin from sugar cane (Elsevier).

Blauth, S.L., Yao, Y., Klucinec, J.D., Shannon, J.C., Thompson, D.B., and Guilitinan, M.J. (2001). Identification of Mutator insertional mutants of starch-branching enzyme 2a in corn. Plant Physiol. *125*, 1396–1405.

Blauth, S.L., Kim, K.-N., Klucinec, J., Shannon, J.C., Thompson, D., and Guiltinan, M. (2002). Identification of Mutator insertional mutants of starch-branching enzyme 1 (sbe1) in Zea mays L. Plant Mol. Biol. *48*, 287–297.

Blount, Z.D. (2015). The unexhausted potential of E. coli. Elife *4*, e05826.

Boel, E., Brady, L., Brzozowski, A.M., Derewenda, Z., Dodson, G.G., Jensen, V.J., Petersen, S.B., Swift, H., Thim, L., and Woldike, H.F. (1990). Calcium binding in alpha-amylases: an X-ray diffraction study at 2.1-A resolution of two enzymes from Aspergillus. Biochemistry *29*, 6244–6249.

Bornhorst, J.A., and Falke, J.J. (2000). Purification of proteins using polyhistidine affinity tags. Methods Enzymol. *326*, 245–254.

Borovsky, D., Smith, E.E., and Whelan, W.J. (1975a). Temperature-dependence of the action of Q-enzyme and the nature of the substrate for Q-enzyme. FEBS Lett. *54*, 201–205.

Borovsky, D., Smith, E.E., and Whelan, W.J. (1975b). Purification and Properties of Potato 1,4-alpha-d-Glucan: 1,4-alpha-d-Glucan 6-alpha-(1,4-alpha-Glucano)-Transferase. Evidence against a Dual Catalytic Function in Amylose-Branching Enzyme. Eur. J. Biochem. *59*, 615–625.

Borovsky, D., Smith, E.E., and Whelan, W.J. (1976). On the mechanism of amylose branching by potato Q-enzyme. Eur. J. Biochem. *62*, 307–312.

Borovsky, D., Smith, E., Whelan, W., French, D., and Kikumoto, S. (1979). The mechanism of Q-enzyme action and its influence on the structure of amylopectin. Arch. Biochem. Biophys. *198*, 627–631.

Boyer, C.D., Daniels, R.R., and Shannon, J.C. (1976). Abnormal Starch Granule Formation in Zea Mays L. Endosperms Possessing the Amylose-Extender Mutant1. Crop Sci. *16*, 298.

Boyer, L., Roussel, X., Courseaux, A., Ndjindji, O.M., Lancelon-Pin, C., Putaux, J.-L., Tetlow, I.J., Emes, M.J., Pontoire, B., D'Hulst, C., et al. (2016). Expression of Escherichia coli glycogen branching enzyme in an *Arabidopsis* mutant devoid of endogenous starch branching enzymes induces the synthesis of starch-like polyglucans. Plant. Cell Environ. *39*, 1432–1447.

Bradford, M.M. (1976). A rapid and sensitive method for the quantitation of microgram quantities of protein utilizing the principle of protein-dye binding. Anal. Biochem. *72*, 248–254.

Bräsen, C., Esser, D., Rauch, B., and Siebers, B. (2014). Carbohydrate Metabolism in Archaea: Current Insights into Unusual Enzymes and Pathways and Their Regulation. Microbiol. Mol. Biol. Rev. *78*, 89–175.

Brayer, G.D., Luo, Y., and Withers, S.G. (1995). The structure of human pancreatic alpha-amylase at 1.8 A resolution and comparisons with related enzymes. Protein Sci. *4*, 1730–1742.

Brooks, B.W., and Murray, R.G.E. (1981). Nomenclature for Micrococcus radiodurans and Other Radiation-Resistant Cocci: Deinococcaceae fam. nov. and Deinococcus gen. nov., Including Five Species. Int. J. Syst. Bacteriol. *31*, 353–360.

Brown, B.I., and Brown, D.H. (1966). Lack of an alpha-1,4-glucan: alpha-1,4-glucan 6-glycosyl transferase in a case of type IV glycogenosis. Proc. Natl. Acad. Sci. U. S. A. *56*, 725–729.

Bruinenberg, P.M., Hulst, A.C., Faber, A., and Voogd, R.H. (1996). A process for surface sizing or coating of paper.

Brummell, D.A., Watson, L.M., Zhou, J., McKenzie, M.J., Hallett, I.C., Simmons, L., Carpenter, M., and Timmerman-Vaughan, G.M. (2015). Overexpression of STARCH BRANCHING ENZYME II increases short-chain branching of amylopectin and alters the physicochemical properties of starch from potato tuber. BMC Biotechnol. *15*, 28.

Brzozowski, A.M., and Davies, G.J. (1997). Structure of the Aspergillus oryzae alpha-amylase complexed with the inhibitor acarbose at 2.0 A resolution. Biochemistry *36*, 10837–10845.

Buisson, G., Duée, E., Haser, R., and Payan, F. (1987). Three dimensional structure of porcine pancreatic alpha-amylase at 2.9 A resolution. Role of calcium in structure and activity. EMBO J. *6*, 3909–3916.

Buléon, A., Colonna, P., Planchot, V., and Ball, S. (1998a). Starch granules: structure and biosynthesis. Int. J. Biol. Macromol. *23*, 85–112.

Buléon, A., Gérard, C., Riekel, C., Vuong, R., and Chanzy, H. (1998b). Details of the

Crystalline Ultrastructure of C-Starch Granules Revealed by Synchrotron Microfocus Mapping. Macromolecules *31*, 6605–6610.

Burrell, M.M. (2003). Starch: the need for improved quality or quantity--an overview. J. Exp. Bot. *54*, 451–456.

Camps, M. (2010). Modulation of ColE1-like plasmid replication for recombinant gene expression. Recent Pat. DNA Gene Seq. *4*, 58–73.

Cantor, E.J., and Chong, S. (2001). Intein-Mediated Rapid Purification of Cre Recombinase. Protein Expr. Purif. *22*, 135–140.

Cao, H., and Preiss, J. (1996). Evidence for essential arginine residues at the active sites of maize branching enzymes. J. Protein Chem. *15*, 291–304.

Carroll, J.O., Boyce, C., Wong, T.M., and Starace, C.A. (1985). Bread antistaling method.

Cassidy, A., Bingham, S.A., and Cummings, J.H. (1994). Starch intake and colorectal cancer risk: an international comparison. Br. J. Cancer *69*, 937–942.

Che, L.-M., Li, D., Wang, L.-J., Dong Chen, X., and Mao, Z.-H. (2007). Micronization and Hydrophobic Modification of Cassava Starch. Int. J. Food Prop. *10*, 527–536.

Chen, J., Liu, Y., Wang, Y., Ding, H., and Su, Z. (2008). Different effects of L-arginine on protein refolding: Suppressing aggregates of hydrophobic interaction, not covalent binding. Biotechnol. Prog. *24*, 1365–1372.

Chi, M.-C., Chen, Y.-H., Wu, T.-J., Lo, H.-F., and Lin, L.-L. (2010). Engineering of a truncated α-amylase of Bacillus sp. strain TS-23 for the simultaneous improvement of thermal and oxidative stabilities. J. Biosci. Bioeng. *109*, 531–538.

Chong, S., Shao, Y., Paulus, H., Benner, J., Perler, F.B., and Xu, M.Q. (1996). Protein splicing involving the Saccharomyces cerevisiae VMA intein. The steps in the splicing pathway, side reactions leading to protein cleavage, and establishment of an in vitro splicing system. J. Biol. Chem. *271*, 22159–22168.

Chong, S., Mersha, F.B., Comb, D.G., Scott, M.E., Landry, D., Vence, L.M., Perler, F.B., Benner, J., Kucera, R.B., Hirvonen, C.A., et al. (1997). Single-column purification of free recombinant proteins using a self-cleavable affinity tag derived from a protein splicing element. Gene *192*, 271–281.

Christianson, D.D., and Bagley, E.B. (1983). Apparent viscosities of dispersions of swollen corn starch granules. Cereal Chem. *60*, 116–121.

Collado, L.S., and Corke, H. (1999). Heat-moisture treatment effects on sweetpotato starches differing in amylose content. Food Chem. *65*, 339–346.

Conrad, B., Hoang, V., Polley, A., and Hofemeister, J. (1995). Hybrid Bacillus amyloliquefaciens X Bacillus licheniformis alpha-amylases. Construction, properties and

sequence determinants. Eur. J. Biochem. *230*, 481–490.

Cori, G.T., and Cori, C.F. (1943). Crystalline Muscle Phosphorylase. IV. Formation of Glycogen. J. Biol. Chem. *151*, 57–63.

Counotte, G.H., and Prins, R.A. (1979). Calculation of Km and Vmax from substrate concentration versus time plot. Appl. Environ. Microbiol. *38*, 758–760.

Couto, S.R., and Sanromán, M.Á. (2006). Application of solid-state fermentation to food industry—A review. J. Food Eng. *76*, 291–302.

Crabb, D.W., and Mitchinson, C. (1997). Enzymes involved in the processing of starch to sugars. Trends Biotechnol. *15*, 349–352.

Crabb, W.D., and Shetty, J.K. (1999). Commodity scale production of sugars from starches. Curr. Opin. Microbiol. *2*, 252–256.

Craig, S.A., McDonald, A.M., Manners, D.J., and Stark, J.R. (1988). The iodine-staining properties and fine structure of some mammalian and invertebrate glycogens. Carbohydr. Res. *179*, 327–340.

Crick, F.H., Barnett, L., Brenner, S., and Watts-Tobin, R.J. (1961). General nature of the genetic code for proteins. Nature *192*, 1227–1232.

Damotte, M., Cattanéo, J., Sigal, N., and Puig, J. (1968). Mutants of Escherichia coli K 12 altered in their ability to store glycogen. Biochem. Biophys. Res. Commun. *32*, 916–920.

Dauvillée, D., Deschamps, P., Ral, J.-P., Plancke, C., Putaux, J.-L., Devassine, J., Durand-Terrasson, A., Devin, A., and Ball, S.G. (2009). Genetic dissection of floridean starch synthesis in the cytosol of the model dinoflagellate Crypthecodinium cohnii. Proc. Natl. Acad. Sci. U. S. A. *106*, 21126–21130.

Declerck, N., Machius, M., Wiegand, G., Huber, R., and Gaillardin, C. (2000). Probing structural determinants specifying high thermostability in Bacillus licheniformis α-amylase. J. Mol. Biol. *301*, 1041–1057.

Demain, A.L., and Vaishnav, P. (2009). Production of recombinant proteins by microbes and higher organisms. Biotechnol. Adv. *27*, 297–306.

Deremaux, L., Petitjean, C., and Wills, D. (2007). Soluble, highly branched glucose polymers for enteral and parenteral nutrition and for peritoneal dialysis.

Devillers, C.H., Piper, M.E., Ballicora, M.A., and Preiss, J. (2003). Characterization of the branching patterns of glycogen branching enzyme truncated on the N-terminus. Arch. Biochem. Biophys. *418*, 34–38.

Dias, A.R.G., Zavareze, E. da R., Helbig, E., Moura, F.A. de, Vargas, C.G., and Ciacco, C.F. (2011). Oxidation of fermented cassava starch using hydrogen peroxide. Carbohydr. Polym. *86*, 185–191.

Dickmanns, A., Ballschmiter, M., Liebl, W., and Ficner, R. (2006). Structure of the novel α-amylase AmyC from *Thermotoga maritima*. Acta Crystallogr. Sect. D Biol. Crystallogr. *62*, 262–270.

DiMauro, S., and Lamperti, C. (2001). Muscle glycogenoses. Muscle Nerve *24*, 984–999.

Dong, A., Meyer, J.D., Kendrick, B.S., Manning, M.C., and Carpenter, J.F. (1996). Effect of Secondary Structure on the Activity of Enzymes Suspended in Organic Solvents. Arch. Biochem. Biophys. *334*, 406–414.

Dowd, J.E., and Riggs, D.S. (1965). A Comparison of Estimates of Michaelis-Menten Kinetic Constants from Various Linear Transformations. J. Biol. Chem. *240*, 863–869.

Drake, E.N., and Brown, C.E. (1977). Application of nmr to biochemical kinetics. A laboratory experiment in physical biochemistry. J. Chem. Educ. *54*, 124.

Dumez, S., Wattebled, F., Dauvillee, D., Delvalle, D., Planchot, V., Ball, S.G., and D'Hulst, C. (2006). Mutants of Arabidopsis lacking starch branching enzyme II substitute plastidial starch synthesis by cytoplasmic maltose accumulation. Plant Cell *18*, 2694–2709.

Dumon-Seignovert, L., Cariot, G., and Vuillard, L. (2004). The toxicity of recombinant proteins in Escherichia coli: a comparison of overexpression in BL21(DE3), C41(DE3), and C43(DE3). Protein Expr. Purif. *37*, 203–206.

Van Eijk, J.H., and Docter, C. (1993). Dough product and method for improving bread quality.

Erra-Pujada, M., Debeire, P., Duchiron, F., and O'Donohue, M.J. (1999). The type II pullulanase of Thermococcus hydrothermalis: molecular characterization of the gene and expression of the catalytic domain. J. Bacteriol. *181*, 3284–3287.

Flipse, E., Suurs, L., Keetels, C.J.A.M., Kossmann, J., Jacobsen, E., and Visser, R.G.F. (1996). Introduction of sense and antisense cDNA for branching enzyme in the amylose-free potato mutant leads to physico-chemical changes in the starch. Planta *198*, 340–347.

Fox, J., Kennedy, L.D., Hawker, J.S., Ozbun, J.L., Greenberg, E., Lammel, C., and Preiss, J. (1973). De novo synthesis of bacterial glycogen and plant starch by ADPG: -glucan 4-glucosyl transferase. Ann. N. Y. Acad. Sci. *210*, 90–103.

French, D. (1984). Organization of starch granules. In Starch: Chemistry and Technology, (Orlando: Academic Press), pp. 183–237.

Funane, K., Libessart, N., Stewart, D., Michishita, T., and Preiss, J. (1998). Analysis of essential histidine residues of maize branching enzymes by chemical modification and site-directed mutagenesis. J. Protein Chem. *17*, 579–590.

Fyfe, J.C., Giger, U., Van Winkle, T.J., Haskins, M.E., Steinberg, S.A., Wang, P., and Patterson, D.F. (1992). Glycogen Storage Disease Type IV: Inherited Deficiency of Branching Enzyme Activity in Cats. Pediatr. Res. *32*, 719–725.

Fyfe, J.C., Kurzhals, R.L., Hawkins, M.G., Wang, P., Yuhki, N., Giger, U., Van Winkle, T.J., Haskins, M.E., Patterson, D.F., and Henthorn, P.S. (2007). A complex rearrangement in GBE1 causes both perinatal hypoglycemic collapse and late-juvenile-onset neuromuscular degeneration in glycogen storage disease type IV of Norwegian forest cats. Mol. Genet. Metab. *90*, 383–392.

Gallant, D.J., Bouchet, B., and Baldwin, P.M. (1997). Microscopy of starch: evidence of a new level of granule organization. Carbohydr. Polym. *32*, 177–191.

Gao, M., Fisher, D.K., Kim, K.N., Shannon, J.C., and Guiltinan, M.J. (1997). Independent genetic control of maize starch-branching enzymes IIa and IIb. Isolation and characterization of a Sbe2a cDNA. Plant Physiol. *114*, 69–78.

Garg, S.K., Alam, M.S., Kishan, K.V.R., and Agrawal, P. (2007). Expression and characterization of α-(1,4)-glucan branching enzyme Rv1326c of Mycobacterium tuberculosis H37Rv. Protein Expr. Purif. *51*, 198–208.

Garnier, J., Gibrat, J.F., and Robson, B. (1996). GOR method for predicting protein secondary structure from amino acid sequence. Methods Enzymol. *266*, 540–553.

Gidley, M.J. (1985). Quantification of the structural features of starch polysaccharides by N.M.R. spectroscopy. Carbohydr. Res. *139*, 85–93.

Gidley, M.J., and Bulpin, P. V. (1989). Aggregation of amylose in aqueous systems: the effect of chain length on phase behavior and aggregation kinetics. Macromolecules *22*, 341–346.

Giles, H.F., Wagner, J.R., and Mount, E.M. (2005). Extrusion : the definitive processing guide and handbook (William Andrew Pub).

Glaring, M.A., Skryhan, K., Kötting, O., Zeeman, S.C., and Blennow, A. (2012). Comprehensive survey of redox sensitive starch metabolising enzymes in Arabidopsis thaliana. Plant Physiol. Biochem. *58*, 89–97.

Goldsmith, E., Sprang, S., and Fletterick, R. (1982). Structure of maltoheptaose by difference Fourier methods and a model for glycogen. J. Mol. Biol. *156*, 411–427.

Greenberg, E., and Preiss, J. (1964). The occurrence of adenosine diphosphate glucose: glycogen transglucosylase in bacteria. J. Biol. Chem. *239*, 4314–4315.

Greenfield, N.J. (2006). Using circular dichroism collected as a function of temperature to determine the thermodynamics of protein unfolding and binding interactions. Nat. Protoc. *1*, 2527–2535.

Greenfield, N., and Fasman, G.D. (1969). Computed circular dichroism spectra for the evaluation of protein conformation. Biochemistry *8*, 4108–4116.

Guan, H.-P., and L Keeling, P. (1998). Starch Biosynthesis : Understanding the Functions and Interactions of Multiple Isozymes of Starch Synthase and Branching Enzyme. Trends Glycosci. Glycotechnol. *10*, 307–319.

Guan, H.P., and Preiss, J. (1993). Differentiation of the Properties of the Branching Isozymes from Maize (Zea mays). Plant Physiol. *102*, 1269–1273.

Guan, H., Kuriki, T., Sivak, M., and Preiss, J. (1995). Maize branching enzyme catalyzes synthesis of glycogen-like polysaccharide in glgB-deficient Escherichia coli. Proc. Natl. Acad. Sci. U. S. A. *92*, 964–967.

Guan, H., Li, P., Imparl-Radosevich, J., Preiss, J., and Keeling, P. (1997). Comparing the properties of Escherichia coli branching enzyme and maize branching enzyme. Arch. Biochem. Biophys. *342*, 92–98.

Guan, H.P., Baba, T., and Preiss, J. (1994a). Expression of branching enzyme I of maize endosperm in Escherichia coli. Plant Physiol. *104*, 1449–1453.

Guan, H.P., Baba, T., and Preiss, J. (1994b). Expression of branching enzyme II of maize endosperm in Escherichia coli. Cell. Mol. Biol. (Noisy-Le-Grand). *40*, 981–988.

Gunja, Z.H., Manners, D.J., and Maung, Khin, K. (1960). Studies on carbohydrate-metabolizing enzymes. 3. Yeast branching enzyme. Biochem. J. *75*, 441–450.

Gunja-Smith, Z., Marshall, J.J., Mercier, C., Smith, E.E., and Whelan, W.J. (1970). A revision of the Meyer-Bernfeld model of glycogen and amylopectin. FEBS Lett. *12*, 101–104.

Gupta, R., Gigras, P., Mohapatra, H., Goswami, V.K., and Chauhan, B. (2003). Microbial α-amylases: a biotechnological perspective. Process Biochem. *38*, 1599–1616.

Hannig, G., and Makrides, S.C. (1998). Strategies for optimizing heterologous protein expression in Escherichia coli. Trends Biotechnol. *16*, 54–60.

Hardacre, A.K., and Turnbull, H.L. (1986). The Growth and Development of Maize (Zea mays L.) at Five Temperatures. Ann. Bot. *58*, 779–787.

Hawker, J.S., Ozbun, J.L., Ozaki, H., Greenberg, E., and Preiss, J. (1974). Interaction of spinach leaf adenosine diphosphate glucose alpha-1,4-glucan alpha-4-glucosyl transferase and alpha-1,4-glucan, alpha-1,4-glucan-6-glycosyl transferase in synthesis of branched alpha-glucan. Arch. Biochem. Biophys. *160*, 530–551.

Haworth, W.N., Peat, S., and Bourne, E.J. (1944). Synthesis of Amylopectin. Nature *154*, 236–236.

Hendriksen, H., Pedersen, S., and Bisgård-Frantzen, H. (1998). A process for textile warp sizing using enzymatically modified starches.

Henrissat, B., and Bairoch, A. (1996). Updating the sequence-based classification of glycosyl hydrolases. Biochem. J. *316 (Pt 2*, 695–696.

Hilden, I., Leggio, L.L., Larsen, S., and Poulsen, P. (2000). Characterization and crystallization of an active N-terminally truncated form of the Escherichia coli glycogen branching enzyme. Eur. J. Biochem. *267*, 2150–2155.

Hizukuri, S. (1986). Polymodal distribution of the chain lengths of amylopectin, and its significance. Carbohydr. Res. *147*, 342–347.

Hizukuri, S., Kaneko, T., and Takeda, Y. (1983). Measurement of the chain length of amylopectin and its relevance to the origin of crystalline polymorphism of starch granules. Biochim. Biophys. Acta - Gen. Subj. *760*, 188–191.

Hobbs, L. (2009). Sweeteners from Starch: Production, Properties and Uses. In Starch: Chemistry and Technology, (Elsevier Inc.), pp. 797–832.

Hong, S., and Preiss, J. (2000). Localization of C-terminal domains required for the maximal activity or for determination of substrate preference of maize branching enzymes. Arch. Biochem. Biophys. *378*, 349–355.

Hoover, R. (2000). Acid-Treated Starches. Food Rev. Int. *16*, 369–392.

Hormdok, R., and Noomhorm, A. (2007). Hydrothermal treatments of rice starch for improvement of rice noodle quality. LWT - Food Sci. Technol. *40*, 1723–1731.

Hu, X., Xu, X., Jin, Z., Tian, Y., Bai, Y., and Xie, Z. (2011). Retrogradation properties of rice starch gelatinized by heat and high hydrostatic pressure (HHP). J. Food Eng. *106*, 262–266.

Huang, Z.-Q., Lu, J.-P., Li, X.-H., and Tong, Z.-F. (2007). Effect of mechanical activation on physico-chemical properties and structure of cassava starch. Carbohydr. Polym. *68*, 128–135.

Hurley, T.D., Walls, C., Bennett, J.R., Roach, P.J., and Wang, M. (2006). Direct detection of glycogenin reaction products during glycogen initiation. Biochem. Biophys. Res. Commun. *348*, 374–378.

Iglesias, A., and Preiss, J. (1992). Bacterial glycogen and plant starch biosynthesis. Biochem. Educ. *20*, 196–203.

Imamura, H., Fushinobu, S., Yamamoto, M., Kumasaka, T., Jeon, B.-S., Wakagi, T., and Matsuzawa, H. (2003). Crystal structures of 4-alpha-glucanotransferase from Thermococcus litoralis and its complex with an inhibitor. J. Biol. Chem. *278*, 19378–19386.

Ito, H., Hamada, S., Isono, N., Yoshizaki, T., Ueno, H., Yoshimoto, Y., Takeda, Y., and Matsui, H. (2004). Functional characteristics of C-terminal regions of starch-branching enzymes from developing seeds of kidney bean (Phaseolus vulgaris L.). Plant Sci. *166*, 1149–1158.

Jacobs, H., and Delcour, J.A. (1998). Hydrothermal Modifications of Granular Starch, with Retention of the Granular Structure: A Review. J. Agric. Food Chem. *46*, 2895–2905.

James, M.G., Denyer, K., and Myers, A.M. (2003). Starch synthesis in the cereal endosperm. Curr. Opin. Plant Biol. *6*, 215–222.

Jane, J., Xu, A., Radosavljevic, M., and Seib, P. (1992). Location of Amylose in Normal Starch Granules. I. Susceptibility of Amylose and Amylopectin to Cross-Linking Reagents. *69*, 405–409.

Janecek, S. (1997). alpha-Amylase family: molecular biology and evolution. Prog. Biophys. Mol. Biol. *67*, 67–97.

Janeček, Š. (2005). Amylolytic families of glycoside hydrolases: focus on the family GH-57. *60*, 177–184.

Jayakody, L., and Hoover, R. (2008). Effect of annealing on the molecular structure and physicochemical properties of starches from different botanical origins – A review. Carbohydr. Polym. *74*, 691–703.

Jenkins, P.J., and Donald, a M. (1995). The influence of amylose on starch granule structure. Int. J. Biol. Macromol. *17*, 315–321.

Jeong, H.-Y., and Lim, S.-T. (2003). Crystallinity and Pasting Properties of Freeze-Thawed High Amylose Maize Starch. Starch - Stärke *55*, 511–517.

Jespersen, H.M., MacGregor, E.A., Sierks, M.R., and Svensson, B. (1991). Comparison of the domain-level organization of starch hydrolases and related enzymes. Biochem. J. *280*, 51–55.

Jespersen, H.M., MacGregor, E.A., Henrissat, B., Sierks, M.R., and Svensson, B. (1993). Starch- and glycogen-debranching and branching enzymes: prediction of structural features of the catalytic (beta/alpha)8-barrel domain and evolutionary relationship to other amylolytic enzymes. J. Protein Chem. *12*, 791–805.

Jobe, A., and Bourgeois, S. (1972). lac repressor-operator interaction. J. Mol. Biol. *69*, 397–408.

Jobling, S. (2004). Improving starch for food and industrial applications. Curr. Opin. Plant Biol. *7*, 210–218.

Juge, N., Søgaard, M., Chaix, J.C., Martin-Eauclaire, M.F., Svensson, B., Marchis-Mouren, G., and Guo, X.J. (1993). Comparison of barley malt alpha-amylase isozymes 1 and 2: construction of cDNA hybrids by in vivo recombination and their expression in yeast. Gene *130*, 159–166.

Kagawa, Y., Nojima, H., Nukiwa, N., Ishizuka, M., Nakajima, T., Yasuhara, T., Tanaka, T., and Oshima, T. (1984). High guanine plus cytosine content in the third letter of codons of an extreme thermophile. DNA sequence of the isopropylmalate dehydrogenase of Thermus thermophilus. J. Biol. Chem. *259*, 2956–2960.

Kanai, R., Haga, K., Yamane, K., and Harata, K. (2001). Crystal structure of cyclodextrin glucanotransferase from alkalophilic Bacillus sp. 1011 complexed with 1-deoxynojirimycin at 2.0 A resolution. J. Biochem. *129*, 593–598.

Kandra, L. (2003). α-Amylases of medical and industrial importance. J. Mol. Struct. *666*–

667, 487–498.

Kasprzak, M.M., Lærke, H.N., Larsen, F.H., Knudsen, K.E.B., Pedersen, S., and Jørgensen, A.S. (2012). Effect of enzymatic treatment of different starch sources on the in vitro rate and extent of starch digestion. Int. J. Mol. Sci. *13*, 929–942.

Katsuya, Y., Mezaki, Y., Kubota, M., and Matsuura, Y. (1998). Three-dimensional structure of Pseudomonas isoamylase at 2.2 A resolution. J. Mol. Biol. *281*, 885–897.

Katz, J.R. (1930). Uber die anderungen in Rontgenspektrum der starke brim baker and beam altbacken warden des brutes. Zeitschrift Fur Phys. Chemie *150*, 37–59.

Kaur, B., Ariffin, F., Bhat, R., and Karim, A.A. (2012). Progress in starch modification in the last decade. Food Hydrocoll. *26*, 398–404.

Kawabata, Y., Toeda, K., Takahashi, T., Shibamoto, N., and Kobayashi, M. (2002). Preparation of Highly Branched Starch by Glycogen Branching Enzyme from Neurospora crassa N2-44 and Its Characterization. J. Appl. Glycosci. *49*, 273–279.

Kelly, S.M., and Price, N.C. (2000). The use of circular dichroism in the investigation of protein structure and function. Curr. Protein Pept. Sci. *1*, 349–384.

Khoshnoodi, J., Blennow, A., Ek, B., Rask, L., and Larsson, H. (1996). The Multiple Forms of Starch-Branching Enzyme I in Solanum Tuberosum. Eur. J. Biochem. *242*, 148–155.

Kiel, J. a, Boels, J.M., Beldman, G., and Venema, G. (1991). Molecular cloning and nucleotide sequence of the glycogen branching enzyme gene (glgB) from Bacillus stearothermophilus and expression in Escherichia coli and Bacillus subtilis. Mol. Gen. Genet. *230*, 136–144.

Kim, E.-J., Ryu, S.-I., Bae, H.-A., Huong, N.T., and Lee, S.-B. (2008). Biochemical characterisation of a glycogen branching enzyme from Streptococcus mutans: Enzymatic modification of starch. Food Chem. *110*, 979–984.

Kim, K.N., Fisher, D.K., Gao, M., and Guiltinan, M.J. (1998). Molecular cloning and characterization of the Amylose-Extender gene encoding starch branching enzyme IIB in maize. Plant Mol. Biol. *38*, 945–956.

Kirk, O., Borchert, T.V., and Fuglsang, C.C. (2002). Industrial enzyme applications. Curr. Opin. Biotechnol. *13*, 345–351.

Kittleson, J.T., Cheung, S., and Anderson, J.C. (2011). Rapid optimization of gene dosage in E. coli using DIAL strains. J. Biol. Eng. *5*, 10.

Klein, C., and Schulz, G.E. (1991). Structure of cyclodextrin glycosyltransferase refined at 2.0 A resolution. J. Mol. Biol. *217*, 737–750.

Klein, B., Vanier, N.L., Moomand, K., Pinto, V.Z., Colussi, R., da Rosa Zavareze, E., and Dias, A.R.G. (2014). Ozone oxidation of cassava starch in aqueous solution at

different pH. Food Chem. *155*, 167–173.

Klucinec, J.D., and Thompson, D.B. (2002). Structure of Amylopectins from *ae* - Containing Maize Starches. Cereal Chem. J. *79*, 19–23.

Koay, A., Rimmer, K.A., Mertens, H.D.T., Gooley, P.R., and Stapleton, D. (2007). Oligosaccharide recognition and binding to the carbohydrate binding module of AMP-activated protein kinase. FEBS Lett. *581*, 5055–5059.

Koch, K., Andersson, R., and Åman, P. (1998). Quantitative analysis of amylopectin unit chains by means of high-performance anion-exchange chromatography with pulsed amperometric detection. J. Chromatogr. A *800*, 199–206.

Korma, A.S., Alahmad, K., Niazi, S., Ammar, A., Zaaboul, F., and Zhang, T. (2016). Chemically Modified Starch and Utilization in Food Stuffs. Int. J. Nutr. Food Sci. *5*, 264.

Kraak, A. (1992). Industrial applications of potato starch products. Ind. Crops Prod. *1*, 107–112.

Krisman, C.R. (1973). A Possible Intermediate In The Initiation Of Glycogen Biosynthesis. Ann. N. Y. Acad. Sci. *210*, 81–89.

Kuakpetoon, D., and Wang, Y.-J. (2001). Characterization of Different Starches Oxidized by Hypochlorite. Starch - Stärke *53*, 211–218.

Kuriki, T., Okada, S., and Imanaka, T. (1988). New type of pullulanase from Bacillus stearothermophilus and molecular cloning and expression of the gene in Bacillus subtilis. J. Bacteriol. *170*, 1554–1559.

Kuriki, T., Takata, H., Okada, S., and Imanaka, T. (1991). Analysis of the active center of Bacillus stearothermophilus neopullulanase. J. Bacteriol. *173*, 6147–6152.

Kuriki, T., Guan, H., Sivak, M., and Preiss, J. (1996). Analysis of the active center of branching enzyme II from maize endosperm. J. Protein Chem. *15*, 305–313.

Kuriki, T., Stewart, D.C., and Preiss, J. (1997). Construction of Chimeric Enzymes out of Maize Endosperm Branching Enzymes I and II : Biochemistry *272*, 28999–29004.

Laemmli, U.K. (1970). Cleavage of structural proteins during the assembly of the head of bacteriophage T4. Nature *227*, 680–685.

Lavintman, N., and Cardini, C.E. (1973). Particulate UDP-glucose: Protein transglucosylase from potato tuber. FEBS Lett. *29*, 43–46.

Lawal, O.S., Adebowale, K.O., Ogunsanwo, B.M., Barba, L.L., and Ilo, N.S. (2005). Oxidized and acid thinned starch derivatives of hybrid maize: functional characteristics, wide-angle X-ray diffractometry and thermal properties. Int. J. Biol. Macromol. *35*, 71–79.

Lawson, C.L., van Montfort, R., Strokopytov, B., Rozeboom, H.J., Kalk, K.H., de Vries,

G.E., Penninga, D., Dijkhuizen, L., and Dijkstra, B.W. (1994). Nucleotide sequence and X-ray structure of cyclodextrin glycosyltransferase from Bacillus circulans strain 251 in a maltose-dependent crystal form. J. Mol. Biol. *236*, 590–600.

Le, Q.-T., Lee, C.-K., Kim, Y.-W., Lee, S.-J., Zhang, R., Withers, S.G., Kim, Y.-R., Auh, J.-H., and Park, K.-H. (2009). Amylolytically-resistant tapioca starch modified by combined treatment of branching enzyme and maltogenic amylase. Carbohydr. Polym. *75*, 9–14.

Leach, H.W., and Schoch, T.. J. (1961). Structure of the Starch Granule. II. Action of Various Amylases on Granular Starches. Cereal Chem. *38*, 34–46.

Lee, S.Y. (1996). High cell-density culture of Escherichia coli. Trends Biotechnol. *14*, 98–105.

Lee, B.-H., Yan, L., Phillips, R.J., Reuhs, B.L., Jones, K., Rose, D.R., Nichols, B.L., Quezada-Calvillo, R., Yoo, S.-H., and Hamaker, B.R. (2013). Enzyme-Synthesized Highly Branched Maltodextrins Have Slow Glucose Generation at the Mucosal α-Glucosidase Level and Are Slowly Digestible In Vivo. PLoS One *8*, e59745.

Lee, C.-K., Le, Q.-T., Kim, Y.-H., Shim, J.-H., Lee, S.-J., Park, J.-H., Lee, K.-P., Song, S.-H., Auh, J.H., Lee, S.-J., et al. (2008). Enzymatic synthesis and properties of highly branched rice starch amylose and amylopectin cluster. J. Agric. Food Chem. *56*, 126–131.

Leggio, L. Lo, Ernst, H.A., Hilden, I., Larsen, S., Innovation, D.C., and K, D.-C. (2002). A structural model for the N-terminal N1 module of E . coli glycogen branching enzyme. Structure 109–118.

Lewicka, K., Siemion, P., Kurcok, P., and Kurcok, P. (2015). Chemical Modifications of Starch: Microwave Effect. Int. J. Polym. Sci. *2015*, 1–10.

Libessart, N., and Preiss, J. (1998). Arginine residue 384 at the catalytic center is important for branching enzyme II from maize endosperm. Arch. Biochem. Biophys. *360*, 135–141.

van Lieshout, J.F.T., Verhees, C.H., Ettema, T.J.G., van der Sar, S., Imamura, H., Matsuzawa, H., van der Oost, J., and de Vos, W.M. (2003). Identification and Molecular Characterization of a Novel Type of α-galactosidase from *Pyrococcus furiosus*. Biocatal. Biotransformation *21*, 243–252.

Liu, Weis, R., and Glieder, A. (2004). Enzymes from Higher Eukaryotes for Industrial Biocatalysis. *42*, 237–249.

Liu, F., Ahmed, Z., Lee, E.A., Donner, E., Liu, Q., Ahmed, R., Morell, M.K., Emes, M.J., and Tetlow, I.J. (2012). Allelic variants of the amylose extender mutation of maize demonstrate phenotypic variation in starch structure resulting from modified protein-protein interactions. J. Exp. Bot. *63*, 1167–1183.

Lou, J., Dawson, K.A., and Strobel, H.J. (1997). Glycogen biosynthesis via UDP-glucose

in the ruminal bacterium Prevotella bryantii B1(4). Appl. Environ. Microbiol. *63*, 4355–4359.

Louis-Jeune, C., Andrade-Navarro, M.A., and Perez-Iratxeta, C. (2012). Prediction of protein secondary structure from circular dichroism using theoretically derived spectra. Proteins Struct. Funct. Bioinforma. *80*, 374–381.

Ma, B., Zhang, K., Hendrie, C., Liang, C., Li, M., Doherty-Kirby, A., and Lajoie, G. (2003). PEAKS: powerful software for peptide de novo sequencing by tandem mass spectrometry. Rapid Commun. Mass Spectrom. *17*, 2337–2342.

van der Maarel, M.J.E.C., and Leemhuis, H. (2013). Starch modification with microbial alpha-glucanotransferase enzymes. Carbohydr. Polym. *93*, 116–121.

van der Maarel, M.J.E.., van der Veen, B., Uitdehaag, J.C.., Leemhuis, H., and Dijkhuizen, L. (2002). Properties and applications of starch-converting enzymes of the α-amylase family. J. Biotechnol. *94*, 137–155.

van der Maarel, M.J.E.C., Capron, I., Euverink, G.-J.W., Bos, H.T., Kaper, T., Binnema, D.J., and Steeneken, P.A.M. (2005). A Novel Thermoreversible Gelling Product Made by Enzymatic Modification of Starch. Starch - Stärke *57*, 465–472.

Van Der Maarel, M.J.E.C., Dijkhuizen, L., Vos, A., and Sanders, P. (2003). Properties of the Glucan Branching Enzyme of the Hyperthermophilic Bacterium Aquifex aeolicus. Biocatal. Biotransformation *21*, 199–207.

MacGregor, E.A., and Svensson, B. (1989). A super-secondary structure predicted to be common to several alpha-1,4-D-glucan-cleaving enzymes. Biochem. J. *259*, 145–152.

MacGregor, E.A., Janecek, S., and Svensson, B. (2001). Relationship of sequence and structure to specificity in the alpha-amylase family of enzymes. Biochim. Biophys. Acta *1546*, 1–20.

Machida, S., Ogawa, S., Xiaohua, S., Takaha, T., Fujii, K., and Hayashi, K. (2000). Cycloamylose as an efficient artificial chaperone for protein refolding. FEBS Lett. *486*, 131–135.

Madsen, N.B., and Cori, C.F. (1958). The binding of glycogen and phosphorylase. J. Biol. Chem. *233*, 1251–1256.

Makhmoudova, A., Williams, D., Brewer, D., Massey, S., Patterson, J., Silva, A., Vassall, K.A., Liu, F., Subedi, S., Harauz, G., et al. (2014). Identification of multiple phosphorylation sites on maize endosperm starch branching enzyme IIb, a key enzyme in amylopectin biosynthesis. J. Biol. Chem. *289*, 9233–9246.

Manners, D.J. (1989). Recent Developments in Our Understanding of Amylopectin Structure. Carbohydr. Polym. *11*, 87–112.

Manners, D.J. (1991). Recent developments in our understanding of glycogen structure. Carbohydr. Polym. *16*, 82–37.

Manners, D.J., and Matheson, N.K. (1981). The fine structure of amylopectin. Carbohydr. Res. *90*, 99–110.

Matsui, I., Yoneda, S., Ishikawa, K., Miyairi, S., Fukui, S., Umeyama, H., and Honda, K. (1994). Roles of the aromatic residues conserved in the active center of Saccharomycopsis alpha-amylase for transglycosylation and hydrolysis activity. Biochemistry *33*, 451–458.

Matsuura, Y., Kusunoki, M., Harada, W., and Kakudo, M. (1984). Structure and Possible Catalytic Residues of Taka-Amylase A. J. Biochem. *95*, 697–702.

McBride, A., Ghilagaber, S., Nikolaev, A., and Hardie, D.G. (2009). The glycogen-binding domain on the AMPK beta subunit allows the kinase to act as a glycogen sensor. Cell Metab. *9*, 23–34.

McIntyre, D.D., and Vogel, H.J. (1990). Two-Dimensional Nuclear Magnetic Resonance Studies of Starch and Starch Products. Starch - Stärke *42*, 287–293.

McIntyre, D.D., and Vogel, H.J. (1991). Nuclear Magnetic Resonance Studies of Homopolysaccharides Related to Starch. Starch - Stärke *43*, 69–76.

McIntyre, D.D., Ho, C., and Vogel, H.J. (1990). One-Dimensional Nuclear Magnetic Resonance Studies of Starch and Starch Products. Starch - Stärke *42*, 260–267.

Meléndez, R., Meléndez-Hevia, E., and Cascante, M. (1997). How did glycogen structure evolve to satisfy the requirement for rapid mobilization of glucose? A problem of physical constraints in structure building. J. Mol. Evol. *45*, 446–455.

Meléndez, R., Meléndez-Hevia, E., Mas, F., Mach, J., and Cascante, M. (1998). Physical constraints in the synthesis of glycogen that influence its structural homogeneity: a two-dimensional approach. Biophys. J. *75*, 106–114.

Meléndez-Hevia, E., Waddell, T.G., and Shelton, E.D. (1993). Optimization of molecular design in the evolution of metabolism: the glycogen molecule. Biochem. J. *295*, 477–483.

Meyer, T.S., and Lamberts, B.L. (1965). Use of coomassie brilliant blue R250 for the electrophoresis of microgram quantities of parotid saliva proteins on acrylamide-gel strips. Biochim. Biophys. Acta *107*, 144–145.

Michaelis, L., and Menten, M. (1913). Die kinetic der inver tinwirkung. Biochem. Z. *49*, 333–369.

Mikkelsen, R., Binderup, K., and Preiss, J. (2001). Tyrosine residue 300 is important for activity and stability of branching enzyme from Escherichia coli. Arch. Biochem. Biophys. *385*, 372–377.

Miroux, B., and Walker, J.E. (1996). Over-production of proteins in Escherichia coli: mutant hosts that allow synthesis of some membrane proteins and globular proteins at high levels. J. Mol. Biol. *260*, 289–298.

Miyazaki, M., Van Hung, P., Maeda, T., and Morita, N. (2006). Recent advances in application of modified starches for breadmaking. Trends Food Sci. Technol. *17*, 591–599.

Mizuno, K., Kawasaki, T., Shimada, H., Satoh, H., Kobayashi, E., Okumura, S., Arai, Y., and Baba, T. (1993). Alteration of the structural properties of starch components by the lack of an isoform of starch branching enzyme in rice seeds. J. Biol. Chem. *268*, 19084–19091.

Mohtar, N.S., Abdul Rahman, M.B., Raja Abd Rahman, R.N.Z., Leow, T.C., Salleh, A.B., and Mat Isa, M.N. (2016). Expression and characterization of thermostable glycogen branching enzyme from Geobacillus mahadia Geo-05. PeerJ *4*, e2714.

Morell, M.K., and Myers, A.M. (2005). Towards the rational design of cereal starches. Curr. Opin. Plant Biol. *8*, 204–210.

Morell, M.K., Blennow, a, Kosar-Hashemi, B., and Samuel, M.S. (1997). Differential expression and properties of starch branching enzyme isoforms in developing wheat endosperm. Plant Physiol. *113*, 201–208.

Morris, G.A. (1986). Modern NMR techniques for structure elucidation. Magn. Reson. Chem. *24*, 371–403.

Moses, S.W., and Parvari, R. (2002). The variable presentations of glycogen storage disease type IV: a review of clinical, enzymatic and molecular studies. Curr. Mol. Med. *2*, 177–188.

Mukerjea, R., and Robyt, J.F. (2012). De novo biosynthesis of starch chains without a primer and the mechanism for its biosynthesis by potato starch-synthase. Carbohydr. Res. *352*, 137–142.

Mullis, K., Faloona, F., Scharf, S., Saiki, R., Horn, G., and Erlich, H. (1986). Specific enzymatic amplification of DNA in vitro: the polymerase chain reaction. Cold Spring Harb. Symp. Quant. Biol. *51 Pt 1*, 263–273.

Murakami, T., Kanai, T., Takata, H., Kuriki, T., and Imanaka, T. (2006). A novel branching enzyme of the GH-57 family in the hyperthermophilic archaeon Thermococcus kodakaraensis KOD1. J. Bacteriol. *188*, 5915–5924.

Murphy, P. (2000). Starch. In Handbook of Hydrocolloids. In Handbook of Hydrocolloids 2nd Edition, G.O. Phillips, and P.A. Williams, eds. (USA: CRC Press), pp. 41–65.

Myers, A.M., Morell, M.K., James, M.G., and Ball, S.G. (2000). Recent progress toward understanding biosynthesis of the amylopectin crystal. Plant Physiol. *122*, 989–997.

Nakajima, R., Imanaka, T., and Aiba, S. (1986). Comparison of amino acid sequences of eleven different ?-amylases. Appl. Microbiol. Biotechnol. *23*, 355–360.

Nakamura, Y. (2002). Towards a better understanding of the metabolic system for

amylopectin biosynthesis in plants: rice endosperm as a model tissue. Plant Cell Physiol. *43*, 718–725.

Nakamura, Y., Utsumi, Y., Sawada, T., Aihara, S., Utsumi, C., Yoshida, M., and Kitamura, S. (2010). Characterization of the reactions of starch branching enzymes from rice endosperm. Plant Cell Physiol. *51*, 776–794.

Nakorn, K.N., Tongdang, T., and Sirivongpaisal, P. (2009). Crystallinity and Rheological Properties of Pregelatinized Rice Starches Differing in Amylose Content. Starch - Stärke *61*, 101–108.

Neelam, K., Vijay, S., and Lalit, S. (2012). Various Techniques for the Modification of Starch and the Applications of its Derivatives. Int. Res. J. Pharm. *3*, 25–31.

Neira-Velázquez, M.G., Rodríguez-Hernández, M.T., Hernández-Hernández, E., and Ruiz-Martínez, A.R.Y. (2013). Polymer Molecular Weight Measurement. In Handbook of Polymer Synthesis, Characterization, and Processing, (Hoboken, NJ, USA: John Wiley & Sons, Inc.), pp. 355–366.

Nichetti, D., and Manas-Zloczower, I. (1998). Viscosity model for polydisperse polymer melts. J. Rheol. (N. Y. N. Y). *42*, 951.

Nichols, S.E. (2000). Glucan-containing compositions and paper.

Nilsson, G.S., Gorton, L., Bergquist, K.-E., and Nilsson, U. (1996). Determination of the Degree of Branching in Normal and Amylopectin Type Potato Starch with1H-NMR Spectroscopy Improved resolution and two-dimensional spectroscopy. Starch - Starke *48*, 352–357.

Nirenberg, M., Leder, P., Bernfield, M., Brimacombe, R., Trupin, J., Rottman, F., and O'Neal, C. (1965). RNA codewords and protein synthesis, VII. On the general nature of the RNA code. Proc. Natl. Acad. Sci. U. S. A. *53*, 1161–1168.

Nishi, A., Nakamura, Y., Tanaka, N., and Satoh, H. (2001). Biochemical and genetic analysis of the effects of amylose-extender mutation in rice endosperm. Plant Physiol. *127*, 459–472.

Noguchi, J., Chaen, K., Vu, N.T., Akasaka, T., Shimada, H., Nakashima, T., Nishi, A., Satoh, H., Omori, T., Kakuta, Y., et al. (2011). Crystal structure of the branching enzyme I (BEI) from Oryza sativa L with implications for catalysis and substrate binding. Glycobiology *21*, 1108–1116.

Ohdan, T., Sawada, T., and Nakamura, Y. (2011). Effects of Temperature on Starch Branching Enzyme Properties of Rice. J. Appl. Glycosci. *58*, 19–26.

Omelchenko, M. V, Wolf, Y.I., Gaidamakova, E.K., Matrosova, V.Y., Vasilenko, A., Zhai, M., Daly, M.J., Koonin, E. V, and Makarova, K.S. (2005). Comparative genomics of Thermus thermophilus and Deinococcus radiodurans: divergent routes of adaptation to thermophily and radiation resistance. BMC Evol. Biol. *5*, 57.

Ozbun, J.L., Hawker, J.S., and Preiss, J. (1972). Soluble adenosine diphosphate glucose--1,4-glucan -4-glucosyltransferases from spinach leaves. Biochem. J. *126*, 953–963.

Pal, K., Kumar, S., Sharma, S., Garg, S.K., Alam, M.S., Xu, H.E., Agrawal, P., and Swaminathan, K. (2010). Crystal Structure of Full-length *Mycobacterium tuberculosis* H37Rv Glycogen Branching Enzyme. J. Biol. Chem. *285*, 20897–20903.

Palomo, M., Kralj, S., van der Maarel, M.J.E.C., and Dijkhuizen, L. (2009). The unique branching patterns of Deinococcus glycogen branching enzymes are determined by their N-terminal domains. Appl. Environ. Microbiol. *75*, 1355–1362.

Palomo, M., Pijning, T., Booiman, T., Dobruchowska, J.M., van der Vlist, J., Kralj, S., Planas, A., Loos, K., Kamerling, J.P., Dijkstra, B.W., et al. (2011). Thermus thermophilus glycoside hydrolase family 57 branching enzyme: crystal structure, mechanism of action, and products formed. J. Biol. Chem. *286*, 3520–3530.

Patron, N.J., and Keeling, P.J. (2005). Common Evolutionary Origin of Starch Biosynthetic Enzymes in Green and Red Algae1. J. Phycol. *41*, 1131–1141.

Pei-Ling, L., Xiao-Song, H., and Qun, S. (2010). Effect of high hydrostatic pressure on starches: A review. Starch - Stärke *62*, 615–628.

Pérez, S., and Bertoft, E. (2010). The molecular structures of starch components and their contribution to the architecture of starch granules: A comprehensive review. Starch - Stärke *62*, 389–420.

Pilling, E., and Smith, A.M. (2003). Growth ring formation in the starch granules of potato tubers. Plant Physiol. *132*, 365–371.

Pitcher, J., Smythe, C., Campbell, D.G., and Cohen, P. (1987). Identification of the 38-kDa subunit of rabbit skeletal muscle glycogen synthase as glycogenin. Eur. J. Biochem. *169*, 497–502.

Polekhina, G., Gupta, A., van Denderen, B.J.W., Feil, S.C., Kemp, B.E., Stapleton, D., and Parker, M.W. (2005). Structural basis for glycogen recognition by AMP-activated protein kinase. Structure *13*, 1453–1462.

Pope, B., and Kent, H.M. (1996). High efficiency 5 min transformation of Escherichia coli. Nucleic Acids Res. *24*, 536–537.

Preiss, J. (1984). Bacterial glycogen synthesis and its regulation. Annu. Rev. Microbiol. *38*, 419–458.

Privé, G.G. (2007). Detergents for the stabilization and crystallization of membrane proteins. Methods *41*, 388–397.

Qiu, L., Hu, F., and Peng, Y. (2013). Structural and mechanical characteristics of film using modified corn starch by the same two chemical processes used in different sequences. Carbohydr. Polym. *91*, 590–596.

Rahman, S., Regina, A., Li, Z., Mukai, Y., Yamamoto, M., Kosar-Hashemi, B., Abrahams, S., and Morell, M.K. (2001). Comparison of starch-branching enzyme genes reveals evolutionary relationships among isoforms. Characterization of a gene for starch-branching enzyme IIa from the wheat genome donor Aegilops tauschii. Plant Physiol. *125*, 1314–1324.

Raines, R.T., McCormick, M., Van Oosbree, T.R., and Mierendorf, R.C. (2000). The S.Tag fusion system for protein purification. Methods Enzymol. *326*, 362–376.

Regina, A., Bird, A., Topping, D., Bowden, S., Freeman, J., Barsby, T., Kosar-Hashemi, B., Li, Z., Rahman, S., and Morell, M. (2006). High-amylose wheat generated by RNA interference improves indices of large-bowel health in rats. Proc. Natl. Acad. Sci. U. S. A. *103*, 3546–3551.

Regina, A., Kosar-Hashemi, B., Ling, S., Li, Z., Rahman, S., and Morell, M. (2010). Control of starch branching in barley defined through differential RNAi suppression of starch branching enzyme IIa and IIb. J. Exp. Bot. *61*, 1469–1482.

Render, J.A., Common, R.S., Kennedy, F.A., Jones, M.Z., and Fyfe, J.C. (1999). Amylopectinosis in Fetal and Neonatal Quarter Horses. Vet. Pathol. *36*, 157–160.

Richardson, P.H., Jeffcoat, R., Shi, Y.-C., Smith, A.M., Denyer, K., Martin, C., PREISS, J., Sidebottom, C., Kirkland, M., Strongitharm, B., et al. (2000). High-Amylose Starches: From Biosynthesis to Their Use as Food Ingredients. MRS Bull. *25*, 20–24.

Ring, S.G., Colonna, P., I'Anson, K.J., Kalichevsky, M.T., Miles, M.J., Morris, V.J., and Orford, P.D. (1987). The gelation and crystallisation of amylopectin. Carbohydr. Res. *162*, 277–293.

Roach, P.J. (2002). Glycogen and its metabolism. Curr. Mol. Med. *2*, 101–120.

Roach, P.J., Depaoli-Roach, A.A., Hurley, T.D., and Tagliabracci, V.S. (2012). Glycogen and its metabolism: some new developments and old themes. Biochem. J. *441*, 763–787.

Roberts, J.C. (John C. (1996). The chemistry of paper (Cambridge: Royal Society of Chemistry).

Robin, J.P., Mercier, C., Charbonniere, R., and Guilbot, A. (1974). Lintnerized Starches: Gel Filtration and Enzymatic Studies of Insoluble Residues from Prolonged Acid Treatment of Potato Starch. Cereal Chem. *51*, 389–406.

Romeo, T., Kumar, A., and Preiss, J. (1988). Analysis of the <i>Escherichia coli<i> glycogen gene cluster suggests that catabolic enzymes are encoded among the biosynthetic genes. Gene *70*, 363–376.

Röper, H. (2002). Renewable Raw Materials in Europe-Industrial Utilisation of Starch and Sugar. Starch - Stärke *54*, 89–99.

Rosano, G.L., and Ceccarelli, E.A. (2014). Recombinant protein expression in Escherichia coli: advances and challenges. Front. Microbiol. *5*, 172.

Rost, B., Yachdav, G., and Liu, J. (2004). The PredictProtein server. Nucleic Acids Res. *32*, W321–W326.

Roussel, X., Lancelon-Pin, C., Viksø-Nielsen, A., Rolland-Sabaté, A., Grimaud, F., Potocki-Véronèse, G., Buléon, A., Putaux, J.-L., and D'Hulst, C. (2013). Characterization of substrate and product specificity of the purified recombinant glycogen branching enzyme of Rhodothermus obamensis. Biochim. Biophys. Acta *1830*, 2167–2177.

Rowen, D.W., Meinke, M., and LaPorte, D.C. (1992). GLC3 and GHA1 of Saccharomyces cerevisiae are allelic and encode the glycogen branching enzyme. Mol. Cell. Biol. *12*, 22–29.

Rutenberg, M.W., and Solarek, D. (1984). Starch Derivatives: Production and Uses. In Starch: Chemistry and Technology, (Elsevier), pp. 311–388.

Rydberg, U., Andersson, L., Andersson, R., Aman, P., and Larsson, H. (2001). Comparison of starch branching enzyme I and II from potato. Eur. J. Biochem. *268*, 6140–6145.

Sánchez-Rivera, M.M., García-Suárez, F.J.L., Velázquez del Valle, M., Gutierrez-Meraz, F., and Bello-Pérez, L.A. (2005). Partial characterization of banana starches oxidized by different levels of sodium hypochlorite. Carbohydr. Polym. *62*, 50–56.

Sandhu, K.S., Kaur, M., Singh, N., and Lim, S.-T. (2008). A comparison of native and oxidized normal and waxy corn starches: Physicochemical, thermal, morphological and pasting properties. LWT - Food Sci. Technol. *41*, 1000–1010.

Santos, C.R., Tonoli, C.C.C., Trindade, D.M., Betzel, C., Takata, H., Kuriki, T., Kanai, T., Imanaka, T., Arni, R.K., and Murakami, M.T. (2011). Structural basis for branching-enzyme activity of glycoside hydrolase family 57: Structure and stability studies of a novel branching enzyme from the hyperthermophilic archaeon Thermococcus Kodakaraensis KOD1. Proteins Struct. Funct. Bioinforma. *79*, 547–557.

Satoh, H., Nishi, A., Yamashita, K., Takemoto, Y., Tanaka, Y., Hosaka, Y., Sakurai, A., Fujita, N., and Nakamura, Y. (2003). Starch-Branching Enzyme I-Deficient Mutation Specifically Affects the Structure and Properties of Starch in Rice Endosperm 1. *133*, 1111–1121.

Sawada, T., Nakamura, Y., Ohdan, T., Saitoh, A., Francisco, P.B., Suzuki, E., Fujita, N., Shimonaga, T., Fujiwara, S., Tsuzuki, M., et al. (2014). Diversity of reaction characteristics of glucan branching enzymes and the fine structure of α-glucan from various sources. Arch. Biochem. Biophys. *562*, 9–21.

Schäffner, J., Winter, J., Rudolph, R., and Schwarz, E. (2001). Cosecretion of chaperones and low-molecular-size medium additives increases the yield of recombinant disulfide-bridged proteins. Appl. Environ. Microbiol. *67*, 3994–4000.

Schwalbe, H.C. (1966). Starch adhesive and process for its preparation.

Schwall, G.P., Safford, R., Westcott, R.J., Jeffcoat, R., Tayal, A., Shi, Y.C., Gidley, M.J.,

and Jobling, S.A. (2000). Production of very-high-amylose potato starch by inhibition of SBE A and B. Nat. Biotechnol. *18*, 551–554.

Seo, B., Kim, S., Scott, M.P., Singletary, G.W., Wong, K., James, M.G., and Myers, A.M. (2002). Functional Interactions between Heterologously Expressed Starch-Branching Enzymes of Maize and the Glycogen Synthases of Brewer ' s Yeast 1. Society *128*, 1189–1199.

Sharma, S.S., Chong, S., and Harcum, S.W. (2006). Intein-mediated protein purification of fusion proteins expressed under high-cell density conditions in E. coli. J. Biotechnol. *125*, 48–56.

Shaw, A., Bott, R., and Day, A.G. (1999). Protein engineering of α-amylase for low pH performance. Curr. Opin. Biotechnol. *10*, 349–352.

Shevchenko, A., Wilm, M., Vorm, O., and Mann, M. (1996). Mass spectrometric sequencing of proteins silver-stained polyacrylamide gels. Anal. Chem. *68*, 850–858.

Shiloach, J., and Fass, R. (2005). Growing E. coli to high cell density--a historical perspective on method development. Biotechnol. Adv. *23*, 345–357.

Shinohara, M.L., Ihara, M., Abo, M., Hashida, M., Takagi, S., and Beck, T.C. (2001). A novel thermostable branching enzyme from an extremely thermophilic bacterial species, Rhodothermus obamensis. Appl. Microbiol. Biotechnol. *57*, 653–659.

Singh, S.M., and Panda, A.K. (2005). Solubilization and refolding of bacterial inclusion body proteins. J. Biosci. Bioeng. *99*, 303–310.

Singh, J., Kaur, L., and McCarthy, O.J. (2007). Factors influencing the physico-chemical, morphological, thermal and rheological properties of some chemically modified starches for food applications—A review. Food Hydrocoll. *21*, 1–22.

Smith, A.M. (2008). Prospects for increasing starch and sucrose yields for bioethanol production. Plant J. *54*, 546–558.

Smith, D.B., and Johnson, K.S. (1988). Single-step purification of polypeptides expressed in Escherichia coli as fusions with glutathione S-transferase. Gene *67*, 31–40.

Smith, A.M., Denyer, K., and Martin, C. (1997). THE SYNTHESIS OF THE STARCH GRANULE. Annu. Rev. Plant Physiol. Plant Mol. Biol. *48*, 67–87.

Smythe, C., and Cohen, P. (1991). The discovery of glycogenin and the priming mechanism for glycogen biogenesis. Eur. J. Biochem. *200*, 625–631.

Sørensen, H.P., and Mortensen, K.K. (2005). Advanced genetic strategies for recombinant protein expression in Escherichia coli. J. Biotechnol. *115*, 113–128.

de Souza, P.M., and de Oliveira Magalhães, P. (2010). Application of microbial α-amylase in industry - A review. Braz. J. Microbiol. *41*, 850–861.

Spendler, T., and Jorgensen, O.B. (1997). Use of a Branching Enzyme in Baking.

Sreerama, N., and Woody, R.W. (2003). Structural composition of betaI- and betaII-proteins. Protein Sci. *12*, 384–388.

Stam, M.R., Danchin, E.G.J., Rancurel, C., Coutinho, P.M., and Henrissat, B. (2006). Dividing the large glycoside hydrolase family 13 into subfamilies: towards improved functional annotations of alpha-amylase-related proteins. Protein Eng. Des. Sel. *19*, 555–562.

Stenesh, J. (1998). Biochemistry (Plenum).

Stolt, M., Oinonen, S., and Autio, K. (2000). Effect of high pressure on the physical properties of barley starch. Innov. Food Sci. Emerg. Technol. *1*, 167–175.

Strocchi, M., Ferrer, M., Timmis, K.N., and Golyshin, P.N. (2006). Low temperature-induced systems failure inEscherichia coli: Insights from rescue by cold-adapted chaperones. Proteomics *6*, 193–206.

Studier, F.W., and Moffatt, B.A. (1986). Use of bacteriophage T7 RNA polymerase to direct selective high-level expression of cloned genes. J. Mol. Biol. *189*, 113–130.

Stute, R., Heilbronn, R.W., Klingler, R.W., Boguslawski, S., Eshtiaghi, M.N., and Knorr, D. (1996). Effects of High Pressures Treatment on Starches. Starch - Starke *48*, 399–408.

Su, W.-F. (2013). Principles of Polymer Design and Synthesis (Berlin, Heidelberg: Springer Berlin Heidelberg).

Sun, C., Sathish, P., Ahlandsberg, S., and Jansson, C. (1998). The two genes encoding starch-branching enzymes IIa and IIb are differentially expressed in barley. Plant Physiol. *118*, 37–49.

Svensson, B. (1994). Protein engineering in the alpha-amylase family: catalytic mechanism, substrate specificity, and stability. Plant Mol. Biol. *25*, 141–157.

Szente, L., and Szejtli, J. (2004). Cyclodextrins as food ingredients. Trends Food Sci. Technol. *15*, 137–142.

Szweda, P., Pladzyk, R., Kotlowski, R., and Kur, J. (2001). Cloning, expression, and purification of the Staphylococcus simulans lysostaphin using the intein-chitin-binding domain (CBD) system. Protein Expr. Purif. *22*, 467–471.

Szymońska, J., Krok, F., and Tomasik, P. (2000). Deep-freezing of potato starch. Int. J. Biol. Macromol. *27*, 307–314.

Szymońska, J., Krok, F., Komorowska-Czepirska, E., and Rębilas, K. (2003). Modification of granular potato starch by multiple deep-freezing and thawing. Carbohydr. Polym. *52*, 1–10.

Takata, H., Kuriki, T., Okada, S., Takesada, Y., Iizuka, M., Minamiura, N., and Imanaka,

T. (1992). Action of neopullulanase. Neopullulanase catalyzes both hydrolysis and transglycosylation at alpha-(1----4)- and alpha-(1----6)-glucosidic linkages. J. Biol. Chem. *267*, 18447–18452.

Takata, H., Takaha, T., Kuriki, T., Okada, S., Takagi, M., and Imanaka, T. (1994). Properties and active center of the thermostable branching enzyme from Bacillus stearothermophilus. Appl. Environ. Microbiol. *60*, 3096–3104.

Takata, H., Takaha, T., Okada, S., Hizukuri, S., Takagi, M., and Imanaka, T. (1996a). Structure of the cyclic glucan produced from amylopectin by Bacillus stearothermophilus branching enzyme. Carbohydr. Res. *295*, 91–101.

Takata, H., Takaha, T., Okada, S., Takagi, M., and Imanaka, T. (1996b). Cyclization reaction catalyzed by branching enzyme. J. Bacteriol. *178*, 1600–1606.

Takata, H., Takaha, T., Nakamura, H., Fujii, K., Okada, S., Takagi, M., and Imanaka, T. (1997). Production and some properties of a dextrin with a narrow size distribution by the cyclization reaction of branching enzyme. J. Ferment. Bioeng. *84*, 119–123.

Takata, H., Ohdan, K., Takaha, T., Kuriki, T., and Okada, S. (2003). Properties of Branching Enzyme from Hyperthermophilic Bacterium, Aquifex aeolicus, and Its Potential for Production of Highly-branched Cyclic Dextrin. J. Appl. Glycosci. *50*, 15–20.

Takata, H., Kato, T., Takagi, M., and Imanaka, T. (2005). Cyclization reaction catalyzed by Bacillus cereus branching enzyme, and the structure of cyclic glucan produced by the enzyme from amylose. J. Appl. Glycosci. *52*, 359–365.

Takeda, Y., Guan, H.-P., and Preiss, J. (1993). Branching of amylose by the branching isoenzymes of maize endosperm. Carbohydr. Res. *240*, 253–263.

Tanaka, N., Fujita, N., Nishi, A., Satoh, H., Hosaka, Y., Ugaki, M., Kawasaki, S., and Nakamura, Y. (2004a). The structure of starch can be manipulated by changing the expression levels of starch branching enzyme IIb in rice endosperm. Plant Biotechnol. J. *2*, 507–516.

Tanaka, N., Fujita, N., Nishi, A., Satoh, H., Hosaka, Y., Ugaki, M., Kawasaki, S., and Nakamura, Y. (2004b). The structure of starch can be manipulated by changing the expression levels of starch branching enzyme IIb in rice endosperm. Plant Biotechnol. J. *2*, 507–516.

Tao, H., Yan, J., Zhao, J., Tian, Y., Jin, Z., and Xu, X. (2015). Effect of Multiple Freezing/Thawing Cycles on the Structural and Functional Properties of Waxy Rice Starch. PLoS One *10*, e0127138.

Terpe, K. (2003). Overview of tag protein fusions: from molecular and biochemical fundamentals to commercial systems. Appl. Microbiol. Biotechnol. *60*, 523–533.

Tester, R.F., and Debon, S.J.. (2000). Annealing of starch — a review. Int. J. Biol. Macromol. *27*, 1–12.

Tetlow, I.J. (2006). Understanding storage starch biosynthesis in plants : a means to quality improvement.

Tetlow, I.J. (2011). Starch biosynthesis in developing seeds. Seed Sci. Res. *21*, 5–32.

Tetlow, I.J. (2012). Starch : origins, structure and metabolism (Society for Experimental Biology).

Tetlow, I.J., and Emes, M.J. (2014). A review of starch-branching enzymes and their role in amylopectin biosynthesis. IUBMB Life *66*, 546–558.

Tetlow, I.J., Wait, R., Lu, Z., Akkasaeng, R., Bowsher, C.G., Esposito, S., Kosar-Hashemi, B., Morell, M.K., and Emes, M.J. (2004). Protein phosphorylation in amyloplasts regulates starch branching enzyme activity and protein-protein interactions. Plant Cell *16*, 694–708.

Tharanathan, R.N. (2005). Starch-Value Addition by Modification. Crit. Rev. Food Sci. Nutr. *45*, 371–384.

Thiemann, V., Saake, B., Vollstedt, A., Schäfer, T., Puls, J., Bertoldo, C., Freudl, R., and Antranikian, G. (2006). Heterologous expression and characterization of a novel branching enzyme from the thermoalkaliphilic anaerobic bacterium Anaerobranca gottschalkii. Appl. Microbiol. Biotechnol. *72*, 60–71.

Tolvanen, P., Mäki-Arvela, P., Sorokin, A.B., Salmi, T., and Murzin, D.Y. (2009). Kinetics of starch oxidation using hydrogen peroxide as an environmentally friendly oxidant and an iron complex as a catalyst. Chem. Eng. J. *154*, 52–59.

Tomasik, P., and Schilling, C.H. (2004). Chemical Modification of Starch. Adv. Carbohydr. Chem. Biochem. *59*, 175–403.

Tomono, K., Mugishima, A., Suzuki, T., Goto, H., Ueda, H., Nagai, T., and Watanabe, J. (2002). Interaction between Cycloamylose and Various Drugs. J. Incl. Phenom. Macrocycl. Chem. *44*, 267–270.

Torija, M.-J., Novo, M., Lemassu, A., Wilson, W., Roach, P.J., François, J., and Parrou, J.-L. (2005). Glycogen synthesis in the absence of glycogenin in the yeast *Saccharomyces cerevisiae*. FEBS Lett. *579*, 3999–4004.

Towbin, H., Staehelin, T., and Gordon, J. (1979). Electrophoretic transfer of proteins from polyacrylamide gels to nitrocellulose sheets: procedure and some applications. Proc. Natl. Acad. Sci. U. S. A. *76*, 4350–4354.

Tsumoto, K., Umetsu, M., Kumagai, I., Ejima, D., Philo, J.S., and Arakawa, T. (2004). Role of Arginine in Protein Refolding, Solubilization, and Purification. Biotechnol. Prog. *20*, 1301–1308.

Utsumi, Y., Yoshida, M., Francisco, Jr., P.B., Sawada, T., Kitamura, S., and Nakamura, Y. (2009). Quantitative Assay Method for Starch Branching Enzyme with Bicinchoninic Acid by Measuring the Reducing Terminals of Glucans. J. Appl. Glycosci. *56*, 215–222.

Vagenende, V., Yap, M.G.S., and Trout, B.L. (2009). Mechanisms of Protein Stabilization and Prevention of Protein Aggregation by Glycerol. Biochemistry *48*, 11084–11096.

Valberg, S.J., Ward, T.L., Rush, B., Kinde, H., Hiraragi, H., Nahey, D., Fyfe, J., and Mickelson, J.R. (2001). Glycogen branching enzyme deficiency in quarter horse foals. J. Vet. Intern. Med. *15*, 572–580.

Vamadevan, V., and Bertoft, E. (2015). Structure-function relationships of starch components. Starch - Stärke *67*, 55–68.

Venn, B.J., and Mann, J.I. (2004). Cereal grains, legumes and diabetes. Eur. J. Clin. Nutr. *58*, 1443–1461.

van der Vlist, J., Faber, M., Loen, L., Dijkman, T.J., Asri, L. a. T.W., and Loos, K. (2012). Synthesis of Hyperbranched Glycoconjugates by the Combined Action of Potato Phosphorylase and Glycogen Branching Enzyme from Deinococcus geothermalis. Polymers (Basel). *4*, 674–690.

Völksen, W. (1949). The discovery of starch saccharification (acid hydrolysis) by G. S. C. Kirchhoff in 1811. Starch - Stärke *1*, 30–36.

Waffenschmidt, S., and Jaenicke, L. (1987). Assay of reducing sugars in the nanomole range with 2,2'-bicinchoninate. Anal. Biochem. *165*, 337–340.

Wang, L., and Wang, Y.-J. (2001). Structures and Physicochemical Properties of Acid-Thinned Corn, Potato and Rice Starches. Starch - Stärke *53*, 570.

Wang, Y.-J., and Wang, L. (2003). Physicochemical properties of common and waxy corn starches oxidized by different levels of sodium hypochlorite. Carbohydr. Polym. *52*, 207–217.

Ward, T., Valberg, S., Adelson, D., Abbey, C., Binns, M., and Mickelson, J. (2004). Glycogen branching enzyme (GBE1) mutation causing equine glycogen storage disease IV. Mamm. Genome *15*, 570–577.

Watanabe, T., and French, D. (1980). Structural features of naegeli amylodextrin as indicated by enzymic degradation. Carbohydr. Res. *84*, 115–123.

Weisburg, W.G., Giovannoni, S.J., and Woese, C.R. (1989). The Deinococcus-Thermus phylum and the effect of rRNA composition on phylogenetic tree construction. Syst. Appl. Microbiol. *11*, 128–134.

Woo, K.S., and Seib, P.A. (2002). Cross-Linked Resistant Starch: Preparation and Properties. Cereal Chem. J. *79*, 819–825.

Wu, H.C.H., and Sarko, A. (1978). The double-helical molecular structure of crystalline a-amylose. Carbohydr. Res. *61*, 27–40.

Wu, J., and Filutowicz, M. (1999). Hexahistidine (His6)-tag dependent protein

dimerization: a cautionary tale. Acta Biochim. Pol. *46*, 591–599.

Wu, J., Yang, J.T., and Wu, C.S. (1992). Beta-II conformation of all-beta proteins can be distinguished from unordered form by circular dichroism. Anal. Biochem. *200*, 359–364.

Wu, S., Liu, Y., Yan, Q., and Jiang, Z. (2014). Gene cloning, functional expression and characterisation of a novel glycogen branching enzyme from Rhizomucor miehei and its application in wheat breadmaking. Food Chem. *159*, 85–94.

Würsch, P., and Gumy, D. (1994). Inhibition of amylopectin retrogradation by partial beta-amylolysis. Carbohydr. Res. *256*, 129–137.

Wurzburg, O.B. (1986). Modified Starches: Properties and Uses (Boca Raton, FL: CRC Press).

Yoo, S.-H., Spalding, M.H., and Jane, J. (2002). Characterization of cyanobacterial glycogen isolated from the wild type and from a mutant lacking of branching enzyme. Carbohydr. Res. *337*, 2195–2203.

Young, C.L., Britton, Z.T., and Robinson, A.S. (2012). Recombinant protein expression and purification: A comprehensive review of affinity tags and microbial applications. Biotechnol. J. *7*, 620–634.

Yu, R. -j., Hong, A., Dai, Y., and Gao, Y. (2004). Intein-mediated Rapid Purification of Recombinant Human Pituitary Adenylate Cyclase Activating Polypeptide. Acta Biochim. Biophys. Sin. (Shanghai). *36*, 759–766.

Yu, S., Xu, J., Zhang, Y., and Kopparapu, N.K. (2014). Relationship between Intrinsic Viscosity, Thermal, and Retrogradation Properties of Amylose and Amylopectin. *32*, 514–520.

Zallie, J. (1988). Benefits of quick setting starches. Manuf. Confect. *66*, 41–43.

Zang, L.H., Howseman, A.M., and Shulman, R.G. (1991). Assignment of the 1H chemical shifts of glycogen. Carbohydr. Res. *220*, 1–9.

Zavareze, E. da R., and Dias, A.R.G. (2011). Impact of heat-moisture treatment and annealing in starches: A review. Carbohydr. Polym. *83*, 317–328.

Zeeman, S.C., Kossmann, J., and Smith, A.M. (2010). Starch: its metabolism, evolution, and biotechnological modification in plants. Annu. Rev. Plant Biol. *61*, 209–234.

Zhang, L.-M. (2001). A Review of Starches and Their Derivatives for Oilfield Applications in China. Starch - Stärke *53*, 401–407.

Zhang, G., and Hamaker, B.R. (2009). Slowly Digestible Starch: Concept, Mechanism, and Proposed Extended Glycemic Index. Crit. Rev. Food Sci. Nutr. *49*, 852–867.

Zhang, G., Venkatachalam, M., and Hamaker, B.R. (2006). Structural Basis for the Slow Digestion Property of Native Cereal Starches. Biomacromolecules *7*, 3259–3266.

Zhou, Z., Robards, K., Helliwell, S., and Blanchard, C. (2003). Effect of rice storage on pasting properties of rice flour. Food Res. Int. *36*, 625–634.

Zona, R., and Janeček, Š. (2005). Relationships between SLH motifs from different glycoside hydrolase families. *60*, 115–121.

Zona, R., Chang-Pi-Hin, F., O'Donohue, M.J., and Janecek, S. (2004). Bioinformatics of the glycoside hydrolase family 57 and identification of catalytic residues in amylopullulanase from Thermococcus hydrothermalis. Eur. J. Biochem. *271*, 2863–2872.